Vaccine immunomodulation and protection mechanisms against *Mycobacterium avium* subsp. *paratuberculosis*: Focus on innate responses

Iraia Ladero Auñón

Submitted to
Universidad del País Vasco/ Euskal Herriko Unibertsitatea (UPV/EHU)
Departamento de Calidad y Seguridad Alimentaria

For the degree of
PhD

June 2021

Supervised by: Dr. Natalia Elguezabal & Dr. Juan Anguita

A Aitatxu y Amatxu,

a Lorena e Hirune,

a Ibon

y a Miko♥

"The strength of the team is each individual member. The strength of each member is the team."

Phil Jackson

Agradecimientos

En primer lugar, quiero mostrar mi agradecimiento a todas las entidades financiadoras sin las cuales la realización del presente trabajo de tesis no hubiera sido posible. Por un lado, al Departamento de Desarrollo Económico, Sostenibilidad y Medio Ambiente del Gobierno Vasco por la concesión de la beca pre doctoral en 2017. Por otro lado, al INIA, por haber respaldado el proyecto PROBAK (RTA 2017-00089-00-00) en el cual ha estado enclavado el presente trabajo de Tesis. Finalmente, por la financiación de mi estancia en el Royal Veterinary College de Londres, a la Organización Europea de Biología Molecular (EMBO), y a la Federación Europea de Asociaciones de Microbiología (FEMS).

Agradezco a Natalia la paciencia y dedicación que ha demostrado durante mi aprendizaje. Por haberme guiado en esta importante etapa de mi carrera científica, pero también por haberme dejado dar rienda suelta a mis ideas y haberme permitido aprender de mis errores. También a Juan, por lo atento y rápido que ha sido siempre que he necesitado de su apoyo y sabios consejos. Gracias a Joseba por su atención y confianza y por estar siempre dispuesto a "poner el tanque boca abajo".

Gracias a Elena, compañera de poyata, sudor y lágrimas, gran compañera y amiga, siempre capaz de reconfortar a los demás. Gracias a Ainara por todas sus pócimas secretas y por SSS (Sacar Siempre una Sonrisa). A Félix, siempre dispuesto cuando se rompe algo (ruedas) o falta enantyum. Gracias a AlfonsoU por su predisposición y destreza con la toma de muestras.

Gracias a l@s compañer@s del becariado, a l@s que se quedan y a las que se fueron, amig@s realmente, ha sido un verdadero placer conoceros y

espero que sigamos en contacto siempre. En especial a mi favorita english-mate Mili (Maitane), por su apoyo moral y por esas cañas que podrían arreglar el mundo, a la encantadora doctora Serrano, por sus grandes consejos y a María, nunca hay que olvidarse de llevar los intermitentes instalados ;)

En general a toda la plantilla de Neiker, que son muchos y en algún momento todos me han ofrecido su apoyo de alguna manera. A la gente del edificio rojo, concretamente, Fernando Blanco (un crack), que me ha librado tantas veces del pánico con el fluorímetro. Y cómo no, a toda la gente de Sanidad Animal, la calidad humana y profesional que me he encontrado han sido excelentes. En especial a personas amables como Nekane, Bea, Mertxe, Miguel o Iker que siempre están dispuestas a ayudar. También a Diego B. del CiCbioGUNE y a R. Arrazuria por haber dedicado su tiempo a colaborar y haber sido tan agradables.

I also want to thank the people I met in the RVC of London, for welcoming me as a part of the team and showing me around. I had a really good experience there and I hope to see you again at some point. Especially grateful to Dirk Werling for having allowed me to spend that time with them and having been such a good host and supervisor.

Finalmente, quiero agradecer a los míos, a mis queridísimos Ibon, Sis, Aita y Ama, por su infinita paciencia y apoyo incondicionales y a mis variopintos amig@s por haber estado siempre que lo he necesitado. Y cómo no, gracias a mi siempre pequeña Hirune por su aportación técnica en la laburpena. Gracias a todos por escucharme, aguantarme y haberme animado a emprender este duro pero apasionante camino.

Table of Contents

List of Tables

List of Figures

List of Abbreviations

ACD	Acid Citrate Dextrose
AFB	Acid-Fast Bacilli
APC	Antigen Presenting Cell
BCG	Bacillus Calmette Guérin
BHI	Brain Heart Infusion (Agar)
BSA	Bovine Serum Albumin
bTB	Bovine Tuberculosis
CC	Challenge Control group
CD	Cluster of Differentiation
cDNA	Complementary DNA
CFU	Colony-Forming Unit
ConA	Concanavalin A
CPDA	Citrate phosphate dextrose adenine
Cpstb	*Corynebacterium pseudotuberculosis*
CPV	*Corynebacterium pseudotuberculosis* based vaccine
Cq	Quantification Cycle
CR	Complement Receptor
Ct	Cycle threshold
CV	Control vaccine (Silirum®)
DAMPs	Damage-associated Molecular Patterns
DAPI	4′,6-diamidino-2-phenylindole
DDA	Dimethyldiocta-decylammonium bromide
DC	Dendritic cell
DEPC	Diethylpyrocarbonate
DIVA	Differentiating Infected from Vaccinated Animals
DNA	Deoxyribonucleic Acid

dPCR	Digital polymerase chain reaction
DPX	Dibutyl phthalate xylene
DTH	Delayed-type hypersensitivity (response)
Ecoli	*Escherichia coli*
EDTA	Ethylenediamine tetraacetic acid
ELISA	Enzyme-Linked Immunosorbent assay
ET	Extracellular Trap
FAP-P	Fibronectin attachment protein
FBS	Fetal Bovine Serum
Fc	Fragment crystallizable
FITC	Fluorescein 5(6)-isothiocyanate
FN	Fibronectin
FSC	Forward Side Scatter
GALT	Gut-associated lymphoid tissue
GFP	Green Fluorescent Protein
HEYM	Herrold's egg yolk medium
HMGB	High Mobility Group Box
hTB	Human Tuberculosis
IAC	Internal amplification control
IC	Infected Control group
ICAM	Intracellular adhesion molecule
IDR	Intradermal reaction
IFN	Interferon
IgA	Immunoglobulin A
IgG	Immunoglobulin G
IgM	Immunoglobulin M

IGRA	Interferon-gamma release assay
IHC	Immunohistochemistry
IL	Interleukin
IM	Intramuscular
iNOS	Inducible nitric oxide synthase
IP	Intraperitoneal
LAV	Live attenuated vaccine
LPS	Lipopolysaccharide
MΦ	Macrophage
M-CSF	Macrophage-Colony Stimulating Factor
Maa	*Mycobacterium avium* subsp. *avium*
ManLAM	Mannosylated lipoarabinomannan
Map	*Mycobacterium avium* subsp. *paratuberculosis*
MAPK	Mitogen-activated protein kinase
Mbv	*Mycobacterium bovis*
MBV	*Mycobacterium bovis* based vaccine
MC1+	Mannose receptor C-type 1
MDM	Monocyte derived macrophages
MHC	Major Histocompatibility Complex
MIQE	Minimum information necessary for evaluating qPCR experiments
MJ	Mycobactin J
MLN	Mesenteric lymph node
MOI	Multiplicity of infection
MPV	*Mycobacterium avium* subsp. *paratuberculosis* based vaccine
MR	Mannose receptor

mRNA	Messenger RNA
Mtb	*Mycobacterium tuberculosis*
NADH	Nicotinamide adenine dinucleotide
NC	Non-challenged Control group
NET	Neutrophil Extracellular Trap
NIC	Non-infected Control group
NK	Natural Killer
NO	Nitric oxide
NTC	No template control
NV	Non-vaccinated group
OADC	Oleic acid, dextrose and catalase
OD	Optical Density
OIE	The World Organization for Animal Health
ON	Overnight
PBMCs	Peripheral mononuclear cells
PBS	Phosphate Buffered Saline
PC	Primer Concentration
PCA	Principal Component Analysis
PCR	Polymerase Chain Reaction
PMA	Phorbol 12-myristate 13-acetate
PMN	Polymorphonuclear neutrophil
PPA-3	Map Protoplasmatic antigen 3
PPD	Purified Protein Derivative
PTB	Paratuberculosis
qPCR	Real-time Polymerase Chain Reaction
QuilA	*Quillaja saponaria* saponin-based vaccine adjuvant

RNA	Ribonucleic acid
ROS	Reactive oxygen species
ROX	6-carboxy-X-rhodamine
RPMI	Roswell Park Memorial Institute medium
RT-	Retrotranscriptase minus control
RT-qPCR	Real-time Reverse Transcription Polymerase Chain Reaction
Saur	*Staphylococcus aureus*
SC	Subcutaneous
SD	Standard deviation
SDS	Sodium dodecyl sulfate
SED	Subepithelial dome
SEM	Standard error of the mean
SM	Map sonicate
SR	*Sacculus rotundus*
SS	Saline Solution
SSC	Side Scatter
STA	Specific target amplification
TCR	T cell receptor
TGF	Transforming Growth Factor
Th	T helper lymphocyte
TLR	Toll-like receptor
Tm	Primer melting temperature
TNF	Tumor necrosis factor
VA	Vermiform appendix
VID	Intradermally vaccinated group
VOR	Orally Vaccinated Group

Laburpena

Paratuberkulosia (PTB) edo Johne-ren gaixotasuna *Mycobacterium avium* subspecies *paratuberculosis*-ek (Map) eragindako gaixotasuna da. Batez ere etxeko hausnarkariei eragiten die, halaber, badaude hausnarkariak zein hausnarkariak ez diren basa-espezie batzuek, PTBz gaixotu ahal direnak ere. PTB enteritis granulomatoso kronikoa da, animalietan beherakoak eta pisu galera progresiboa eragiten duena. Antzekotasun klinikoa dela eta, gizakiek pairatzen duten Crohn gaixotasuna PTBarekin erlazionatu da. Hala ere, orain arte egin diren ikerketak ez dira nahikoak izan Map giza gaixotasun horren agente etiologiko gisa esleitzeko edo baztertzeko.

Map zelula barneko derrigorrezko bakteria izanik, hestearen azpi-epitelioan dagoen makrofagoa infektatzen du. Kutsadura ahoz gertatzen da, oro har, animaliak oso gazteak direnean, bakterioak eramaten dituzten gorotzekin kutsatuta dauden elikagaien bidez edo zuzenean emeen esnearen bidez. Sarrera bide nagusia ileonean aurki daitezkeen Peyerren Plakak dira, izan ere, haien M zelulen bidez Map-ek epitelioa zeharkatzea eta azpi epitelioko lamina propiora heltzea lortzen du. Behin lamina propiora heldu direla, bertan dauden makrofagoek Map bacterioak fagozitatu egiten dituzte, eta horiek Map suntsitzetik urrun, nitxo gisa jarduten dute. Makrofagoaren fagosomaren barnetik, Map-ek fagolisosomaren heltzea eragozten du, eta horrek aldi berean, fagosomaren azidotzea eta suntsipena sahiesten du.

PTBa oso motel garatzen den gaixotasuna da, hori dela eta, animaliek infekzio latente eta subkliniko egoeretan denbora luzez egon daitezke. Oso zaila da gaixotasunaren forma isilak eta subklinikoak pairatzen dituzten animaliak hautematea, alde batetik, ez dutelako sintomarik azaltzen eta

bestetik, gorotzetatik kanporatzen diren bakterioak eta plasman aurki daitezkeen antigorputz espezifikoak detektatzea zaila delako, baita eskuragarri dauden diagnostiko proben sentsibilitatea txikia delako. Gainera, paratuberkulosiaren aurkako tratamendu farmakologiko eraginkorrik ez dagoenez, Map borrokatzeko erabilgarri dagoen metodo bakarra txertoa da, zeina zenbait neurri higienikoekin eta gaixotu diren animalien hilketarekin batera ezarri beharra dagoen. Hausnarkari txikietan txertoa onartzen den arren, behi-aziendan erabiltzea debekatuta dago, txertoaren eraginez lortutako erantzun immunologikoak erreakzio intradermalaren (IDR) diagnostiko proba oztopatzen baitu, behi tuberkulosia (bTB) errotik kentzeko programa ofizialetan erabiltzen dena. Horrez gain, txertoak PTBaren diagnostikoa ere oztopatzen du, ez baitago infekzioa txertaketatik bereiztea ahalbidetzen duen probarik (DIVA). Gainera, merkaturatuta dauden txertoak ez dute Map-aurkako babes osoa bermatzen.

Hori horrela izanik, txerto berrien garapena beharrezkoa da, txertoen konposizioaren aldakuntzak ikertzeko ez ezik, horien administrazio bide desberdinak ikertzeko ere, antigenoen aurkezpen lekuaren arabera erantzun immunologikoa aldatzen baita. Arreta berezia merezi duen beste fenomeno bat txertoen babes gurutzatua da, zeinak patogeno erlazionatu edo guztiz desberdinen aurkako babesa ematen duten. Zentzu horretan, frogatu da PTB-ren aurkako Silirum® txerto komertzialak txertatutako artaldeen bizitza produktiboa areagotzen duela, baita ohikoak diren beste gaixotasun batzuen intzidentzia murrizten duela ere.

Efektu ezagunak eta kontrolatuak dituzten txerto berriak diseinatzeko, erantzun immunologikoaren maila desberdinetan dituzten ondorioak arretaz aztertu behar dira. PTB-an, tradizioz, Map-en itu zelulak diren makrofagoen ezagutzari buruzko ikerketa lehenetsi da. Neutrofiloek, ordea, interes txikia sortu dute, nahiz eta kanpoko patogenoen edo kalte fisiko edo kimikoen arriskuen aurrean lekura bertaratzen diren lehen globulu zuriak izan. Neutrofiloak leukozito ugarienak dira, eta horien funtzio mikrobizida nagusiak fagozitosia, oxigeno espezie erreaktiboak sortzea, horien granuluen edukia zelulaz kanpoko ingurunera kanporatzea eta zelulaz kanpoko tranpak askatzea dira. Neutrofiloen zelulaz kanpoko tranpak DNAz, histonaz eta gaitasun mikrobizidak dituzten beste proteina batzuez osatuta daude.

Map-k sortutako hesteetako infekzioaren hasierako faseetan, zelula egoiliarrek askatutako alarma seinaleei erantzuten dieten neutrofiloen presentzia deskribatu da. Hala ere, infekzioa aurrera egin ahala, PTB-ko lesioetan neutrofilo gutxi behatu dira. Izan ere, PTBa jasaten duten animalietan oinarritzen diren zenbait ikerketa transkriptomikoek erakutsi dute animalia horietan neutrofiloen errekrutatze eta migrazioan parte hartzen duten molekula desberdinen adierazpena gutxitu egiten dela.

Tesi-lan honetan, zenbait txerto-prototipo aurkeztu dira, zeinak hainbat administrazio bidetan aplikatu diren, bTB-ren IDRren probarekin interferentziarik izan ez dadin. Horrez gain, haren infekzioaren aurkako babesean eta sistema immunean dituen eraginak aztertu dira.

Txertoen prototipoek interferentzia hori saihesten dutela egiaztatzeko, kui eredua erabili da, oso erabilia izan dena tuberkulin antigenoen potentzia

frogatzeko IDR probetan, hipersentsibilitate erantzun atzeratua (DTH) erakusten dutelako. Txertoen infekzioaren aurkako eraginkortasuna, ordea, untxi ereduan frogatu da, lehenik txertoak bideratzeko dermis barneko (VID) eta ahozko (VOR) bideak alderatu dira, eta ondoren, ahoz bideratutako prototipo desberdinak frogatu dira; bi kasuetan larruazalpean aplikatutako txerto komertzialarekin alderatuta.

Babesari dagokionez, bide intradermalak emaitza oso onak adierazi zituen. Izan ere, VID taldeak ageriko lesiorik gabeko animalien proportzio handiena aurkeztu zuen, eta PCR bidez Map-rekiko ehun positiboak dituzten animalien proportzio txikiena. Azterketa immunohistokimikoek agerian utzi zuten txertoen estrategien arabera makrofagoek polarizazio egoera desberdinekin erantzun zutela. VID taldeak nagusiki M1 erantzun polarizatua aurkeztu zuen, IFN-γ eta TNF-ren adierazpen altua eta CD163 (M2 markatzailea) adierazpen baxua erakutsiz.

Txertatu gabeko baina desafiaturiko taldearekin alderatuta, oro har, txertatutako talde guztiek lesio granulomatoso aktibo gutxiago erakutsi zituzten, kalprotektina maila baxuarekin lotuta. VID taldeak nolabaiteko erreaktibitatea erakutsi zuen larruazaleko frogetan, ez ordea, ahozko txertoa, non guztiz negatiboa izan zen. Datu horiek erakutsi dute PTB-aren aurkako txertatzeak eta hauen administrazio bidea: 1) makrofagoen polarizazioan eragina dutela, 2) infekzioaren emaitzan eragina dutela eta 3) bTB-aren diagnostikoan erabilitako IDR frogan ere eragina izan dezakeela.

Txertoaren administrazioa ahozko bidera aldatuz gero interferentziaren arazoa saihestu daitekeela frogatu ondoren; hurrengo

helburua ahozko txerto prototipoaren erantzun immunologikoa hobetzea izan zen, babesari dagokionez ez baitzen eraginkorra izan. Horretarako, untxi eredua erabilita txerto mikobakteriano eta ez-mikobakterianoen multzoa formulatu eta probatu egin zen. Inaktibatutako bakterioetan oinarritutako txertoak QuilA laguntzaile batekin formulatu ziren, eta bakteria bizidun atenuatuetan oinarritutako prototipoa, berriz, laguntzailerik gabe. Horrez gain, neutrofiloen entrenamenduarekin erlazionatutako erantzun immuneak aztertu ziren, odol periferikoko zelula mononuklearren (PBMCs) erantzunak eta erantzun humorala hain zuzen ere. Gainera, Map aurkako babes homologo eta heterologoen ondorioak *in vivo* aztertu ziren ehun kulturgintzako teknikak erabilita.

Ahozko txertoek, bai txerto biziekin eta bai inaktibatuekin, mukosaren immunitatea aktibatu ahal izan zuten, zeinak IgA serumaren handipena eta odol periferikoko zelula mononuklearretan (PBMC) *IL4* adierazpen altua aurkezten duen. Gainera, Map-ren aurkako neutrofiloen fagozitosi periferikoa txertoaren bidez hobetu zen eta, horrez gain, Map eta bestelako patogenoen aurkako zelulaz kanpoko tranpen askapena aldatu egin zen, bai txertoak eraginda bai Map infekzioak eraginda. Horrek guztiak, txertoak immunitate entrenatua sortu zuela esan nahi du. Bestalde, Map antigenoekin *ex vivo* estimulatutako txertatutako animalien PBMC-ak berezko aktibazio azkarraren zitokinen profila erakutsi zuten. Laburbilduz, gure datuek ahozko txerto inaktibatuak neutrofiloen babes-jarduera eta berezko erantzun immunitarioak eta egokitzaileak estimulatu ditzaketela erakusten dute.

Horrez gain, bi ikerketen emaitzek iradokitzen dute txertoen ondoriozko erantzun humoraletatik eratorritako antigorputzek Map-arekiko infekzioaren aurka babesa ematen dutela. Neutrofiloetan behatutako jarduera fagozitikoaren hazkuntza tenporala desagertzen denean, antigorputzek neutrofiloen jarduera handitua ordezkatzea lortu zuten, bakteriak opsonizatuz, fagozitoek bakteriak azkar detektatu eta suntsitu ahal izateko.

Behin txertoek behar bezala entrenatutako neutrofiloek infekzioaren garapena zuzentzeko gaitasuna zutela eta baita ere makrofagoen erantzuna untxiaren ereduan polariza dezaketela ezarri ondoren, neutrofiloen eta makrofagoen arteko interakzioa mikobakterioen infekzio batean positiboa den edo ez argitu nahi izan zen. Horretarako, behi odoletik monozitoak isolatu eta makrofagoetara bihurtu ziren. Ondoren, animalia beraren neutrofiloak eta makrofagoak batera edo bereizirik kultibatu ziren eta Map edo BCG anduiekin infektatu ziren. Zelulaz kanpoko tranpa askatzea, mikobakterioen heriotza eta IL-1β eta IL-8 askapena kuantifikatu egin ziren. Neutrofiloek zelulaz kanpoko tranpak askatu zituzten mikobakterien aurka bereizirik kultibatu zirenean, ordea, ko-kultiboetan makrofagoekin kontaktu zuzenan zeudenean, askatutako tranpa kopurua askoz txikiagoa zen.

Makrofagoak oso eraginkorrak izan ziren BCG bakterioaren hilketan, baina ez ziren batere eraginkorrak izan Map-en aurka. Aitzitik, neutrofiloek bi mikobakterio motak hiltzeko antzeko eragirkortasuna erakutsi zuten. Map-ekin infektaturiko ko-kulturek bi zelula-moten konbinazioaren efektu hilgarria erakutsi zuten, BCG-rekin infektatutako ko-kulturek, berriz, espero zitekeena baino eragin hilgarri handiagoa erakutsi zuten, zeinak lankidetza

sinergiko onuragarria adierazten duen. Bi kasuetan, IL-1β eta IL-8 mailak baxuagoak izan ziren ko-kultiboetan, makrofagoak soilik zeuden kultiboekin alderatuta. Datu horiek adierazten dute bi zelula moten lankidetza onuragarria izan daitekeela inflamazioaren erreakzioa murrizteko.

Tesi-lan honen emaitzek iradokitzen dute neutrofiloek Map suntsitzeko eraginkorrak diren mekanismoak dituztela, zeinak PTB gaixotasuna pairatzean huts egiten dutenak, dirudienez, infekzioaren lekura makrofagoak iritsi ondoren. Hori dela eta, neutrofiloen jarduera hobetzea lortzen duten txerto eraginkorrak erabiltzeak, infekzioaren aurkako babesari dagokionez, arrakasta izateko aukerak handitu dezake. Zentzu horretan, lan honek ahoz bideraturiko txertoen prototipo itxaropentsuak aurkezten ditu, bTB-ren diagnostiko probarekin interferentziaren arazoa gainditzeko gaitasuna ere erakutsi dutenak.

Resumen

La paratuberculosis (PTB) o enfermedad de Johne es una enfermedad causada por *Mycobacterium avium* subespecies *paratuberculosis* (Map) que afecta principalmente a rumiantes domésticos, aunque hay una gran variedad de especies salvajes, tanto rumiantes como no rumiantes que también son susceptibles. Se trata de una enteritis granulomatosa crónica que cursa con episodios de diarrea y adelgazamiento progresivo. Por la similitud en la clínica, la enfermedad de Crohn sido relacionada con la PTB, aunque los estudios que se han llevado a cabo hasta ahora no han sido suficientes para atribuir o descartar a Map como agente etiológico de esa enfermedad humana.

Map es una bacteria intracelular obligada cuya célula diana es el macrófago situado en la zona subepitelial del intestino. El contagio se produce por la vía oral, generalmente cuando los animales son muy jóvenes, por contaminación de los alimentos con heces que vehiculan la bacteria o directamente a través de la leche materna. Su principal vía de entrada son las Placas de Peyer del ileon, a través de cuyas células M, Map consigue atravesar el epitelio y llegar a la zona subepitelial de la lámina propia. Una vez allí las bacterias son fagocitadas por los macrófagos, quienes muy lejos de destruirla, acaban sirviendo de nicho para Map. Desde el interior del fagosoma del macrófago, Map impide la maduración del fagolisosoma evitando la acidificación del mismo y su propia destrucción.

La PTB es una enfermedad de muy lento desarrollo, pudiendo permanecer los animales en un estado de infección latente o silente o en estados subclínicos de la enfermedad durante largos periodos de tiempo. Es muy difícil detectar a los animales que padecen formas silenciosas o

subclínicas de la enfermedad debido a la ausencia de síntomas, a la dificultad de detección de la bacteria en heces de la bacteria y a la dificultad en la detección de anticuerpos específicos en plasma, todo ello unido a la insuficiente sensibilidad de las pruebas de diagnóstico disponibles. Además, al no existir un tratamiento farmacológico eficaz contra la PTB, el único método efectivo consiste en aplicar la vacunación junto con una serie de medidas higiénico sanitarias y el sacrificio de animales enfermos. A pesar de que la vacunación sí está permitida en pequeños rumiantes, su uso en el ganado bovino está prohibido debido a que respuesta inmunitaria derivada de la vacunación interfiere en la prueba de diagnóstico de intradermorreacción (IDR), utilizada en los programas oficiales de erradicación de la tuberculosis bovina (bTB). Además, la vacunación también interfiere en el propio diagnóstico de la PTB, al no disponer de un test que permita diferenciar infección de vacunación (DIVA), por no mencionar el hecho de que ninguna de las vacunas comerciales ha demostrado ser totalmente eficaz en cuanto a protección frente a Map se refiere.

En este aspecto es necesario el desarrollo de nuevas vacunas, que incluya no solo la investigación de variaciones en la composición, sino también las distintas vías de administración de las mismas, ya que la respuesta inmunitaria varía en función del lugar en que se haya realizado la presentación de antígenos. Otro fenómeno que merece una especial atención es el de las protecciones cruzadas de las vacunas, que confieren protección frente a patógenos emparentados o totalmente distintos. En este sentido la vacuna comercial Silirum® contra la PTB ha demostrado aumentar la vida

productiva en rebaños vacunados y disminuir la incidencia de otras enfermedades frecuentes.

Para diseñar nuevas vacunas con efectos conocidos y controlados es necesario explorar con detenimiento los efectos de las mismas en los distintos niveles de la respuesta inmunitaria. Tradicionalmente, en la PTB se ha priorizado la investigación en el conocimiento de los macrófagos, que son la célula diana de Map. Poco interés han generado, sin embargo, los neutrófilos (PMNs), que son los primeros leucocitos en llegar ante la amenaza de patógenos externos o ante lesiones físicas o químicas. Los PMNs son los leucocitos más numerosos cuyas funciones microbicidas principales son fagocitosis, la formación de especies reactivas de oxígeno, la de degranulación del contenido de sus gránulos citoplasmáticos al medio extracelular y la de liberación de trampas extracelulares (ETs). Las ETs están compuestas por DNA, histonas y otras proteínas con capacidades microbicidas. Durante las primeras etapas de la infección con Map en el intestino se ha descrito la presencia de PMNs que acuden ante las señales de alarma liberadas por las células residentes. Sin embargo, con el tiempo, su presencia en las lesiones de PTB es muy escasa. De hecho, algunos estudios de transcriptómica de animales enfermos de PTB demuestran que en estos animales existe una disminución en la expresión de diversas moléculas implicadas en el reclutamiento y migración de los PMNs.

En este trabajo de tesis se presentan distintos prototipos vacunales que han sido aplicados por distintas rutas de administración para evitar la

interferencia con la prueba de la IDR de la bTB y se han estudiado sus efectos en la protección frente a la infección y en el sistema inmune.

Para verificar que los prototipos vacunales evitan dicha interferencia, en este trabajo se ha utilizado el modelo de cobaya, ampliamente utilizado para testar la potencia de antígenos como la tuberculina, mediante la realización de la IDR por su demostrada respuesta de hipersensibilidad de tipo retardado (DTH). La efectividad frente a la infección se ha probado en el modelo de conejo, comparando primero las vías intradérmica (VID) y oral (VOR) en el primer estudio, y probando distintos prototipos orales después, en comparación con una vacuna comercial aplicada por la vía subcutánea.

La vía intradérmica mostró unos resultados muy satisfactorios en cuanto a protección se refiere, siendo los animales del grupo VID los que menos lesiones visibles mostraron y además también presentaron la menor proporción de tejidos positivos a Map por PCR. El análisis de inmunohistoquímica reveló que los macrófagos respondían con estados de polarización distintos en función de las estrategias de vacunación. El grupo VID presentó una respuesta polarizada predominantemente de macrófagos M1, caracterizados por una mayor expresión de IFN-γ y TNF, y una menor expresión de CD163 (marcador M2). En general, todos los grupos vacunados mostraron lesiones granulomatosas menos activas, asociado a niveles más bajos de calprotectina, en comparación con el grupo desafiado no vacunado. En cuanto a las pruebas de interferencia realizadas en cobaya, el grupo VID mostró cierto grado de reactividad en las pruebas cutáneas, mientras que la misma vacuna por vía oral resultó completamente negativa. Estos datos

mostraron que la vacunación contra la PTB y la vía de administración de la misma: 1) tienen efectos sobre la polarización de los macrófagos, 2) influyen en el resultado de la infección y 3) condicionan los resultados de la prueba de la IDR para el diagnóstico de la bTB.

Tras haber demostrado que el problema de la interferencia se puede evitar potencialmente cambiando la administración de la vacuna a la vía oral, el siguiente objetivo fue mejorar la respuesta inmune proporcionada por el prototipo inicial de vacuna oral, que resultó ser poco eficiente en relación a la protección. Para ello se formularon un conjunto de vacunas micobacterianas y no micobacterianas que fueron testadas en el modelo de conejo. Las vacunas basadas en bacterias inactivadas se formularon con un adyuvante, QuilA, mientras que el prototipo basado en una bacteria viva atenuada se aplicó sin adyuvante. Además, se estudiaron respuestas inmunes relacionadas con el entrenamiento sobre los PMNs, respuestas adquiridas de células mononucleares de sangre periférica (PBMCs) y respuesta humoral. Además, también se examinó la protección *in vivo* homóloga y heteróloga de los distintos tipos vacunales contra Map utilizando técnicas de cultivo de tejidos. La vacunación oral con vacunas vivas o inactivadas pudo activar la inmunidad de la mucosa caracterizada por la elevación de IgA sérica y la expresión de *IL4* en PBMCs. Además, la fagocitosis de PMN de sangre periférica contra Map fue mejorada por la vacunación y la liberación de trampas extracelulares contra Map y patógenos no relacionados fue modificada tanto por la vacunación como por el desafío con Map. Finalmente, las PBMCs de animales vacunados estimulados *ex vivo* con antígenos Map mostraron un perfil de citoquinas de activación rápida de sistema inmune

innato. En conclusión, nuestros datos muestran que la vacunación oral con vacunas inactivadas puede estimular la actividad protectora de los PMNs y las respuestas inmunitarias tanto innatas como adaptativas.

En relación a la respuesta humoral, ambos estudios apuntan a que los anticuerpos derivados de la respuesta humoral debidos a la vacunación tienen un papel protector frente a la infección por Map. Cuando el aumento transitorio en la actividad fagocítica observada en los PMNs desaparece, los anticuerpos presentes a nivel sistémico, conseguían suplir esa carencia opsonizando las bacterias para que los fagocitos las detectasen y las destruyesen rápidamente.

Una vez establecido que los PMNs adecuadamente entrenados presentan capacidad para dirigir el desarrollo de la infección y que las vacunas pueden polarizar también la respuesta de los macrófagos en el modelo de conejo, la siguiente cuestión que se quiso esclarecer fue si la interacción entre PMNs y macrófagos durante una infección por micobacterias es positiva o no. Para ello, a partir de sangre fresca de bovino, se aislaron mocitos y se diferenciaron a macrófagos. Después, se pusieron en cultivo macrófagos y PMNs del mismo animal juntos o por separado en presencia de Map o BCG. Se evaluaron la liberación de trampas extracelulares, la muerte de micobacterias y la liberación de IL-1β e IL-8. Los PMNs liberaron trampas extracelulares contra las micobacterias cuando se encontraban solos y en presencia de macrófagos sin contacto directo con las células, pero resultaron inhibidos en el contacto directo. Los macrófagos resultaron extremadamente eficientes matando la cepa BCG, pero ineficaces contra Map. Por el contrario,

los PMNs mostraron tasas de destrucción similares para ambas micobacterias. Los co-cultivos infectados con Map mostraron el efecto letal esperado de la combinación de ambos tipos de células, mientras que los co-cultivos infectados con BCG mostraron un efecto letal potenciado más allá del esperado, lo que indica una cooperación sinérgica beneficiosa. En ambos casos, los niveles de IL-1β e IL-8 fueron más bajos en los co-cultivos, lo que sugiere una reacción inflamatoria reducida en comparación con la detectada en los macrófagos en solitario. Estos datos indican que la cooperación de ambos tipos de células puede ser beneficiosa en términos de disminuir la reacción inflamatoria.

Los resultados de este trabajo de tesis sugieren que los PMNs disponen de mecanismos de protección efectivos contra Map que parecen fallar durante la enfermedad de PTB después de la llegada de macrófagos al sitio de infección. Por tanto, el uso de vacunas efectivas que consigan potenciar la actividad de los PMNs podría ayudar a aumentar las posibilidades de éxito de las mismas en cuanto a protección frente a la infección se refiere. En este trabajo también se presentan unos prototipos de vacunas orales prometedores en este sentido, que además, han demostrado capacidad para superar la limitación que supone la interferencia en la prueba de diagnóstico de la bTB.

Summary

Paratuberculosis (PTB) or Johne's disease is a disease caused by *Mycobacterium avium* subspecies *paratuberculosis* (Map) that mainly affects domestic ruminants, although there is a wide variety of wild species, both ruminant and non-ruminant that are susceptible. It is a chronic granulomatous enteritis with episodes of diarrhea and progressive weight loss. Due to the similarity between both diseases, Crohn's disease has been related to PTB, although the studies published so far have not definitively either attribute or discard Map as an etiological agent of this human disease.

Map is an obligate intracellular bacterium whose target cell is the macrophage located in the subepithelial zone of the intestine. The infection occurs orally, generally when the animals are very young, by contamination of feed with feces that carry the bacteria or directly vehiculated by milk. Its main route of entry is the Peyer's patches of the ileum, where M cells aid Map to cross the epithelium and reach the subepithelial area of the lamina propria. Once there, the bacteria are phagocytosed by macrophages that far from destroying them, end up serving as a shelter for Map. Within the macrophage phagosome, Map prevents the maturation of the phagolysosome by preventing the acidification of the phagosome and its destruction.

PTB disease progresses very slowly, and infected animals can remain in a silent and subclinical infection state for long periods of time. It is very difficult to diagnose animals that suffer from silent or subclinical forms of the disease due to the absence of symptoms, the difficulty to detect bacteria in the feces and detect specific antibodies in plasma, which add to the insufficient sensitivity of the available diagnostic tests. Furthermore, since

there is no effective pharmacological treatment against PTB, the only effective method is applying hygienic management measures and the test and cull strategy together with vaccination. However, although vaccination is allowed in small ruminants, its use in cattle is prohibited due to the interference caused by the immune responses derived from the vaccine with the intradermal reaction (IDR) diagnostic test, used in official programs of eradication of bovine tuberculosis (bTB). Furthermore, vaccination also interferes in the diagnosis of PTB itself, as there is no test that allows differentiating infection from vaccination (DIVA), not to mention the fact that none of the commercial vaccines has proven to be completely effective in terms of protection against Map.

In this regard, the development of new vaccines is necessary, which must encompass not only the investigation of variations in the composition of vaccines, but also the different routes of administration, since the immune response varies depending on where the antigen presentation occurs. Another phenomenon that deserves special attention involves cross-protection of vaccines against related or unrelated pathogens. In this sense, the commercial Silirum® vaccine against PTB has been shown to increase the productive life of vaccinated herds and reduce the incidence of other common diseases.

In order to design new vaccines with known and controlled effects, it is necessary to carefully explore their effects on the different levels of the immune response. Traditionally, the priority has been on research into the knowledge of macrophages, which are the target cell of Map. However, neutrophils (PMNs) have generated little interest, even though they are the

first white blood cells to reach the site of contact with external pathogens or physical or chemical injury. PMNs are the most numerous leukocytes, and upon the interaction with pathogens they exert their microbicidal functions of phagocytosis, reactive oxygen species production, degranulation of the content of their granules to the extracellular environment and the release of extracellular traps (ETs). ETs are composed of DNA, histones, and other proteins with microbicidal activities. During the early stages of infection with Map in the intestine, PMNs reach the infection site attracted by the alarm signals released by resident cells. However, over time, their presence in PTB lesions is very rare. In fact, some transcriptomic studies in animals suffering from PTB show that in these animals there is a decrease in the expression of various molecules involved in the recruitment and migration of neutrophils.

In this thesis work, different vaccine prototypes are presented that have been applied by different routes of administration to avoid interference with the diagnosis test for bTB, and their effects on protection against infection have been studied. In order to verify that the vaccine prototypes avoid such interference, the guinea pig model, widely used in testing the potency of antigens such as tuberculin, was used to perform the IDR due to its demonstrated delayed-type hypersensitivity response (DTH). The effectiveness against infection has been tested in the rabbit model, comparing the intradermal (VID) and oral (VOR) routes firstly, and then testing different oral prototypes in a second approach, compared with a subcutaneously applied commercial vaccine.

The intradermal route showed satisfactory results in terms of protection, being the animals of the VID group the ones that showed a lower number of visible lesions and also the lowest proportion of positive tissues to Map by PCR. The immunohistochemical analysis revealed that macrophages responded with different polarization states depending on vaccination strategies. The VID group presented predominantly polarized M1 macrophages, characterized by greater expression of IFN-γ and TNF, and lower expression of CD163 (M2 marker). In general, all vaccinated groups showed less active granulomatous lesions, associated with lower levels of calprotectin, compared to the unvaccinated challenged group. The VID group showed a certain degree of reactivity in the skin test, while the same oral vaccine was completely negative. These data showed that vaccination against PTB and its delivery route: 1) have an effect on macrophage polarization, 2) influence the outcome of infection and 3) condition the results of the IDR test for the diagnosis of bTB.

After having shown that the problem of interference can be potentially avoided by changing the administration of the vaccine to the oral route, the next objective was to improve the immune response provided by the initial prototype of oral vaccine, which was not very efficient in terms of protection. For this, a set of mycobacterial and non-mycobacterial vaccines were formulated and tested in the rabbit model. Vaccines based on inactivated bacteria were formulated with an adjuvant, QuilA, while the prototype based on live attenuated bacteria was applied without adjuvant. In addition, immune responses related to training on neutrophils, acquired responses on peripheral

blood mononuclear cells (PBMCs) and humoral responses were studied. In addition, the homologous and heterologous *in vivo* protection of the different vaccine types against Map was also examined using tissue culture techniques. Oral vaccination with live or inactivated vaccines was able to activate mucosal immunity characterized by elevated serum IgA and *IL4* expression in peripheral blood mononuclear cells (PBMC). Furthermore, PMN phagocytosis against Map was enhanced by vaccination and the release of extracellular traps against Map and unrelated pathogens was modified by both vaccination and Map challenge. Finally, PBMCs from vaccinated animals stimulated *ex vivo* with Map antigens showed a cytokine profile of rapid activation of the innate immune system. In conclusion, our data show that oral vaccination with inactivated vaccines can stimulate the protective activity of PMNs and both innate and adaptive immune responses.

Regarding the humoral response, both studies suggest that antibodies derived from vaccination have a protective role against Map infection. When the transitory increase in the observed phagocytic activity of PMNs disappears, the antibodies at the systemic level managed to compensate the lack of neutrophil training opsonizing the bacteria so that phagocytes rapidly detect and destroy them.

Once it was established that adequately trained PMNs have the ability to direct the development of infection and that vaccines can also polarize the response of macrophages in the rabbit model, the next question to be clarified was whether the interaction between PMNs and macrophages during a mycobacterial infection is positive or not. For this purpose, and using bovine

blood, macrophages and PMNs isolated from the same animal were grown together or separately in the presence of Map or BCG. The release of extracellular traps, the death of mycobacteria, and the release of IL-1β and IL-8 were evaluated. PMNs released extracellular traps against mycobacteria when cultured alone but were inhibited in the presence of macrophages when co-cultured in direct contact. Macrophages were extremely efficient in killing the BCG strain, but ineffective against Map. In contrast, PMNs showed similar killing rates for both mycobacteria. Co-cultures infected with Map showed the expected lethal effect of the combination of both cell types, while co-cultures infected with BCG showed a potentiated lethal effect beyond that expected, indicating a beneficial synergistic cooperation of both cell types. In both cases, the levels of IL-1β and IL-8 were lower in the co-cultures, suggesting a reduced inflammatory reaction compared to that detected in macrophages alone. These data indicate that the cooperation of both cell types may be beneficial in terms of reducing the inflammatory reaction.

The results of this thesis work suggest that PMNs are effective in destroying Map and may exert protective mechanisms against Map that appear to fail during PTB disease after macrophage arrival at the site of infection. Therefore, the use of effective vaccines that are able to enhance the activity of PMNs could help to increase the chances of success in terms of protection against Map infection. In this regard, this thesis work also presents some promising oral vaccine prototypes, which have also shown the ability to overcome interference problems with the bTB diagnostic test.

Introduction

Paratuberculosis (PTB) disease

History and etiology of PTB

Paratuberculosis (PTB), also known as Johne's disease, is a chronic granulomatous enteritis that primarily affects domestic and wild ruminants (deer, bighorn sheep, moose, mouflon, antelope, bison, buffaloes) (O'Brien *et al.*, 2020). However, it has also been described in other non-ruminant mammals (rabbit, mouse, rat, stoat, badger, ferret, fox, racoon, wild boar, *et cetera*) and various species of birds, among others (Fox *et al.*, 2020).

The first document describing PTB disease is dated from 1895 by Heinrich Albert Johne and Langdon Frothingham (Jöhne and Frothingham, 1895), although there is enough evidence to assume that earlier reports referred to the same disease in 1826 (D'Arboval, 1826). It was described as an infectious enteritis of slow progression affecting bovines of all ages (primarily between 3-6 years), rarely diagnosed in animals younger than a year and frequently associated to pregnant cows, in which symptoms aggravate after birth. Chronic diarrhea, sometimes intermittent, led to progressive emaciation and ultimately to death. A broad list of similar cases from many countries around the globe sprang during the following years evidencing the wide distribution of the disease (Twort and Ingram, 1912).

As well as other bacteria belonging to the *Mycobacterium* genus, *Mycobacterium avium* subspecies *paratuberculosis* (Map), the etiological agent of the disease, is covered by a complex wall, composed of peptidoglycan and arabinogalactan, which confers resistance to adverse

environmental conditions such as heat or desiccation (Collins, 2010) and a variety of commonly utilized disinfectants (Twort and Ingram, 1912), such as sodium hypochlorite or ethanol. Mycobacteria are considered Gram positive in spite of their wide and resistant cell wall that makes them impervious to Gram staining, resulting in a variable degree of staining or no staining at all (Alderwick *et al.*, 2015). They are considered acid-fast-bacilli (AFB), acquiring a characteristic pinkish red color when using the Ziehl-Nielsen staining.

Map was first isolated in 1912 by Twort and Ingram (Twort and Ingram, 1912), who cultured the bacteria in a growth medium formulated with a supplement based on killed mycobacteria, with special success using timothy-grass bacilli or *Mycobacterium phlei.* He concluded that the culture media needed a component present in other mycobacteria that was lacking in Map. This component is now known as mycobactin J, a lipidic siderophore present in the cell wall of mycobacteria, but absent in Map. Although Map has been described to grow in 7H11 without it (Aduriz *et al.*, 1995), mycobactin J improves Map growth in 7H11 and is needed as a supplement in most culture media for Map's growth *in vitro* (Whittington *et al.*, 2011). The way Map achieves iron uptake *in vivo* has not yet been elucidated, however, it has been proposed that it could take advantage of the conditions found inside macrophage vacuoles, where the range of pH (4.5-6.5) allows iron dissociation from lactoferrin becoming available for its use (Lambrecht and Collins, 1993). Alternatively, it has been proposed that the Map genome contains genes encoding for an alternative iron-uptake system (Wang *et al.*, 2016).

Map is a slow growing coco-bacilli that tends to stick together forming clumps in suspension. In solid cultures, colonies appear of a white-cream color and wrinkled with irregular margins usually adopting the characteristic fried egg shape. As they age, colonies tend to darken and take the appearance of a rose. They need a minimum of three weeks to start forming colonies, but it could take between four to six months before ensuring a negative result (Whittington, 2020).

Symptomatology and stages of PTB

Historically the PTB has been classified in four stages (Tiwari *et al.*, 2006; Imada *et al.*, 2020): Silent, subclinical, clinical and advanced clinical.

Animals at the *silent* stage of the disease are infected but do not shed the bacteria nor express any symptoms and antibodies indicative of a humoral response cannot be detected through the conventional serological enzyme-linked immunosorbent assay (ELISA) test. The only way of diagnosing this stage is through histological techniques and microscopic observation of AFB, culture in specific growth media or directed molecular methods such as the polymerase chain reaction (PCR) (Whittington *et al.*, 2017).

The *subclinical* form of the disease is characterized by the lack of evident symptoms, in which animals shed a low and discontinuous bacterium load in feces. The serological detection of antibodies is possible at this stage, although at low levels and there is a high number of false negative results.

In contrast, the *clinical* stage consists of a progressive enteritis characterized by intermittent to chronic diarrhea that progressively emaciates

animals despite showing normal or increased appetite. Serological tests and fecal PCRs or cultures are most useful in this stage (Tiwari *et al.*, 2006). Most animals do not reach the next PTB stage due to the application of the test and cull strategy used to control the disease or to the lack of health condition and production losses. The *advanced clinical* stage is characterized by weak cachectic animals, showing physical wasting and profuse diarrhea. Sometimes they may present submandibular oedema due to the hypoproteinemia derived from enteric protein loss (Tiwari *et al.*, 2006).

Pathological lesions

Intestinal macroscopic lesions are most evident in the ileum, jejunum and the ileocecal valve, but they could appear throughout the intestinal tube (Corpa *et al.*, 2000; Storset *et al.*, 2001). They are not exclusive of PTB, consisting of enlarged pale mesenteric nodes, thickening of the affected intestinal tissue, and lymphangiectasia and lymphedema of the mesenteric ducts. The mesentery acquires a white oedematose aspect, derived from the infiltration of immune cells, due to the inflammatory process (Clarke and Little, 1996; Whittington *et al.*, 2017). Serosal and mesenteric vessels are visible due to the increase in their thickness. The enteric mucosa, also thickened, presents transverse folds and ulcerations (Lybeck *et al.*, 2020).

There are several classifications that englobe the histopathological microscopic lesions of PTB. Most of them are based on the observed microscopic changes of lesion appearance and the cell type composition as the disease advances parallel to the evolution in the severity of the clinical symptoms. González *et al* (González *et al.*, 2005), classified PTB lesions into

three categories and the third category into 3 sub-categories that are not necessarily sequential. Nevertheless, it is highly likely that a progression exists in the cases where the disease advances from silent or subclinical to clinical stages, as demonstrated in a study analyzing consecutive biopsies of 77 sheep (Dennis *et al.*, 2011) and evidence found in other studies (Pérez *et al.*, 1997; Vázquez *et al.*, 2013). This classification takes into account the following parameters: the presence and shape of granulomatous lesions, their abundance and distribution, the presence and abundancy of AFB and the composition of leucocyte infiltrates.

Focal lesions consist of mild small scattered and well demarcated granulomas composed primarily by macrophages and few Langhans giant cells, although lymphocytes could also be present and scarce AFB. It is restricted to lymphoid tissues mostly from ileal and jejunal mesenteric lymph nodes and sometimes can also be observed in the distal ileal Peyer's patches (González *et al.*, 2005).

Multifocal lesions consist of multiple well demarcated focal lesions, with identical composition as focal lesions, but with differences in their abundance and distribution. Multifocal lesions are not restricted to the lymphoid tissues, but they are also distributed through the lamina propria of the intestine, with granulomas in some of the villi, adjacent to not affected villi and scarce AFB. Multifocal lesions are more abundant in the ileum and the ileocecal valve, whereas the jejunum is less affected (González *et al.*, 2005).

Diffuse lesions are found in animals with more severe enteritis. These lesions are composed by multiple and not so well delimited granulomas distributed through the mucosa and submucosa of the intestine and the lymphoid tissue of the jejunum, ileum and ileocecal valve. Diffuse lesions are infiltrated with numerous inflammatory cells that provoke the thickening of the wall and a variable number of AFB. Depending on the number of AFB and the leucocyte composition of the infiltrates they are subdivided into three categories: 1) *diffuse multibacillary or hystiocytic lesions* are characterized by the abundance of Map bacteria and infiltrates composed of macrophages and giant Langhans cells, 2) *diffuse lymphocitic or paubacillary lesions* present a majority of lymphoid infiltrates and very few AFB. Finally, an intermediate category is defined, 3) *diffuse intermediate lesions*, that share characteristics with both the multibacillary and the paubacillary diffuse forms (González *et al.*, 2005).

Apart from the intestinal tissue and associated lymph nodes, animals with advanced intestinal lesions also contain Map in peripheral lymph nodes, liver and skeletal muscle due to systemic infection (Bower *et al.*, 2011; Smith *et al.*, 2014). It is thought that Map uses the blood stream to spread to other tissues since it has been isolated from blood of infected cattle and sheep (Koenig *et al.*, 1993; Bower *et al.*, 2010).

Considering the traditional immunopathological classification together with epidemiological aspects and diagnostic results, three stages of the disease have been proposed (Vázquez *et al.*, 2014): apparently free of PTB, latent and patent. This classification suggests similarities with the

epidemiology of tuberculosis in humans. Animals are classified as *apparently free* of PTB, when they cannot be diagnosed and do not show microscopic lesions. The *latent* stage is characterized by the presence of mild PTB lesions, and no symptomatology. In contrast, the *patent* stage, is an active form of the disease characterized by animals showing a variable degree of symptoms and presenting advanced multifocal and diffuse lesions. Opposed to the latent stage, the patent stage is shown to be more frequent in animals younger than a year and is decreasingly frequent as animals age.

Diagnosis

The diagnosis of the clinical forms of PTB *in vivo* is based on the clinical-epidemiological diagnosis followed by laboratorial confirmation consisting of microbiological and serological tests. The most employed stategies are serum or milk antibody ELISA to detect humoral responses against Map, PCR for the detection of Map-specific genes or Map isolation from fecal or milk samples using specific growth media. The *post mortem* diagnosis of the disease is based on the detection of compatible gross and microscopic lesions together with the observation of AFB using the Ziehl-Neelsen staining, combined with Map isolation from tissues using a selective culture medium or a PCR for the detection of Map-specific genes.

Traditional Map culture techniques (Twort and Ingram, 1912) (Merkal *et al.*, 1982a) usually require a decontamination step to eliminate ubiquitous bacteria and at some stage, the incorporation of antimicrobial compounds to avoid undesirable microorganism growth. Once colonies have grown, recognition of typical Map colonies in a solid medium is needed

followed by phenotypic and/or genotypic identification of Map (Whittington, 2020). Map isolation is still considered the gold standard method for PTB diagnosis. However, due to the slow growing of Map, and the requirements for its isolation this method results highly time consuming and it could take weeks or months to have the results ready. Efforts have been made to overcome this issue, as an example, the recently developed culture medium, TiKa (Bull *et al.*, 2017) incorporates a preliminary step for Map resuscitation and growth stimulation that greatly accelerates Map growth.

Molecular methods based on the detection of Map specific genes, such as the multicopy *IS900* by PCR or real time PCR (qPCR) have proven high specificity and sensitivity rates, reaching 94% and 93% in milk samples, respectively (Butot *et al.*, 2019) in contrast to culture methods (specificity: 83% and sensitivity: 89%). However, when analyzing tissue or fecal samples such sensitivity decreases due to the presence in the samples of a variety of polymerase inhibitors (Schrader *et al.*, 2012) or the low bacterial load (Park *et al.*, 2014). Additionally, there have been described a number of sequences that show high homology to *IS900* (Cousins *et al.*, 1999; Taddei *et al.*, 2008) that compromise its specificity. It is worth mentioning other specific genes that have been evaluated in order to increase specificity (such as *ISMap02*, *ISMapv2*, *f57*, *MAP2765c*, *MAP0865*), although at the expense of losing sensitivity due to the lower number of copies of these genes in Map genome in comparison to *IS900* (Plain *et al.*, 2020). There are several strategies that have demonstrated being useful for overcoming some of the drawbacks of PCR and qPCR related to enzymatic inhibitions or low sample sequences that include: 1) combining molecular and culture techniques (Secott *et al.*, 1999;

Paolicchi *et al.*, 2003); 2) employing simultaneous detection of two targets by PCR (Stabel and Bannantine, 2005; Sevilla *et al.*, 2014) and 3) improving sample processing through bacteria concentration or DNA extraction techniques (Park *et al.*, 2014; Mita *et al.*, 2016; Schwalm *et al.*, 2018). Near future promising methods will include using the currently available digital PCR (dPCR) (Ricchi *et al.*, 2017).

There are various immunological methods that detect host's specific responses derived from previous encounters with Map. The methods that measure the cellular immune response include the IFN-γ release assay (IGRA), which measures cell specific responses when stimulating whole blood with Map antigens (ej. PPD J) (Corneli *et al.*, 2021) and the intradermal reaction skin test (IDR) that measures cell-mediated immunity responses to Map antigens *in vivo* (Kalis et al., 2003). The test that measures the humoral response of the host against Map antigens that is most widely used is the ELISA. Serum antibody increases have traditionally been linked to PTB clinical stages (Clarke, 1997; Pérez et al., 1997; Storset et al., 2001). The antibody ELISA test is commonly used for detecting Map- specific antibodies in serum or milk, due to its low cost and rapid results. Map ELISA test's sensitivity is low (5-30%), although it increases with the age of the animal, whereas the specificity is high (95%)(Nielsen and Toft, 2006). Considerations regarding the interpretation of ELISA tests results before taking any action on the animals are: 1) the humoral response is a late infection indicator (Matthews et al., 2021); 2) not all the animals with high antibody titers are shedding the bacteria, they could be Map-infected but not Map-infectious,

thus they may not represent a risk at the sampling moment (Li et al., 2017); 3) antibody fluctuations during lactation occur, for instance antibody titters are higher in the milk at the beginning of the lactation period, and higher in the serum at the end (Nielsen et al., 2002). ELISAs are good indicators of Map prevalence within the herd and for disease surveillance (Nielsen, 2020). For this application it is highly recommended to carry out periodic tests instead of one test in the herd to monitor the evolution of individual antibody rises and falls and control the general herd prevalence (Nielsen et al., 2013). This facilitates decisions on those animals that have been tested positive more than once to the ELISA test or present increasing levels of antibodies (Toft *et al.*, 2005; Meyer *et al.*, 2018).

In general, the abundance of false negatives in all the existing diagnostic methods, makes applying combinations of different techniques necessary in order to improve the *in vivo* detection of infected animals. Even so, the detection of infected animals is underestimated due to the subclinical and silent forms of the disease. It has been proposed that for each PTB diagnosed animal in the herd, there may be 15-25 infected animals that cannot be detected. The detection of these animals is difficult due to absent or weak host responses and the intermittent and low shedding in feces. This phenomena is known as "the iceberg effect" (Bennett *et al.*, 2010).

Treatment

Although various pharmacological agents can reduce clinical symptoms, there is currently no effective treatment for paratuberculosis (St-Jean and Jernigan, 1991; Aduriz *et al.*, 2000). The main drugs with

bactericidal or bacteriostatic action could be used in combination (St-Jean, 1996). The most effective are isoniazid, rifampicin, clofazimine, aminoglycoside antibiotics (streptomycin, kanamycin, gentamicin and amikacin) and dapsone (DDS)(Fecteau and Whitlock, 2011). The most recent antimycobacterial evaluation comes from Pavić et al, who tested *in vitro* the effect of primaquine hybrids against various tuberculous bacteria and found than some compounds were better against Map than ciprofloxacin (Pavić *et al.*, 2018).

In any event, currently antimicrobial therapy is not considered a viable option for the treatment of Map infection because it is an expensive procedure, drugs must be administered over a long period of time, and when treatment is stopped, the disease recurs (Stabel, 1998). Treated animals can still be a source of contagion due to the lack of a totally effective drug (St-Jean and Jernigan, 1991; Aduriz *et al.*, 2000), not to mention the food safety risks derived for its application in animals destined for human consumption, and the risk associated with the development of antimicrobial resistance. As a consequence, the use of antimicrobials has only been justified in animals of high reproductive genetic or productive value (Harris and Barletta, 2001; Fecteau and Whitlock, 2011). In general, veterinarians and farmers rely on PTB infection control programmes, detailed later in the prophylaxis section.

Pathogenesis

Mucosal immunity of the gut

In order to understand Map pathogenesis, knowledge on mucosal immunity of healthy gut-associated lymphoid tissue (GALT) is important. It is explained and summarized throughout Figures 1-6.

Resident immune cells of the subepithelial dome (SED), such as dendritic cells (DC), macrophages, memory and naïve T and B lymphocytes, protect the epithelium from pathogens (Reboldi and Cyster, 2016). A key function of the Peyer's patches is the sampling of antigens (Figure 1), mainly bacteria and food antigens. M cells, specialized phagocytic epithelial cells, facilitate the capture of antigens and their transport from the lumen to the SED in a process named transcytosis (Jung *et al.*, 2010). DCs are also able to directly take antigens directly from the lumen (Coombes and Powrie, 2008). There are other means of antigen transport such as integrin mediated or phagocytosis of opsonized particles by epithelial cells. Antigens can be presented through the Major Histocompatibility Complex class II (MHC II) to lymphocytes of the SED, lymphocytes of the B cell follicles or the adjacent T cell areas or they also can carry them to the mesenteric lymph nodes and present them there to naïve lymphocytes (Jung *et al.*, 2010). Upon activation, lymphocytes expressing homing receptors are released to the blood, which will direct them to the effector place from the circulatory torrent (Kantele *et al.*, 1997).

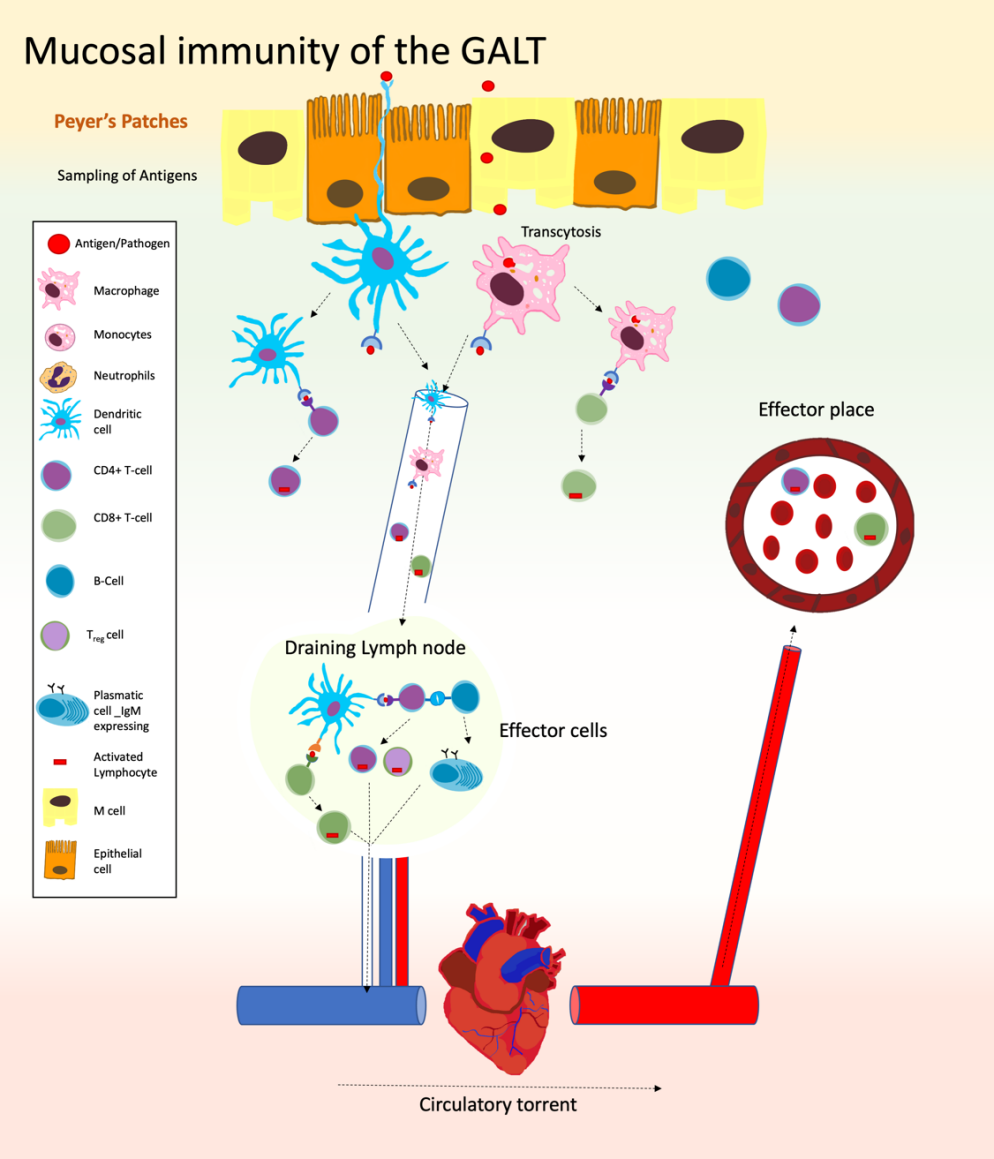

Figure 1. Sampling of antigens in the Peyer's Patches in presence of pathogens.

In the absence of pathogens DC release IL-10 in order to avoid unnecessary inflammation (Schülke, 2018) (Figure 2).

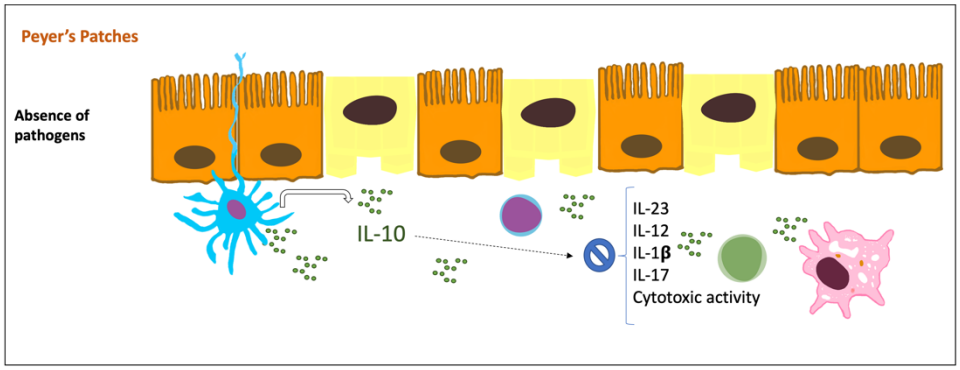

Figure 2. Sampling of antigens in the Peyer's Patches in absence of pathogens.

Upon the encounter of DCs with specific CD4+ lymphocytes, these are differentiated to regulatory T cells (Tregs), which in order to exert their function of tolerance, release suppressive cytokines in the lamina propria, with the correspondent anti-inflammatory effect (Luckheeram *et al.*, 2012; Janssen and Arkitek, 2013) (Figure 3).

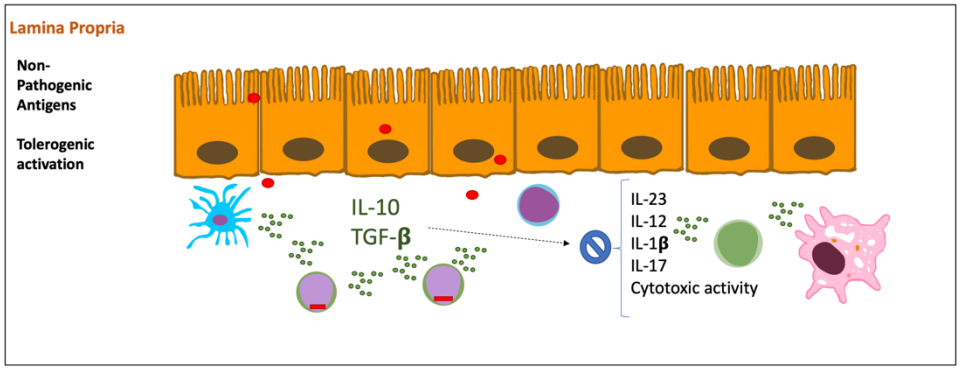

Figure 3.Tolerogenic activation in the presence of innocuous antigens.

Pathogen triggered epithelial barrier disruption initiates inflammation. The epithelium in contact with bacteria is activated, increasing the permeability of the barrier and the release of alarm molecules. This activates

immune cells and shuts IL-10 secretion to enable the immune response to start (Janssen and Arkitek, 2013; Lechuga and Ivanov, 2017). DCs and macrophages are also activated by the environment and start releasing key inflammatory cytokines. Resident cytotoxic lymphocytes are also activated and exert their effector functions, destroying the infected cells expressing the Major Histocompatibility Complex class I (MHC I) receptor on the surface (Cebra *et al.*, 1998) (Figure 4).

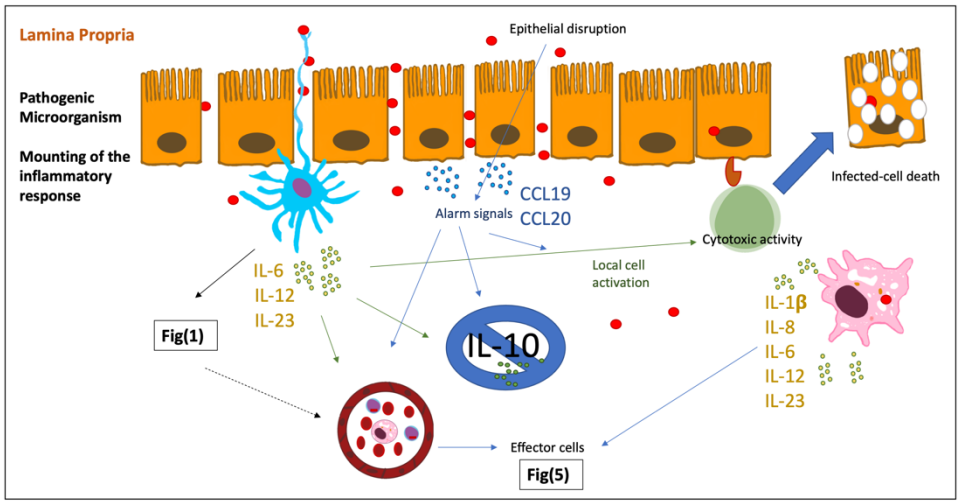

Figure 4. Inflammatory response upon pathogen invasion: part I.

Effector T cells also appear attracted to alarm signals and together with macrophages release effector cytokines for the recruitment of more phagocytic cells and the efficient destruction of pathogens (Janeway *et al.*, 2001). Neutrophils, also known as polymorphonuclear neutrophils (PMNs), are attracted to the site of infection by all the alarm signals and chemotactic cytokines such as IL-8 and they start to exert their microbicidal functions including phagocytosis, extracellular trap (ET) release, degranulation and the

production of reactive oxygen species (ROS). PMNs are not part of the resident cell subset due to their self-damaging nature, but they are required upon invasion because their potent antimicrobial activity is essential (Janssen and Arkitek, 2013; De Oliveira *et al.*, 2016) (Figure 5).

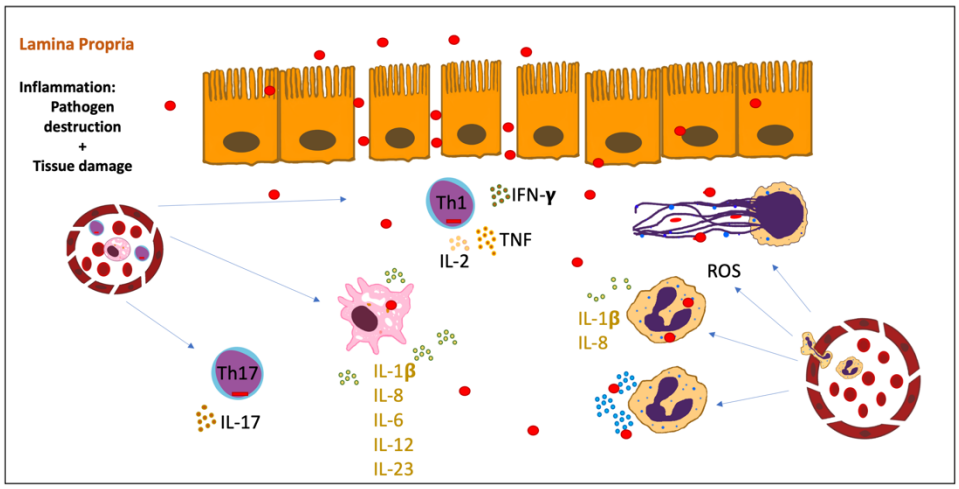

Figure 5. Inflammatory response upon pathogen invasion: part II.

After pathogen elimination, PMNs die by apoptosis and macrophages contribute to the resolution of the inflammation by clearing neutrophil apoptotic debris, toxic and self-damaging molecules and also by producing anti-inflammatory mediators such as IL-10 and transforming growth factor β (TGF-β) (Watanabe *et al.*, 2019). The epithelial wall is restored by replacing the damaged cells with new ones from the intestinal crypts (Andersson-Rolf *et al.*, 2017) (Figure 6).

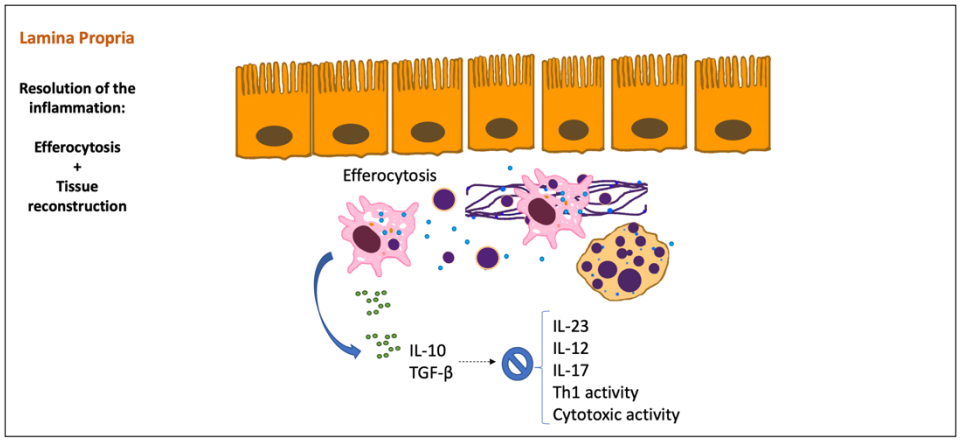

Figure 6. Resolution of inflammation.

Map invasion

Despite the fact that neonatal and young animals are more susceptible to Map due to the immaturity of their immune system, adult individuals can also contract the disease. The transmission takes place through the oral route when animals feed on contaminated fodder with feces of infected shedder animals or milk from clinically infected dams (Smith *et al.*, 2015). Bacteria are activated by the acid of the stomach and reach the small intestine where the colonization starts. In the ileum and jejunum epithelia, Map is endocytosed preferably by M cells of the Peyer's patches, although its entrance through enterocytes and goblet cells has also been described (Sigurdardóttir *et al.*, 2005; Golan *et al.*, 2009). M cells internalize the bacteria by the union of their β1 integrin receptors to fibronectin (FN), constituted by Map's fibronectin attachment protein (FAP-P) and the host's FN (Secott *et al.*, 2001, 2002, 2004). However, Map entrance through villous epithelial cells does not seem to be FN dependent (Secott *et al.*, 2004). In any

case, the translocation of Map causes the disruption of the epithelial barrier, which increases its permeabilization (Khare *et al.*, 2012, 2016) and facilitates the colonization. Consequently, the intestinal mucosa layer is activated by the secretion of the proinflammatory chemokine MIP-2 together with an increased expression of intracellular adhesion molecule 1 (ICAM-1). This event is accompanied by an early inflammatory response that attracts macrophages, PMNs and goblet cells, as a consequence of the increase in the expression of chemo attractants (CXC, IL-8, MCP-1, MCP-2) and pro-inflammatory cytokines such as IL-1β, tumor necrosis factor (TNF), IL-6, and IL-15, which can reach the maximum peak at 4h post infection, as described by *Khare et al* (Khare *et al.*, 2009) based on an ileal loop challenge. However, this response was transient and was reduced as early as 12h post infection. The initial activity of the host against Map invasion at the mucosal level also includes the secretion of mucus to the surface of the mucosa described as fibrin or mucin layer, with the goal to impede more Map entrance (Khare *et al.*, 2009). Once Map is transported across the epithelial barrier to the lamina propria it is phagocytosed by macrophages (Arsenault *et al.*, 2014). Antigen-presenting cells (APCs) can process and present the antigens *in situ* or rapidly transport the bacterium to the lymph nodes, where Map has been detected as soon as 1h after infection (Wu *et al.*, 2007), before disseminating to other tissues.

Several macrophage membrane receptors mediate the phagocytosis of mycobacteria. These include: 1) mannose receptor (MR) that binds mannosylated molecules such as the glycolipid mannosylated

lipoarabinomannan (ManLAM) present in the surface of mycobacteria, 2) complement receptor (CR3), 3) scavenger receptors and 4) Fc receptors for IgG-opsonized pathogens (Pieters, 2001). Recognition of mycobacteria may also involve toll-like receptors (TLRs), and CD14 as co-receptor of TLR4 (Souza *et al.*, 2008).

Once the bacterium is phagocytosed by the macrophage it avoids the host defense by several mechanisms; firstly, abrogating phagosomal maturation and ensuring its survival; and then, avoiding its destruction and the subsequence antigen presentation through MHC II molecules, permitting its replication and dissemination (Kuehnel *et al.*, 2001). The exact mechanism or mechanisms by which Map avoids phagolysosome fusion are not yet known, but studies on *Mycobacterium tuberculosis* (Mtb) indicate that ManLAM is indispensable to inhibit phagosome-lysosome fusion (Yates and Russell, 2005). Related with the abolition of phagolysosome maturation, Map avoids the apoptosis of the infected macrophage, impeding the development of another mechanism of antigen presentation, based on efferocytosis (Kabara and Coussens, 2012). Another important mechanism used by Map for immune evasion is the MAPK p38 signal transduction pathway, that functions in the control of apoptosis, the release of cytokines and neutrophil chemotaxis (Heuertz *et al.*, 1999; Cuenda and Rousseau, 2007), that is activated by Map through TLR2 and TLR4 signaling. Blocking the MAPK p38 pathway abolishes Map-induced IL-10 induction, IL-12p40 decrease and blocks phagosome acidification, enhancing the ability of macrophages to destroy Map (Souza *et al.*, 2006, 2008).

On the other hand, Map is thought to induce a state of immune tolerance in order to remain unnoticed and prevent the bactericidal activity of the innate immune system. Indeed, it has been confirmed that Map downregulates the expression of pro-inflammatory proteins (IL-12p40) and inducible nitric oxide synthase (iNOS) through the downregulation of the CD40 pathway (Sommer *et al.*, 2009; Khare *et al.*, 2012) and the downregulation of the MHC II-antigen-presentation pathway (Carvalho *et al.*, 2011; Khare *et al.*, 2016). The interaction of CD40 on macrophages and CD40L on activated T cells is crucial for the maintenance of the Th1 response and macrophage activation (Sommer *et al.*, 2009). At the same time, anti-inflammatory genes, such as IL-10 and TGF-β are upregulated (Khare *et al.*, 2009; Bannantine and Bermúdez, 2013). Map-induced IL-10 upregulation during infection has been suggested to block host innate immune responses, resulting beneficial for Map survival (Weiss *et al.*, 2005). In fact, Map-inoculated tissue has shown, in the initial stages, a biased lymphocyte response towards Th2 and the repression of phagocytosis related proteins, compared to tissue inoculated with less pathogenic mycobacteria such as *Mycobacterium avium* subspecies *avium* (Maa), which showed a stronger innate response favoring Th1 and phagocytic activity (Khare *et al.*, 2016).

Macrophage infection triggers further macrophage migration to the infected regions, leading to the formation of granulomas, as a means to contain the bacteria. With the evolution of the disease, focal granuloma formation progresses into a more or less extended granulomatous enteritis. The characteristic diffuse lesions that appear in advanced PTB are thought to be a consequence of the host late response to limit Map spread and,

frequently, by the time clinical signs would appear, between 2 and 5 years after infection, the animals have already been removed for other reasons and the disease goes unnoticed (Coussens *et al.*, 2020).

Immune cells and responses against Map

Macrophages

Macrophages from PTB histological lesions acquire a different phenotype depending on the severity of the disease. In mild lesions, associated with silent and subclinical stages of the disease, macrophages have been classically associated with the M1 phenotype (Fernández *et al.*, 2017a). The M1 phenotype is triggered by microbes and inflammatory cytokines and it is characterized by the expression of proteins such as iNOS or TNF in their membrane (Benoit *et al.*, 2008). However, in diffuse lesions, more associated to clinical stages of the disease, macrophages acquire the M2 phenotype (Fernández *et al.*, 2017a), triggered by IL-4, IL-10 cytokines and glucocorticoids, and characterized by the expression of protein markers such as CD163, IL-10, or TGF-β in their membrane. However, recent studies link the subclinical cases to an equilibrated M1/M2 ratio in contrast to control animals or clinically infected animals, showing a M1 and M2 pattern, respectively (Jenvey *et al.*, 2019). According to their activities, M1 macrophages exert inflammatory and microbicidal functions, diminished efferocytosis, increased phagocytosis and enhanced expression of pro-inflammatory cytokines, reactive oxygen species (ROS), and nitric oxide (NO), whereas M2 macrophages have differentiated immunomodulatory properties, lower ROS and NO and pro-inflammatory cytokine production,

states associated with enhanced efferocytosis of apoptotic cells (Benoit *et al.*, 2008; Korns *et al.*, 2011). The bactericidal protection exerted by M1 phenotype has been reported to be substantiated in the production of IL-12 and IFN-γ (Casanova, 1999). Indeed, the M2 phenotype is associated with the chronicity of diseases and M1 restoration has been demonstrated to be beneficial in terms of bacterial clearance (Benoit *et al.*, 2008). Nevertheless, prolonged M1 phenotypes, associated with sepsis (Bozza *et al.*, 2007), are related to be detrimental for the host and have fatal consequences (O'Reilly *et al.*, 1999).

Polymorphonuclear neutrophils (PMNs)

Abundant research has been carried out studying the action of macrophages on PTB. However, not much attention has been paid to PMNs. Although their presence in the early phases of the infection is well documented in PTB (Sigurdardóttir *et al.*, 1999; Khare *et al.*, 2009), their involvement in tissues from cows with clinical PTB is not frequent (Coussens, 2004) and this is probably the reason why this immune cell type has not been deeply analysed in the context of PTB.

Dotta and collaborators (Dotta *et al.*, 1999) tested PMNs isolated from cows with subclinical PTB in an *in vitro* model for their migratory properties. PMNs from infected cattle showed poorer migratory traits, when activated with zymosan, than those from healthy animals suggesting that PMN activity may be impaired upon Map infection. Indeed, several recent transcriptomic studies have put in evidence the existence of some kind of PMN dampening during PTB manifested by downregulated pathways related to neutrophil

recruitment (Park *et al.*, 2018; Alonso-Hearn *et al.*, 2019) and the decreased expression of antimicrobial peptides in PMNs, including β-defensins (David *et al.*, 2014) and cathelicidins (Alonso-Hearn *et al.*, 2019).

As an illustrative example of the relevance of PMNs against mycobacterial diseases, they have been shown to play a protective role against Mtb (Kroon *et al.*, 2018; Hilda *et al.*, 2020) and *M. marinum* (Wright *et al.*, 2021). Furthermore, vaccination against Mtb, based on the *Mycobacterium bovis* (Mbv), Bacillus Calmette Guerin strain (BCG), has been shown to induce protection dependent on PMNs (Bickett *et al.*, 2020), demonstrating that they can endure functional reprogramming (Moorlag *et al.*, 2020). Indeed, BCG vaccination has been demonstrated to improve PMN functionality, inducing innate training, through reinforcement of specific Th1 and Th17 responses resulting in a reduction of the bacterial burden (Trentini *et al.*, 2016).

PMNs have long been considered as short-lived, non-specialized cells. However, recent research on these predominant immune cells, has redefined them as efficient and versatile effector cells (Tecchio and Cassatella, 2016; Warren *et al.*, 2017). PMNs kill microbes through a set of immune functions, including phagocytosis, ROS production, exocytosis of lytic enzymes with potent antimicrobial activity (Jimbo *et al.*, 2017) and the release of ETs (Brinkmann *et al.*, 2004; Cassatella *et al.*, 2009).

ET formation is now considered as an important effector mechanism of PMNs against pathogens (Brinkmann *et al.*, 2004), that has also recently been documented in macrophages in response to some pathogens (Benati *et*

al., 2010; Aulik *et al.*, 2012; Wong and Jacobs, 2013; Muñoz-Caro *et al.*, 2014). ETs consist of extracellular sticky threads of DNA, histones and microbicidal proteins (such as myeloperoxidase, elastase, lactoferrin, High Mobility Group Box 1, HMGB1; cathepsin G; proteinase 3; LL-37) that capture and destroy microorganisms (Fuchs *et al.*, 2007; Santocki and Kolaczkowska, 2020). Pathogens and other danger associated molecular patterns (DAMPs), exogenous particles, platelets, antibodies and inflammatory cytokines such as IL-8 and TNF (Skendros *et al.*, 2018; Shrestha *et al.*, 2020) are able to trigger ET release in PMNs.

Several studies have addressed the cooperation of PMNs and macrophages at the inflammation site (Silva *et al.*, 1989; Silva, 2010), where macrophages phagocytose apoptotic PMNs and restore tissue damage. This mechanism, named efferocytosis, is also known to serve as an indirect pathogen presentation mechanism and as a way for PMNs to deliver internalized pathogens to macrophages (Silva *et al.*, 1989). During efferocytosis, macrophages also acquire antimicrobial molecules lacking in mature macrophages, such as lactoferrin (Silva *et al.*, 1989; Tan *et al.*, 2008; Lutaty *et al.*, 2018). PMNs have shown to contain high quantities of lactoferrin (Momotani *et al.*, 1988a), which, together with other granular proteins, is known to be present in ETs (Santocki and Kolaczkowska, 2020). However, although macrophages of healthy ileums do not contain lactoferrin nor ferritin, some macrophages have been shown to contain ferritin in Map infected Peyer's patches. Moreover, lactoferrin is present in PTB lesions in granulomas more associated to PMNs and giant cells than to macrophages (Momotani *et al.*, 1988a). As mentioned before, the *in vivo* iron uptaking

system in Map is yet to be elucidated as well as PMNs and their interactions with macrophages in PTB.

The Classical Th1/Th2 paradigm

Classically, PTB stages have been associated to different immune responses. Silent and subclinical stages have been linked to Th1 responses, where lymphocyte CD4+ and CD8+ cellular responses are dominant and related to the control of the disease. However, advanced or clinical PTB, has been related to B cell activation, and the shift to a Th2 humoral response, associated with the progression of the disease to clinical stages (Chiodini *et al.*, 1984; Burrells *et al.*, 1998; Smeed *et al.*, 2007).

Studies on lymphocyte function describe an early T cell activation, induced by IL-1 secretion combined with antigen presentation by macrophages through the MHC II, while Map antigen presentation to CD8+ lymphocytes would be done through the MHC I. Then, following activation, T cells release IL-2, which triggers clonal expansion of specific T CD4+ and CD8+ lymphocytes (Stabel, 2000). Early immune responses are crucial for the progression of the disease. Indeed, at early stages a strong Th1 response by CD4+ and γδ T cells with high IFN-γ release are related to the successful intracellular destruction of Map by macrophages (De Silva *et al.*, 2013, 2018). Moreover, low early IFN-γ responses have been related to increased susceptibility to infection (De Silva *et al.*, 2013) and strong early IFN-γ responses have been linked to resilience (De Silva *et al.*, 2018) in sheep. However, a prompt disruption of CD4+ T cell responses seems to occur together with the downregulation of the MHC II antigen-presentation

pathway (Purdie *et al.*, 2012; Stabel *et al.*, 2020) and a disruption of γδ T and B cells, but not in CD8+ T cell responses (De Silva *et al.*, 2015) that has been associated to an upregulation of MHC I gene expression in cattle (Purdie *et al.*, 2012).

Nevertheless, the progression of the disease is linked to cell exhaustion (Okagawa *et al.*, 2015), and a switch to Th2 responses and high antibody titters. *Diffuse paubacillary lesions* in sheep have shown a Th1/Th17 response with higher IL-12, IL-17A and IFN-γ levels, while *diffuse multibacillary lesions* are described to be driven almost exclusively by Th2 responses (Nicol *et al.*, 2016) characterized by IL-4, IL-5 and IL-10 expression (Whittington *et al.*, 2012).

Regulatory T cells (Treg) and γδ T cells

T cells that express TCRγδ constitute 45-50% of the total peripheral T cells in bovines (Tizard, 2017a) and in young animals these could reach 66% (Tizard, 2017b). γδ T cells are resident sentinel cells in the ileum (among other mucosal surfaces), where infection with Map is assumed to start.

It has been proposed that the shift to Th2 could be prompted by Treg cells (CD4+, CD25+ and FoxP3+), that would limit the Th1 response through IL-10 and TGF-β production, which are indeed increased in Map infected animals (De Almeida *et al.*, 2008). However, Tregs seem to be absent in late PTB lesions (Roussey *et al.*, 2016) and γδ T cells $WC1.1^{+}$, $WC1.2^{+}$, that express CD4+, CD25+ and FoxP3+, are considered the mayor regulatory T cells in bovines (Hoek *et al.*, 2009; Guzman *et al.*, 2014; Tizard, 2017c).

Indeed, the number of $WC1^+$ γδ T cells expressing IL-10 was found to be higher in ileal tissues from clinical cattle compared to subclinical cases (Albarrak *et al.*, 2018). In addition, an increase in the number of γδ T cells, accompanied by a CD4+ decrease, has been described as the animals progress from subclinical to clinical infection in the mesenteric lymph nodes and lamina propria of Map-infected cattle (Koets *et al.*, 2002). Whether WC1+ γδ T cells impede Th1 responses during late stages of PTB by releasing anti-inflammatory cytokines like IL-10 is yet unknown (Albarrak, 2018). However, there is a recognized pro-inflammatory role of $WC1^+$γδ T cells, expressing IFN-γ and promoting a Th1 response against Map and Mbv infections (Kennedy *et al.*, 2002; Plattner *et al.*, 2009, 2013, 2014).

The $WC1^-$ γδ T cell subset has been less studied than the $WC1^+$. Map viability from infected monocytes differentiated in the presence of $WC1^-$ γδ T cells resulted significantly lower compared to that from infected MDMs in a reported Map infection *ex vivo* assay. Additionally, the presence of $WC1^-$ γδ T cells during the *in vitro* differentiation of monocyte-derived dendritic cells was associated with significantly higher expression of MHC II than in the absence of γδ T cells (Baquero and Plattner, 2017a). Moreover, $WC1^-$ γδ T cells have also been described to produce IFN-γ against Map *in vivo* and *in vitro* (Plattner *et al.*, 2013; Baquero and Plattner, 2017b).

The humoral response

The protective effect of antibodies against Map has traditionally been questioned, in part due to the link that has classically associated the humoral response with the clinical phases of the disease (Clarke, 1997; Pérez *et al.*,

1997; Storset *et al.*, 2001) and also because of the intracellular character of Map (Tessema *et al.*, 2001). The shift from cellular Th1 response to the humoral Th2 response has been related to clinical stages and loss of infection control by the host (Stabel, 2000; Coussens, 2004; Sweeney, 2011). However, there are several studies that support the protective role of antibodies. In fact, a study involving a therapeutic vaccination after natural infection of Map, associates the success of the treatment to the humoral response involving antibody production rather than to the cellular Th1 response (Santema *et al.*, 2013). Another study on PTB vaccination also demonstrates that humoral response is necessary for vaccine protection (Pooley *et al.*, 2019). In a recent review Stabel *et al* (Stabel *et al.*, 2020) suggest that another evasion mechanism by Map could be delaying the antibody production by B cells, based on studies supporting the protective role of antibodies and the need to profound into B cells and antibody function in PTB (Koets *et al.*, 2015) and human tuberculosis (hTB) (Chan *et al.*, 2014) infections.

Th17: an alternative T cell response

Apart from the classical Th1/Th2 dichotomy, recent studies involving Th17 responses intend to explain the role of Th17-related cytokines (IL-1, IL-6, TGF-β and IL-23) and specific Th17 cytokines (IL-17 and IL-22) (Coussens *et al.*, 2020). IL-17 is produced by Th17 CD4+ cells and a set of innate cells such as NK cells and γδ T cells (Onishi and Gaffen, 2010). Initial studies described an increase in the expression of IL-17A in paratuberculous cows, suggesting that as the disease progresses, this type of immune response prevails (Dudemaine *et al.*, 2014). Another study reported the upregulation in

mRNAs encoding for IL-6, IL-1, IL-23, and IL-17A cytokines of acquiring a Th17-like phenotype in PBMCs exposed to Map *ex vivo* (Roussey *et al.*, 2014). Moreover, PBMCs isolated from animals that were positive to Map with the serum ELISA test, revealed higher expression of IL-23 receptor (IL-23R) and IL-17A mRNA, compared to Map negative animals. Additionally, higher IL-17A levels in plasma have been found in Map -positive-tested cows in comparison to those that had tested negative (DeKuiper and Coussens, 2019a). In addition, subclinical PTB lesions showed higher IL-17A expression than those advanced lesions (Roussey *et al.*, 2016). IL-23, although not necessary for Th17 induction, is required *in vivo* for the stabilization and proliferation of Th17 cells (Onishi and Gaffen, 2010). It is a potent pro-inflammatory cytokine that prevents the entrance of undesirable bacteria, thus helping to maintain the homeostasis in the intestinal barrier (Fatkhullina *et al.*, 2018). Notwithstanding, some propose that IL-23 is responsible for the chronic inflammation of the intestine in PTB, though its role is yet to study (Coussens *et al.*, 2020).

Relevant mediators of the inflammatory responses

In addition to lymphocyte linked cytokines, pro-inflammatory IL-1β and IL-8 are also critical components in the formation of granulomas associated to mycobacterial infections. Although essential for pathogen resistance, IL-1β and IL-8 also can contribute to tissue damage during chronic diseases and acute injuries. IL-1β, key mediator of the inflammatory response, attracts immune cells further to the site of the infection and leads to a general activation of the immune system. In an experimental study carried

out in mice, IL-1β prevented Map infection (Kenefick *et al.*, 1994). It has been suggested, however, that IL-1β effects on macrophage attraction (Lamont *et al.*, 2012; Lemon *et al.*, 2015) could result in benefits for Map, providing the bacteria with more target cells that can contribute to its dissemination (Lamont *et al.*, 2012). Additionally, a study involving RNA-seq analysis of monocyte derived macrophages infected *in vitro* with Map found upregulation of IL-1 and IL-10 cytokines, among others (Casey *et al.*, 2015). Upregulation of IL-10 expression induced by mycobacteria has been proposed to inhibit host innate immune responses during Map infection resulting in enhanced pathogen survival (Weiss *et al.*, 2005).

IL-8 is considered to be a major ET inducer for PMNs (Gupta *et al.*, 2005), and to have an important role in leucocyte recruitment, granuloma formation, and respiratory burst in response to Mtb, leading to enhanced phagocytosis and killing of Mtb (Krupa *et al.*, 2015). PMN absence in PTB lesions could be due to a defect in IL-8 signalling. In fact, some studies report the expression of IL-8 to be impaired in Map infected animals (Khare *et al.*, 2012; Alonso-Hearn *et al.*, 2019).

Table 1. Cytokines involved in PTB and their effects.

Cytokine	Secreted by	Opposed molecule	Effects	Events in ptb	References
IFN-γ	**To a greater extent:** CD4+, CD8+, NK and γδ T cells **To a lesser extent:** B lymphocytes DCs	IL-10 IL-4 TGF-β	• Th1 polarizing cytokine • Cell activation through the JAK-STAT pathway • Suppression of the activity of Th2 lymphocytes • NK activation • MΦ activation and increase of Ag presentation • M1 phenotype polarization • Favors MHC expression in MΦs	• Map blocks the ability of MΦ to be activated by IFN-γ, increasing the negative regulators (SOCS1 y SOCS2) (inhibiting jack/stat signaling) • Higher IFN-γ release upon *in vitro* stimulation with Map correlates with PTB lesion severity • IHC: more cells labeled with IFN-γ in mild lesions compared to advanced lesions. • Map inhibits IFN-γ induced signaling in bovine monocytes • Early high IFN-γ levels related to intracellular destruction of Map by MΦs	(Li *et al.*, 2006; Darwich *et al.*, 2009; Arsenault *et al.*, 2012; De Silva *et al.*, 2013, 2018; Fernández *et al.*, 2017b; Marino *et al.*, 2017; Tizard, 2017b)
IL-12	Monocytes MΦ DCs B lymphocytes PMNs Keratinocytes	IL-10 IL-4 TGF-β	• Th1 polarizing cytokine • Stimulates the production of IFN-γ and TNF from T cells • Enhancement of the cytotoxic activity of NK cells and CD8+ cytotoxic T lymphocytes • Stimulation of the expression of IL-12 receptors: IL-12R-β1 and IL-12R-β2	• Map downregulates the expression of IL-12p40 through the downregulation of the CD40 and MHC II pathways • Blocking the MAPK p38 pathway activated by Map infection resulted in lower IL-10 expression, increased acidification of the phagosome, increased expression of IL-12 and Map killing *in vitro*	(Weiss *et al.*, 2005; Sommer *et al.*, 2009; Carvalho *et al.*, 2011; Khare *et al.*, 2012, 2016; Tizard, 2017b, 2017d)
IL-2	**To a greater extent:** CD4+ and CD8+ activated lymphocytes	IL-1 (promotion of Th17) TGF-β	• Growth factor for T and B lymphocytes • Increased responsiveness to IL-12 and IL-4 to promote Th1 and Th2 phenotypes • Inhibits the IL-6 to IL-23 to IL-21 cytokine cascade that drives Th17 cell differentiation	• Related to early Th1 responses against Map infection	(Stabel, 2000; Kryczek *et al.*, 2007; Liao *et al.*, 2013; Tizard, 2017b)

	To a lesser extent: NK lymphocytes DCs		• Regulation of Treg lymphocyte survival and function		
TNF	Sentinel cells MΦ Monocytes Mastocytes T and B lymphocytes Endothelial cells	IL-10 TGF-β	• Immune cell recruitment and migration • Induces IL-1, IL-6 and IL-8 production • Inflammatory cell activation and enhancement of MΦ and neutrophil function • Inflammatory reaction and acute phase stimulation (related to IL-1) • Induction of granuloma formation	• Early increase upon Map invasion • Related to early Th1 responses against Map infection • Increased *in vitro* expression in Map infected bovine MΦs	(Alzuherri *et al.*, 1996; Khare *et al.*, 2009; Dudemaine *et al.*, 2014; Tizard, 2017e)
IL-4	Activated: Th2 CD4+ Lymphocytes, Basophils, mastocytes and eosinophils	IL-12 IFN-γ	• Anti-inflammatory effects blocking IL-1, TNF and IL-6 synthesis. • Promotes Th2 lymphocyte differentiation and proliferation through STAT6 pathway • Apoptosis inhibitor • Antibody production IgG, IgA, IgE • Inhibition of Th17 • Inhibition of IFN-γ • Mastocyte activation	• IL-4 has not been associated to susceptibility or resistance to disease, although lower expression levels of IL-4 have been seen in PBMCs of clinically and subclinically infected animals compared to healthy controls • Higher secretion of IL-4 in PBMCs of clinically and subclinically infected animals when stimulated with Map sonicate • Diffuse multibacillary lesions are described to be driven almost only by Th2 responses characterized by IL-4, IL-5 and IL-10 expression	(Coussens *et al.*, 2004; Karcher *et al.*, 2008; Whittington *et al.*, 2012; Nicol *et al.*, 2016; Tizard, 2017b; Stabel *et al.*, 2020)
IL-1β	Activated MΦs, NK cells, monocytes, and PMNs.	IL-10 IL-6 IL-1RA CD121b	• Inflammatory reaction and acute phase stimulation (related to TNF) • Causes fever and neutrophilia • Favors PMN adhesion to the endothelium (migration) • Involved in the proliferation, differentiation and apoptosis of cells	• Early increase upon Map invasion • Early T cell activation, induced by IL-1 secretion by recently infected MΦs • Map is thought to take advantage of IL-1β secretion by attracting more MΦs	(Alzuherri et al., 1996; Stabel, 2000; Khare et al., 2009; Lamont et al., 2012; Lemon et

				• Th17-like phenotype in PBMCs exposed to Map ex vivo: increased mRNAs encoding for IL-6, IL-1, IL-23, and IL-17A	al., 2015; Tizard, 2017e)
IL-8	MΦs Endothelial cells PMNs	IL-10 IL-6	• Attracts and activates PMNs, activates ROS and degranulation • Pro-inflammatory	• Early increase upon Map invasion • Reported to be impaired in Map infected animals	(Khare *et al.*, 2009, 2012; Roussey *et al.*, 2014; Tizard, 2017e; Alonso-Hearn *et al.*, 2019)
IL-6	MΦs T lymphocytes Mastocytes DC Eosinophils Basophils Keratinocytes	IL-1 IL-2	• Mediator of the inflammatory reaction and acute phase stimulation • Mediator of tissue repair after inflammation related with the efferocytosis process driven by MΦs • Stimulates Th17 and Th2 • Suppresses Treg cells	• Early increase upon Map invasion • Th17-like phenotype in PBMCs exposed to Map *ex vivo:* increased mRNAs encoding for IL-6, IL-1, IL-23, and IL-17A	(Alzuherri *et al.*, 1996; Fielding *et al.*, 2008; Khare *et al.*, 2009; Roussey *et al.*, 2014; Tizard, 2017e)
IL-23	Activated DCs Monocytes MΦs Innate lymphoid cells γδ T cells	IL-2	• Stimulation of Th17 cells to produce IL-17 and IL-22 • Activation, recruitment and migration of inflammatory immune cells • Promotes angiogenesis • T lymphocyte and NK cytotoxic activity stimulation • T cell proliferation • IFN-γ production	• Higher levels of IL23A in the ileal mucosa of the paucibacillary form in comparison with the asymptomatic or multibacillary forms • Th17-like phenotype in PBMCs exposed to Map *ex vivo:* increased mRNAs encoding for IL-6, IL-1, IL-23, and IL-17A • It is thought that IL-23 is responsible for the chronic inflammation of the intestine in PTB, though its role is yet to study	(Gossner *et al.*, 2012; Dudemaine *et al.*, 2014; Roussey *et al.*, 2014; Tizard, 2017c; Coussens *et al.*, 2020)
IL-17	Th17 CD4+ T cells	IL-2 IFN-γ	• Generation, recruitment and activation of PMNs via G-CSF • Pro-inflammatory effect promoting innate immunity responses • Promotes angiogenesis	• Associated to diffuse paucibacillary lesions (Th1/Th17) • Th17-like phenotype in PBMCs exposed to Map *ex vivo:* increased mRNAs encoding for: IL-6, IL-1, IL-23, and IL-17A	(Dudemaine *et al.*, 2014; Roussey *et al.*, 2014, 2016; Tizard, 2017c; DeKuiper and

			• Stimulates the secretion of inflammation mediators: G-CSF, IL-6, IL-1β, IL-9, TNF, IL-8, ICAM-1 • Activation, recruitment and migration of inflammatory immune cells	• Higher IL-17A levels in plasma of Map infected cows in comparison to healthy cows • Subclinical PTB lesions showed higher IL-17A expression than those advanced lesions	Coussens, 2019a)
IL-10	**To a greater extent:** M2 MΦ DC Tregs **To a lesser extent:** Th, B and NK cells Mastocytes Epithelial cells.	TNF, IFN-γ, IL-12	• Inhibition of innate and adaptative immune responses • Decreases MHC II molecule expression • Long standing anergy towards specific antigens • Inhibition of TNF, IFN-γ, IL-12, IL-4, IL-5, CXCL8, GM-CSF and G-CSF production	• Anti-inflammatory genes, such as IL-10 are upregulated during Map infection • Map-induced IL-10 upregulation during infection has been suggested to block host innate immune responses, resulting beneficial for Map survival • Diffuse multibacillary lesions are described to be driven by Th2 responses linked to IL-4, IL-5 and IL-10 expression • IL-10 was found to be higher in ileal tissues from clinical cattle compared to subclinical cases • Blocking the MAPK p38 pathway activated by Map infection, decreased IL-10 expression, increased acidification of the phagosome, increased expression of IL-12 and Map killing *in vitro*	(Weiss *et al.*, 2005; Khare *et al.*, 2009; Whittington *et al.*, 2012; Bannantine and Bermúdez, 2013; Nicol *et al.*, 2016; Tizard, 2017c; Albarrak *et al.*, 2018)
TGF-β	Platelets Activated MΦs PMNs B and T lymphocytes	TNF IFN-γ	• Promotes M2 phenotype and prevents M1 phenotype of MΦs • Inhibits B cell proliferation and blocks B cell activation and class switching to most isotypes except for IgA. • Inhibition of Th1 and Th2 proliferation, through IL-2 blockade. •Development, maintenance, and induction of Tregs • Promotion of Th17 development and maintenance	• Anti-inflammatory genes, such as IL-10 and TGF-β are upregulated during Map infection • Mycobacteria induce MΦs to produce TGF-β and suppress their antibacterial activity to aid their pathogenesis.	(Yamane *et al.*, 2003; Li *et al.*, 2006; Khare *et al.*, 2009; Hatton, 2011; Bannantine and Bermúdez, 2013; Tizard, 2017c)

NK: natural killer, DC: dendritic cell, MΦ: macrophage, Ag: antigens, IHC: immunohistochemistry, PBMC: peripheral blood mononuclear cell, ROS: reactive oxygen species.

Prophylaxis: justification of needs and methods

Impact of PTB, control measures and implications in Public Health

PTB results in monetary losses to the livestock industry worldwide (Sweeney, 1996) that can be difficult to measure (Imada *et al.*, 2020), although efforts have been made and it has been estimated that the expenses per animal and year in dairy cattle range between 21US$-234€, depending on the country (Whittington *et al.*, 2019). Production losses are consequence of sub-clinical and clinical infections, that have an impact in milk production, weight gain, fertility, susceptibility to other diseases, and animal losses due to premature cull or deaths (Ott *et al.*, 1999; Weber, 2006; Gonda *et al.*, 2007; Richardson and More, 2009; García and Shalloo, 2015). Most of the efforts made in many countries to control PTB disease consist of implementing control programs based on the test and cull strategy, which are shown to be effective as long as they are implemented together with hygiene and biosecurity practices (Dorshorst *et al.*, 2006; Marcé *et al.*, 2010; Smith *et al.*, 2017). Furthermore, the worst drawback of the test and cull strategy is the lack of sensitivity of current diagnostic techniques, which do not detect the animals that must be slaughtered. Additionally, the lack of economic resources and the prioritization of other diseases considered more important, are among the reasons given by the governments for not implementing PTB control programs in farms (Whittington *et al.*, 2019).

On the other hand, although there is not enough evidence yet to attribute the disease to Map, this bacterium has been associated to Crohn's disease in humans (Bull *et al.*, 2003; Grant, 2005; Juste *et al.*, 2009a). The

issue is so controversial that researchers from all over the globe have composed a scientific forum, to manifest the urgency in clarifying this issue (Kuenstner *et al.*, 2017). They claim, that, in any case, its presence in commercial products for human feeding such as milk (Ayele *et al.*, 2005; Carvalho *et al.*, 2012), meat (Savi *et al.*, 2015) or infant preparations (Botsaris *et al.*, 2016) make Map a potential zoonotic threat (Ekundayo and Okoh, 2020) and have requested the international agencies to implement preventive measures in order to preserve public health (Kuenstner *et al.*, 2017).

Vaccination

Since the first vaccine against PTB in cattle that was developed in France (Vallée and Rinjard, 1926), the most commonly used vaccines are subcutaneously administered and formulated with oil or wax adjuvants (Table 2). These adjuvants provoke extremely high and persistent immune responses. In fact, the current commercially available vaccines are killed (Gudair®, Silirum® and Mycopar®) (Reddacliff *et al.*, 2006; Bastida and Juste, 2011; Hines *et al.*, 2014; Tewari *et al.*, 2014) or live-atenuated Map (Neoparasec®, LioJohne®) (Tejedor, 1994; Molina *et al.*, 1996; Bastida and Juste, 2011) suspended in oil based adjuvants. However, the major shortcoming of this type of vaccines is the formation of a subcutaneous nodule at the inoculation site, which can even get ulcerated (Lei *et al.*, 2008; Musk *et al.*, 2019) and the derived risks from accidental self-inoculation (Windsor *et al.*, 2005).

Table 2. Commercial PTB vaccines.

Name	*Route*	*Composition*	*Animal species*	*Currently Available*
Gudair®	SC 1dose	Inactivated Map 316F Mineral oil (Marcol) Water-in-oil (Montanide)	Sheep and Goat	√
Silirum®	SC 1dose	Inactivated Map 316F Water-in-oil (Montanide)	Cattle	√
Paratuberculosis Autovaxine®	SC 1dose	Inactivated Map Water-in-oil	Sheep and Goat	√
Mycopar®	SC 1dose	Killed *Mycobacterium avium* subspecies *avium* (Maa) 18 strain Oil adjuvant (secret)	Cattle	
Neoparasec®	SC 1dose	Live attenuated Map 316F Water-in-oil (secret)	Cattle Sheep and Goat	
LioJohne®	SC 1dose	Live attenuated Map 316F Oil adjuvant (unknown)	Sheep	

There is a common agreement regarding vaccination as the most effective prophylactic approach in the fight against PTB. In fact, when combining it with good management practices, vaccination has shown to: 1) reduce clinical sign manifestation, 2) reduce bacteria shedding (Juste *et al.*,

2009b; Alonso-Hearn *et al.*, 2012; Tewari *et al.*, 2014), 3) reduce in-herd transmission (Juste *et al.*, 2009b; Bastida and Juste, 2011), 4) improve milk production (Juste *et al.*, 2009b), 5) extend the productive life of the animals (Alonso-Hearn *et al.*, 2012) and 6) reduce overall mortality (Juste *et al.*, 2021). Nevertheless, vaccination does not exert full protection from contracting the infection (Reddacliff *et al.*, 2006; Muñoz, 2014) and there is also a diagnostic gap: the impossibility of differentiating between vaccinated and infected animals (DIVA) (Bull, 2020; Juste *et al.*, 2020). Finally, the derived cross immune effects interfere with the official tests used in many countries in the bovine tuberculosis (bTB) eradication programs and thus, vaccination is not allowed in cattle in most countries (Garrido *et al.*, 2013). In small ruminants, however, vaccination is recommended as a PTB control method (Juste and Pérez, 2011).

Novel antigen search (Serrano *et al.*, 2017a) is one of the approaches that has been tested to avoid interferences associated to PTB vaccination in cattle. Indeed, previous studies had suggested that introducing variations in the official tests (Hope *et al.*, 2005) could help to overcome this drawback, but legislative modifications are not easily implementable. In consequence, new immunogen development avoiding cross reactivity with bTB diagnosis seems to be the most feasible option. Diverse immunogenic products have been tested (Table 3), such as: 1) subunit vaccines (Koets *et al.*, 2006; Rigden *et al.*, 2006) and recombinant proteins (Kathaperumal *et al.*, 2008) use Map specific immunogenic antigens alone or in combination. These are a good alternative, albeit they are expensive to produce; 2) DNA vaccines use vectors to deliver Map antigens (Park *et al.*, 2008; Bull *et al.*, 2014). There are some

promising prototypes (Faisal *et al.*, 2013a); although they need to increase the protection efficacy (Juste *et al.*, 2020); 3) live attenuated vaccines (LAV) are thought to be a good alternative, because they trigger a strong cellular response (Chen *et al.*, 2012; Faisal *et al.*, 2013b; Shippy *et al.*, 2017; Phanse *et al.*, 2020), however, there are yet safety and legal issues to overcome such as the liberation of genetically modified organisms to the environment (Bull, 2020; Juste *et al.*, 2020). Finally, natural and innocuous alternatives such as the use of probiotics like Dietzia (Click, 2011), alone or in combination with vaccines are worth exploring since the infection with Map is able to produce changes in the microbiota (Arrazuria *et al.*, 2016a).

Table 3. Alternative vaccine formulations tested in animals

Vaccine	Route	Composition	Species	References
Subunit	*SC* *SC (Th)*	*Heatshock protein Hsp70*	*Cattle*	*(Koets et al., 2006)* *(Santema et al., 2012)*
Subunit	*SC*	*Lipoprotein p22* *Water-in-oil adjuvant*	*Sheep*	*(Rigden et al., 2006)*
Subunit LAM	*SC*	*Lipoarabinomannan*	*Cattle*	*(Jolly et al., 2013)*
Fusion protein MAP 74F	*SC*	*Trypsin-like serin protease & PPE MAP1519*	*Mice*	*(Chen et al., 2008)*
Fusion protein expressed in Salmonella sp.	*SC*	*Map antigens: Ag85A, Ag85B SOD*	*Goat*	*(Faisal et al., 2013a)*

Recombinant protein cocktail	*SC*	*Map antigens: 85A, 85B, 85C, and SOD* *MPLA & IL-12 adjuvants*	*Cattle*	*(Kathaperumal et al., 2008)*
Recombinant protein cocktail	*SC*	*MAP1087, 1204, 1272c, 2077c* *DDA adjuvant*	*Cattle*	(Stabel and Bannantine, 2021)
DNA gene constructs	*IM*	*DNA (85A, 85B, 85C, SOD, and 35 kDa) gene constructs*	*Mice*	*(Park et al., 2008)*
DNA mammalian expression vector plasmid pEGFP-N1	*IM*	*plasmid encoding for 85A-BCG and HSP65*	*Sheep*	*(Sechi et al., 2006)*
DNA Construct of 4 MAP genes in an adenovirus	*ID*	*Modified Vaccinia virus ankara recombinant for Map Ags (HAV)*	*Mice* *Cattle*	*(Bull et al., 2007)* *(Bull et al., 2014)*
LAV MAP3323c gene knockout target	*SC*	*Mycotiol system. Anti-sigma-R factor (ΔsigH) with and wo* *QuilA adjuvant*	*Mice*	*(Ghosh et al., 2015)*
LAV MAP3006c gene knockout target	*SC*	*(lipN/pgsN) with QuilA adjuvant* *(pgsN) with and wo QuilA adjuvant*	*Goat* *Cattle*	*(Shippy et al., 2017)* *(Phanse et al., 2020)*
LAV MAP3963 gene knockout target	*SC*	*Sam-dependent methyltransferase (umaA1)*	*Mice*	(Shin *et al.*, 2006; Settles *et al.*, 2014)

LAV MAP3025c gene knockout target	*SC*	*3-isopropylmalate dehydratase (leuD)*	*Goat*	*(Faisal et al., 2013b)*
LAV MAP3291c gene knockout target	*IP*	*Membrane protein involved in giant cell apoptosis (mpt64)*	*Mice*	*(Chen et al., 2012)*

SC: subcutaneous, IM: intramuscular, IP: intraperitoneal, LAV: live attenuated vaccine, Th: therapeutic.

Alternative vaccination routes

Leaving aside the formulations, recent studies have demonstrated that changes in the vaccination route could also lead to alternative outcomes for both protection and interference with bTB. The delivery route can distinctly modulate the immune response of the stimulated APCs, which, depending on their location, can generate a variety of T cell responses (Diebold, 2008).

In this sense, the Mbv vaccination route has shown promising effects avoiding interference with bTB diagnosis in wild boar (Garrido *et al.*, 2011) and cattle (Jones *et al.*, 2016). The intramuscular route showed a bovine purified protein derivative (PPD)-dose-dependent IFN-γ response, but the oral route did not show any positive reactors. Additionally, oral vaccination in goats, using an inactivated Mbv prototype, has recently been reported not to interfere with the ante-mortem diagnosis of tuberculosis (Roy *et al.*, 2017), implying that the bTB official diagnostic test results could also be influenced by the vaccination route.

The fundaments of using the oral route for vaccination against PTB, are the following three: 1) This route would imitate better the natural

exposure to Map and activate the immunity of the mucosa, 2) The oral route would be an easy route of administration, oral vaccines would not require the expertise of a veterinarian, so farmers could apply the dosage themselves and 3) This route is safe for the personnel responsible of its administration. The few studies that have been carried out with not so promising results include oral subunit vaccination in a goat model (Hines *et al.*, 2014), whole cell inactivated vaccination in sheep (Nisbet *et al.*, 1962; Gilmour and Angus, 1974) or live attenuated vaccines (Park *et al.*, 2011). Inadequate dosing or absence of adjuvant has been suggested to be behind unsuccessful results (Bull, 2020).

On the other hand, intradermal vaccination, as a result of the development of innovative designs such as micro needles or needle free injection devices, represents an appealing alternative route of vaccine delivery. It has shown to be more effective than the intramuscular or the subcutaneous vaccination in the prevention of many pathogens (Propst *et al.*, 1998; Holland *et al.*, 2008). Surprisingly however, this route has not been explored against Map infection.

Heterologous protection

Added to the protection against PTB, a commercially available inactivated Map vaccine has shown heterologous protection against other mycobacteria (Serrano *et al.*, 2017b) that could be a result of innate training mechanisms or cross-reactive T cell mediated adaptive mechanisms due to the homology between mycobacteria. In fact, the application of this vaccine has also been linked to an overall mortality reduction in dairy cattle (Juste *et*

al., 2021) suggesting that trained immunity such as that observed with the BCG vaccine in human newborns against Mtb, *Candida albicans* and *Staphylococcus aureus,* can indeed be behind this effect (Covián *et al.*, 2019). These findings, open the door to focus on a better comprehension of host-pathogen interactions and vaccination-mediated immune protection that will in turn help the development of innovative vaccines.

Research models for Vaccine development in PTB

Animal models

In the absence of sophisticated artificial models, animal models are yet necessary to understand the course of infection and the pathology and for testing prophylactic immunogens in PTB. The most explored animals have been goats, cattle, deer, sheep, mouse and rabbits. Experimental trials in the bovine species are most useful due to the reproducibility of the observed effects in natural conditions. However, the bovine models are time consuming as well as extremely expensive and although tissue cultures can result positive as soon as 12 weeks after the challenge, lesions cannot be expected to be seen so early (Talaat *et al.*, 2020). The deer model has also been explored, and presents timing advantages since the lesions require less time to appear and they have also showed increased susceptibility to certain strains (Mackintosh *et al.*, 2004; MacKintosh *et al.*, 2012; O'Brien *et al.*, 2020; Talaat *et al.*, 2020). On the other hand, they are difficult to manipulate and they also present expensive homing requirements. The goat model has been considered a good model and has been largely used for vaccine testing (Kathaperumal *et al.*, 2009; Faisal *et al.*, 2013a; Hines *et al.*, 2014). It has advantages associated

with the shorter time for lesion development (9-10 months) and homing expenses compared to cattle, however, compared with laboratory species they are yet expensive and the space for animal stabling represents an obstacle (Talaat *et al.*, 2020). The sheep model has also been used (Gilmour and Angus, 1974; Sechi *et al.*, 2006) and the advantages and disadvantages are similar to those described for the goat model (Talaat *et al.*, 2020); in favor of this model it could be said that sheep are known to be easier to manipulate than goats. For host-pathogen interaction short-term models of ruminants have been developed (Talaat *et al.*, 2020) such as the intestinal loop model (Momotani *et al.*, 1988b; Khare *et al.*, 2009), the ileal canulation model (Streeter *et al.*, 1991; Hein *et al.*, 2004) or the everted intestine sleeve model (Sigurdardóttir *et al.*, 2005). Vaccine evaluation is generally carried out in ruminants, however, due to the production cost of some of the vaccines tested in recent years, more economic, smaller laboratory animal models have begun to be used.

Probably inherited from human research, and due to the aforementioned reasons, the mouse has been widely used to test the virulence of Map mutants (Shin *et al.*, 2006; Bannantine *et al.*, 2014) to the study of Map-host interaction during infection (Scandurra *et al.*, 2010; Shin *et al.*, 2015) and for the screening of vaccines (Chen *et al.*, 2008; Roupie *et al.*, 2012; Bannantine *et al.*, 2014; Settles *et al.*, 2014). Despite the advantages of the murine model, there are important anatomical, physiological and immunological differences between ruminants and mice, which mean that this animal model does not show the clinical signs observed in cattle, nor the intestinal lesions characteristic of the disease (Talaat *et al.*, 2020). Moreover,

recent results with live attenuated vaccines show that the predictive capacity of the mouse results suboptimal (Scandurra *et al.*, 2010; Bull, 2020). Thus, a more accurate and adequately standardized (Bull, 2020) laboratory disease model is needed (Juste *et al.*, 2020) for conducting preliminary vaccine prototype screenings. The lack of suitable laboratory animal models has also hampered advances in the study of PTB pathogenesis. The complexity of the task resides in part in the inexistence of small laboratory ruminants.

Different groups have tested the rabbit PTB model (Mokresh *et al.*, 1989; Mokresh and Butler, 1990; Vaughan *et al.*, 2005). The rabbit not only possesses an herbivorous digestive system, but it is also naturally susceptible to infection with Map (Mokresh *et al.*, 1989; Beard *et al.*, 2001). This model has been described to show more PTB associated symptomatology than rodents, involving diarrhea and weight loss (Vaughan *et al.*, 2005; Talaat *et al.*, 2020). The leporid model has aided the study of pathogenesis of PTB (Vaughan *et al.*, 2005) and the study of the effect of diets (Arrazuria *et al.*, 2015a), the effect on microbiota (Arrazuria *et al.*, 2016a) and the effect of vaccination sequence (Arrazuria *et al.*, 2016b). However, its use also presents technical disadvantages such as the lack of research immunological reagents for rabbits, which limits its use.

Guinea pigs have also been explored as a PTB infection model with the idea of reducing the costs associated with experimental ruminant models (Francis, 1943; Merkal *et al.*, 1982b), albeit they did not succeed due to their lack of susceptibility to Map infection. They are, however, a recognized good human TB model (Padilla-Carlin *et al.*, 2008). Guinea pigs develop DTH

responses after Mtb infective exposure, which has made of the guinea pig the perfect model to test and standarize new diagnostic antigens and vaccine reactions in hTB and bTB (Angus, 1978; Padilla-Carlin *et al.*, 2008; World Organisation for Animal Health (OIE), 2018).

In vitro *and* Ex vivo *models*

Complementary to *in vivo* models, there has been an effort to design *in vitro* assays for the initial screening of vaccines, searching of diagnostic markers and correlates of protection, studying the immune responses and permitting the reduction in the use of laboratory animals. The amoeba model system has been proposed as an initial tool for virulence factor selection (Phillips *et al.*, 2020). On the other hand, the *ex vivo* MDM model has been successfully used (Park *et al.*, 2011) as an initial screening technique, however its effectiveness in predicting *in vivo* protection has been questioned (Scandurra *et al.*, 2010; Bannantine *et al.*, 2014; Lamont *et al.*, 2014). A co-culture system of monocytes and lymphocytes has been proposed to predict vaccine protectiveness *ex vivo* (Pooley *et al.*, 2018). The culture and *ex vivo* stimulation of primary cells, for example PBMCs, isolated from treated, naturally infected, challenged or healthy animals has demonstrated being very useful providing on immunological responses (Park *et al.*, 2011; Faisal *et al.*, 2013b; De Silva *et al.*, 2015; DeKuiper and Coussens, 2019a). These are very useful at predicting animals' immunological status and also permit studying the effect of vaccines against Map or other pathogens.

Background and Objectives

Vaccination against paratuberculosis has proven to be effective as a control measure, although vaccine failure exists and therefore prevention of the infection is not complete. Added to this, current vaccines cause interference with the serological tests used to diagnose the disease and their use is restricted due to interference with the diagnosis of bovine tuberculosis. New vaccines are needed and knowledge gaps in PTB pathogenesis should be filled in order to accelerate PTB vaccinology. Most host-pathogen research has focused on the action of macrophages since they are the main immune cell subset invaded by *Mycobacterium avium* subsp. *paratuberculosis* (Map). Indeed, it is inside macrophages where this pathogen is able to survive and replicate. Recent transcriptomic studies evidence an impairment of PMN recruitment during Map infection, suggesting that PMNs could be more important than previously thought.

In this context, this thesis explores the effect of new immunogens administered by alternative routes aimed at overcoming the problems associated with the current commercially available vaccines.

Furthermore, this work investigates the role of the innate immune system in the disease and host protection.

1. The **overall objective** of the project is to develop effective vaccination strategies against paratuberculosis, exerting protection without interfering with the serological diagnostic techniques of paratuberculosis and the official routine techniques for the diagnosis of bovine tuberculosis, in addition to studying the non-specific effects derived from vaccination against paratuberculosis.

2. The **specific objectives** of the thesis work are:
   2.1. To analyze whether the effects of oral and intradermal vaccination with a Map inactivated vaccine or other products **interfere** with the result of routine official tests in the diagnosis of bovine tuberculosis.
   2.2. To analyze the **protective** effect against Map infection of different vaccines in rabbits, taking into account bacteriological, immunological and histopathological parameters.
   2.4. To analyze the **trained immune response** in animals treated with different vaccines using *ex vivo* functional assays to evaluate their potential against other important pathogens that affect livestock.
   2.5. To study the interaction of **innate professional phagocytes**, PMNs and macrophages with Map *in vitro*.

Materials, Methods and Results

Materials, Methods and Results

Study I

Alternative Vaccination Routes against paratuberculosis modulate local Immune response and Interference with tuberculosis diagnosis in laboratory animals

The results of this study have been published:

Arrazuria R, **Ladero I**, Molina E, Fuertes M, Juste R, Fernández M, Pérez V, Garrrido J, Elguezabal N. Alternative vaccination routes against paratuberculosis modulate local immune response and interference with tuberculosis diagnosis in laboratory animals. *Veterinary Sciences*, January 2020.

Synopsis

This study evaluates an experimental inactivated Map vaccine through the oral (VOR) and intradermal (VID) routes of vaccination against Map and their effect on local immune responses in comparison to a commercial vaccine administered through the subcutaneous route (CV). The guinea pig model was to predict the effects of these routes on interference with the on-farm tests for bTB surveillance. The VID group showed certain degree of reactivity to the skin test, whereas the same vaccine administrated orally was completely negative. For efficacy assessment against Map, histopathological (macroscopic and microscopic lesions in the *sacculus rotundus,* vermiform appendix and associated lymphatic tissues) and bacteriological (Map-PCR in *sacculus rotundus,* vermiform appendix and associated lymphatic tissues) parameters were considered at the experiment endpoint. The VID group presented the highest proportion of animals with no visible lesions and the lowest proportion of animals with Map positive tissues. In order to characterize the polarization of local macrophages, immunohistochemistry analysis in *sacculus rotundus* and vermiform appendix was carried out using M1 and M2 specific markers. The VID group presented a dominantly M1 polarized response related with the control over the infection. In general, all vaccinated groups showed less active granulomatous lesions indicated by lower calprotectin expression of local macrophages. These data show that PTB vaccination has an effect on macrophage polarization and that the route influences infection outcome and can also have an impact on bTB diagnosis.

Materials and Methods

1.1 Vaccination and Challenge Experiment

1.1.1 Experimental Design

The protection and immune response study design is summarized in Figure 7. New Zealand white female rabbits of 7 weeks of age (n = 25) were purchased from authorized experimental animal dealers (Granja San Bernardo, Tulebras, Spain). Upon arrival at NEIKER facilities (Derio, Spain), animals were randomly allocated into five experimental groups with 5 animals each: non-infected control group (NIC); infected control group (IC); experimental intradermal vaccine group (VID); experimental oral vaccine group (VOR); and control vaccine group (CV) and left on a 15 day adaptation period being fed with weaning growth pellets ad-libitum until the age of 12 weeks. Afterwards, animal feed was limited to 30–35 g of dry matter/kg bodyweight per day whereas water was available ad-libitum.

Intradermal and oral vaccinations were carried out with an experimental whole-cell Map strain chemically inactivated vaccine that does not include any adjuvant in its formulation. As a control, subcutaneous vaccination was performed with Silirum® (CZV, Porriño, Pontevedra, Spain), a whole-cell inactivated commercial vaccine that carries a highly refined mineral oil adjuvant, that is approved for its use in cattle in some countries and that is the current standard for vaccination, being an appropriate control.

On day 1, vaccination was performed in the corresponding groups (VID, VOR, CV) with 1 ml of 12.5 mg antigen (calculated by the wet weight method to be 2.3×10^7 CFU). Fifteen days after, a second dose was administered to the VID and VOR groups. VID and CV vaccination were performed distributing the dose in two shots performed on the back. VID was administered using a 29G needle on two previously shaved sections and CV using a 25G needle. VOR vaccine was administered via needle-less syringe. Afterwards, on three consecutive days (day 26, 27, and 28) all animals except the ones belonging to the NIC group were orally challenged via needle-less syringe with a dose of 10^9 CFU per day of Map strain K10 obtained as described previously (Arrazuria *et al.*, 2015a).

Weight recording and blood sampling was done at different time points (S0–S6). Blood was centrifuged at 1500 g for 10 min RT to obtain plasma which was stored at −20 °C for further analysis. All animals were euthanized at the end point (195–200 days) with an intracardiac pentobarbital dose (200 mg/kg) after deep sedation with xylazine (5 mg/kg) and ketamine (35 mg/kg). Immediately afterwards, a complete necropsy was performed focusing on the digestive system. The observed gross pathology was scored as follows: Normal appearance (0), mild thickening of ileum and/or distal jejunum (1), moderate ileum and/or jejunum thickening plus lymphangiectasia (2). Presence of white spots corresponding to caseous necrosis foci in *sacculus rotundus* (SR) and/or vermiform appendix (VA) (3). Presence of white spots in SR and/or VA plus ileum and/or jejunum thickening or lymphangiectasia (4). Thereafter, tissue samples of SR, VA,

mesenteric lymph node (MLN), liver and tonsil were collected and the size of the SR, VA, and MLN was noted.

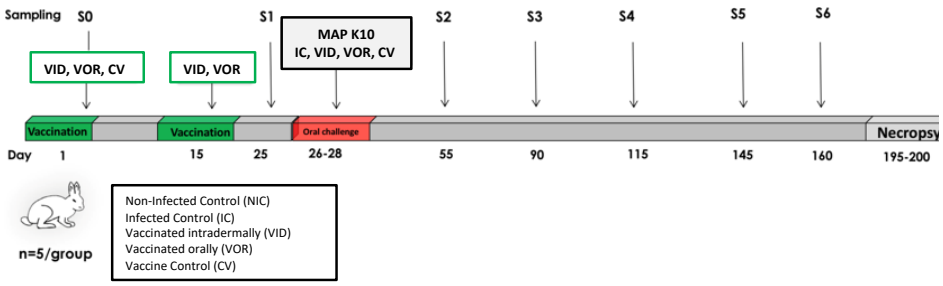

Figure 7. Vaccination effect on immune response after Map challenge. Experimental design with interventions and time points.

1.1.2 Tissue Gene Extraction and Map PCR

Collected tissues (SR and VA) stored at −20 °C were thawed overnight (ON) at 4 °C and tissue DNA was extracted with DNA Extract-VK (Vacunek S.L, Derio, Spain) according to the manufacturer's instructions and as described previously (Arrazuria *et al.*, 2015a). Extracted DNA was stored at −20 °C until assayed. A real time multiplex PCR detecting *IS900* and *ISMAP02* DNA sequences of Map was performed with 350 ng/µl as described by Sevilla et al. (Sevilla *et al.*, 2014). PCR results were analyzed using the 7500 System SDS software v. 1.4 (Applied Biosystems, Alcobendas, Spain). Threshold cycle (Ct) and baseline were automatically determined by the software and verified by visual examination of the threshold line in amplification plots. Ct values equal or below 38 for both *IS900* and *ISMAP02* probes were considered positive, Ct values over 38 for both target probes and under 38 for internal amplification control (IAC) were considered negative.

1.1.3 PPA-3 Enzyme Linked Immunosorbent Assay (ELISA)

To assess humoral immunity, an in-house indirect ELISA was performed using paratuberculosis protoplasmic antigen 3 (PPA-3) (Allied Lab, Fayette, MO, USA) as described previously (Arrazuria *et al.*, 2016b). Briefly, microtiter plates were coated with 100 µl of PPA-3 (0.04 mg/mL) diluted in 0.5% sodium carbonate buffer (pH 9.6) and incubated at 4 °C ON. After coating, plates were washed once with wash solution (0.05% Tween 80/0.85% sodium chloride). Plasma samples were thawed, adsorbed with *Mycobacterium phlei* in saline solution (5 g/l) diluted 1:100 in 0.05% Tween 80 in PBS (PBS-T), added to coated plates (100 µl/well) and incubated 2 h at RT in a humid chamber. Following incubation plates were washed three times with wash solution (300 µl/well). Recombinant protein G peroxidase (Sigma-Aldrich, St Louis, MI, USA) 0.025 µg/ml in PBS-T was added (100 µl/well) and plates were incubated at RT for 2 h. The plates were washed again three times with wash solution (300 µl/well) and then peroxidase substrate (0.01% ABTS, Sigma Aldrich, St Louis, MI, USA) was added and plates were further incubated at RT for 30 min in darkness. The reaction was stopped by the addition of 2% hydrofluoric acid (100 µl/well). The absorbance was measured at 405 and 450 nm using an automated ELISA plate reader (Multiskan EX®, Thermo Lab Systems, Helsinki, Finland). The reading obtained at 450 nm was subtracted from the reading of 405 nm and results were expressed as an ELISA index calculated by subtracting the negative control mean absorbance to the sample mean absorbance. Optical density (OD) values were normalized across plates using the following calculation: ELISA index = (Mean sample

OD) × (Mean OD of the highest positive control/Mean OD of the positive control of the plate).

1.1.4 Histopathology

Samples from SR and VA, mesenteric lymph node, liver and tonsil were collected and fixed in 10% neutral buffered formalin solution for a minimum of 24 h, trimmed and dehydrated through graded alcohols. Afterwards, samples were embedded in paraffin wax and sectioned at 3–5µm. These sections were mounted on glass slides and stained with haematoxylin and eosin (HE) according to standard procedures. Slides were examined blindly by an experienced pathologist giving an histopathology score. Severity of the lesions were graded as 0 if absent, and from 1 to 3 if present based on the number and extent of granulomatous lesions. Those graded as 1 were characterized by the presence of few granulomas, composed of about 50–60 macrophages, only in the interfollicular areas of the intestinal lymphoid tissue. In the other 2 categories, granulomatous lesions were seen affecting the lymphoid tissue and intestinal lamina propria with different intensity.

1.1.5 Immunohistochemistry

For immunohistochemistry analysis sections of 3–5 µm were placed on poly-L-lysine coated slides and immunohistochemically stained using the Envision + System (Dako, Agilent Technologies, Glostrup, Denmark). Different monoclonal antibodies raised against antigens expressed by

macrophages, including M1 and M2 subpopulations, and proliferation markers were used (Table 4).

Briefly, sections were deparaffinized and antigen retrieval was performed in the PT Link system (Dako, Agilent Technologies, Glostrup, Denmark) at 96 °C using a pH 6 or pH 9 retrieval solution (Table 4). After hydration, the sections were incubated in 3% hydrogen peroxide in methanol for 30 min to eliminate endogenous peroxidase. Rehydrated slides were rinsed in PBS of pH 7.4, and sections were incubated with the primary antibodies diluted in PBS (Table 4) ON at 4 °C in a humidified chamber. After washing in PBS, sections were incubated for 40 min at room temperature with EnVision + horseradish peroxidase solution (Dako, Agilent Technologies, Sta Clara, CA, USA) for the monoclonal antibody. After washing in PBS, antibody localization was determined using 3,3-diaminobenzidine (Sigma-Aldrich Corp., Madrid, Spain). Sections were counterstained with Mayer's hematoxylin for 10 s. Slides were mounted with DPX (dibutyl phthalate xylene) and observed under a light microscope. Appropriate species and isotype-matched immunoglobulins were used as negative controls.

For this study, only those immunolabeled cells with a clear macrophage morphology (abundant cytoplasm and ovoid nucleus) or lymphocyte morphology in the case of IFN-γ analysis that were forming part of the granulomas present in the different lesion types were considered and evaluated. In each slide, 20 representative fields containing granulomatous lesions were selected, photographed and analyzed. Cell counting and image

analysis were performed using the Image J processing and analysis software (US National Institutes of Health, Bethesda, MD, USA).

Table 4. Immune markers detected in the immunohistochemistry analysis.

Antigen (Clone)	**Specificity and Target Cells**	**Antigen Retrieval Solution**	**Antibody Dilution**	**Reference**
Bovine TNF (CC327)	Expressed in M1 macrophages.	6	1:200	(Fernández *et al.*, 2017a)
Bovine IFN-γ (CC330)	Released by lymphocytes, macrophages and dendritic cells. Induces M1 macrophage polarization.	6	1:100	(Soulas *et al.*, 2011)
Human calprotectin (MAC387)	Expressed in activated, recently recruited macrophages among other cells.	9	1:200	(Fernández *et al.*, 2017a)
Human CD163 (EDHu-1)	Expressed in M2 macrophages.	6	1:300	(Fernández *et al.*, 2017a)

For staining comparison among animals, samples were scored semi-quantitatively using a complete immunohistochemistry-score (IHC-score) that considers both the staining intensity and the percentage of positively immunolabeled cells as described previously (Begg *et al.*, 2011). Briefly, for each type of lesion, the IHC-score was calculated by adding the products of the percentage of cells (0–100) labeled at a given staining intensity present in each selected field and the staining intensity score (0, none; 1, weak; 2,

moderate; and 3, intense). Thus, the IHC-score obtained in each random field could range between 0 and 300.

1.2 Interference with bTB Diagnosis

The interference study experimental design is summarized in Figure 8. Dunkin Hartley female guinea pigs of 4 weeks of age (n = 9) were purchased from authorized experimental animal dealers (Envigo, Barcelona, Spain). Upon arrival at NEIKER facilities (Derio, Spain), animals were randomly allocated into three experimental groups with 3 animals each: experimental intradermal vaccine group (VID), experimental oral vaccine group (VOR); and control vaccine group (CV). Animals were fed guinea pig growing pellets and water ad-libitum throughout the experiment. After a 15 day adaptation period, groups VID and VOR were vaccinated. VID animals received intradermal injections of the experimental whole-cell Map inactivated vaccine in two sites of their right flank, whereas VOR animals received the experimental whole-cell Map inactivated vaccine orally. 15 days after, both groups received a second dose in identical conditions and the CV animals were vaccinated subcutaneously with the commercial vaccine (Silirum®). All vaccine doses were composed of 12.5 mg of antigen measured by wet weight (Achkar and Casadevall, 2013). After 5 weeks the left flank of all animals was shaved and treated with depilatory crème and three intradermal injections of 100 µl of saline, 1:100 dilution of avian PPD (A PPD) (CZ Veterinaria, Porriño, Spain) and 1:100 bovine PPD (B PPD) (CZ Veterinaria, Porriño, Spain) following a Latin square pattern were applied. The diameters of the reddish circles that form around the injection sites (delayed type

hypersensitivity reaction) were measured after 48 h. Animals were euthanized on day 53 by intracardiac pentobarbital (200 mg/kg) injection after deep sedation with ketamine (50 mg/kg) and xylazine (5 mg/kg).

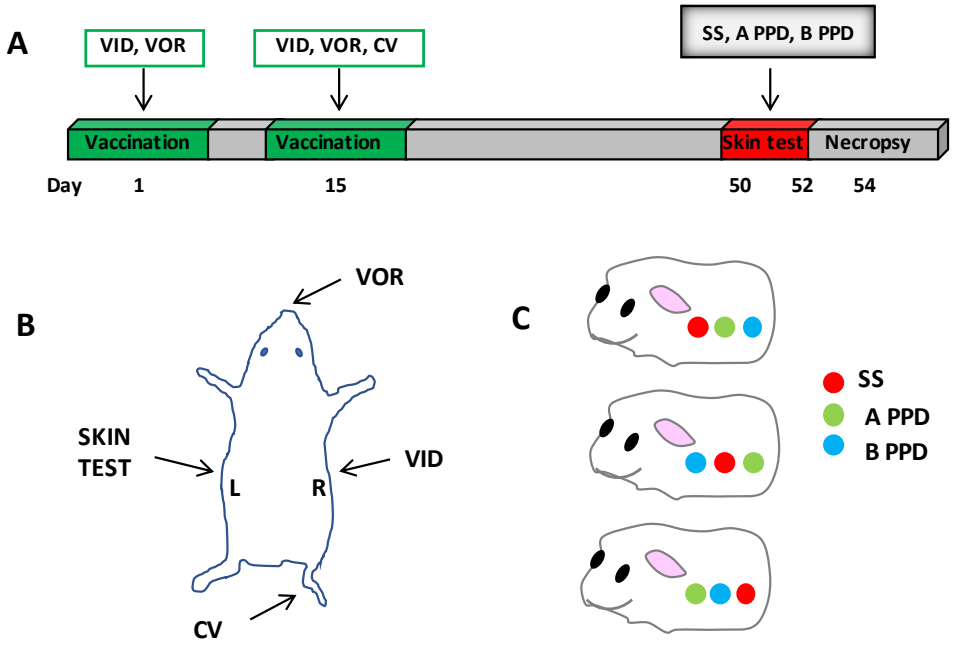

Figure 8. Vaccination interference with tuberculin testing in guinea pigs. Experimental Design. (A) Experimental interventions and time points, (B) vaccination and skin test inoculation sites, (C) latin square diagram of tuberculin inoculation sites. VID: intradermal vaccine, VOR: oral vaccine, CV: control vaccine, SS: saline, A PPD: avian PPD, B PPD: bovine PPD, L: left flank, R: right flank.

1.3 Statistical Analysis

To test data normal distribution Shapiro–Wilk test was applied. Data normally distributed (weight gain percentage: calculated as the percentage of the initial weight, size of SR, VA and MLN) were analyzed by one-way analysis of variance (ANOVA) test for route as the independent variable,

followed by a Dunnett's multiple comparison test to compare all groups against the control group and Tukey post-hoc test to compare among the different groups. A two-way repeated measures ANOVA was applied to test differences in ELISA index values among groups at different sampling points.

The histopathology index was calculated as the sum of the scores per tissues divided by the number of examined tissues. Non-normally distributed data (gross pathology score, sum of all tested tissues, histopathology score, IHC-score) were tested using the non-parametric Kruskal-Wallis test, followed by Dunn's post-hoc test for multiple comparisons among groups.

Figures were generated using GraphPad Prism 7 (GraphPad Software Inc., La Jolla, San Diego, CA, USA), Tableau software and Microsoft Excel 2010 while R statistical software was used for data analysis. For all tests a probability value of <0.05 was considered significant.

Results

2.1.Vaccination and Challenge Experiment

2.1.1 Weight Gain, Gross Pathology and Map Detection

Weight gain during experimental period calculated as the percentage of weight gain in relation to the initial weight, was significantly higher (p = 0.024) in animals from the NIC group compared to the CV group (Figure 9).

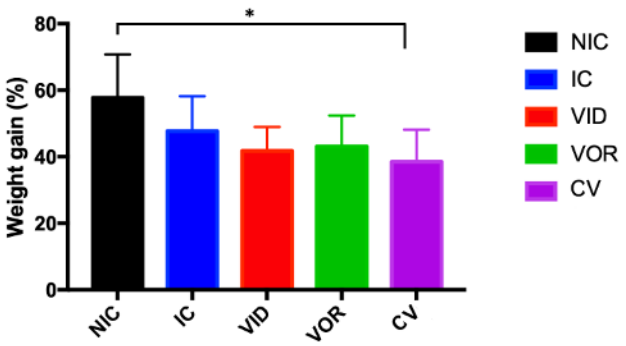

*Figure 9. Weight gain during experimental period. Bars represent the mean and the error bars the standard error of the mean (SEM). * Significant differences were detected by Dunnet's post hoc between the non-infected control group (NIC) and the control vaccine (CV) group (p = 0.024).*

At necropsy, lesions compatible with PTB infection consisting of mild and moderate ileum and distal jejunum thickness, intestinal and mesentery lymphangiectasia and presence of white spots corresponding to caseous necrosis foci in SR and VA were observed (Figure 10). These lesions were present in 60% of animals belonging to the IC group, 40% of the VID group and 80% of VOR and CV groups (Table 5). Map was detected by PCR in 80% of animals of the IC, VOR, and CV groups and in 40% of animals belonging to the VID group (Table 5).

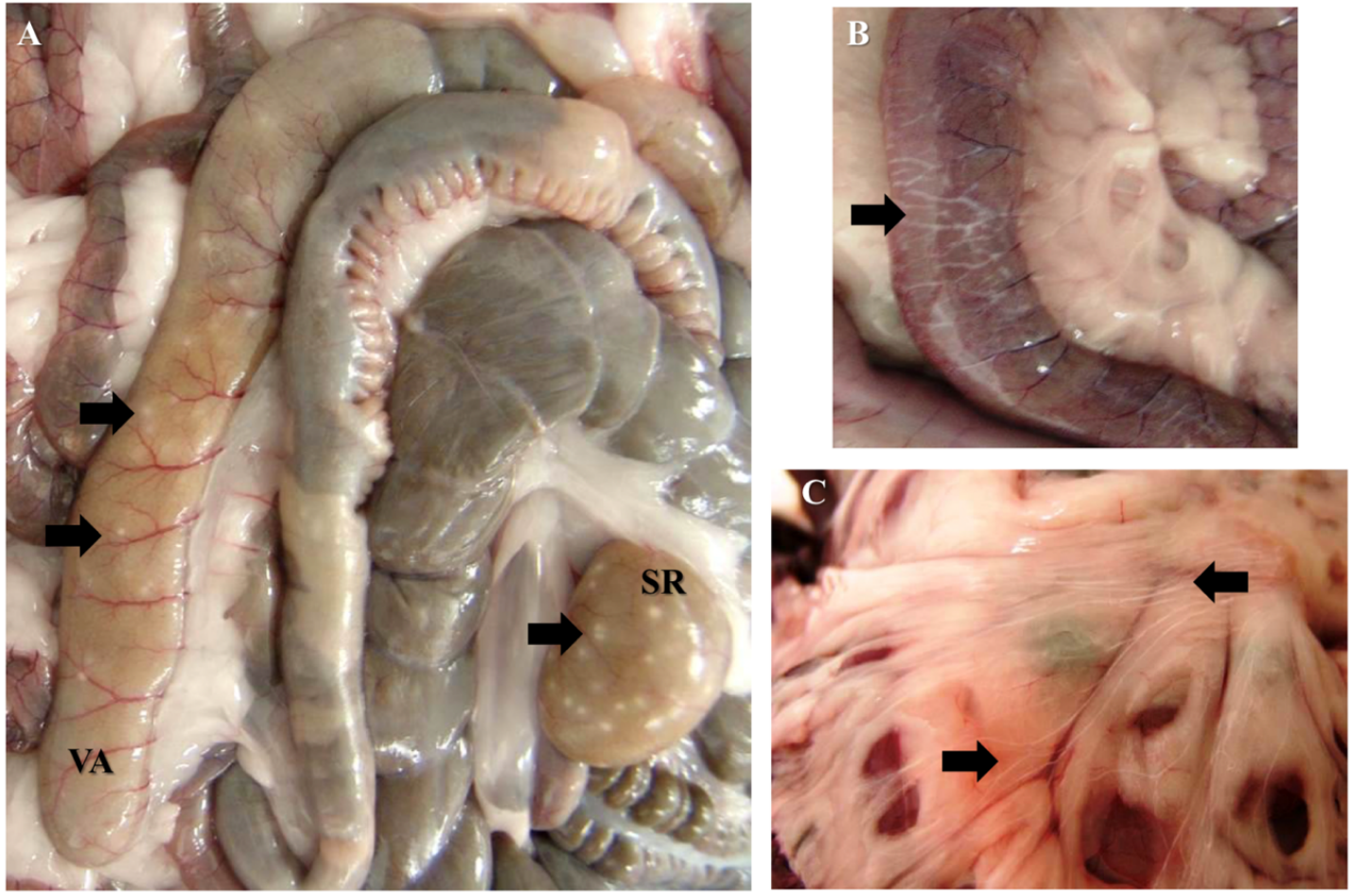

Figure 10. Gross pathology observed in the digestive system. A) Pale white reactive spots in sacculus rotundus *(SR) and vermiform appendix (VA). B) Intestinal lymphangiectasia. C) Dilatation of lymphatic vessels in the mesentery.*

Table 5. Infection outcome in Map infected rabbits.

		Map PCR		Histopathology Score		
Group	**ID**	**SR**	**VA**	**SR**	**VA**	**Gross Pathology Score**
IC	37	+	−	2	2	2
	38	+	−	1	1	0
	40	−	+	3	3	4
	43	−	−	2	2	4
	44	+	+	2	3	0
VID	16	−	−	1	2	0
	17	−	−	2	1	0
	31	+	+	1	1	3
	32	−	+	2	2	0
	33	−	−	2	2	3
VOR	18	−	−	2	2	1
	19	−	+	2	2	1
	34	+	+	1	1	0
	35	+	−	1	2	3
	36	−	+	2	3	4
CV	14	−	−	1	1	0
	15	+	−	1	1	2
	28	−	+	1	1	1
	29	+	+	1	1	4
	30	+	+	1	2	3

Infected controls (IC), experimental intradermal vaccine animals (VID), experimental oral vaccine animals (VOR), control vaccine (CV) animals. Sacculus rotundus *(SR) and vermiform appendix (VA). Histopathology score: 0 if no lesion, and from 1 to 3 if present based on the number and extent of granulomatous lesions. Gross pathology score: normal appearance (0), mild thickness of ileum and/or distal jejunum (1), moderate ileum and/or jejunum thickness plus lymphangiectasia (2), presence of white reactive spots in SR and/or VA (3), presence of white reactive spots in SR and/or VA plus ileum and/or jejunum thickness or lymphangiectasia (4).*

2.1.2 Humoral Response

Humoral immune response measured by ELISA and an index was calculated during the experiment (Figure 11). As expected, the humoral

immune response did not show any difference between groups at the baseline sampling (S0). NIC and IC animals did not show an antibody level increase throughout experiment samplings (data not shown). At day 55 (S2), animals of the CV group showed an increase in anti-PPA-3 antibody levels. At this point, the ELISA index was significantly higher in CV group compared to the experimental vaccine groups (VID, VOR) ($p < 0.0001$). CV animals continued with significantly higher antibody levels after 90 days (S3) and 115 days (S4) of the beginning of the experiment. In these two samplings points, all pairwise comparisons involving the CV group yielded a p-value < 0.0001.

When sampling period increments representing crucial experimental interventions such as vaccination (S2 − S0), vaccination plus challenge (S3 − S0) and the end of the experiment compared to the beginning (S6 − S0) were analyzed, the CV group showed highest antibody values and significant differences compared to the other vaccinated groups in periods (S2 − S0; vaccination) and (S3 − S0; vaccination + challenge). In the last sampling point (S6), after 160 days of the beginning the experiment, the CV group showed a decrease in PPA-3 antibody levels, although these were still higher than in the rest of the experimental groups ($p < 0.001$).

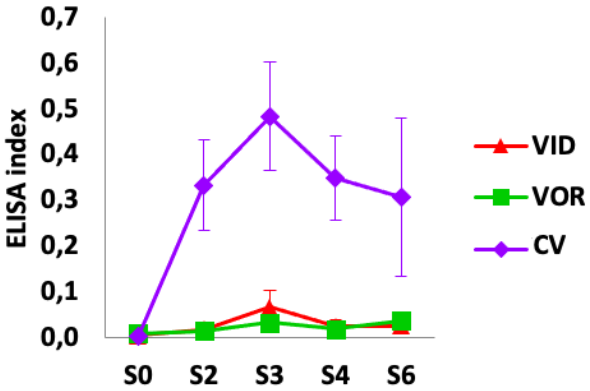

Figure 11. Anti-Map antibody levels time course. ELISA index of the vaccinated animal groups.

In the CV group vaccination site nodules were measured showing variability in size which was expressed as cm^2. Vaccination site nodule size was positively correlated to anti-PPA-3 antibody levels in the CV group (Pearson: 0.935, p: 0.02) (Figure 13A-C).

2.1.3 Histology

Granulomatous lesions were detected in SR and VA in all infected groups. The histology score of these two lymphoid tissues is detailed in Table 5.

The IC group presented the highest number of microscopically affected tissues (SR, VA, tonsils, liver and MLN) followed by the VOR group, that did not show lesions in liver. Interestingly, the VID group showed lesions in liver but not in mesenteric lymph nodes in contrast to the VOR group. Finally, the CV group was the one with the lowest number of affected tissues. The histopathology index was significantly lower in the CV group

compared to the IC group (p = 0.011) suggesting a healing or protective capacity of CV (Figure 12).

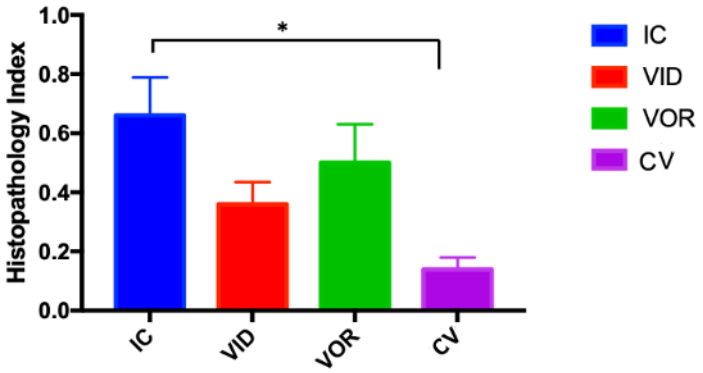

*Figure 12. Histopathology index of challenged animals. This index was calculated as the sum of the scores per tissues divided by the number of examined tissues of the experimental groups. Error bars represent the standard error of the mean. * p < 0.05.*

Histology of vaccination site of VID animals showed a small necrotic area in the skin with dispersed acid-fast bacilli (Figure 13D-F).

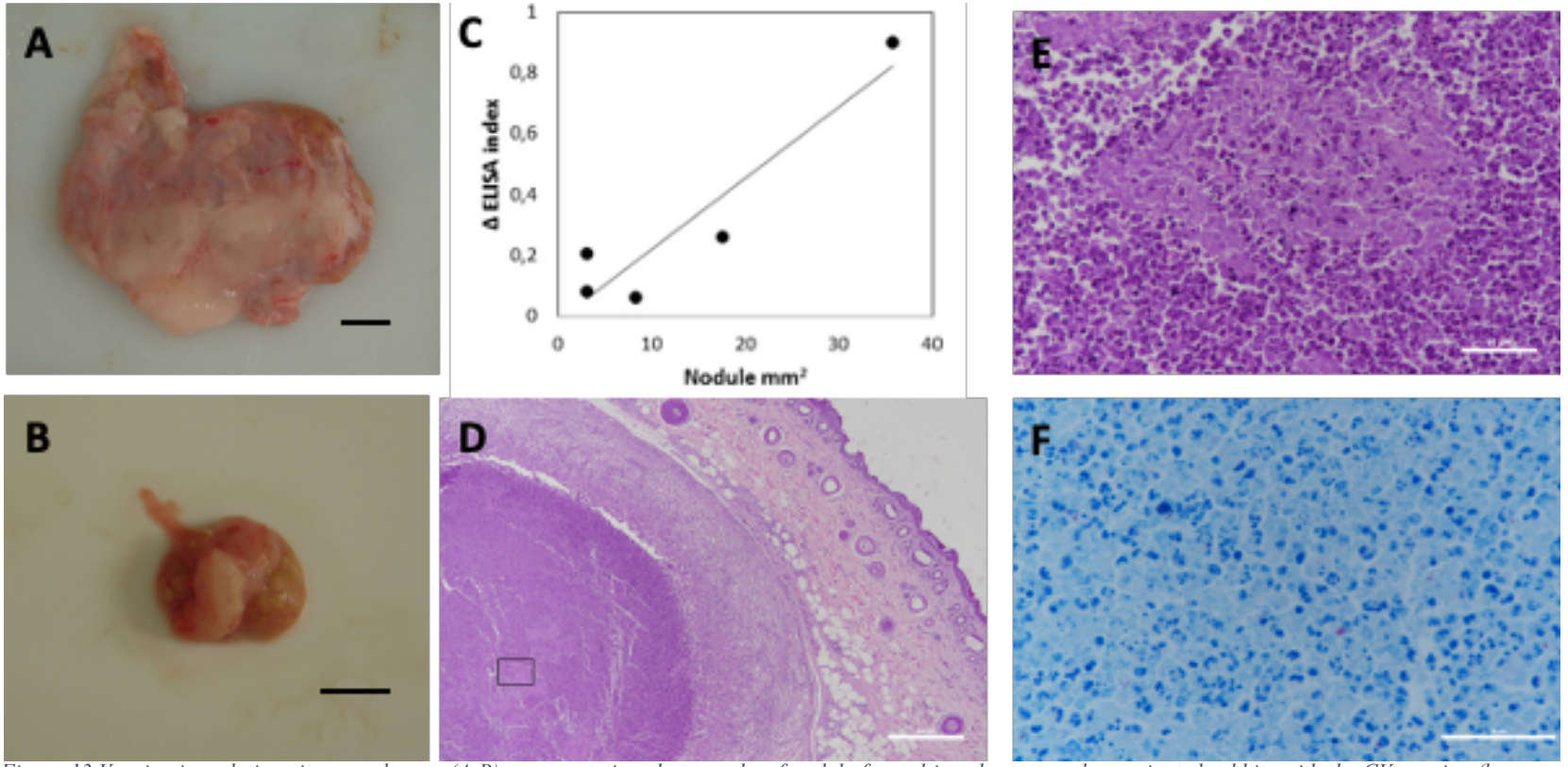

Figure 13.Vaccine inoculation site granulomas. (A-B) representative photographs of nodule formed in subcutaneously vaccinated rabbits with the CV vaccine (bars are equivalent to 1 cm), (C) dot plot showing correlation between vaccination nodule and ELISA index (S6–S0) in the CV group (Pearson: 0.935, p: 0.02). The trend line represents the least square estimation. (D) Cutaneous pyogranuloma in intradermic vaccination site on guinea pig (haematoxilin-eosin staining; bar = 500 mm). (E) Magnification of (D), necrosis and neutrophil inflammatory infiltrate in intradermic injection site (haematoxilin-eosin staining; bar = 50 mm). (F) Acid-fast bacilli in necrotic areas of intradermic injection site (Ziehl-Nelsen staining; bar = 50 mm).

2.1.4 Cell Subsets on Granulomatous Lesions

Representative micrographs of the immunohistochemical characterization of SR granulomatous lesions are shown on Figure 15. The calculated IHC score for the selected markers on the granulomatous lesions of SR and VA are shown on Figure 14. There were less IFN-γ positive cells in the granulomatous lesions of SR in the CV group compared to the VID, VOR and IC groups ($p = 0.013$, $p = 0.046$, $p = 0.023$, respectively) (Figure 14A). The same pattern of IFN-γ detection among study groups was observed in VA, where CV presented less cells immunolabelled for IFN-γ compared to VID, VOR and IC ($p = 0.016$, $p = 0.012$ and $p < 0.001$, respectively). In addition, in the VA the IC group presented significantly higher IFN-γ IHC scores compared to VID and VOR ($p = 0.010$ and $p = 0.013$).

The IHC score for TNF (Figure 14B) in the granulomatous lesions of the SR showed lower values in the IC group compared to VID and CV ($p < 0.001$ and $p < 0.001$), and in VOR comparing with VID and CV ($p = 0.013$ and $p = 0.021$). In the VA, the levels of this marker were much lower than in the SR and again the IC group presented lower values than VID and CV ($p = 0.002$ and $p < 0.001$) and the VOR group was the one that showed the highest TNF levels, higher than the IC ($p < 0.001$), VID ($p < 0.001$) and CV ($p = 0.020$) groups.

Regarding CD163 immunostaining (Figure 14C) in the SR, the VOR, and CV groups showed higher levels compared to other groups. The VOR group had higher values than IC ($p < 0.001$) and VID ($p = 0.004$). In the same way this marker was higher in the CV group, compared to the IC group ($p < 0.001$)

and VID ($p < 0.001$). A similar pattern was observed in the VA for this marker (Figure 14C). In this tissue, the CV group presented higher values than IC ($p < 0.001$) and VID ($p < 0.001$). Likewise, VOR group showed higher levels than IC group ($p < 0.001$) and VID ($p < 0.001$), although in this case VOR group levels were higher than in the SR.

Calprotectin detection was higher in the IC group compared to the vaccinated groups in both SR (VID, VOR, and CV, $p < 0.001$ for all pairwise comparisons) and VA (VID, VOR, and CV, $p < 0.001$ for all pairwise comparisons) (Figure 14D). In addition, in the SR the VOR group showed higher levels of calprotectin than VID ($p = 0.003$) or CV ($p < 0.001$) groups. The same occurred in the VA, where the VOR group presented higher levels of calprotectin compared to VID ($p = 0.022$) and CV ($p< 0.001$). In the VA, the VID group presented higher levels of calprotectin compared to the CV group ($p = 0.022$).

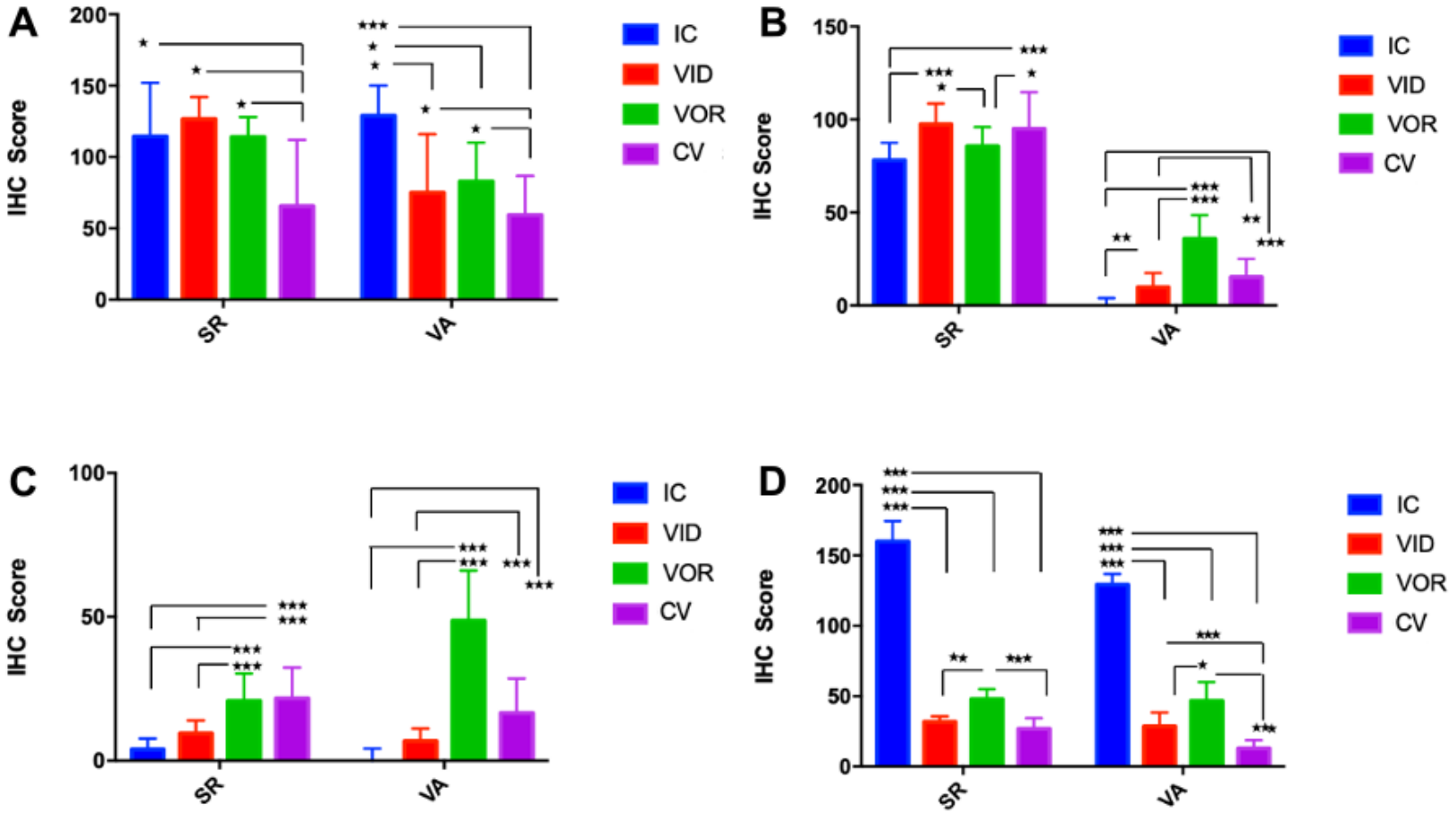

Figure 14. Macrophage polarization status. Mean IHC-score in sacculus rotundus *(SR) and vermiform appendix (VA) in the infected controls (IC), experimental intradermal vaccine (VID), experimental oral vaccine (VOR), and control vaccine (CV) animals for (A) IFN-γ; (B) TNF; (C) CD163; (D) calprotectin. Error bars represent the Confidence Interval of 95%. * $p < 0.05$; ** $p < 0.01$; *** $p < 0.001$.*

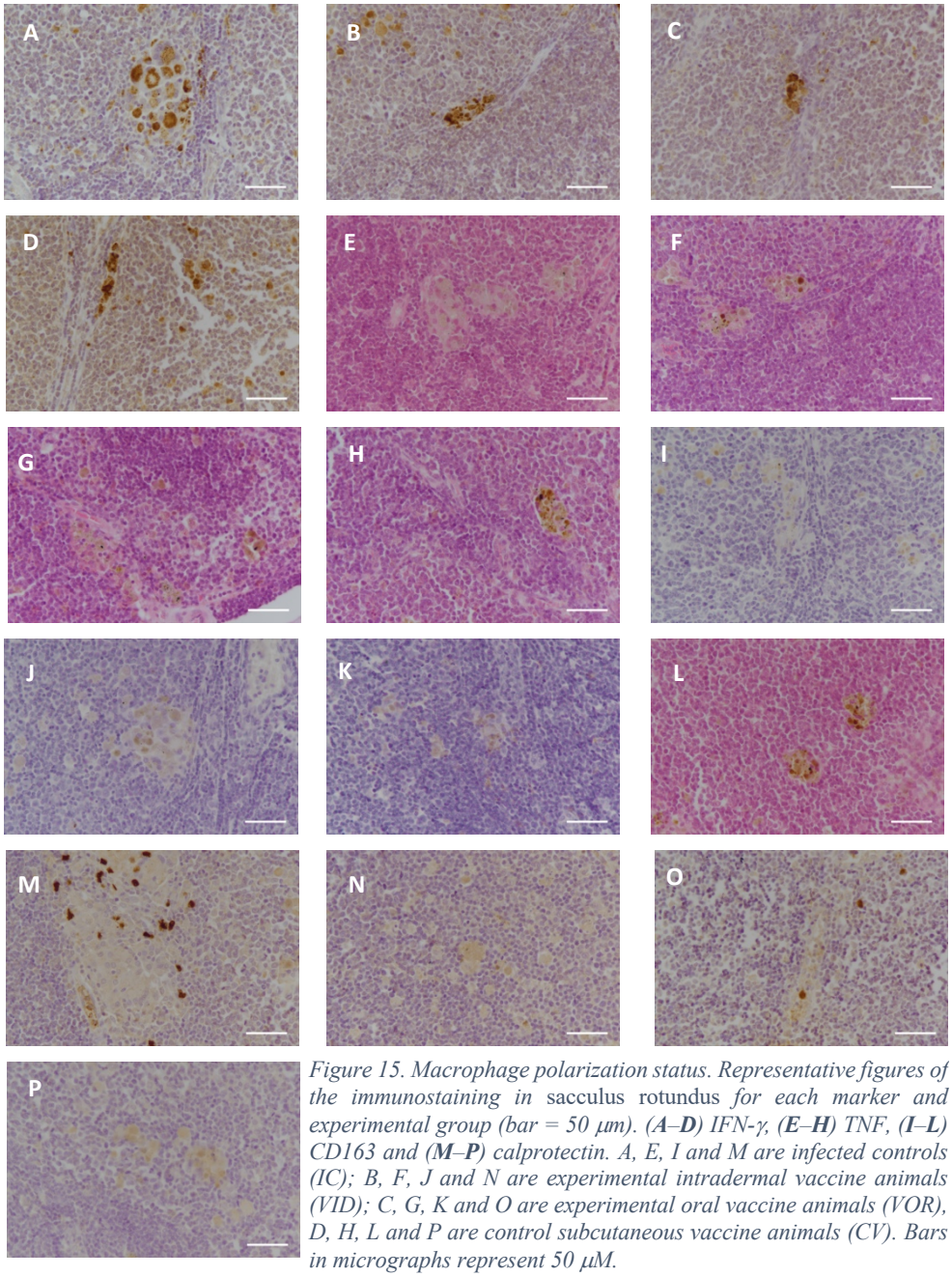

Figure 15. Macrophage polarization status. Representative figures of the immunostaining in sacculus rotundus *for each marker and experimental group (bar = 50 μm). (**A**–**D**) IFN-γ, (**E**–**H**) TNF, (**I**–**L**) CD163 and (**M**–**P**) calprotectin. A, E, I and M are infected controls (IC); B, F, J and N are experimental intradermal vaccine animals (VID); C, G, K and O are experimental oral vaccine animals (VOR), D, H, L and P are control subcutaneous vaccine animals (CV). Bars in micrographs represent 50 μM.*

2.2. Interference with bTB diagnosis

The skin test interference analysis in guinea pigs revealed that VOR animals did not show skin reaction to A or B PPD, whereas CV and VID animals showed reactions for both tuberculins (Figure 16). CV animals presented significantly higher values compared to VID for the B PPD ($p = 0.006$). This test confirmed what was observed in rabbits in the sense that the orally administered experimental vaccine (VOR) did not trigger a detectable specific response either humoral or cellular, while the CV initiated both pathways. The VID, however, yielded a cellular immune response that could be related to the protection trend observed in the microbiological and histological parameters.

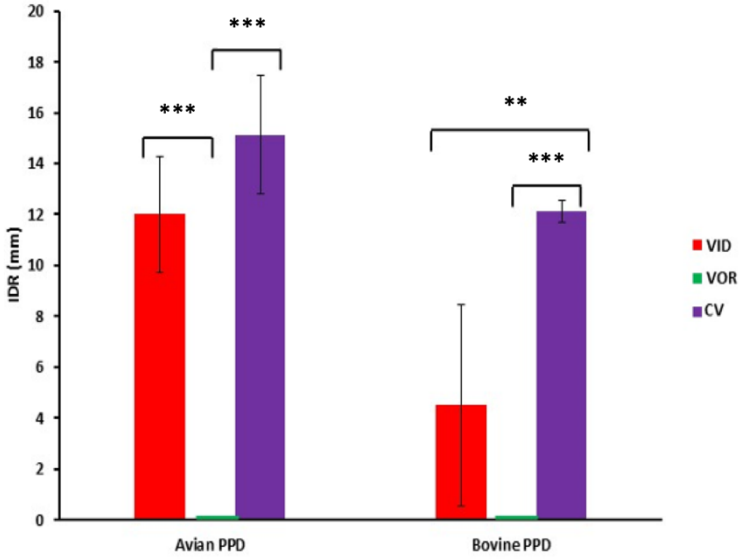

*Figure 16. Mean skin reaction measured values to avian and bovine purified protein derivative (PPD) after sensitization in experimental intradermal vaccine (VID), experimental oral vaccine (VOR) and control vaccine (CV) animal groups. Error bars represent the standard error of the mean. * $p < 0.01$; ** $p < 0.001$; *** $p < 0.0001$.*

Materials, Methods and Results

Study II

Oral vaccination stimulates neutrophil functionality and exerts protection in a *Mycobacterium avium* subsp. *paratuberculosis* infection model

The results of this study have been accepted:

Ladero-Auñon I, Molina E, Oyanguren M, Barriales D, Fuertes M, Sevilla I, Luo L, Arrazuria R, De Buck J, Anguita J, Elguezabal N. "Oral vaccination stimulates neutrophil functionality and exerts protection in a *Mycobacterium avium* subsp. *paratuberculosis* infection model". Accepted in *npj Vaccines*, July 2021.

Synopsis

The first study has shown that the interference with the bTB diagnostic test can potentially be avoided by changing the administration of the vaccine to the oral route. Therefore, the aim of this study was to compare the oral route with a set of mycobacterial and non-mycobacterial vaccines in order to investigate homologous and heterologous *in vivo* protection against Map in the rabbit infection model. In this study, the inactivated vaccines were administered with the QuilA adjuvant whereas the live attenuated vaccine was formulated without adjuvant. All experimental vaccines were compared with a commercial vaccine administered through the subcutaneous route. Oral vaccination with inactivated or live vaccines was able to activate mucosal immunity as seen by elevation of serum IgA and the expression of *IL4* in peripheral blood mononuclear cells (PBMCs). Training effects on polymorphonuclear neutrophils (PMNs) were assessed measuring phagocytosis by flow cytometry and extracellular trap release by fluorimetry. PMN phagocytosis against Map was enhanced by vaccination and extracellular trap release against Map and non-related pathogens was modified by both, vaccination and Map-challenge, suggesting the existence of trained immunity. Finally, PBMCs from vaccinated animals stimulated *in vitro* with Map antigens showed a rapid innate activation cytokine profile. These results suggest that oral vaccination against PTB can stimulate neutrophil activity and both innate and adaptive immune responses, that correlate with protection.

Materials and Methods

1.1.Ethics statement

All animal procedures were carried out following European, National and Regional regulations on animals used in experimentation and other scientific purposes. The protocols were evaluated and approved by the Ethics Committee at NEIKER (NEIKER-OEBA-2018-0001) and authorized by the Regional Council (BFA-38012).

1.2.Vaccine and bacteria inoculum preparation

All bacteria used for *ex vivo* and *in vivo* challenge assays were grown to the exponential phase at 37 °C under aerobic conditions.

Vaccines. The MPV vaccine (inactivated Map strain 316F vaccine) was prepared as described previously in Study I (1.1.1). The CPV vaccine (inactivated *Corynebacterium pseudotuberculosis* field strain vaccine) was grown in BHI until mid-exponential phase and was inactivated following the same inactivation protocol as that described for MPV. The MBV vaccine (inactivated Mbv strain 1403 vaccine) was prepared as described in Garrido et al., 2011 (Garrido *et al.*, 2011). The LAV vaccine (live attenuated vaccine) was created by allelic exchange mutagenesis as previously described (Luo, 2018). The attenuated mutant was grown on 7H9 OADC MJ hygromycin (75 µg/ml). The culture was allowed to grow in aerobic conditions at 37 °C, with shaking at 140 rpm until exponential phase (OD_{600} = 0.6-0.8).

Oral challenge. Bovine Map cattle field strain 764 used for challenge was grown on Middlebrook 7H9 broth supplemented with 10% OADC, 0.4%

glycerol and 2 g/l mycobactin J (7H9 OADC MJ) for three weeks and adjusted to 1,5x10^8 CFU/ml based on data from growth curves and plating assuming that 0.7 OD is 1x10^8 bacteria/ml for Map.

Ex vivo assays. Map-K10-GFP (Map-GFP) was grown on 7H9 OADC MJ kanamycin (25 µg/ml) for three weeks. M. bovis (Mbv) strain 2008/2575 was grown on 7H9 OADC for three weeks. *Escherichia coli* (Ecoli), *S. aureus* (Saur) and *C. pseudotuberculosis* (Cpstb) field strains were grown on Brain Heart Infusion (BHI) broth for 24 h in the case of E. coli and Saur and 48 h for Cpstb. Inocula were adjusted after measuring the optical density at 600 nm and based on data from growth curves and plating assuming that 0.7 OD is 1x10^8 bacteria/ml for Map, Mbv and Cpstb, 0.4 OD is 2x10^8 bacteria/ml for Saur and 0.7 OD is 5.6x10^8 bacteria/ml for Ecoli.

1.3.Experimental design

New Zealand White female rabbits of seven weeks of age were purchased from authorized experimental animal dealers (Granja Cunícola San Bernardo, Tulebras, Spain) and left on a 15 day acclimatization period. A schematic representation of the experimental design is shown in Figure 17. Thirty five rabbits were housed in cages being divided into seven groups of five animals each: non-vaccinated and non-challenged group (NC), non-vaccinated challenged group (CC), subcutaneously vaccinated group with the commercially available vaccine Silirum® (CV) and four orally vaccinated groups: live attenuated vaccine (LAV) (Luo, 2018), inactivated Map strain 316F vaccine (MPV) (Study I), inactivated Mbv strain 1403 vaccine (MBV) and inactivated Cpstb field strain vaccine (CPV). Before challenge, at initial

time points, NC and CC, were considered as one group and named NV (non-vaccinated). The NC group was housed in a separate room. The inactivated commercial vaccine was administered subcutaneously as a single dose (12.5 mg of antigen in 1 ml) on day 1. All orally administrated inactivated vaccines were formulated with Quil-A® adjuvant (InvivoGen) at 50 μg/dose. Oral vaccines (LAV, MPV, MBV and CPV) were administered in two doses of 12.5 mg of antigen calculated by wet weight following guidelines for PTB vaccination trials (Hines *et al.*, 2007) in 2 ml for LAV, MPV and CPV (ranging 3,21-4,06 $x10^7$ /dose) and 10^7 CFU for MBV on days 1 and 15. On days 32, 33 and 34 all groups except for NC were challenged orally with one dose of $3x10^8$ CFU of Map strain 764 in 2ml of PBS. Blood sampling for Map PPA-3 ELISA was performed monthly throughout the study. Neutrophils were isolated from blood for ET release assays on weeks 4 (PV1) and 12 (PV3) and for phagocytosis assays on weeks 4 (PV1), 12 (PV3) and 16 (PV4). Also, blood was extracted in heparin for autologous plasma used in phagocytosis assays on weeks 4 (PV1), 12 (PV3) and 16 (PV4). At the end point, 24 weeks after the start of the experiment, all animals were euthanized by intracardiac administration of pentobarbital (Vetoquinol) after deep sedation with xylazine (Calier) and ketamine (Merial). Tissue samples from the *sacculus rotundus* (SR), vermiform appendix (VA), mesenteric lymph nodes (MLN), tongue, tonsils and cecal content from SR were then collected and stored at −20 °C for Map isolation, since this was considered the experimental endpoint parameter.

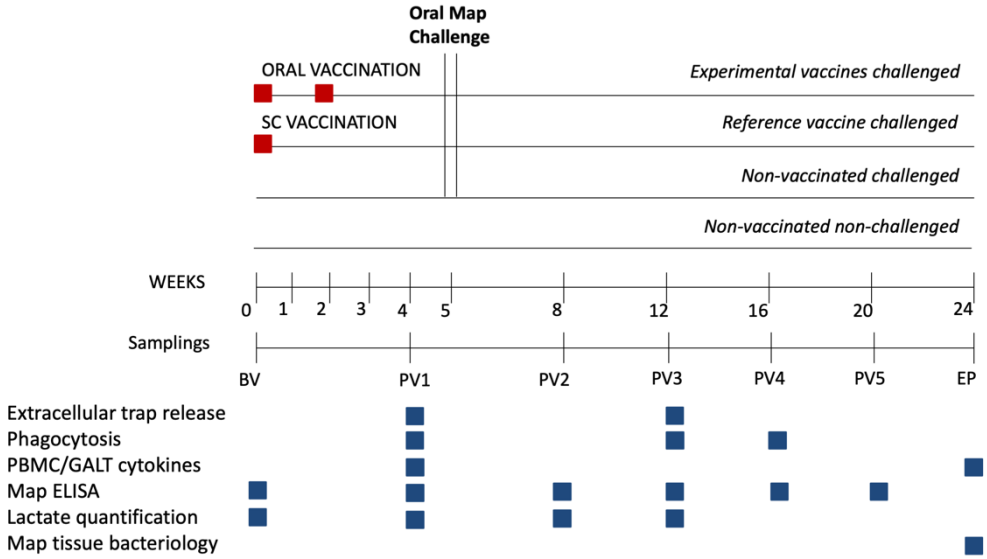

Figure 17. Experimental scheme used to study trained immunity in ex vivo *functional assays and protection* in vivo *after infectious challenge with Map.*

1.4.Interference with bTB Diagnosis

Dunkin Hartley female guinea pigs of 4 weeks of age (n = 15) were purchased from authorized experimental animal dealers (Envigo, Barcelona, Spain). Upon arrival at NEIKER facilities (Derio, Spain), animals were randomly allocated into three experimental groups with 3 animals each: CV, MPV, MBV, LAV and CPV. Animals were fed guinea pig growing pellets and water ad-libitum throughout the experiment. After a 15 day adaptation period, groups MPV, MBV, LAV and CPV were vaccinated orally. 15 days after, those groups received a second dose in identical conditions and the CV animals were vaccinated subcutaneously with the commercial vaccine (Silirum®). All vaccine doses were composed of 12.5 mg of antigen measured by wet weight (Achkar and Casadevall, 2013). The interference

study was performed as described in Study I, M&M (1.2) and Figure 8 for oral and subcutaneous vaccines.

1.5.Lactate quantification assay

Lactate levels in plasma samples were quantified using the Lactate-Glo™ Assay (Promega). The assay was performed following the manufacturer's instructions using 50 µl of samples diluted 1:100 and ten two-fold serial dilutions of a lactate standard run in duplicate in 96-well plates. The assay was performed adding 50 µl of a Lactate Detection Reagent (containing 0.25 µl of Reductase, 0.25 µl of Reductase substrate, 0.25 µl of Lactate Dehydrogenase, 0.25 µl of NADH) and 50 µl of Luciferin Detection Solution. After one hour of incubation at RT in the dark, luminescence was recorded using a plate-reading luminometer (Promega). Lactate quantity was obtained extrapolating sample luminescence values from the standard curve.

1.6.PBMC isolation

Seventeen ml of blood were collected from the auricular artery in Acid Citrate Dextrose (ACD) vacutainer tubes. Red blood cells were eliminated by blood dilution 1:2 with 2.4% Dextran/ 0.9% NaCl. After mixing by tube inversion, tubes were left undisturbed for 30 min until two different phases were visible. The upper clearer layer, rich in leukocytes, was transferred to a 50 ml tube to pellet the cells by centrifugation at 300 g for 10 min. After the supernatant was removed, 10 ml of rabbit leukocyte buffer (NaCl 138 mM, KCl 27 mM, Na_2HPO_4 8.1 mM, KH_2PO_4 1.5 mM, glucose 5.5 mM) was added to the pellet and the cell suspension was layered on top of 10 ml

Histopaque® 1119 (Sigma-Aldrich) and centrifuged at 700 g for 35 min at RT, with no brake. The PBMC layer localized between the saline and the Histopaque® 1119 solution was aspirated and transferred to a new tube for serial washing in saline. PBMCs were counted on a BIORAD TC20 counter and frozen in RPMI supplemented with FBS (40%) and DMSO (10%) at -80 °C until use.

1.7.PMN isolation

PMNs were isolated from the same 17 ml of blood sample passed through Histopaque® 1119 used for PBMC isolation following a modified protocol from Siemsen et al. (Siemsen *et al.*, 2014). After the PBMC layer was aspirated and Histopaque® 1119 was eliminated, PMNs localized in the pellet together with remaining red blood cells were aspirated to a new tube and went through hypotonic lysis with 3 ml of distilled water for 30 s. One ml of KCl 0.6 M was then added and the samples were centrifuged at 300 g for 10 min. PMNs were suspended in rabbit leucocyte buffer and counted on a Bio-Rad TC20™ counter. This isolation protocol yielded PMNs with 94.4 ± 5.9 % purity and 98.68 ± 1.1 % viability (Figure 18).

1.8.Neutrophil phagocytosis

Phagocytosis was performed in suspension following a previously reported method with modifications (Hellebrekers *et al.*, 2017). Briefly, freshly isolated PMNs suspensions were prepared in RPMI without phenol red supplemented with 2% FBS at 10^7 cells/ml. Opsonization of bacteria was performed by incubation in rotation al 37 °C of 400 µl suspensions of a 1:1

dilution of heat-inactivated (52 °C, 15 min) autologous plasma in RPMI with L-glutamine and without phenol red (Gibco). Autologous opsonized and non-opsonized Map-GFP was added to vials with PMNs at MOI 10. Next, PMNs and bacteria were gently mixed and incubated on a wheel shaker at 37 °C at 16 rpm for 20 min.

Live-Dead cells were determined by Hoechst 33258 (Invitrogen) staining 15 min at 4 °C. Cell suspensions were analyzed using a CytoFLEX Flow Cytometer (Beckman Coulter). Details about gating strategy are detailed in Figure 18. Briefly, PMNS were identified according to their specific FSC/SSC patterns. Dead cells were excluded based on their fluorescence in the PB450 channel. Doublets were discriminated using FSC-Area/FSC-Width. PMNs ingesting Map-GFP were identified based on their fluorescence in the FITC channel. Data from the experiments were depicted as percentages of GFP positive PMNs of at least 10,000 events. Flow cytometry data were analyzed with CytExpert v2.3 software (Beckman Coulter). Phagocytosis percentages were expressed as the number of Map- GFP positive cells divided by the total number of live and single PMNs.

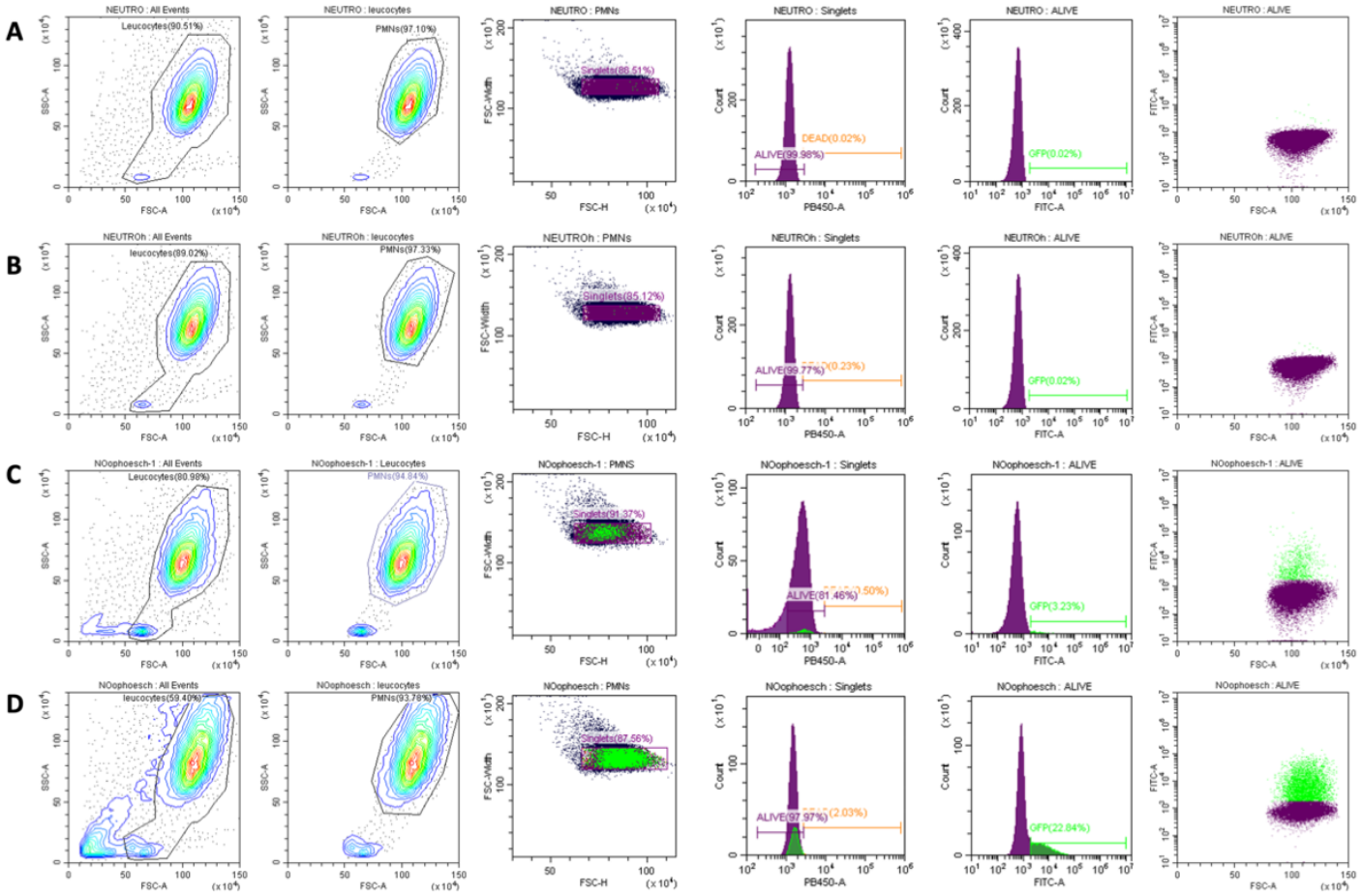

Figure 18. Gating strategy used for the phagocytosis analysis. (A) PMNs without live-dead staining and without Map-GFP (B) PMNs with live-dead staining and without Map-GFP (C) PMNs of the NC group with live-dead staining and with Map-GFP (D) PMNs of the NC group with live-dead staining and with Map-GFP. In the first column details about leucocyte gating based on FSC and SSC; in the second step PMN-gating based on FSC and SSC (purity information); in the third column doublet discrimination strategy; in the fourth column dead cell discrimination strategy; in the fifth column GFP associated PMN selection and in the sixth column a scatter plot based on FITC-FSC of single-alive-PMNs.

1.9.Neutrophil extracellular trap (NET) release quantification

The protocol followed for NET release is a modification of Köckritz-Blickwede et al (Köckritz-Blickwede *et al.*, 2010). Briefly, freshly isolated PMNs were seeded into 96 well plates at a density of $2x10^5$ cells/well. Stimulation was performed with PMA (Sigma-Aldrich) at 25 nM and *S. aureus*, *E. coli*, Cpstb, Mbv and Map a multiplicity of infections (MOI) of 5. Plates were incubated for 4 h at 37 °C, 5% CO_2. Non-stimulated PMNs were used as a negative control. The NETs generated by PMNs were digested with 500 mU/ml of s7 nuclease (Roche) for 10 min at 37 °C, 5% CO_2. Nuclease activity was stopped with 5 mM EDTA and culture supernatants were collected and stored at 4 °C, ON. Total DNA was extracted from non-stimulated neutrophils with DNazol supplemented with 1% polyacryl carrier (Molecular Research Center) following the manufacturer's instructions. Extracted DNA was solubilized in TE buffer. Both NETs and genomic DNA was quantified using the Quant-iTTM PicoGreen® assay (Thermofisher) according to the manufacturer´s instructions. The plates were read in a fluorescence microplate reader (Synergy HTX, Biotek) with filter settings at 488 nm excitation and 520 nm emission. Data from controls with no cells and non-stimulated cells were subtracted. The percentage of released NET-DNA was calculated by dividing the amount of isolated NET-DNA by the DNA genomic content and NETosis levels were expressed as percentages.

1.10. Neutrophil extracellular trap (NET) visualization

Visualization was performed on NETs developed on 16 well chamber slides (Thermo Scientific) in identical conditions as those described for NET

quantification in the 96 well plates. After the 4 h incubation period, PMN preparations were fixed with formaldehyde 4% for 15 min. Two washes with PBS were performed and chambers were kept in PBS at 4 °C until staining was performed. Before staining, cells were permeabilized for 15 min with PBS 0.1% TRITON 100 and blocked with PBS 1% Goat serum, 0.05% Tween 20 and 3% BSA. The immunofluorescence staining was performed with the mouse anti-pan-histone (Merk MAB3422) (1:200) ON at 4 °C. After 3 washing steps with PBS, cells were incubated with anti-mouse Alexa Fluor 594 (Invitrogen) (1:500) for 30 min at RT. After 3 washing steps, cover slips were mounted on the slides with a drop of mounting medium containing DAPI. Micrographs were taken with on a fluorescence microscope (Leica-DMi8).

1.11. Map culture and sonication

Bovine Map cattle field strain 764 strain used for *in vivo* challenge was sonicated and used for *in vitro* stimulation. Briefly, Map was grown in 7H9 OADC MJ broth for (approximately three weeks at 37 °C in aerobic conditions) to an optical density of 0.4 OD at 600 nm. The culture was centrifuged at 10,000 *g* for 20 min and the pellet was washed twice with cold PBS. The pellet was suspended in PBS and sonicated three cycles of 5 min at 18W on ice in a Vibra Cell 75186 sonicator. Protein concentration was determined on a spectrophotometer NanoDrop® and was adjusted to 100 µg/ml.

1.12. PBMC stimulation

PBMCs were thawed, washed twice and incubated in complete medium (RPMI 1640 with 10% FBS) at 37 °C and 5% CO_2. The cells were then washed, counted, suspended in complete medium and seeded at $1x10^6$ cells/well on 24 well plates and incubated 1 h at 37 °C and 5% CO_2 prior to stimulation. Stimulation was performed with Concanavalin A (Sigma-Aldrich) (ConA) (2.5 µg/ml) (Data not shown), Map sonicate (SM) (10 µg/ml) or left untreated (PBS). Cultures were incubated for 24 h at 37 °C and 5% CO_2 and centrifuged at 300 g for 8 min for RNA extraction.

1.13. RNA isolation and conversion to cDNA of PBMCs and gut associated lymphoid tissue

RNA isolation from basal and stimulated PBMCs and gut associated lymphoid tissue (GALT; *sacculus rotundus*) was performed using the RNeasy® minikit (Qiagen). Briefly, RLT buffer supplemented with 2-mercaptoethanol was added to $5x10^6$ pelleted cells (350 µl) or to 20 mg of tissue (600 µl). Disruption and homogenization were performed on Tissuelyser II (Qiagen) for both cells (one cycle of 30 Hz for 9 min) and tissues (two cycles of 20-30 Hz for 2 min with a stainless-steel bead 7 mm per tube). All samples were stored at -80 ºC until use. From this point, the RNA isolation procedure followed the manufacturer's instructions. The RNA was treated with DNAse I (Invitrogen) (1 µl of Buffer 10x, 1 µl of DNAse, 0.5 µl of RNAse out, the sample volume and DEPC water up to 10 µl of final reaction volume for a maximum of 1-2 µg of RNA). DNAse treated RNA yield was quantified using a NanoDrop® spectrophotometer. All the samples

were adjusted to 50 ng/ml RNA concentration and were reverse transcribed to cDNA.

cDNA synthesis and RT minus controls of RNA from GALT and PBMCs were performed on a final volume of reaction 10 µl and 20 ng/µl of RNA concentration. The reaction contained 4 µl of sample, 0.5 µl of Random Primers, 0.5 µl Oligo Dt, 0.75 µl of DEPC-water (1.25 µl for RT- controls), 2 µl of Buffer 5x, 1 µl of MgCl2, 0.5 µl of nucleotide mix, 0.25 µl of RNAsin, and 0.5 µl of GoScript ™ reverse transcriptase (0 µl for RT- controls) using the GoTaq® 2-Step RT-qPCR System (Promega). The RT thermocycler program was the one recommended by the manufacturer (25 °C 5 min anneal, 42 °C 60 min extend, 70 °C 15 min inactivate, 4° C ∞ chill).

Primers for transcripts of IFN-γ, TNF, IL-2, IL1-β, IL-4, IL-12B, IL-10 and IL-23A cytokines and *IPO8, PGK1, RPLP0, UBE2D1, YWHAZ* reference genes were designed using the IDT online PrimerQuest Tool following MIQE guidelines (Bustin *et al.*, 2009). Primer sequences are detailed on Table 6.

Table 6. Primer sequences for each gene, amplicon characteristics and PCR conditions.

Target gene (amplicon size)	Sequences	TmºC	GC%	PC (µM)
IFN-γ	5′TACTTTGGCATGGACTGTATT3′	58.6	38	0.7
(122)	5′CATAAAGCATGGTGGAGAA3′	58.7	42.1	0.7
IL-1β	5′CTCCTGCCAACCCTACAACA3′	57.1	55	0.3
(152)	5′GGACGGGTTCTTCTTCAA3′	52,4	50	0.3
IL-2	5′TATATGCCCAAGAAGGTCACA3′	61.9	42.8	0.4
(205)	5′TGGTAACTGTCTCATCGTATTCAC3′	61.8	41.6	0.4
IL-4	5′CAGTTCTACCTCCACCACAAG3′	61.2	52.3	0.2
(90)	5′GTTCCTGTCGAGTCCTCTC3′	58.9	57.8	0.2
IL-10	5′GCGACAATGTCACCGATTT3′	63.6	47.3	0.7
(98)	5′TGTAGACGCCTTCCTCTTG3′	60.6	52.6	0.7
IL-12B	5′CATCAGAGACATCATCAAACCT3′	60.6	40.9	0.5
(64)	5′GGAATTCTTCAATGGCTTCA3′	61.6	40	0.5
TNF	5′CTAGCCCACGTAGTAGCAAAC3′	60.4	52.3	0.5
(154)	5′AGAGAACCTGGGAGTAGATGAG3′	60.3	50	0.5
IL23A	5′CAGCAGCTCTCCCAGAA3′	56.2	58.8	0.5
(170)	5′AACTGAGTGTTGTCCCTTAGTC3′	55.8	45.5	0.3
RPLP0	5′CGTGAGAGTGACATCGTCTTTA3′	61.9	45.4	0.3
(111)	5′GGATGATCTTAAGGAAGTAGTTGGA3′	62.3	40	0.3
PGK1	5′TGGGCAAGGATGTTCTGTT3′	63.2	47.3	0.4
(112)	5′ACATGAAAGCGGAGGTTCT3′	61.3	47.3	0.4
YWHAZ	F 5′GCCCTTAACTTCTCTGTGTTCT3′	60.4	45.4	0.4
(136)	5′GCGTGCTGTCTTTGTATGATTC3′	63.5	45.4	0.4
IPO8	5′AGCTAGATCGTGCTGGGTA3′	60	52.6	0.3
(100)	5′GATCAGGCTCTTCTTGGCTAAT3′	62.5	45.4	0.2
UBE2D1	F 5′CCTGTGGGAGATGACTTGTTC3′	63.5	52.3	0.5
(82)	R 5′GGAAGAAGACTCCACCTTGATA3′	61.1	45.4	0.5

*Tm: primer melting temperature; PC: primer concentration. For primer design, exon-exon junctions were taken into account, with at least one of each primer pairs between two exons. Target transcript sequences were obtained from the NCBI database. Dimers and hairpins were checked with IDT Oligo Analyzer Tools (*https://eu.idtdna.com/site/account/login?returnurl=%2Fcalc%2Fanalyzer*) and those with high possibilities of conforming secondary structures were discarded. Primer selection parameters were set to be: no more than 3 Gs or Cs in the last five nucleotides of the 3'end, CG% between 40-60%, primer size between 17-25 nucleotids, Tm differences between primer pairs of less than 2ºC and product size 100-200 bp but down to 64 in a case where no suitable primers could be identified. Primers were ordered from Sigma-Aldrich and each pair was cross-tested for optimal working concentrations ranging 0.2-0.7 µM.*

1.14. Cytokine expression level quantification

Fluidigm (Specific target amplification (STA) and qPCR using the BioMarkTM HD system) for cytokine expression level determination was performed at SGIker UPV-EHU. The commercially available Multiplex PCR kit (Qiagen) was used for the STA of the samples in a final reaction volume of 5 µl, containing 1.25 µl of the cDNA and 100 nM of primer concentration.

The thermocycler program performed for STA consisted on a stage 1: 95 °C for 15 min and a stage 2: 12 cycles at 95 °C for 15 s followed for 4 min at 60 °C, at the end, a final step at 4 °C ∞. Then, STA samples were treated with Exonuclease I (Thermo Scientific) adding 2 µl of a master mix (1.4 µl DEPC water, 0.2 µl Exonuclease I Reaction Buffer, 0.2 µl Exonuclease I (20 units/ µl), to each 5 µl of STA sample and the following program was applied: 37 °C for 30 min (Digestion), 80 °C for 15 min (Inactivation Exo I) and 4 °C ∞ (chill). Then STAs were diluted 1:20 in TE (10 mM Tris, 0.1 mM EDTA).

The expression analysis of the pre-amplified Exonuclease I-treated cDNA was carried out in the qPCR BioMark HD (Fluidigm) nanofluidic system in combination with 192.24 Dynamic Arrays IFC (192 samples, 24 assays). SsoFast^{TM} EvaGreen® Supermix with Low ROX (Bio-Rad Laboratories). Final testing conditions for each pair of primers are detailed on Table 6. The 9 target genes were migrated in duplicates. PCR (GE 192x24 Fast PCR + Melt v2) protocol was performed: Stage 1 (Hot start): 95 °C for 5 s, stage 2 (Ramp rate 5.5 ºC/s): 30 cycles at 96 °C for 5 s and 60 °C for 20 s and stage 3 (Melting Curve): 60 ºC for 3 s and from 60 ºC to 95 ºC (ramp rate slow 1 ºC/3 s).

Cts (Cycle threshold) and Cqs (Quantification Cycle) results were analyzed using the Fluidigm Real-Time PCR Analysis Software version 4.1.3. Thresholds were manually adjusted for each primer pair. Apart from duplicates of STA samples, a no template control (NTC), 8 RT minus and five serial 1/5 dilutions from a concentrated sample for the efficiency analysis were included in the run. The MultiD GenEx vs 6.1 software was used for calculating: qPCR efficiency, efficiency correction of Cts, replicate analysis and mean calculation, reference gene stabilization analysis, normalization of Cqs using the best reference genes and relative expression calculation using the comparative $2^{-\Delta\Delta CT}$ method with the efficiency correction. More information on the analysis for the selection of the best reference gene combinations s for each sample type is detailed in Figures 19-21.

A **NORMFINDER**

INTRA-GROUP VARIATION

GROUP	RPLP0	PGK1	IPO8	UBE2D1	YWHAZ
1	0,1683	0,1042	0,0302	0,0353	0,0058
2	0,0122	0,0449	0,0067	0,0135	0,0041
3	0,0464	0,0873	0,0378	0,008	0,0059
4	0,0034	0,0397	0,073	0,0279	0,0076
5	0,0112	0,0257	0,0363	0,0323	0,0058
6	0,4562	1,7302	0,4972	0,014	0,014
7	0,0189	0,0102	0,0066	0,0215	0,0054

INTER-GROUP VARIATION

GROUP	RPLP0	PGK1	IPO8	UBE2D1	YWHAZ
1	0,0741	-0,1965	0,1579	0,1464	-0,1819
2	-0,0754	0,0805	0,0968	0,0003	-0,1022
3	-0,026	0,024	-0,1301	-0,0969	0,229
4	-0,1089	0,0837	0,1206	-0,0144	-0,081
5	-0,031	0,1238	-0,1462	-0,0216	0,0749
6	0,1406	-0,2587	0,0242	-0,0896	0,1835
7	0,0266	0,1432	-0,1232	0,0757	-0,1222

B

Best gene: YWHAZ, SD: 0,0592

Best Combination of two genes: YWHAZ + UBE2D1, SD: 0,0492

Gene Name	SD	Acc. SD	SD	0,1993
YWHAZ	0,1993	0,1993		
RPLP0	0,2054	0,1431	Best Gene	YWHAZ
IPO8	0,234	0,1232		
UBE2D1	0,2738	0,115		

BEST NUMBER OF GENES 4: YWHAZ, RPLP0, IPO8 AND UBE2D1

C

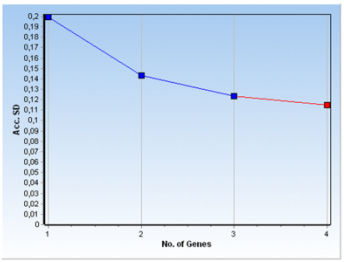

D **GENORM**

Gene Name	M-Value
PGK1	0,41026624
UBE2D1	0,3222696
YWHAZ	0,29957556
RPLP0	0,2594786
IPO8	0,2594786

Figure 19. Best reference gene combination analysis for normalization of RT-qPCR expression in PBMC samples at PV1 (A) NormFinder Intra-group and inter-group variation results. PGK1 gene showed high intra-group variation (>1) in the group 6. All the genes showed low inter-group variation. (B) NormFinder provided best gene, best combination of two genes and best number of reference genes information after elimination of PGK1, the less stable gene. (C) NormFinder graph representation of the best number of reference genes for normalization. (D) GeNorm analysis results. In this case all five genes showed high stability M values (<0.5). UBE2D1, YWHAZ, RPLP0 and IPO8 resulted the most suitable combination of refence genes.

A **NORMFINDER**

INTRA-GROUP VARIATION

GROUP	RPLP0	PGK1	IPO8	UBE2D1	YWHAZ
8	0,0352	0,7615	0,1016	0,0972	0,0127
9	0,0042	0,7171	0,0297	0,7916	0,0042
10	0,0113	0,5967	0,0703	0,0078	0,0938
11	0,0114	0,367	0,038	0,258	0,0025
12	0,0173	1,5236	0,2161	0,2885	0,0032
13	0,0011	0,0888	0,015	0,285	0,0011
14	0,0158	0,048	0,1075	0,1888	0,0043
15	0,0022	0,4484	0,0219	0,1843	0,0158
16	0,0051	0,3938	0,0139	0,6346	0,0038
17	0,0081	0,2347	0,1658	0,1034	0,0011
18	0,0013	0,3623	0,0047	0,2272	0,0047
19	0,02	0,8371	0,0074	0,3378	0,0833
20	0,0044	0,3953	0,0703	0,2661	0,0639
21	0,0495	0,2595	0,0248	0,0636	0,0142
22	0,0243	0,2453	0,2022	0,3008	0,0313
23	0,005	0,1625	0,0282	0,5198	0,009
24	0,0196	0,2367	0,0095	0,3069	0,0658
25	0,0545	0,2687	0,0178	0,3248	0,0003
26	0,0085	0,4509	0,0425	0,3538	0,0125
27	0,0096	0,6041	0,5031	0,1621	0,0052
28	0,0247	0,3973	0,0019	0,1454	0,0077

INTER-GROUP VARIATION

GROUP	RPLP0	PGK1	IPO8	UBE2D1	YWHAZ
8	-0,0345	0,1349	-0,0017	0,0567	-0,1554
9	-0,1554	0,1091	-0,1506	0,2247	-0,0279
10	0,0221	0,009	0,2172	-0,1455	-0,1028
11	0,0673	0,266	0,0822	-0,3979	-0,0176
12	-0,0304	0,4033	0,007	-0,1862	-0,1938
13	-0,1709	0,1903	0,0789	-0,0075	-0,0908
14	0,3102	-0,3317	0,0803	-0,1489	0,0902
15	0,1004	0,0473	-0,0705	-0,0155	-0,0617
16	-0,0978	-0,1561	-0,111	0,3094	0,0556
17	-0,0063	-0,2581	0,1219	0,0071	0,1353
18	0,1855	0,1967	-0,3319	-0,1437	0,0934
19	0,0266	0,2798	-0,1337	-0,1091	-0,0636
20	0,0299	0,5059	-0,2628	-0,0961	-0,1768
21	0,1646	-0,2854	-0,0399	0,038	0,1226
22	0,1137	0,028	0,0742	-0,1212	-0,0947
23	-0,1999	-0,6469	0,0868	0,5905	0,1696
24	-0,1565	-0,4701	0,2154	0,167	0,2442
25	0,0217	-0,2095	0,0532	0,0053	0,1293
26	-0,1587	-0,1889	0,1523	0,126	0,0692
27	-0,1627	0,4748	-0,0076	-0,0856	-0,2189
28	0,131	-0,0982	-0,0598	-0,0675	0,0945

B

Best gene: YWHAZ, SD: 0,1607

Best Combination of two genes: YWHAZ + RPLP0, SD: 0,1356

Gene Name	SD	Acc. SD	SD	0,1384
YWHAZ	0,1384	0,1384		
RPLP0	0,2403	0,1386	Best Gene	YWHAZ
IPO8	0,288	0,1333		
UBE2D1	0,4952	0,1591		

Best number of genes: 3: YWHAZ, RPLP0 AND IPO8

C

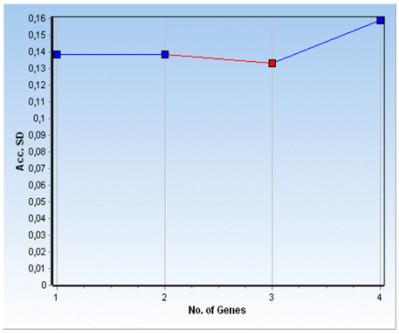

D **GENORM**

Gene Name	M-Value
PGK1	0,5452308
UBE2D1	0,41544932
IPO8	0,30437022
RPLP0	0,27670814
YWHAZ	0,27670814

Figure 20. Best reference gene combination analysis for normalization of RT-qPCR expression in PBMC samples at PV1 after 24h stimulation. (A) NormFinder Intra-group and inter-group variation results. PGK1 gene showed a high intra-group variation (>1) in the group 12 and the highest inter-group variation. (B) NormFinder provided information about best gene, best combination of two genes and best number of reference genes after elimination of PGK1, the less stable gene. (C) NormFinder graph representation of the best number of reference genes for normalization. (D) GeNorm analysis results. PGK1 gene showed insufficient stability M value (>0.5). YWHAZ, RPLP0 and IPO8 resulted the best combination of reference genes.

A **NORMFINDER**

INTRA-GROUP VARIATION

GROUP	RPLP0	PGK1	IPO8	UBE2D1	YWHAZ
1	0,054	0,0317	0,1988	0,0034	0,001
2	0,0187	0,0086	0,03	0,0249	0,0233
3	0,0459	0,031	0,05	0,0256	0,0048
4	0,0458	0,0144	0,1639	0,0045	0,0062
5	0,0397	0,0663	0,1354	0,0175	0,0056
6	0,0178	0,0162	0,0518	0,0076	0,0237
7	0,0233	0,0564	0,0531	0,0033	0,0037

INTER-GROUP VARIATION

GROUP	RPLP0	PGK1	IPO8	UBE2D1	YWHAZ
1	0,126	0,0637	-0,4896	0,1949	0,105
2	-0,1915	-0,0592	0,3374	0,0344	-0,1211
3	-0,0716	-0,0128	0,0796	0,0137	-0,0089
4	0,031	0,0167	0,0288	-0,0661	-0,0103
5	-0,1075	-0,0124	0,1359	0,0109	-0,0269
6	-0,0183	-0,0126	-0,0173	-0,0528	0,1011
7	0,2319	0,0167	-0,0748	-0,1349	-0,0389

B

Best gene: YWHAZ, SD: 0,1067

Best Combination of two genes: YWHAZ + PGK1, SD: 0,1023

Gene Name	SD	Acc. SD	SD	0,0815
YWHAZ	0,0815	0,0815		
UBE2D1	0,1202	0,0726	Best Gene	YWHAZ
PGK1	0,1424	0,0678		
RPLP0	0,223	0,0755		
IPO8	0,3968	0,0997		

BEST NUMBER OF GENES: 3, YWHAZ, UBE2D1 Y PGK1

C

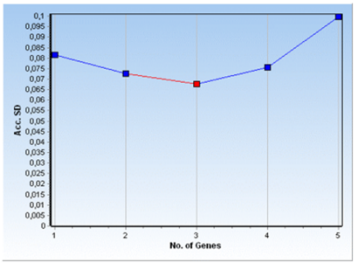

D **GENORM**

Gene Name	M-Value
IPO8	0,28872698
UBE2D1	0,20994529
RPLP0	0,18509162
PGK1	0,17329171
YWHAZ	0,17329171

Figure 21. Best reference gene combination analysis for normalization of RT-qPCR expression in GALT samples. (A) NormFinder Intra-group and inter-group variation results. Al five genes are highly stable. (B) NormFinder provided information about stability values not considering groups, best reference gene, best combination of two genes and best number of reference genes. (C) NormFinder graph representation of the best number of reference genes for normalization. (D) GeNorm analysis results. In this case all five genes showed high stability M<0.5. Although the best number of recommended reference genes was three, as the difference in their M values was small, the normalization was performed with YWHAZ, PGK1, UBE2D1 and RPLP0.

1.15. PPA-3 Enzyme Linked Immunosorbent Assay (ELISA)

Homemade indirect ELISA was performed using Map protoplasmatic antigen 3 (PPA-3) (Allied Lab) as previously described (Arrazuria *et al.*, 2016b) (Study I, M&M 1.1.3).

1.16. Map isolation from tissues

For culture on Herrold's Egg Yolk Medium (HEYM), 0.5 g of collected tissues were processed. Mesenteric lymph node was spliced in tiny pieces and

weighed, whereas vermiform appendix and SR were scraped for collection of mucosa and weighed and samples were processed as described previously (Arrazuria *et al.*, 2015b). Briefly, hexadecylpyridinium chloride (Sigma-Aldrich) 0.76% decontaminated suspensions were centrifuged at 2885 g during 10 min. The supernatant was discarded and the pellet was washed once with sterile water. After a new centrifugation step in the same conditions the pellet was suspended in 2 ml of water and four drops/tube were seeded. All seeded tubes were incubated at 37 °C and checked for Map growth at 8, 12, 16 and 20 weeks.

For culture on 7H11 OADC PANTA TiKa MOPT (Bull *et al.*, 2017), 100 mg of collected tissues were sliced and macerated on a Stomacher®. Afterwards, these were treated with TLB buffer supplemented with collagenase and trypsin, thoroughly mixed and incubated with shaking ON at 37 °C. The digested tissue was centrifuged at 14,000 g for 10 min. The pellet was then re-suspended in 10 ml of TiKa-Kic (TiKa Diagnostics) and incubated for 24 h at 37 °C with gentle shaking. Samples were centrifuged at 10,000 g for 15 min at RT. The pellet was re-suspended in 0.2 ml of sterile PBS and spotted onto 7H11 OADC PANTA TiKa-supplement A MOPT agar plates. Plates were incubated at 37 ± 1 °C and checked for Map growth at 4, 8 and 12 weeks.

Colonies isolated on both medium were confirmed by a real time multiplex PCR detecting *IS900* and *ISMap02* Map sequences (Sevilla *et al.*, 2014). In order to rule out LAV growth in tissues instead of the Map

challenging strain 764, tissues from animals belonging to the LAV vaccinated group were also seeded on 7H9 OADC MJ with hygromycin (75 µg/ml).

1.17. Statistical analyses

The data were assessed for normal distribution with the Shapiro–Wilk test and for homogeneity with the Bartlett's test. For the statistical analysis of comparison between means of variables with a normal distribution, Student's t test or ANOVA was used. For variables with a non-normal distribution, the Mann–Whitney U test or Kruskal-Wallis test with the post-hoc Dunn's multiple comparison test were used. Pearson ($\rho x,y$) coefficient was calculated for correlation between variables.

At PV1, sampling is performed before the challenge and therefore NV control is used as a sum of CC and NC, as at this time of the experiment both groups are non-vaccinated groups.

The efficiency of the amplification of each pair of primers was calculated from the slope of the line resulting from the linear regression of the serial dilutions GenEx software corrects the raw Cqs using the efficiencies. Reference Gene stability analysis and normalization were also performed using the GenEx software, which uses NormFinder (Andersen *et al.*, 2004) and GeNorm (Vandesompele *et al.*, 2002) algorithms. For normalization, the geometric mean of the best combination of reference gene Cqs of each sample was subtracted to each sample Cq for every target gene.

$2^{-\Delta\Delta CT}$ quantification method was performed with respect to the NC group for basal PBMC and SR expression, and with respect to non-stimulated

PBMCs for stimulated PBMCs. The logarithmic transformation of the relative quantities Log2 RQ has been used as input for Fold change, calculation statistical analysis and plot and graph representation. The absolute Fold Changes were calculated using the expression: log2Fold change.

For the PCA analysis the following parameters were taken into account: Phagocytosis of opsonized and non-opsonized Map-GFP at PV1, PV3 and PV4; NETosis percentages against Map, Cpstb, Mbv, Ecoli and Saur at PV1 and PV3; anti-PPA3-IgG/IgM ELISA results at PV1, PV2, PV3, PV4 and PV5; total serum IgA levels at PV1; serum lactate levels at PV1, PV2 and PV3; IFN-γ, IL-10, IL-2, IL-4, IL-12B, IL-1β, TNF and IL-23A cytokine expression of PBMCs at PV1; IFN-γ, IL-10, IL-2, IL-4, IL-12B, IL-1β, TNF and IL-23A cytokine expression of PBMCs stimulated with Map sonicate for 24h at PV1 and IFN-γ, IL-10, IL-2, IL-4, IL-12B, IL-1β, TNF and IL-23A cytokine expression of GALT at EP of the experiment.

All the statistical tests were performed using R studio desktop (version 1.2.5033). (RStudio Team (2019). RStudio: Integrated Development for R. RStudio, Inc., Boston, MA URL http://www.rstudio.com/.) A p-value <0.05 was considered statistically significant.

Results

In order to assess mucosal and systemic immunity activation and disease protection through oral delivery we tested mycobacterial inactivated and live attenuated vaccines and a non-mycobacterial inactivated vaccine in the rabbit Map infection model. Specifically, an inactivated Map vaccine (MPV), a live attenuated vaccine (LAV), an *M. bovis* inactivated vaccine (MBV) and a *C. pseudotuberculosis* inactivated vaccine (CPV). In our experimental design, the isolation of PMNs from this combination of vaccinated animals along with homologous and heterologous stimuli would also permit assessing if these inactivated vaccines are capable of exerting training effects indicative of heterologous protection.

2.1. The oral prototypes did not show interference with bTB diagnosis

The skin test interference analysis in guinea pigs revealed that orally vaccinated animals did not show skin reaction to A or B PPD, whereas CV animals showed reactions for both tuberculins. This test confirms that observed in the Study I (2.2): that the orally administered experimental vaccines do not trigger a detectable specific DTH cellular response when applying the skin test (Supplementary figure).

2.2. Oral vaccination increases phagocytosis of Map by neutrophils

One of the main mechanisms that contribute to bacterial clearance by PMNs is phagocytosis so we assessed if oral vaccination would affect PMN phagocytic capacity. PMNs were isolated at different time points and exposed to Map-GFP *ex vivo*. Oral LAV and CPV and subcutaneous CV vaccination

showed enhanced neutrophil phagocytosis against non-opsonized Map-GFP 4 weeks after first dose of vaccine administration (PV1) compared to non-vaccinated animals (NV) (Figure 22A). This activity was maintained after Map challenge in some cases. At PV3 (12 weeks later) for CPV and CV vaccinated animals (Figure 22C) and even after 16 weeks (PV4), a slight effect was still conserved for CV (Figure 22E). Interestingly, CPV, a non-mycobacterial vaccine was able to activate PMNs for Map phagocytosis indicating that heterologous activation is possible.

Phagocytosis against opsonized Map-GFP with autologous plasma was increased in PMNs isolated from CV, LAV and MBV vaccinated animals 4 weeks after the first dose at PV1 (Figure 22B). PMNS from CV and MPV animals showed enhanced phagocytosis after Map challenge at PV3 (Figure 22D), which was only maintained by CV PMNs at PV4 (Figure 22F).

Map-GFP phagocytosis by PMNs correlated positively with anti-PPA3-antibody levels under opsonized conditions, as expected, at all sampling points (PV1: $\rho=0.77$, $p<0.0001$; PV3: $\rho=0.83$ $p<0.0001$ and PV4: $\rho=0.76$, $p<0.0001$). CV was the group with the highest phagocytic activity and Map-antibody titres. Oral vaccination was less efficient at maintaining a long-lasting elevated specific phagocytic activity of circulating PMNs and at boosting a specific humoral response (IgG and IgM) (Figure 22G).

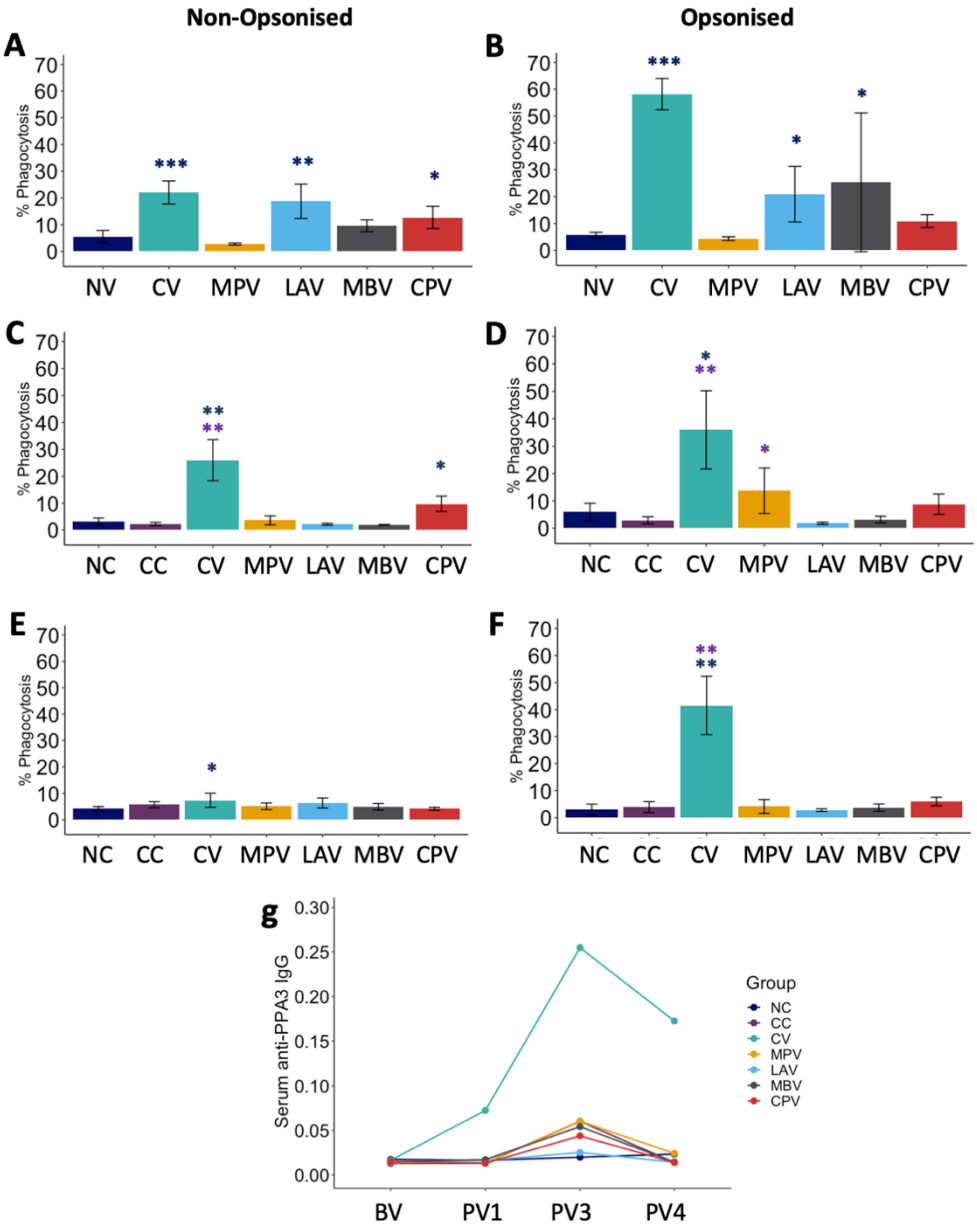

Figure 22. PMN phagocytosis levels against (A, C, E) non-opsonized and (B, D, F) opsonized Mycobacterium avium *subsp.* paratuberculosis *(Map)-GFP at (A, B) PV1 (1 month after first dose vaccination), (C, D) PV3 (2 months after challenge) and (E, F) PV4 (3 months after challenge) of non-vaccinated and non-challenged (NV: NC+CC at BV and PV1); non-challenged (NC), non-vaccinated and challenged (CC), commercial Map inactivated vaccine (CV), killed Map strain oral vaccine (MPV), live attenuated vaccine (LAV), killed* Mycobacterium bovis *vaccine (MBV) and killed* Corynebacterium pseudotuberculosis *vaccine (CPV). (G) Serum anti-PPA3 IgG levels. Blue asterisks represent significant differences compared to the NC group, purple asterisks compared to the CC group and signification levels are *<0.05, **<0.01, *** <0,001.*

2.3. Vaccination and Map challenge induce extracellular trap release by neutrophils

PMNs from healthy animals are also capable of releasing ETs against pathogens such as *S. aureus* (Pilsczek *et al.*, 2010), *E. coli* (Petretto *et al.*, 2019), so we assessed if *ex vivo* NET formation was affected by vaccination and challenge against non-mycobacterial and mycobacterial microorganisms and NETosis levels were represented on a heat-map (Figure 23A).

PMNs isolated from animals vaccinated with MPV showed enhanced NET release against Map and Mbv (heterologous effect) at PV1 compared to NV (Figure 23C and 23E). At this same time point all other tested vaccines showed decreased NET release compared to NV, suggesting that this mechanism is not predominant at this time point in those groups.

At PV3 (two months after challenge and three months after first dose vaccination), NET release was increased in PMNs isolated from CV and CPV animals against Map (Figure 23D), from CPV animals against Mbv (again heterologous training effect) (Figure 23F) and from MPV animals against Cpstb (also heterologous) (Figure 23H).

Interestingly, PMNs from MBV (Figure 23E and 23F) and CPV (Figure 23G and 23H) animals showed an inhibition on ET release when stimulated *ex vivo* with the microorganisms that the vaccines were targeted (secondary exposure), Mbv and Cpstb, respectively. This inhibitory effect was observed in both time-points PV1 and PV3.

ET release against *S. aureus* (Figure 23I) and *E. coli* (Figure 23H) was generally increased at PV3 (2 months after Map challenge and 3 months after first dose vaccination) in all challenged groups.

ET release against Map and Mbv positively correlated both in PV1 and PV3, (PV1: $\rho=0.8$ $p<0.001$ and PV3: $\rho=0.57$, $p<0.0001$), although at PV3 correlation strength dropped, suggesting that although vaccination could exert innate cross protective effect in PMNs, *in vivo* challenge with Map could have reverted this effect or further changed some group's PMNs behaviour against mycobacteria.

2.4. Vaccination enhances PMN aggregation trapping and surrounding Map in vitro

NETosis was also observed by microscopy (Figure 23B). PMN behavior among experimental groups from PV1 varied after in vitro incubation for 4h as seen in micrographs with Map-GFP (Figure 24) and Map (Figure 25). PMNs from vaccinated groups aggregated around Map, arranging to form bigger and more compact clusters structures compared to the NV group. The observed aggregates contained Map-GFP bacteria forming clumps surrounded by PMNs and skeins of chromatin threads. In the NV group, Map-GFP presence outside of PMN aggregates resulted more frequent and the observed clusters of PMNs were smaller and less compact

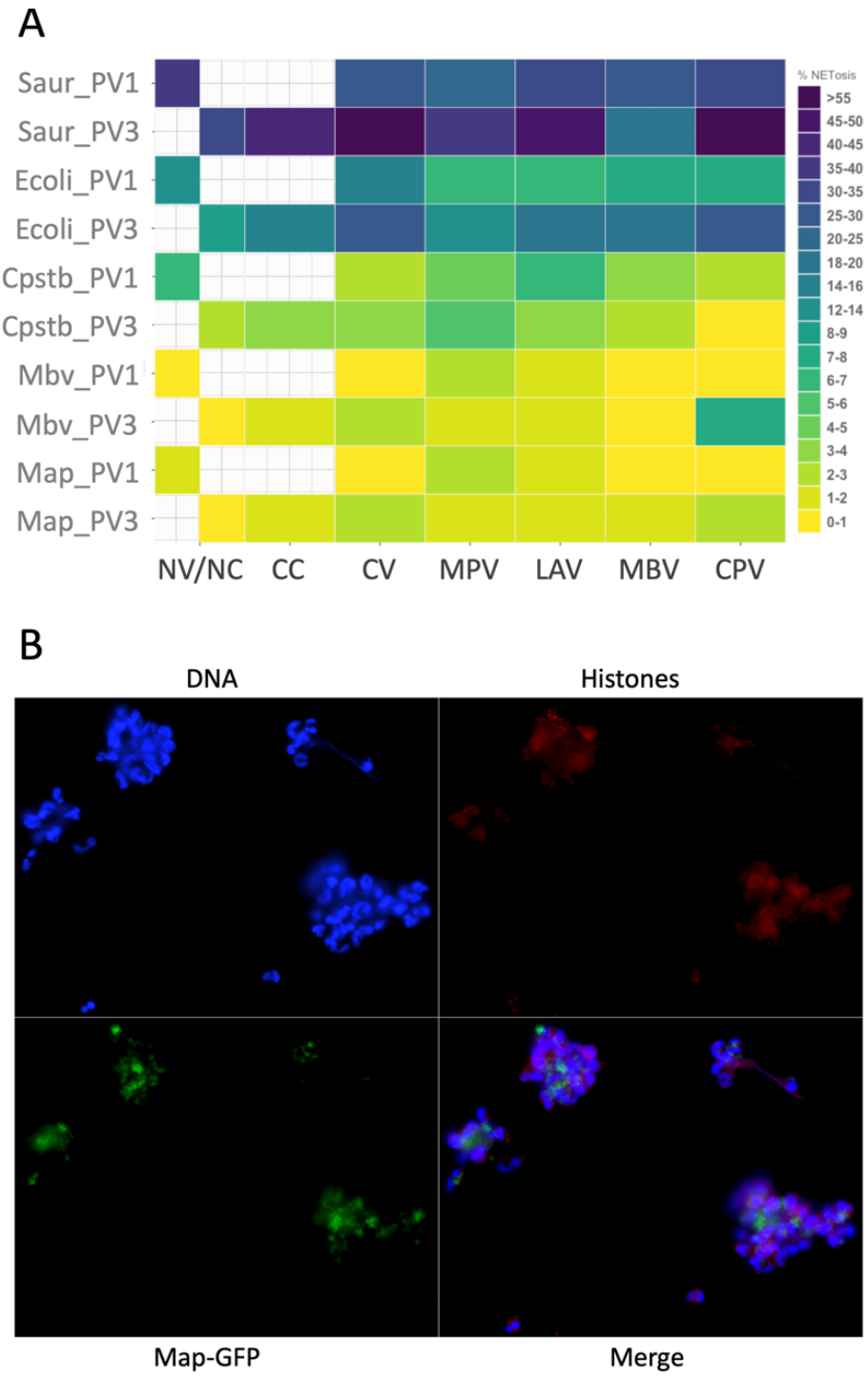

Figure 23. Neutrophil extracellular trap (NET) release levels against Map, Mbv, Ecoli, Saur and Cpstb of animals vaccinated with commercial Map vaccine (CV), killed Map oral vaccine (MPV), live attenuated vaccine (LAV), killed Mbv vaccine (MBV) and killed Cpstb vaccine (CPV). (A) Heatmap representation of % NETosis data. (B) Micrograph image (40x) showing ET release against Map-GFP.

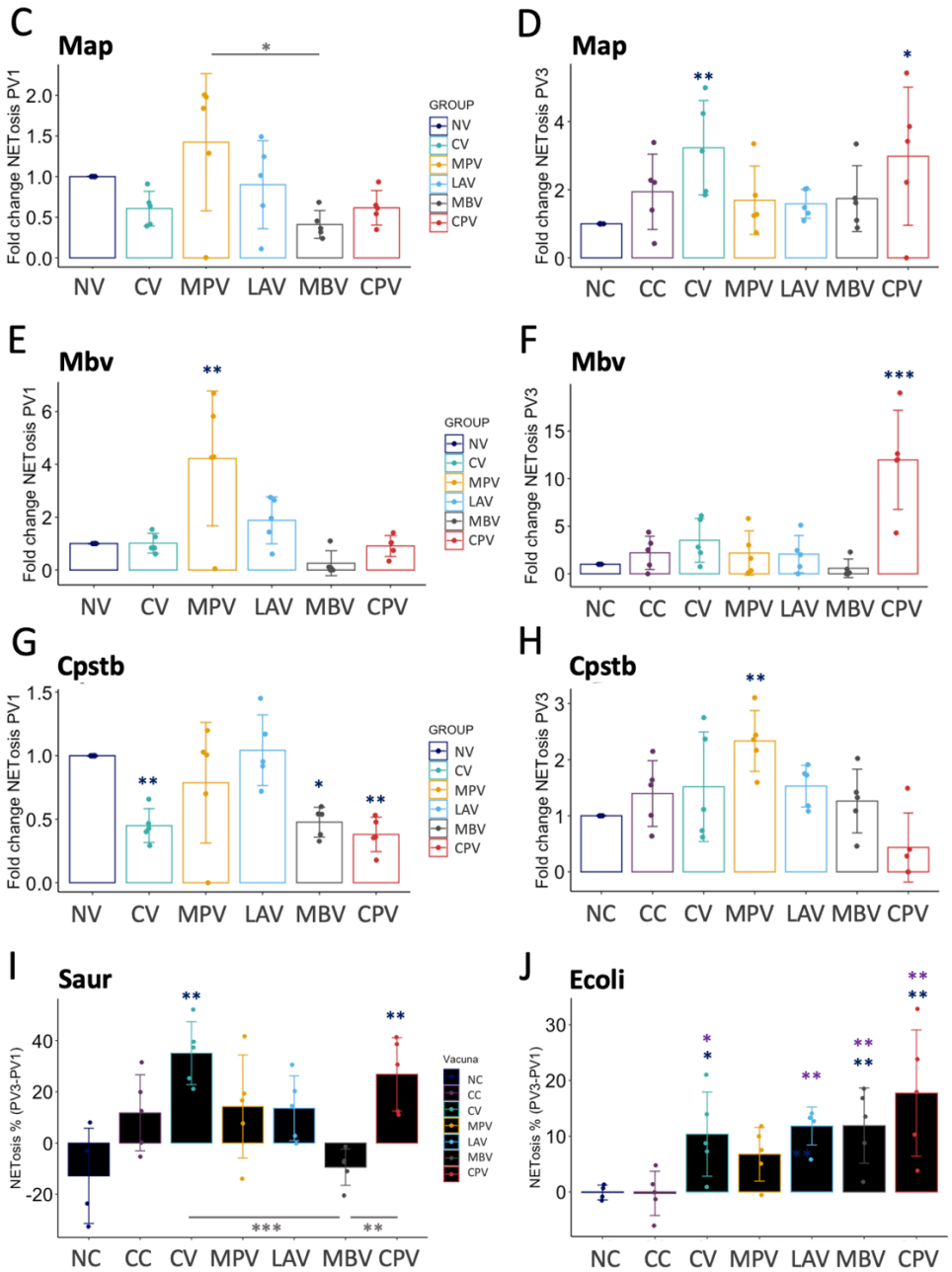

*Figure 23. Neutrophil extracellular trap (NET) release. Fold changes referred to non-vaccinated (NV) animals against (C) Map, (E) Mbv and (G) Cpstb (at time-point PV1 (one month after first dose vaccination) and against (D) Map, (F) Mbv and (H) Cpstb referred to non-challenged (NC) animals at time-point PV3 (2 months after challenge). (I) ET release increase against Saur at PV3 compared to PV1 for all animal groups. (J) ET release increase against Ecoli at PV3 compared to PV1 for all animal groups. Blue-asterisks represent significant differences between vaccinated or challenged groups with NC and purple asterisks represent significant differences between vaccinated groups and CC. *p <0.05, **p <0.01.*

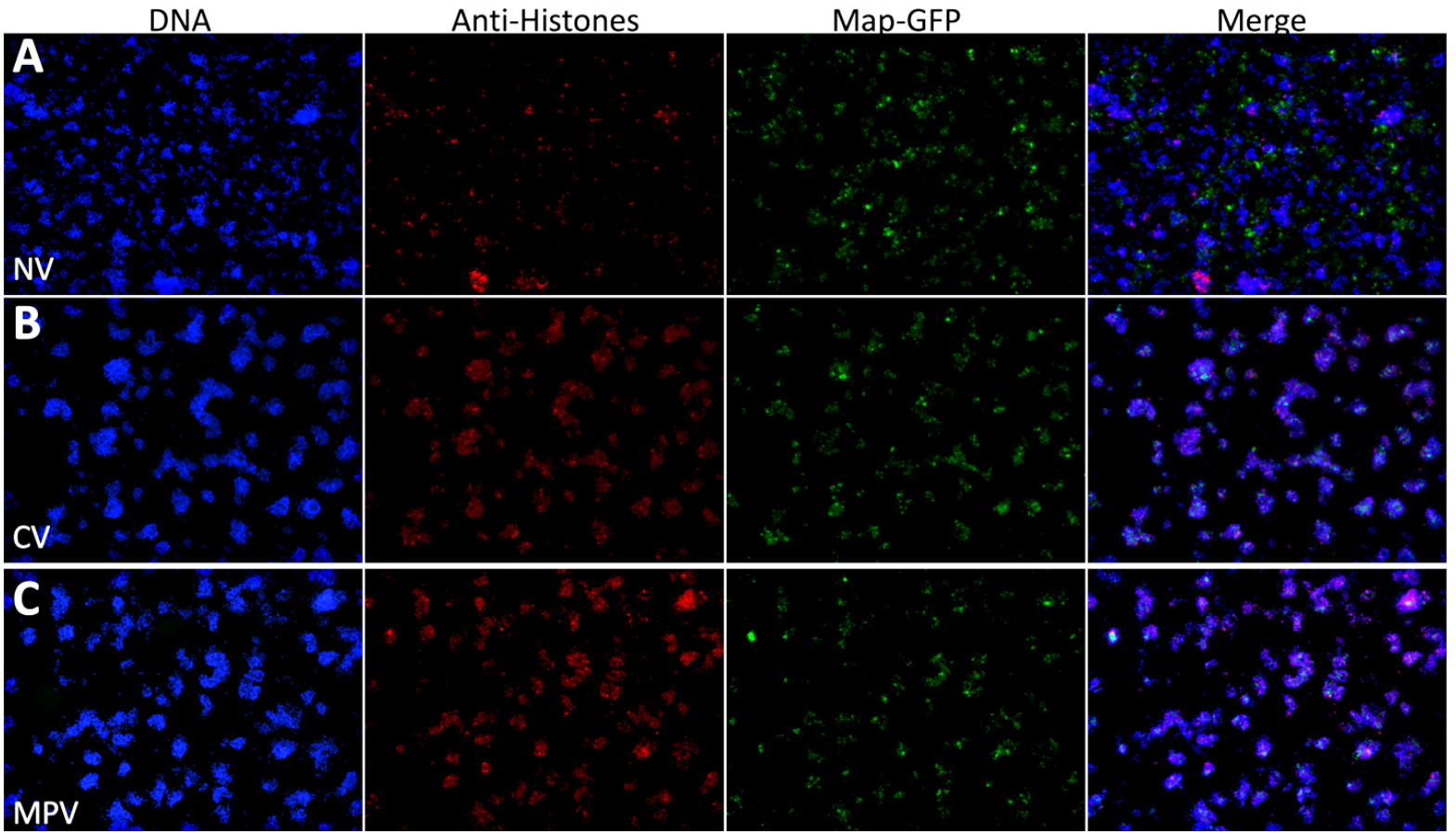

Figure 24. Fluorescence micrographs of PMNs from (A) NV, (B) CV, (C) MPV at PV1 after 4h incubation with Map-GFP (10x). DAPI (blue), anti-histone (red) and Map-GFP (green).

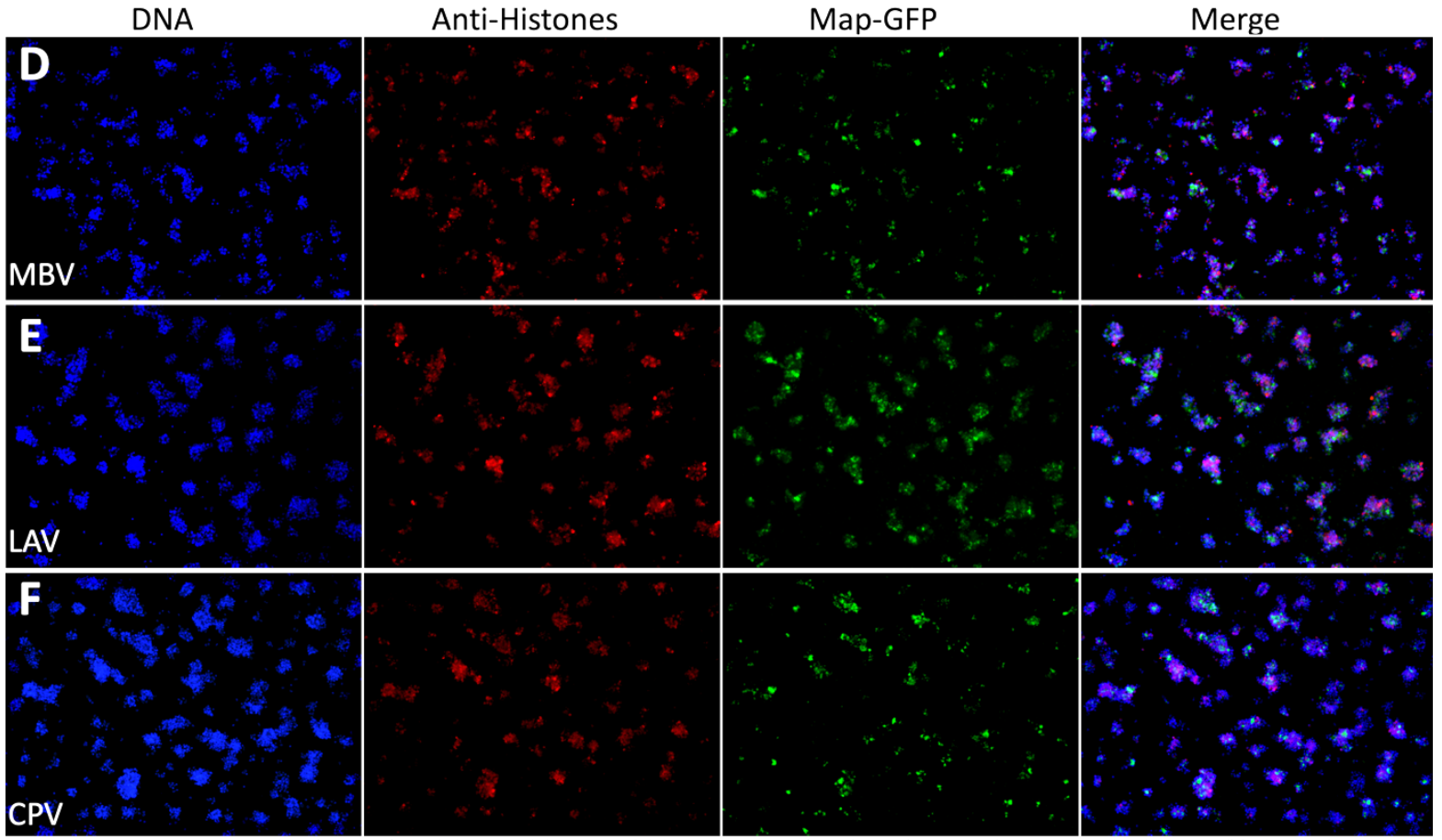

Figure 24. Fluorescence micrographs of PMNs from (D) MBV, (E) LAV and (F) CPV at PV1 after 4h incubation with Map-GFP (10x). DAPI (blue), anti-histone (red) and Map-GFP (green).

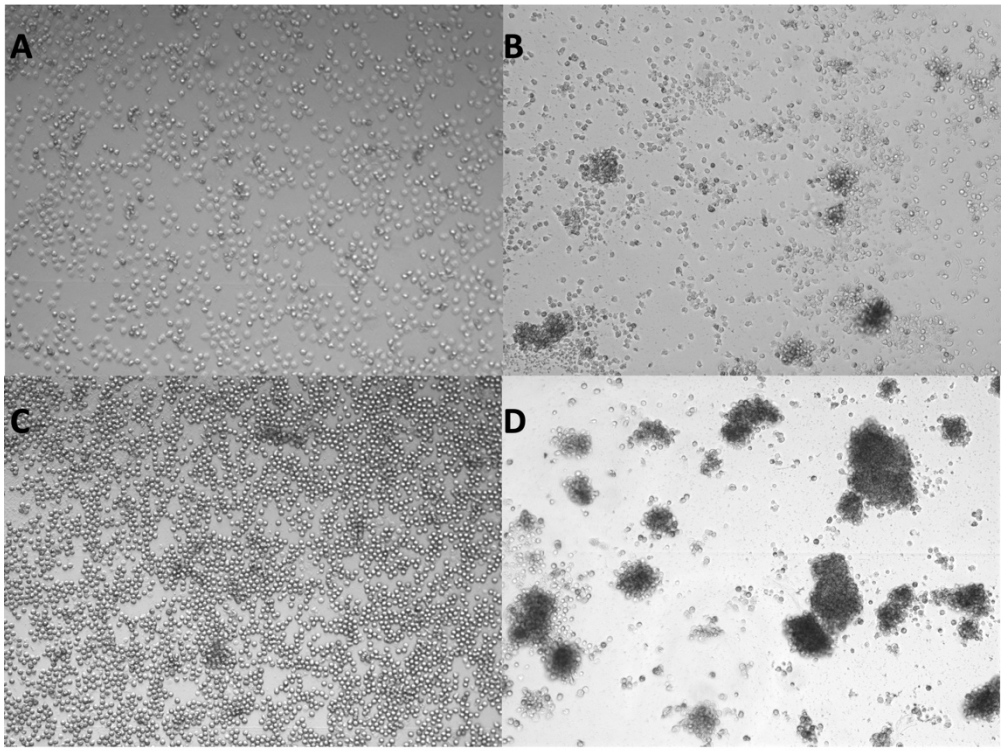

Figure 25. Light microscopy micrographs (10x) at PV1 of NC stimulated with (A) PMA and (B) Map and CV stimulated with (C) PMA and (D) Map.

2.5. Vaccination elevates lactate levels in plasma indicating immune activation

There is evidence on the link between aerobic glycolysis and activated or proliferating cells, due to the increase in their metabolic demand. In order to have more evidence on immune activation by oral vaccination, lactate levels were measured in peripheral plasma samples from BV, PV1, PV2 and PV3 samplings (Figure 26A).

The increase in lactate at PV1 compared to BV was higher compared to the NC group for CV (p=0.011), MBV (p=0.019) and CPV (p=0.009) (Figure 26B) indicating a metabolic demand was taking place after vaccination. MPV also showed a considerable increase at PV1, though it was not significant (p=0.161). On the contrary, LAV, a live Map vaccine did not show a significant increase of peripheral lactate levels. Afterwards at PV2 and PV3 lactate dropped to baseline levels in all orally vaccinated groups.

Lactate levels at PV3 were correlated with non-opsonized phagocytosis rates (ρ=0.67, p<0.00001).

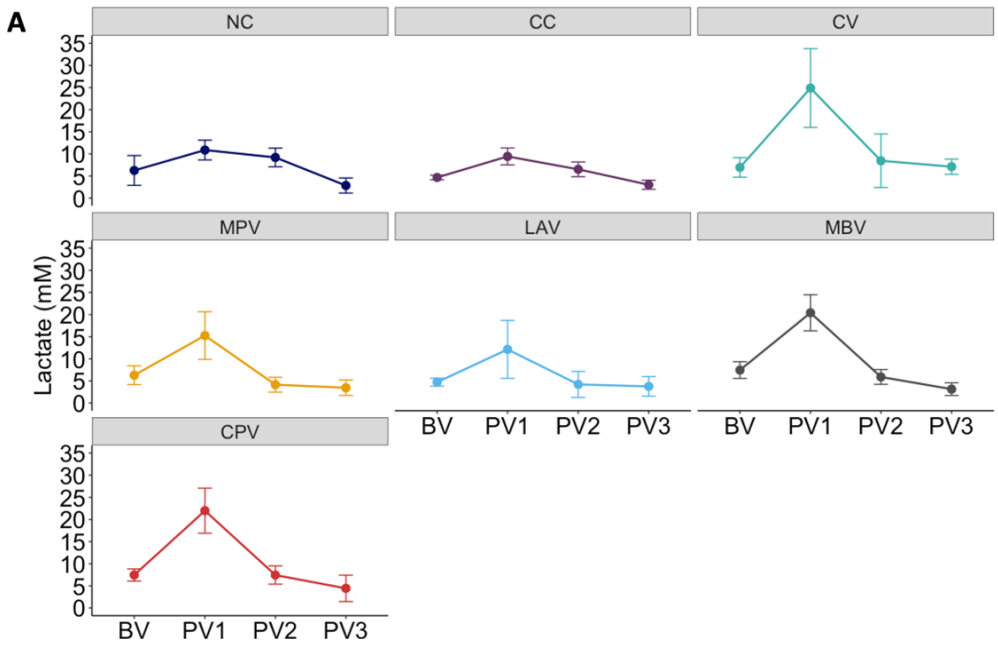

Figure 26. Lactate levels in plasma. (A) Lactate level changes in plasma throughout sampling points.

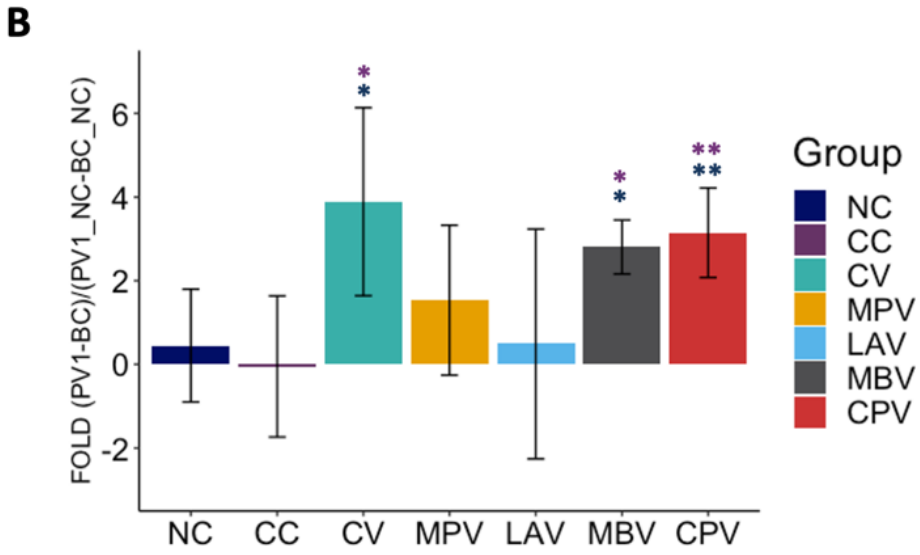

*Figure 26. Lactate levels in plasma. (B) Lactate level increase of vaccinated groups with respect to NC during the period between PV1 (one month after first dose vaccination) and BV (before vaccination). Blue-asterisks represent significant differences between vaccinated or challenged groups with NC and purple asterisks represent significant differences between vaccinated groups and CC. *p <0.05, **p <0.01.*

2.6. Cytokine expression profile and IgA levels suggest that oral vaccines activated mucosal immunity

In order to characterize the cytokine expression in PBMCs stimulated by vaccination, gene expression levels of IFN-γ, TNF, IL-2, IL1-β, IL- 4, IL-12B, IL-10 and IL-23A cytokines were assessed in isolated PBMCs at 1 month after first dose vaccination (PV1) (Figure 27A) and the response of the vaccinated groups were quantified relative to the NC group, and represented on a heat-map (Figure 27B) and further analysed.

Orally administered LAV, is an attenuated vaccine and the only live vaccine included in the study. PBMCs from this group presented the highest

levels of IL-1β after CPV (3.67 fold p= 0.004, in contrast to MPV) (Figure 27C) and the highest basal expression of IFN-γ at PV1 (Figure 27D) indicating a Th1 response. This is partially expected since it shows the nearest infection-like profile compared to the rest of the groups. On the other hand, CV subcutaneous vaccination presented the highest basal expression of TNF expression (2.52 fold p<0.001 with respect to NC) (Figure 27E) and of IL-10 (2.3 fold p =0.010 with respect to NC) (Figure 27F). In contrast, MPV was the group with the lowest IL-10 expression.

As early as 1 month after the first vaccination dose all oral vaccines enhanced IL-4 basal expression compared to NC (Figure 27G). MPV was the group with the highest IL-4 basal expression (2.43 fold, p=0.005), followed by CPV (2.05 fold, p=0.021), MBV (1.83 fold, p=0.046) and LAV (1.82 fold, p=0.046). In contrast, the subcutaneously administered CV group presented the lowest basal expression of IL-4 (2.44 fold lower than MPV, p=0.005). This IL-4 elevation suggests that oral vaccines from our study had activated mucosal immunity. IL-4 elevation is necessary for mucosal and systemic immunity activation and IgA production (Boyaka *et al.*, 2001). Serum IgA levels have been used to predict both vaccine efficacy and the immune status of individuals or herds against enteric infectious diseases (Suda *et al.*, 2021), we decided to measure total IgA in serum at BV and PV1 hypothesizing that oral vaccination would have activated the production of this antibody isotype. Indeed, serum IgA levels increased only in orally vaccinated animals (Figure 27G, blue line), showing highest increase for CPV.

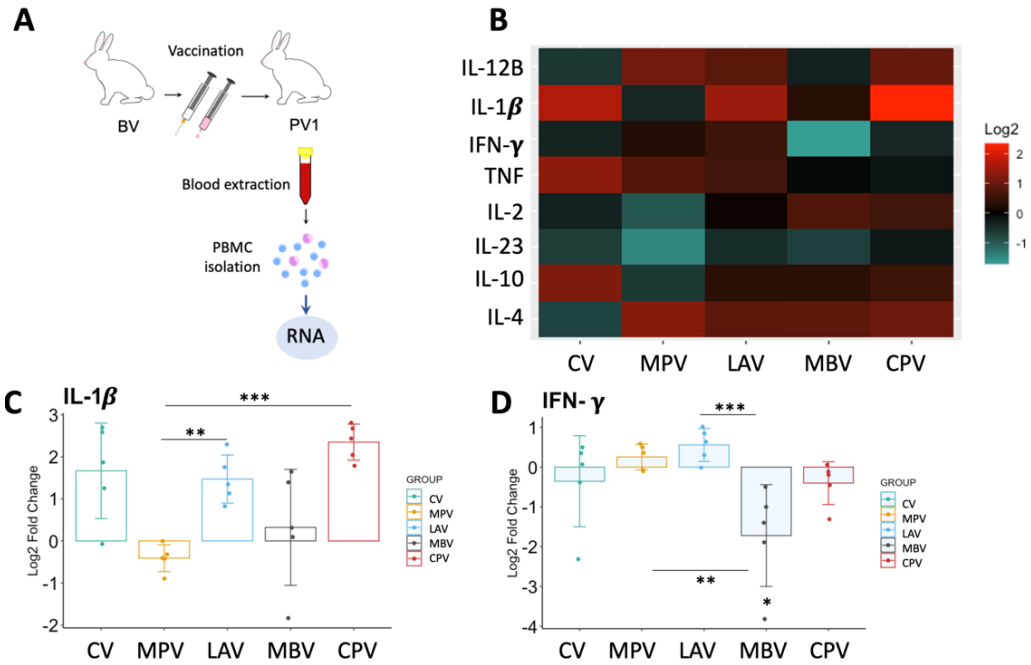

Figure 27. Cytokine relative quantification by RT-qPCR of PBMCs isolated from animals at PV1 (one month after first dose vaccination) relative to the NC. (A) Schematic representation of sample origin. (B) Heatmap representation of cytokine expression of vaccinated groups; in red up-regulated and in green down-regulated gene expression. Bar charts showing log2 fold change between vaccinated groups and NV of (C) IL-1β and (D) IFN-γ.

2.7.MPV vaccine shows the most convenient basal profile of immune modulation whereas CPV induced highest levels of IL-1β

Taking into account the expression of the studied cytokines, MPV is the group showing the best basal pro-inflammatory/Th2 balance at PV1, showing the highest IL-4 expression (2.43 fold p=0.0049 with respect to NC), a significant TNF increase (1.715 fold p=0.04 with respect to NC), and the lowest IL-10 expression. The group showing the highest basal levels of IL-1β was CPV (6.75 fold p<0.0001), in contrast to MPV, which showed the lowest levels, while IL-10 expression was moderate compared to the rest of

the groups (2.3 times higher than MPV p- =0.03). CPV early IL-4 levels were also increased (2.05 fold p=0.021 with respect to NC).

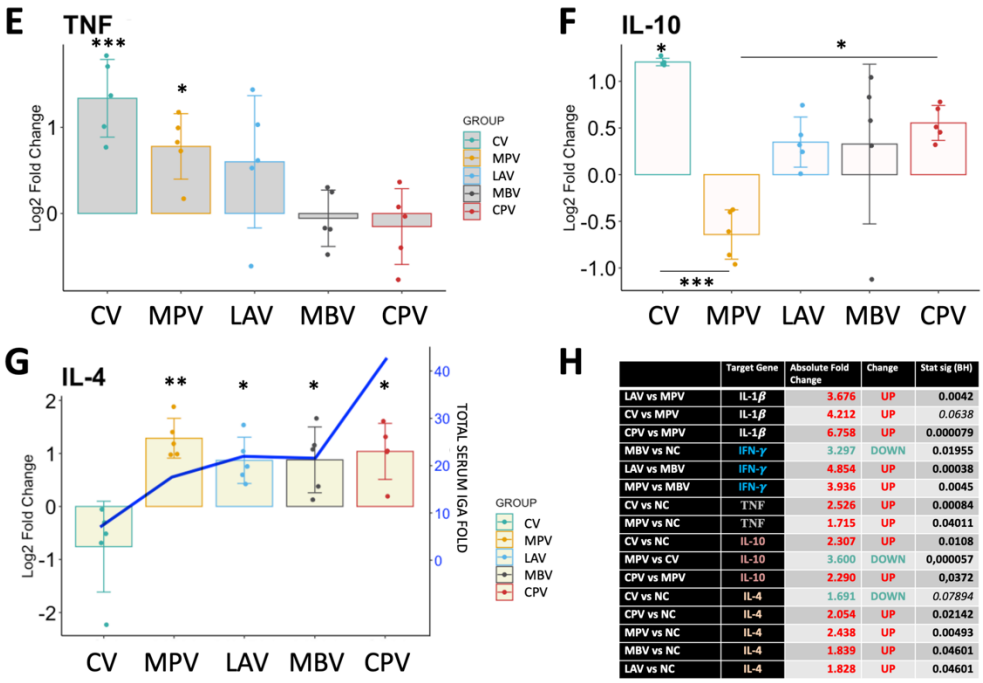

	Target Gene	Absolute Fold Change	Change	Stat sig (BH)
LAV vs MPV	IL-1β	3.676	UP	0.0042
CV vs MPV	IL-1β	4.212	UP	*0.0638*
CPV vs MPV	IL-1β	6.758	UP	0.000079
MBV vs NC	IFN-γ	3.297	DOWN	0.01955
LAV vs MBV	IFN-γ	4.854	UP	0.00038
MPV vs MBV	IFN-γ	3.936	UP	0.0045
CV vs NC	TNF	2.526	UP	0.00084
MPV vs NC	TNF	1.715	UP	0.04011
CV vs NC	IL-10	2.307	UP	0.0108
MPV vs CV	IL-10	3.600	DOWN	0,000057
CPV vs MPV	IL-10	2.290	UP	0,0372
CV vs NC	IL-4	1.691	DOWN	*0.07894*
CPV vs NC	IL-4	2.054	UP	0.02142
MPV vs NC	IL-4	2.438	UP	0.00493
MBV vs NC	IL-4	1.839	UP	0.04601
LAV vs NC	IL-4	1.828	UP	0.04601

Figure 27. Cytokine relative quantification by RT-qPCR of PBMCs isolated from animals at PV1 (one month after first dose vaccination) relative to the NC. Bar charts showing log2 fold change between vaccinated groups and NV of (E) TNF, (F) IL-10 and (G) IL-4 and blue line represents serum total IgA level fold PV1-BV. (H) Table summarizing the significant differences between groups in cytokine expression and the Absolute Fold Change Factor.

2.8.IL-1β basal increase correlated with increased phagocytosis activity of neutrophils

IL-1β basal levels and phagocytosis at PV1 were positively correlated (non-opsonized: spearman ρ=0.54, p = 0.002; opsonized Map: spearman ρ=0.57, p = 0.001). This is partially expected since PBMC derived IL-1β plays a role in neutrophil recruitment, activation and inhibition of neutrophil apoptosis (William *et al.*, 1998; Prince *et al.*, 2004). In addition, the number

of neutrophils isolated from groups with higher phagocytosis rates also correlated with IL-1β expression at PV1 (ρ=0.48, p = 0.007).

2.9. An innate immune activation profile is mounted 24h after *ex vivo* exposure of PMBCs to Map antigens in vaccinated groups

In order to assess the impact of vaccination on the cytokine expression in PBMCs after *ex vivo* exposure to Map antigens, gene expression was relatively quantified from PBMCs isolated at PV1 and stimulated with Map sonicate (SM) for 24h with respect to the expression without stimulation (PBS) (Figure 28A) and represented on a heat-map (Figure 28B).

All the vaccinated groups showed an innate immune activation response (elevated IL-1β, TNF, IL-23A) after exposure to Map antigens in comparison to the NC group (Figure 28D, E and G). The increase of the expression of these pro-inflammatory cytokines reflects modulation of the immune system by both oral and subcutaneous vaccination. IL-10 was also highly increased in all vaccinated groups indicating that regulation of the inflammatory response is taking place (Figure 28H). Actually, no increase of IFN-γ, nor IL-4 expression was achieved in any group with respect to their non-stimulated control. These results can be explained by the high expression of IL-23, which promotes the differentiation of naive CD4+ T cells into Th17 cells that produce IL-6, IL-17, IL-22, and TNF, but not IL-4 and IFN-γ (Iwakura and Ishigame, 2006).

On the other hand, MPV showed the highest IL-12B levels (5-6 fold p=0.014) (Figure 28C) and CV showed the highest IL-2 values (4.13 fold p=0.012, with respect to NC) (Figure 28F).

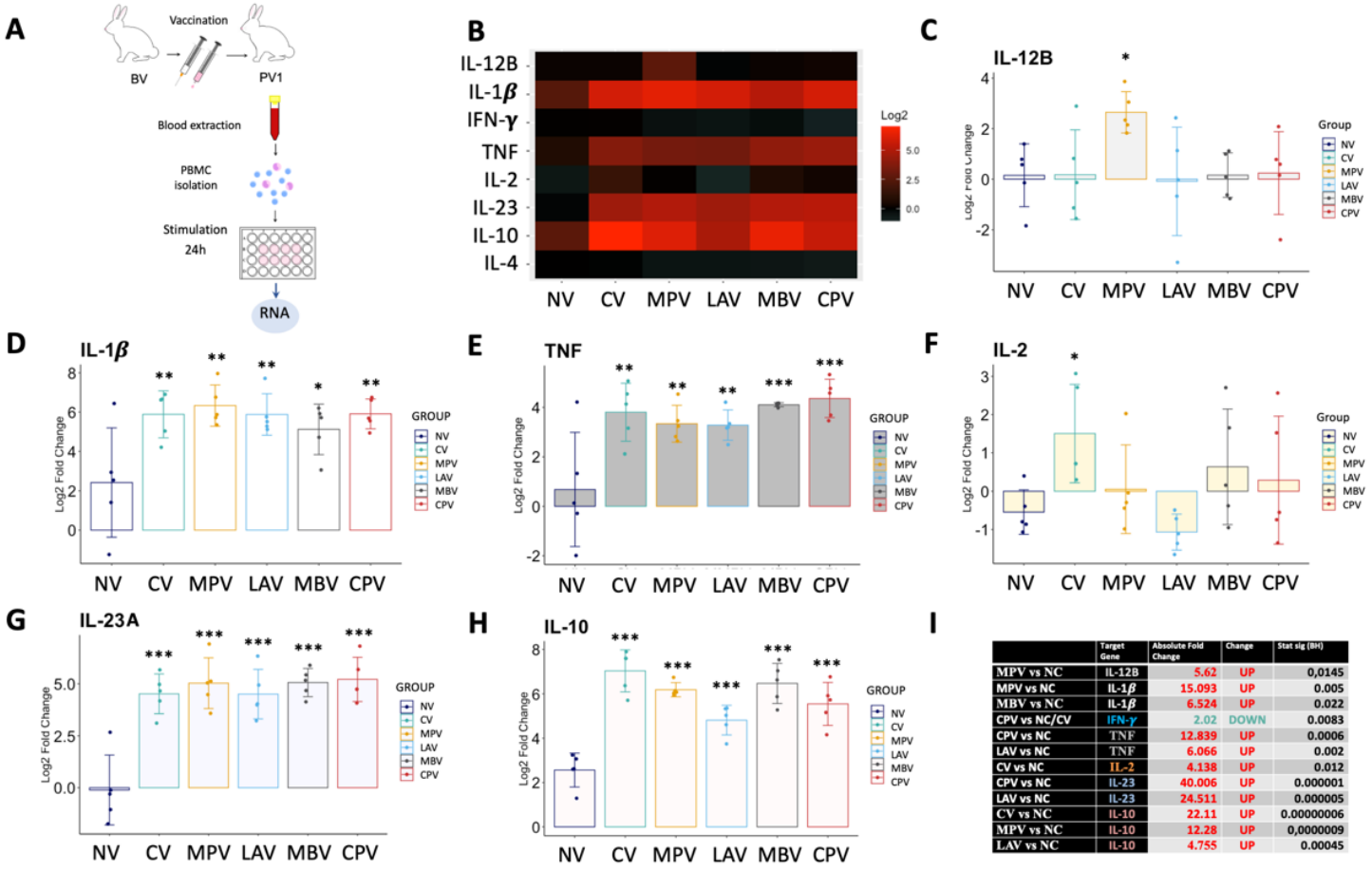

	Target Gene	Absolute Fold Change	Change	Stat sig (BH)
MPV vs NC	IL-12B	5.62	UP	0,0145
MPV vs NC	IL-1β	15.093	UP	0.005
MBV vs NC	IL-1β	6.524	UP	0.022
CPV vs NC/CV	IFN-γ	2.02	DOWN	0.0083
CPV vs NC	TNF	12.839	UP	0.0006
LAV vs NC	TNF	6.066	UP	0.002
CV vs NC	IL-2	4.138	UP	0.012
CPV vs NC	IL-23	40.006	UP	0.000001
LAV vs NC	IL-23	24.511	UP	0.000005
CV vs NC	IL-10	22.11	UP	0.00000006
MPV vs NC	IL-10	12.28	UP	0,0000009
LAV vs NC	IL-10	4.755	UP	0.00045

Figure 28. Cytokine relative quantification by RT-qPCR of PBMCs isolated from animals at PV1, after ex vivo *stimulation with Map sonicate (SM), of the studied vaccination groups relative to their correspondent non-stimulated control (PBS). (A) Schematic representation of sample origin. (B) Heatmap representation of the average expression of cytokines; in red up-regulated and in green down-regulated expression. Bar charts showing log2 fold change between groups (C) IL-12B, (D) IL-1β, (E) TNF, (F) IL-2, (G) IL-23A, (H) IL-10. (I) Table summarizing significant differences between groups in cytokine expression and the Absolute Fold Change Factor. For IL-1β, TNF, IL-23A and IL-10 only the higher and the lower Absolute Fold Change and p-values are detailed.*

2.10. A discrete pro-inflammatory polarization was observed in GALT from challenged animals while CV showed a lymphoproliferative profile.

In order to profile local immune response to Map at the final stage of the experiment expression of the same cytokines studied in the peripheral response was analyzed from GALT (Figure 29A) and challenged groups' responses were relatively quantified with respect to the NC group and represented on a heat-map (Figure 29B).

In general, all challenged groups showed a pro-inflammatory profile in the GALT, based on the higher local expression of IL-12B in these groups (Figure 29C). IL-1β expression was also slightly higher for all challenged groups compared to the NC except for CV (not oral vaccine) (Figure 29D). However, only CC (2.13 fold, p=0.033) and MPV (2.15 fold, p=0.03) showed significant differences.

IL-2 is considered the major T lymphocyte growth factor, being also necessary for memory lymphocyte T differentiation. In this study, the highest local expression of IL-2, was shown by the CV group (Figure 29F). An increase in IL-2 levels could be considered an important indication of vaccine efficacy since it plays an important role in the initiation and maintenance of antigen-specific immune responses (Capitini et al., 2009). Taking into account IL-4 and IL-2 levels, the group showing the highest lymphocyte B and T proliferation balance at the site of infection was the CV vaccinated group, with higher local IL-4 expression compared to CC (2.07 fold; p=0.034) (Figure 29G).

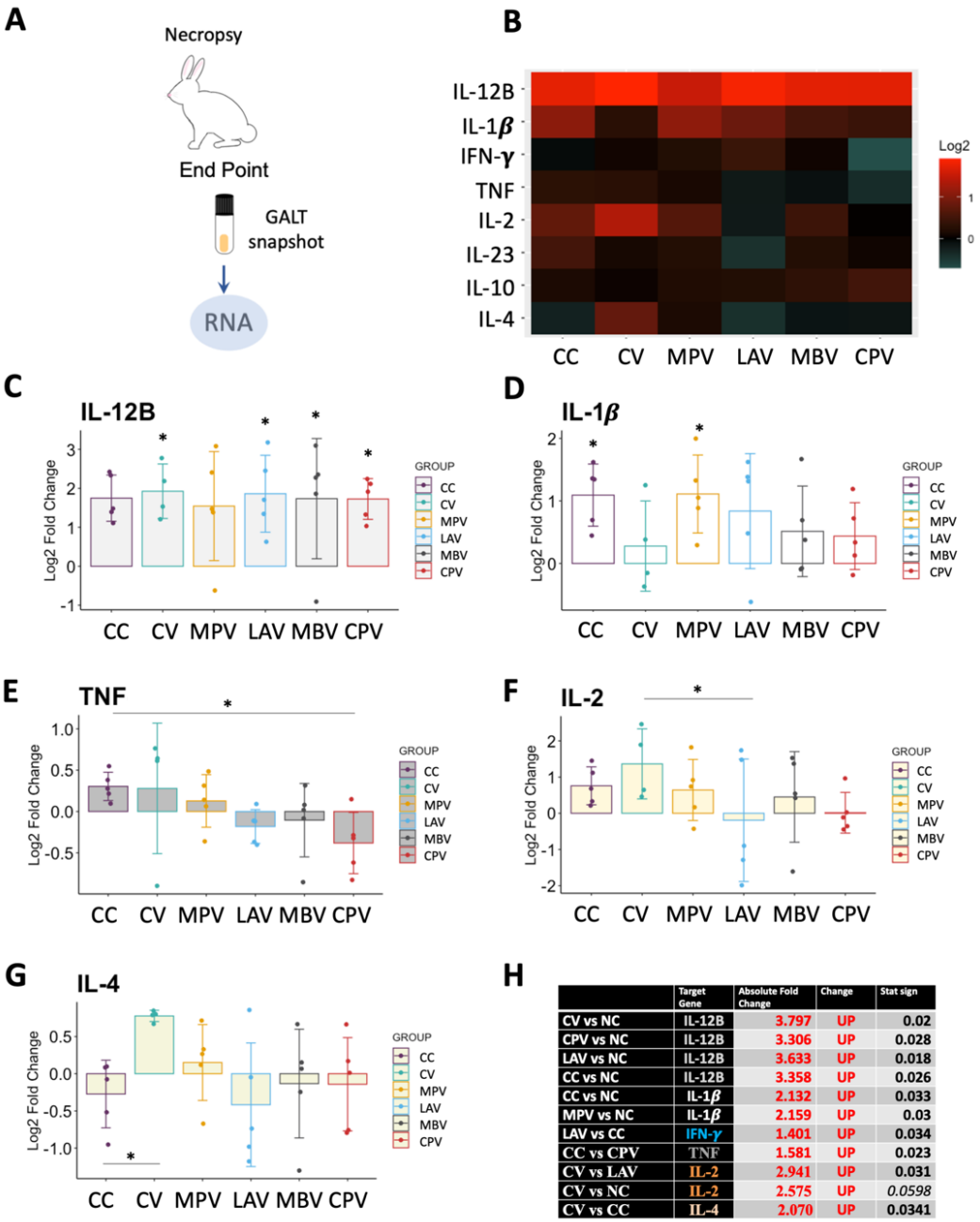

H

	Target Gene	Absolute Fold Change	Change	Stat sign
CV vs NC	IL-12B	3.797	UP	0.02
CPV vs NC	IL-12B	3.306	UP	0.028
LAV vs NC	IL-12B	3.633	UP	0.018
CC vs NC	IL-12B	3.358	UP	0.026
CC vs NC	IL-1β	2.132	UP	0.033
MPV vs NC	IL-1β	2.159	UP	0.03
LAV vs CC	IFN-γ	1.401	UP	0.034
CC vs CPV	TNF	1.581	UP	0.023
CV vs LAV	IL-2	2.941	UP	0.031
CV vs NC	IL-2	2.575	UP	0.0598
CV vs CC	IL-4	2.070	UP	0.0341

Figure 29. Cytokine relative quantification by RT-qPCR in GALT at the end point of the experiment of all challenged groups relative to the NC. (A) Schematic representation of sample origin. (B) Heatmap representation of the average expression of cytokines; in red up-regulated and in green down-regulated gene expression. Bar charts showing log2 fold change between groups. (C) IL-12B, (D) IL-1β, (E) TNF, (F) IL-2, (G) IL-4, (H) Table summarizing significant differences between groups in cytokine expression and the Absolute Fold Change Factor.

The expression of IL-12B and IL-2 resulted positively correlated (ρ=0.42, $p<0.0001$) and the strength of the correlation between IL-12B and IL-2 increased in GALT of those animals with demonstrated Map colonization of tissues (ρ=0.73, p=0.003).

2.11. MPV and CPV vaccinated animals presented lowest Map tissue colonization

In order to partially assess protective effects of the oral vaccines in this subclinical model of infection, Map isolation from tissues was performed on two different culture media augmenting the isolation probability and are shown on Tables 7 and 8.

Map was not isolated in any samples from the NC group as expected. Only one SR from the CV tested positive in HEYM culture. In the CC group three out of five animals were positive for Map in HEYM or TiKa.

Table 7. Bacteriological analysis results of the control groups.

ID	31	33	34	35	1	2	3	4	5	26	27	28	29	30
Group	**NC**				**CV**					**CC**				
HEYM	-	-	-	-	-	-	-	-	SR	-	SR	-	VA	VA
TiKa	-	-	-	-	-	-	-	-	-	-	MLN	-	-	-

White colored boxes and " –" symbol are for negative results; in grey positive results and abreviations indicate the sample tissue: Sacculus rotundus *(SR), vermiform appendix(VA), mesenteric limph node (MLN).*

The bacteriological analysis results from tissue samples of oral vaccine administration groups are shown in Table 8. The best results amongst

orally vaccinated groups are those from MPV and CPV with only one and two positive tissues, respectively.

Table 8. Bacteriological results of oral vaccination groups.

ID	11	12	13	14	15	21	22	23	24	25	16	17	18	19	20	6	7	8	9	10
Group	**MPV**					**LAV**					**MBV**					**CPV**				
HEYM	-	-	-		-	SR	SR, VA	-	-	-	-	VA	SR	SR	SR	-	SR	VA	-	-
TiKa	-	-	MLN	-	-	SR	-	-	SR	-	-	MLN	-	-	MLN	-	-	-	-	-

White colored boxes and " – " symbol are for negative results; in grey positive results and abreviations indicate the sample tissue: Sacculus rotundus *(SR), vermiform appendix (VA), mesenteric limph node (MLN).*

LAV positive cultures in HEYM or TiKa were re-cultured in 7H9 OADC MJ with hygromycin. No colonies were observed confirming that colonies from tissue cultures from this group were belonged to the challenge strain and not from the LAV strain.

2.12. Principal Component Analysis of immune parameters shows a homogeneous and well differentiated immune shaping by MPV and CPV oral vaccines

In order to visualise the global impact of vaccination on activation of immune responses all the immunological parameters were considered for a Principal Component Analysis (PCA). Although, Map isolation from tissues was not considered for the PCA, the groups that the analysis located in the center (LAV, CC and MBV) were coincident with the groups showing highest Map tissue positivity, while the groups located in the periphery were the groups with most Map negative tissues (NC, CV, CPV, and MPV). Moreover,

CV, CPV and MPV, were also represented separately from each other, reflecting the differences in their immune modulation outcome probably due to the differences in vaccine composition and administration route (Figure 30A-C).

The CV vaccinated group displays a large and distant ellipse, consistent with the strong, but heterogeneous effects that are seen in the group (Figure 30A). The strong activity of this vaccine triggers an excessive activation in some of the animals, showing, for instance, higher antibody titres in some animals and lower values in others (#5). In contrast, oral MPV and CPV, display a more compact ellipse, as an indicative of more moderate and homogeneous effects among the members of the groups (Figure 30B).

The fact that CC is displayed very close to NC is mainly due to two facts (Figure 30B-C). Firstly, Map replicates slowly and intends to evade the immune system being hidden in macrophages, thus, provoking minimum reaction is beneficial for its' survival. Secondly, the group suffering less interventions or stimulations, apart from NC, is CC, which only has been challenged, in contrast to the vaccinated groups. Phagocytosis, anti-PPA3 IgG levels and lactate levels at PV3 had high impact on the principal dimension of the PCA (Figure 30E), which explained a 23% of the variation (Figure 30D), while cytokine expression of stimulated and non-stimulated PBMCs, NETs and serum IgA levels had an intermediate impact (Figure 30F). Cytokine levels of the GALT and lactate at PV1 and PV2 had no impact on the three main principal components of the analysis (almost absent in Figure 30E-G). In general, this analysis shows that oral MPV and CPV vaccines, led to homogeneous responses, and a singular response, far from

NC and CC, comparable to the subcutaneously administered CV commercial vaccine, indicating that these can be promising candidates for oral vaccination.

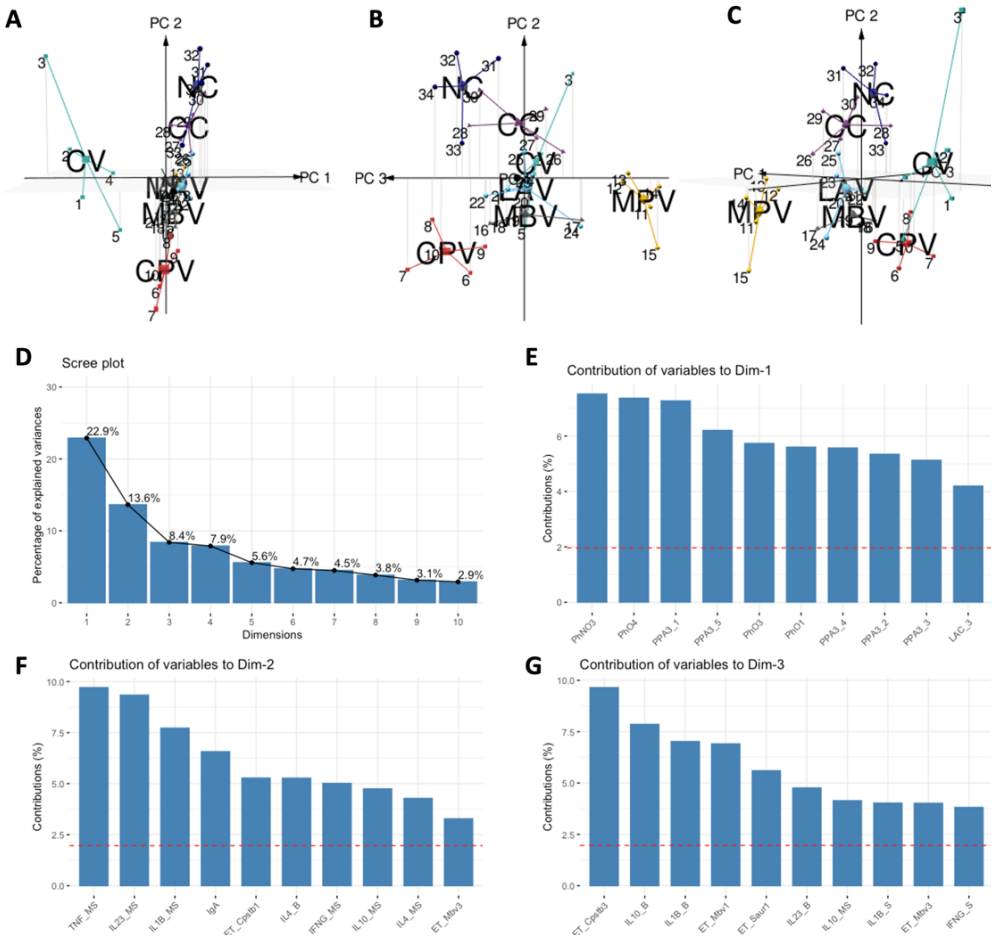

Figure 30. Principal Component Analysis results. (A-C) 3D representation of the spatial disposition that individuals adopt defined by the set of immune variables assessed in the experiment. (D) Percentage of explained variances by the top 10 dimensions of the analysis. (E) Contribution of variables to Dimension 1. (F) Contribution of variables to Dimension 2. (G) Contribution of variables to Dimension 3.

Materials, Methods and Results

Study III

Bovine neutrophils release extracellular traps and cooperate with macrophages in *Mycobacterium avium* subsp. *paratuberculosis* clearance *in vitro.*

The results of this study have been published:

Ladero-Auñon I, Molina E, Holder A, Kolakowski J, Harris H, Urkitza A, Anguita J, Werling D, Elguezabal N. "Bovine Neutrophils Release Extracellular Traps and Cooperate with Macrophages in *Mycobacterium avium* subsp. *paratuberculosis* clearance *in vitro*". *Frontiers in Immunology*, March 2021.

Synopsis

The objective of the third study was to study the interaction of neutrophils with macrophages during an *in vitro* mycobacterial infection. For this purpose, neutrophils and macrophages isolated from the same animal were cultured alone or mixed and were challenged *ex vivo* with Map or *Mycobacterium bovis* Bacillus-Calmette-Guérin (BCG). Extracellular trap release, mycobacteria killing and IL-1β and IL-8 cytokine release were measured. Neutrophils alone released extracellular traps against mycobacteria, although levels were lower when cultured in direct contact. Macrophages were highly efficient at killing BCG, but failed at killing Map. In contrast, neutrophils showed equivalent killing rates for both mycobacteria. Co-cultures infected with Map showed the anticipated killing effect of combining both cell types, whereas co-cultures infected with BCG showed an effect beyond presumed, indicating a potential synergistic cooperation. In both cases, IL-1β and IL-8 levels resulted lower in co-cultures than in macrophages alone, suggestive of a lesser inflammatory reaction. These data suggest that cooperation of both cell types can be advantageous in terms of reducing the inflammatory reaction and that neutrophils could be effective at Map killing during Map infection.

Materials and Methods

1.1 Animals

Blood samples were drawn from healthy Holstein Friesian cows of a commercial dairy farm located in the Basque Country. The herd is enrolled in the national bTB eradication program. Animals on the farm tested negative for bTb by skin-test over the last five years. All animals used in this study (n=4) tested negative for Map shedding in faeces, as confirmed by PCR, and were negative for Map-specific antibodies to Map, as determined by PPA-3 ELISA.

Animals used in this study were submitted only to procedures that according to European (Directive 2010/63/EU of the European Parliament and of the Council of 22 September 2010 on the protection of animals used for scientific purposes. Chapter 1, Article 1, Section 5, paragraphs b and f) and Spanish (Real Decreto 53/2013, de 1 de febrero, por el que se establecen las normas básicas aplicables para la protección de los animales utilizados en experimentación y otros fines científicos, incluyendo la docencia, Article 2, Section 5, Paragraphs b and f) legislation on experimental animals are exempt from its application. The animals, belonging to a registered commercial farm supervised by the local livestock authority (Servicio de Ganadería de la Diputación Foral de Bizkaia) were submitted only to the introduction of a needle in accordance with good veterinary practice and were not killed in relationship with this study.

1.2 Bovine peripheral blood monocyte isolation and generation of macrophages

Blood was taken from the jugular vein using a 16G x 11/2 hypodermic needle into a blood-collection bag containing 63 ml of citrate phosphate dextrose adenine (CPDA; TerumoBCT Teruflex) for a total capacity of 450 ml, which was used for monocyte isolation. One month later, 40 ml of blood from the same cows were collected with a 18G hypodermic needle into a 50 ml tube containing 7 ml of CPDA for PMN isolation. Blood samples were processed within two hours of the extraction.

Peripheral blood mononuclear cells (PBMCs) were separated using Histopaque 1077® and monocytes were selected using mouse anti-human CD14-coupled microbeads and MS columns (Miltenyi) following the manufacturer's recommendations. Greater than 90% of purity of monocytes was achieved as determined by flow cytometry using a mouse anti-bovine CD14 FITC-labelled antibody (BioRad).

For the production of monocyte-derived macrophages (MDMs), monocytes were plated at $1x10^5$ cells/well for co-cultures and at $2x10^5$ cells/well for MDM cultures in wells of 96-well plates for fluorimetric assays to quantify ET release. For immunofluorescence microscopy, monocytes were plated at $1x10^5$ cells/well for co-cultures and at $2x10^5$ cells/well for MDM cultures on 16-well chamber slides (178599PK Thermo Scientific). For contact independent cultures, monocytes were plated at $5x10^5$ cells/well for co-cultures and at $1x10^6$ cells/well in wells of 24-well plates. During maturation to macrophages, monocytes were cultured in RPMI 1640 media

without phenol red (Gibco 11835030), supplemented with 2 mM L-glutamine, 10% foetal bovine serum (FBS), 1% penicillin-streptomycin and 10 ng/ml recombinant bovine M-CSF (Kingfisher Biotech, Inc. RP1353B) at 37 °C and 5% CO_2. The media was replaced every three days and prior to the beginning of the mycobacterial infection assays. After 7 days of culture, MΦ morphology was confirmed by light microscopy (increased size, increased adherence, cytoplasmic granularity and presence of pseudopods).

1.3 Bovine Neutrophil isolation

A week after PBMC isolation, 25 ml of blood were drawn from the same cows by venepuncture and mixed with 25 ml of PBS supplemented with 2% FBS. 25 ml of the mixture were layered on top of 15 ml of Histopaque® 1077 (Sigma) and centrifuged at 1200 x g for 45 min at RT with no brakes. PMNs were located at the lower end of the tube and were subjected to two flash hypotonic lysis using 25 ml of sterile distilled water during 20-30 s, followed by 2.5 ml of a 10% NaCl solution and topped up with PBS-2% FBS, in order to eliminate remaining red blood cells. PMNs were then resuspended in RPMI 1640 with glutamine and without phenol red and counted. Over 90% purity was achieved as determined by FSC and SSC gating and visualization of characteristic nuclei after DAPI staining under a fluorescence microscope.

1.4 Bacterial strains and culture

Map strains K10, Map K10-GFP (kindly provided by Dr. Jeroen de Buck, University of Calgary (Parker and Bermúdez, 1997), *M.bovis* BCG Danish strain 1331 and *M. bovis* BCG Danish strain 1331-GFP were used in the assays. All strains were grown to exponential phase at 37 °C under aerobic

conditions. Map-GFP and BCG-GFP were cultured for three weeks on Middlebrook 7H9 OADC with Kanamycin (25 μg/ml) to select for GFP-plasmid carriers and supplementation with Mycobactin J was added for Map. Map strain K10 and BCG Danish strain 1331 were used for ET isolation and quantification and were cultured in the same medium without kanamycin. Cultures were adjusted after reaching an OD of 0.7 ($3x10^8$ bacteria/ml) and colony forming units (CFU) were confirmed on agar after using 10-fold serial dilutions of bacterial suspensions. In experiments comparing the response to live and killed bacteria, heat-inactivation was performed by heating bacteria for 30 min at 85 ºC. Inactivation of bacteria was confirmed by plating on agar plates.

1.5 Cell cultures and *in vitro* infection

PMNs and MDMs isolated from the same cow were cultured separately or co-cultured together in the same well (CC; see Figures 31A and 33A for details). In order to study cellular changes following paracrine signalling in the absence of cell-to-cell contact between PMNs and MDMs as well as to determine ET formation, a transwell co-culture system was also employed. PMNs were seeded in the transwell insert (pore diameter 0.4 μm; Thermo Fisher Scientific 140620) to generate insert PMNs (TW-PMN), whereas MDMs were seeded into the lower well (TW-MDM). To assess the need for direct cell contact, conditioned MDM media (TW-CM) was produced by incubating MDMs with Map, BCG and Zymosan for 4 h at 37 °C and 5% CO_2, which was subsequently added to the lower well underneath the insert containing PMNs (TW-PMN-CM). ET release quantification and

mycobacteria killing were performed on 24 and 96 well plates. ET visualization was performed on 16-well chamber slides (Nunc Labtek).

Once cell cultures were set, these were stimulated with live or heat-inactivated Map K10-GFP, *M. bovis* BCG -GFP, Map K10, *M. bovis* BCG at either a MOI of 1 (ET release) or a MOI of 5 (survival assay), zymosan (1mg/ml; Sigma Z4250), or left untreated (negative control). The original bacterial strains with no GFP were used for the isolation and quantification of NETs in the fluorometric assay to avoid GFP fluorescence interference.

Cultures were incubated at 37 °C and 5% CO2 for 4 h for ET release evaluation and for 24 h for bacteria killing and cytokine level quantification.

1.6 Isolation and quantification of ETs

ET release was assayed as described by Köckritz-Blickwede *et al* (Köckritz-Blickwede *et al.*, 2010) with some modifications. Briefly, ETs generated by cells were digested with 500 mU/ml of micrococcal nuclease (10107921001 Roche) for 10 min at 37 °C 5% CO_2. The nuclease activity was stopped by the addition of 5 mM EDTA; thereafter, culture supernatants were collected and stored at 4 °C ON. Total DNA was extracted from naive cells with DNeasy® blood & tissue kit (Qiagen) following the manufacturer's instructions. Extracted DNA was solubilized in TE buffer. Both ETs and genomic DNA was quantified using Quant-iT™ PicoGreen™ assay (Thermofisher) according to the manufacturer´s instructions. Plates were read in a fluorescence microplate reader (Synery HTX, Biotek) with filter settings at 488 nm excitation and 520 nm emission. The percentage of DNA released

as ET-DNA was calculated by dividing the amount of quantified ET-DNA by the total amount of genomic DNA.

1.7 Visualisation and quantification of ET by immunofluorescence microscopy

To assess histone staining as a marker for ET formation, cells were seeded into 16-well chamber slides for subsequent antibody staining and microscopy according to Conejeros *et al* (Conejeros *et al.*, 2019). After 4 h of incubation with either Map-GFP, BCG-GFP or zymosan, cells were fixed for 15 min with 4 % formaldehyde. Cells were washed twice with PBS and kept in PBS at 4 °C until staining was performed. Subsequently, cells were permeabilized for 15 min with PBS 0.1% Triton X-100, blocked with 1% goat serum containing 0.05% Tween 20 and 3% BSA-PBS. The immunofluorescence staining was performed ON at 4 °C using a mouse anti-pan-histone antibody (Merk MAB3422; diluted 1:200). Thereafter, cells were washed three-times with PBS and incubated with anti-mouse Alexa Fluor 594 labelled antibody (Invitrogen A-1105, diluted 1:500) for 30 min at RT. Following further three washes with PBS, wells were detached from the slides and mounting medium containing DAPI was added before coverslips were added. Preparations were let dry and observed at 400x magnification on a DMi8 fluorescence inverted microscope (LEICA®). Pictures were taken using a DFC3000 G camera coupled to the microscope.

Quantification was performed by taking snapshots of five fields containing visible ETs with histone staining. Analysis was performed using the Image J software package. Snapshots in 8-bit format were analysed using

the following pipeline. Threshold was adjusted depending on the micrograph, being 4 for low level and 255 for high level. The percentage of picture area occupied by ETs plus nuclei (total DNA) was measured by adjusting the settings for fluorescent particle size: 0-infinity and circularity: 0-1. The percentage of picture area occupied by nuclei were analysed adjusting the settings for particle size: 200-5000 and circularity: 0.3-1. ET percentage was calculated as total DNA percentage minus nuclei percentage. In the case of cultures that did not contain ETs, nuclei were measured, and ET release was considered zero.

1.8 Mycobacteria killing assay

PMNs, MDMs and co-cultures inoculated with BCG -GFP and Map-GFP were prepared. At time 0 (4 ºC control) and 24 h, the supernatants were removed and centrifuged to pellet non-internalized mycobacteria. Supernatants were stored for cytokine analysis. Wells were washed twice with PBS to remove the remaining non-internalized bacteria. Bacterial pellets and washes of remaining bacteria were centrifuged together, and the final pellets were resuspended in 100 µl of filtered PBS. Adherent cells were lysed by vigorous pipetting with 0.5 ml of 0.1% Triton X-100 (Sigma-Aldrich) in sterile water for 10 min at RT.

Two serial 10-fold dilutions of each lysed sample and supernatant were performed in a total volume of 1 ml using filtered PBS. 200 µl of each dilution was inoculated in duplicate in Middlebrook 7H9 OADC-Kanamycin (25 µg/ml) agar plates, supplemented with mycobactin J in the case of Map cultures. Seeded agar plates were allowed to dry at RT until humidity was no

longer visible. Plates were sealed with tape to avoid desiccation and incubated at 37 ± 1 °C for 6 weeks. CFU were counted and 0 h (4 ºC control) CFU were considered total inoculated bacteria, 24 h CFU supernatant bacteria were considered non-internalized and non-killed and 24 h CFU cell bacteria were considered internalized and non-killed bacteria. Killed bacteria were estimated as total inoculated bacteria minus (24 h CFU supernatant bacteria plus 24 h CFU cell bacteria). CFU counts were multiplied by the inverse dilution factor and by the seeded volume. The mean of duplicate plates was calculated and the group mean for each culture type was calculated. Supernatants' fraction and cell-lysis' fractions were divided by the 100% survival control to calculate the survival percentage of each portion and the killing rate.

1.9 Cytokine detection

Commercially available direct ELISA kits were performed to determine bovine IL-1β (ESS0027 Invitrogen®) and IL-8 (3114-1A-6 MABTECH) release in 24 h culture supernatants using the provided manufacturer's instructions. IL-1β ELISA is based on streptavidin-HRP and IL-8 on streptavidin-ALP. Absorbances were measured using an automated ELISA plate reader (Multiskan EX®, Thermo Lab Systems, Finland) and in all cases standard curves were used to determine each cytokine amount in the supernatant samples.

1.10 Statistics

Data were assessed for normal distribution and homoscedasticity using Shapiro-Wilk and Bartlett´s test, respectively. All data are presented as the mean +/- standard deviation (SD), with samples being analysed in triplicates (ET release by fluorimetry) or duplicates (bacterial killing and cytokine release). For ET release, percentage differences between values obtained for the mean of each culture type were calculated using pairwise comparisons (t-tests) with pooled SD for all the stimuli except for values obtained for unstimulated and zymosan stimulated cultures. Here, values were not normally distributed and thus comparisons were calculated using non-pooled SD test.

The number of bacteria (expressed as CFU) in the inoculum (0 h) was considered as 100% viable bacteria. The number of bacteria being alive after 24 h incubation was calculated as the sum of internalized mycobacteria and mycobacteria being present in the supernatant, with the killing rate being the difference between the bacteria at 0 h and the survival at 24 h, expressed as percentage. Mean values obtained for killing rates under different conditions were compared by multiple pairwise comparisons using t tests with non-pooled SD with Benjamini-Hochberg correction. To obtain killing rates for co-cultures, values obtained for the killing rate of individual cultures (PMN, MDM) were divided by two and obtained values were added to each other.

Differences in IL-1β levels were compared by Kruskal-Wallis test with the post-hoc Dunn’s multiple comparison test. IL-8 level differences

were calculated through multiple pairwise comparisons using t tests with pooled SD.

To identify correlations between variables, Pearson ($\rho_{x,y}$) and Spearman (ρ) coefficients were calculated to detect linear and non-linear correlations and in each case the best fitting coefficient value was chosen.

All statistical tests were performed using R studio desktop (version 1.2.5033; (RStudio Team, 2019. RStudio: Integrated Development for R. RStudio, Inc., Boston, MA URL http://www.rstudio.com/), and a p-value of < 0.05 was considered statistically significant.

Results

2.1. PMNs release extracellular traps against both mycobacteria killed and alive in contrast to MDMs

In a first set of experiments, we assessed the induction of ET in PMNs and MDMs, either alone or in co-cultures, in response to Map and BCG. In order to assess whether this mechanism would rely on live or heat-killed bacteria, all culture types were incubated with both live and heat-inactivated Map and BCG. Fluorometric analysis revealed that both cell types cultured individually extruded similar detectable DNA levels in response to zymosan (Figure 31F), whereas lower ET levels were detected when cells were cultured together (Figure 31F). Levels of ET formation in response to live mycobacteria were similar for PMNs and MDMs and lower for CCs although no statistical differences were found (Figures 31B and D). However, in response to killed mycobacteria, PMNs showed higher ET release (Figures 31C and E) compared to MDMs (K-BCG, $p=0.03$; K-Map, $p=0.065$) and to CC (K-BCG, $p=0.04$; K-Map, $p=0.043$).

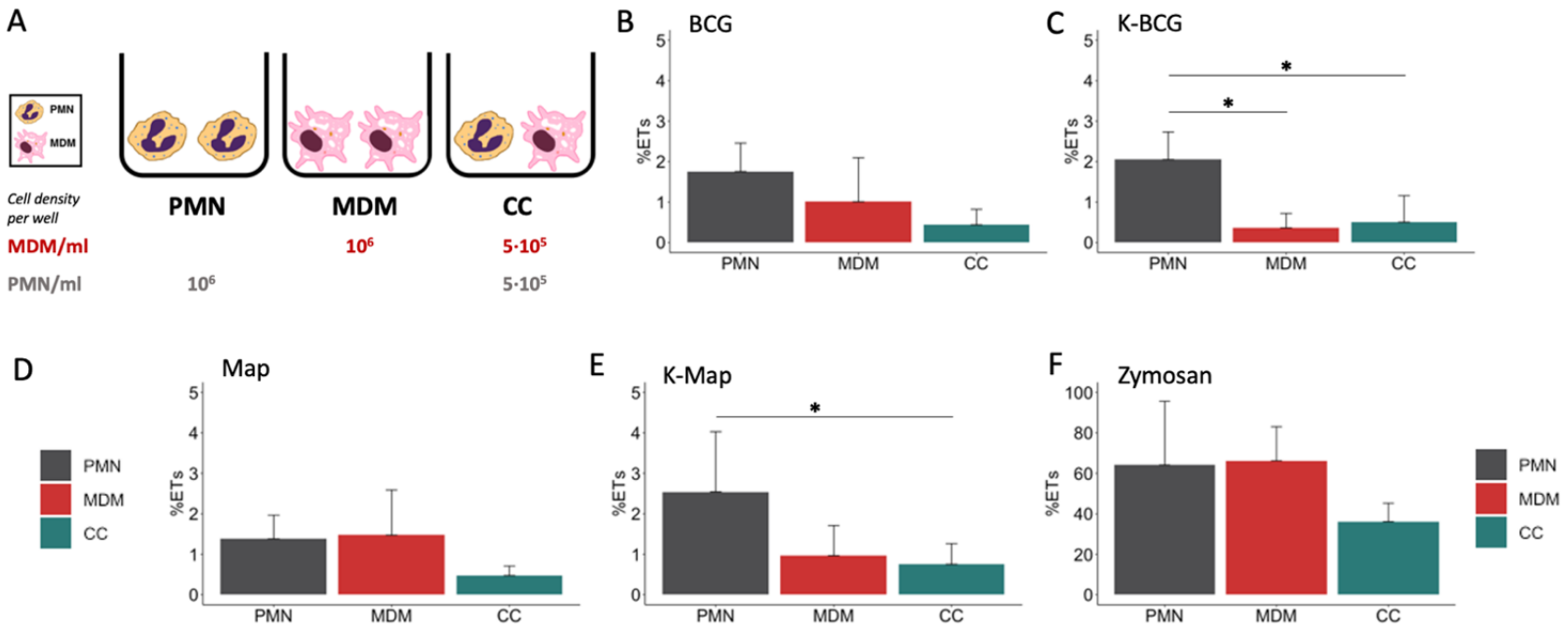

*Figure 31.Fluorimetric ET release quantification of PMNs, MDMs and CCs. (A) Cell culture types and conditions in 96 well plates. ET release quantified by fluorimetry of cultures stimulated with (B) BCG, (C) K-BCG: killed BCG, (D) Map, (E) K-Map: killed Map and (F) Zymosan. Data are composed of combined values obtained of all cows (n=4), with samples run in triplicates. * depicts a p value of $p < 0.05$.*

2.2.PMNs and MDMs alone or in direct co-cultures exert different effector mechanisms against BCG and Map

Although fluorometric quantification analysis revealed significant differences in ET release among cell culture types, further analyses were performed to discriminate between DNA from ET release and DNA liberated by other means. Image analysis quantification of ETs showed that PMNs liberated significantly higher levels of ETs (6.52% - 7.23%) compared to MDMs (0%) and CCs (1.13% - 2.03%) and MDMs (0%) when stimulated with both mycobacteria, independent of whether the bacteria were alive or heat-killed (Figure 32A-D). As seen before, MDMs produced ET-like structures only when stimulated with zymosan (Figure 32E). MDMs and PMNs, cultured either alone or in co-cultures and stimulated with zymosan lost normal nuclei structure, ending in nuclear DNA extrusion (Figure 32E). However, co-cultures seemed to contain fewer ETs, which could be due to MDMs phagocytosing liberated ETs by PMNs or because direct contact of both cell types inhibits ET release.

The microscopic evaluations also revealed that ETs released by PMNs were the main source of histone-staining (shown in red), as this staining was mainly within the extruded ETs and not always associated with DAPI-stained nuclei (Figures 32A and C; PMNs and PMNs and CC). In agreement with data shown in Figure 31, MDMs showed internalized mycobacteria but did not show ET release (Figures 32A and C, MDMs), and anti-histone staining was always associated with the nuclei (as recognised by DAPI staining), independent of bacterial preparation used to stimulate MDM (Figures 32A-

D; MDM). In addition, it seemed that MDMs showed less mycobacterial internalization when co-cultured with PMNs, whereas the opposite was observed with PMNs (Figures 32A and C; CC). However, in Map stimulated CCs, PMN nuclei were not always labelled by the anti-histone antibody, and many PMNs showed condensed nuclei, potentially indicative of apoptosis (Figure 32C; CC).

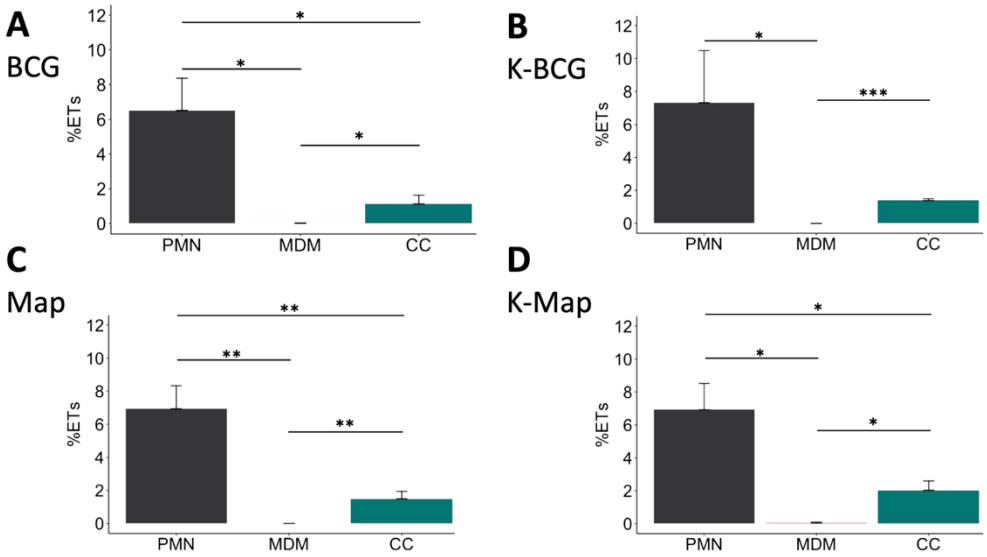

Figure 32. ET release analysis of microscope images. Bar plots representing ET release quantified by immunofluorescence microscopy image analysis corresponding to micrographs (40x) of PMNs, MDMs and CCs stimulated with A) BCG, B) K-BCG, C) Map and D) K-Map. Data composed of combined values obtained of all cows (n=4), with samples run in duplicate and 5 fields quantified per micrograph. (p<0.05; ** p<0.01;*** p<0.001).*

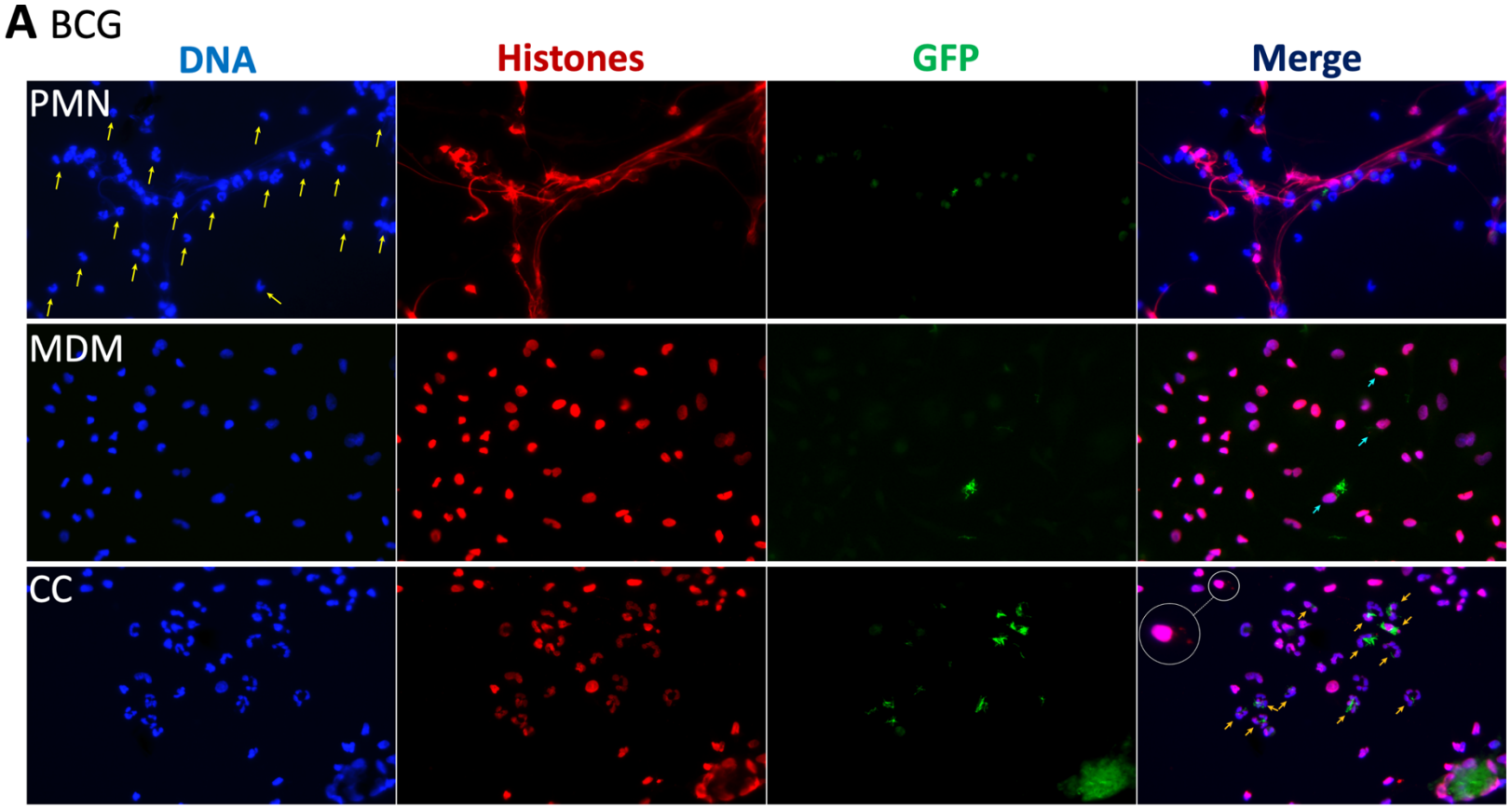

Figure 32A. ET release analysis of microscope images. Representative corresponding examples of micrographs (40x) of PMNs, MDMs and CCs stimulated with BCG. DAPI stained DNA in blue, histones in red and BCG-GFP in green. Yellow arrows indicate nuclei stained with DAPI, which are absent in the red channel corresponding with anti-histone immunolabeling. Light-blue arrows indicate MDM phagocytosis. Orange arrows indicate PMN phagocytosis. A white circle has an augmented image showing a red punctate pattern in MDM cytoplasm.

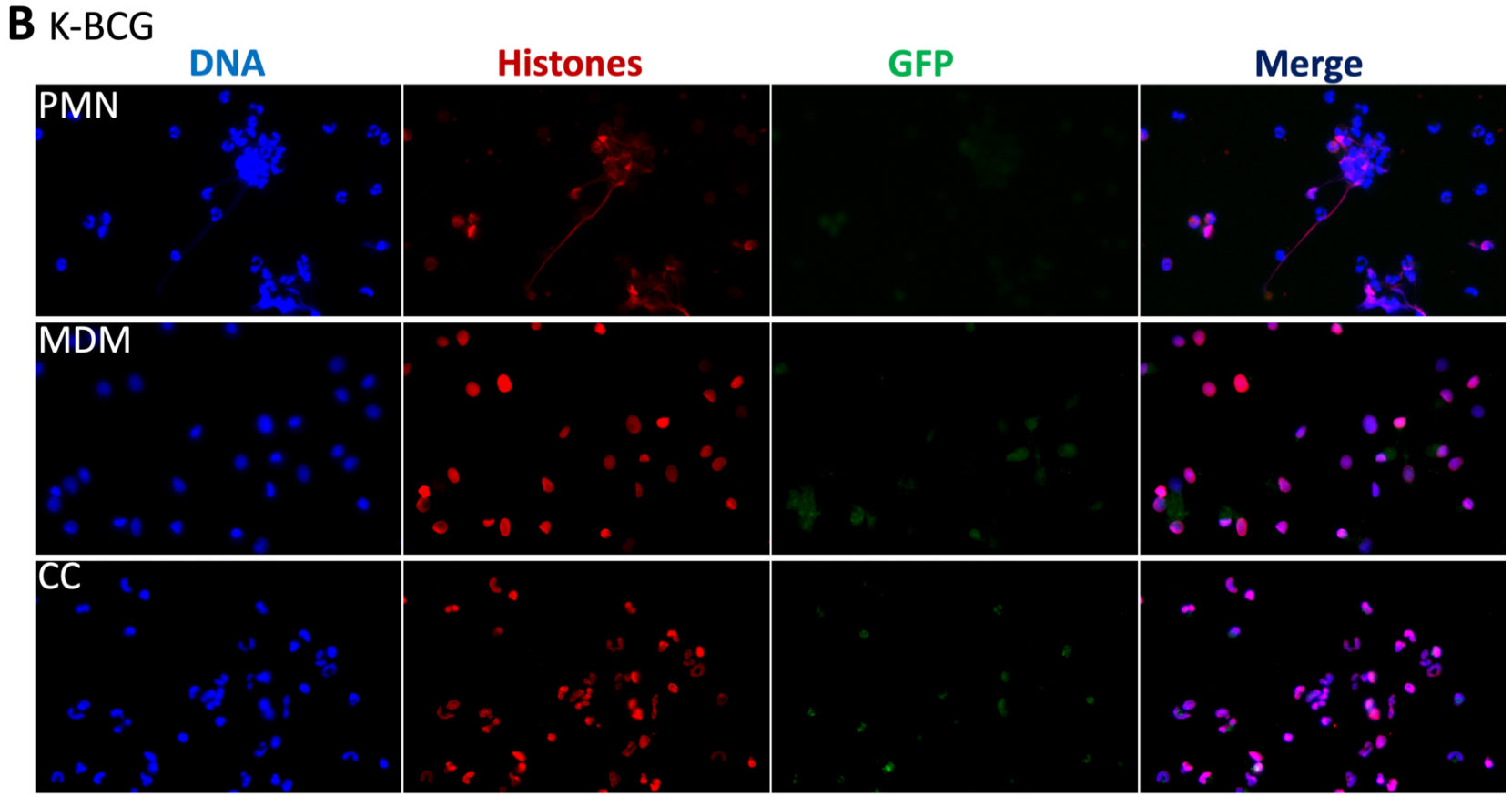

Figure 32B. ET release analysis of microscope images. Representative corresponding examples of micrographs (40x) of PMNs, MDMs and CCs stimulated with K-BCG. DAPI stained DNA in blue, histones in red and K-BCG-GFP in green.

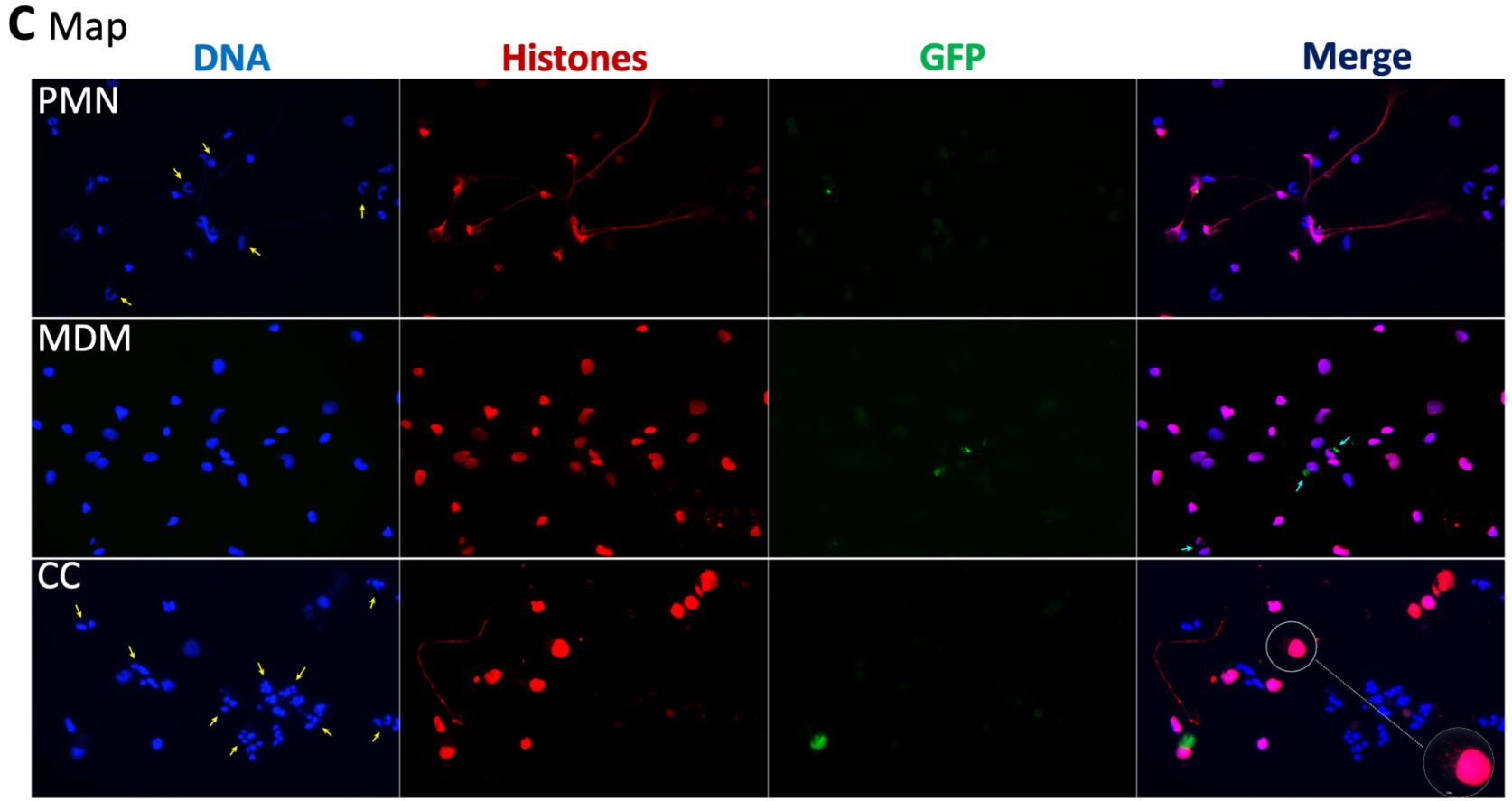

Figure 32C. ET release analysis of microscope images. Representative corresponding examples of micrographs (40x) of PMNs, MDMs and CCs stimulated with Map. DAPI stained DNA in blue, histones in red and Map-GFP in green. Yellow arrows indicate nuclei stained with DAPI, which are absent in the red channel corresponding with anti-histone immunolabeling. Light-blue arrows indicate MDM phagocytosis. A white circle has an augmented image showing a red punctate pattern in MDM cytoplasm.

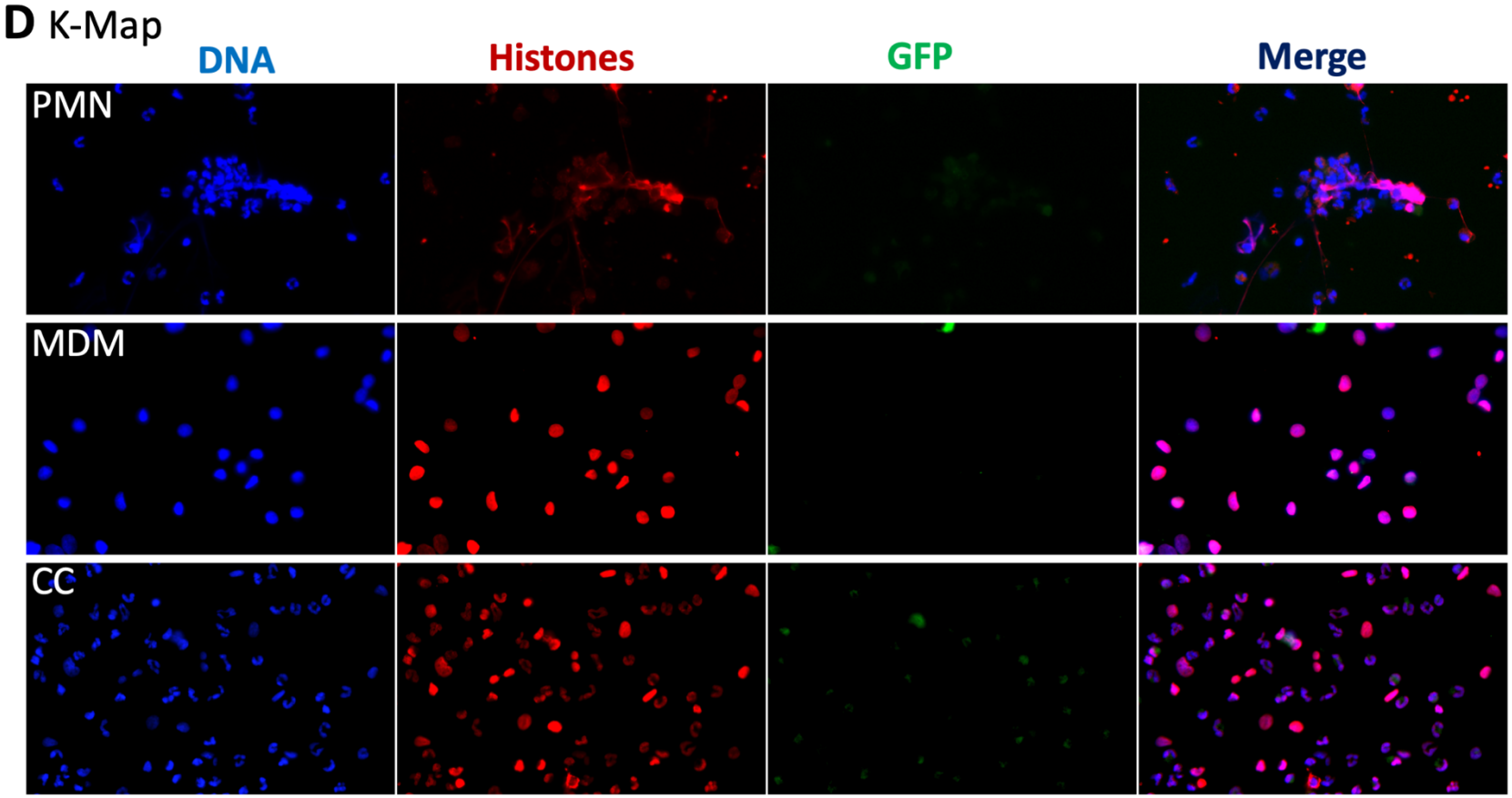

Figure 32D. ET release analysis of microscope images. Representative corresponding examples of micrographs (40x) of PMNs, MDMs and CCs stimulated with K-Map. DAPI stained DNA in blue, histones in red and K-Map-GFP in green.

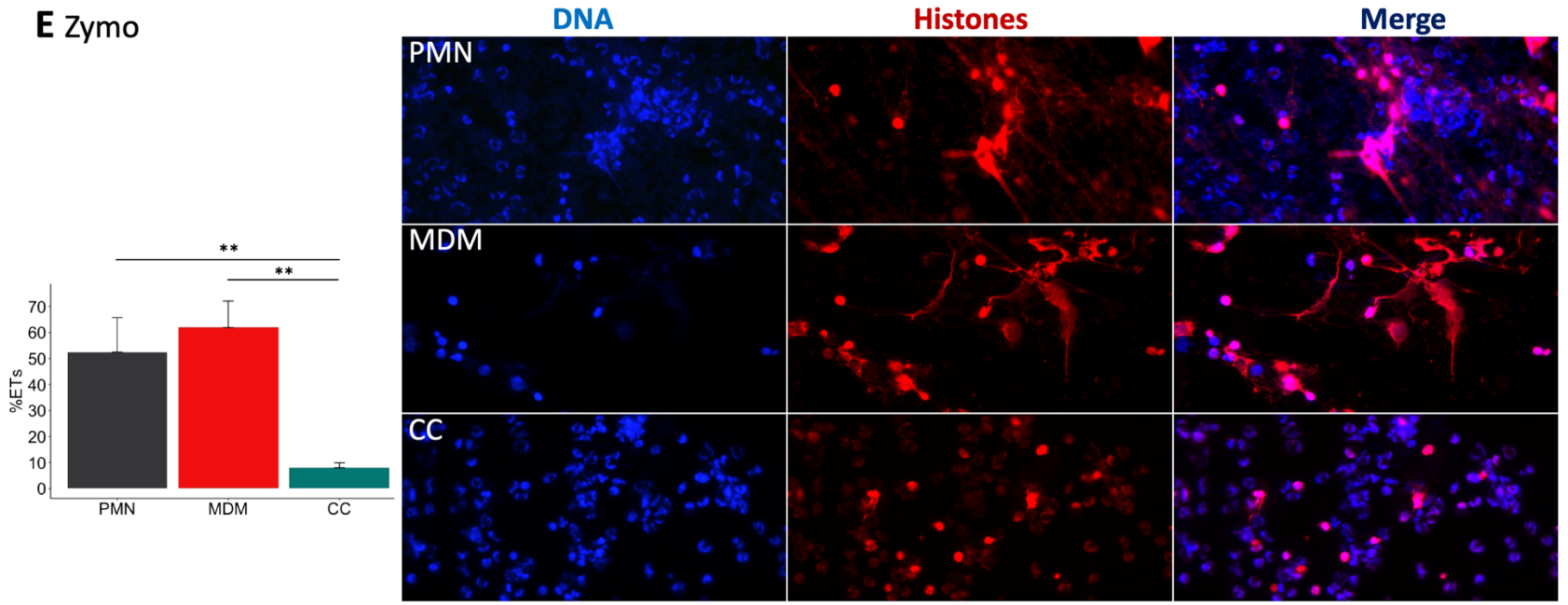

*Figure 32E. ET release analysis of microscope images. In the left of each section bar plots representing ET release quantified by immunofluorescence microscopy image analysis and in the right representative corresponding examples of micrographs (40x) of PMNs, MDMs and CCs stimulated with Zymosan. DAPI stained DNA in blue and histones in red. Data composed of combined values obtained of all cows (n=4), with samples run in duplicate and 5 fields quantified per micrograph (** $p<0.01$)*

Furthermore, ETs were rarely detected and MDMs presented a red punctate pattern in the cytoplasm (Figures 32A and C; CCs) which could support the hypothesis that MDMs phagocytosed histones liberated by PMNs.

2.3. ET release by PMNs in response to mycobacteria is not affected by stimulated MDM soluble factors

Having established that both mycobacterial species induce ET formation in PMNs, but less so in MDMs or co-culture of both cells, we next assessed if ET release was influenced by secreted mediators or required direct cell-cell contact (Figure 33A). To further address the possible paracrine effect of MDMs, PMNs were also cultured in the transwell system (TW-PMN-CM) containing macrophage-conditioned media (CM) (Figure 33B). Additional controls included unstimulated and stimulated PMN kept in the transwell insert on their own (TW-CTRL and TW-PMN, respectively) to exclude an impact on ET release by the transwell culture condition compared to PMNs kept in the lower well (PMN) (see Figures 33A).

PMNs incubated either in the transwell insert (TW-CTRL) or directly in the well (PMN-CTRL) showed no differences in baseline ET release, indicating that the culture conditions did not impact on ET release.

PMNs released equivalent levels of ETs in response to both mycobacteria when cultured either alone in the lower well (PMN) in the presence of MDM conditioned media (TW-PMN-CM), or cultured in the insert of the transwell (TW-PMN) (Figures 33C and D). In contrast, MDMs do not release ETs in transwell co-culture with PMNs when stimulated with mycobacteria (Figures 33C and D), confirming results obtained previously.

Direct cell contact induced the lowest ET release compared to the rest of the co-culture types independent whether cells were stimulated with either mycobacteria ($p<0.05$), and this effect was also present when cells were stimulated with zymosan (Figure 33E). Overall, the response to zymosan followed the response seen to either mycobacteria with the exemption of MDMs that showed a similar ET release compared to PMNs (60-70%) upon stimulation with zymosan.

2.4. PMNs show similar killing levels of Map and BCG, whilst MDMs are more effective at killing BCG

After demonstrating that ET release can be triggered by mycobacteria after 4 h, we next assessed whether ET formation at an early time point may be beneficial in terms of bacterial clearance. For this purpose, the killing capacity of PMNs, MDMs and co-cultures against both mycobacteria after 24 h was quantified. Total inoculated CFU (0 h) and CFU recovered at 24 h for all cultures are shown in Figure 34A and C. MDMs alone and CCs were more effective at killing BCG compared to PMNs alone, whereas PMNs were more effective at killing Map compared to MDMs.

The resulting distribution of live and killed BCG and Map in culture cells and supernatant is shown in Figures 34B and D.

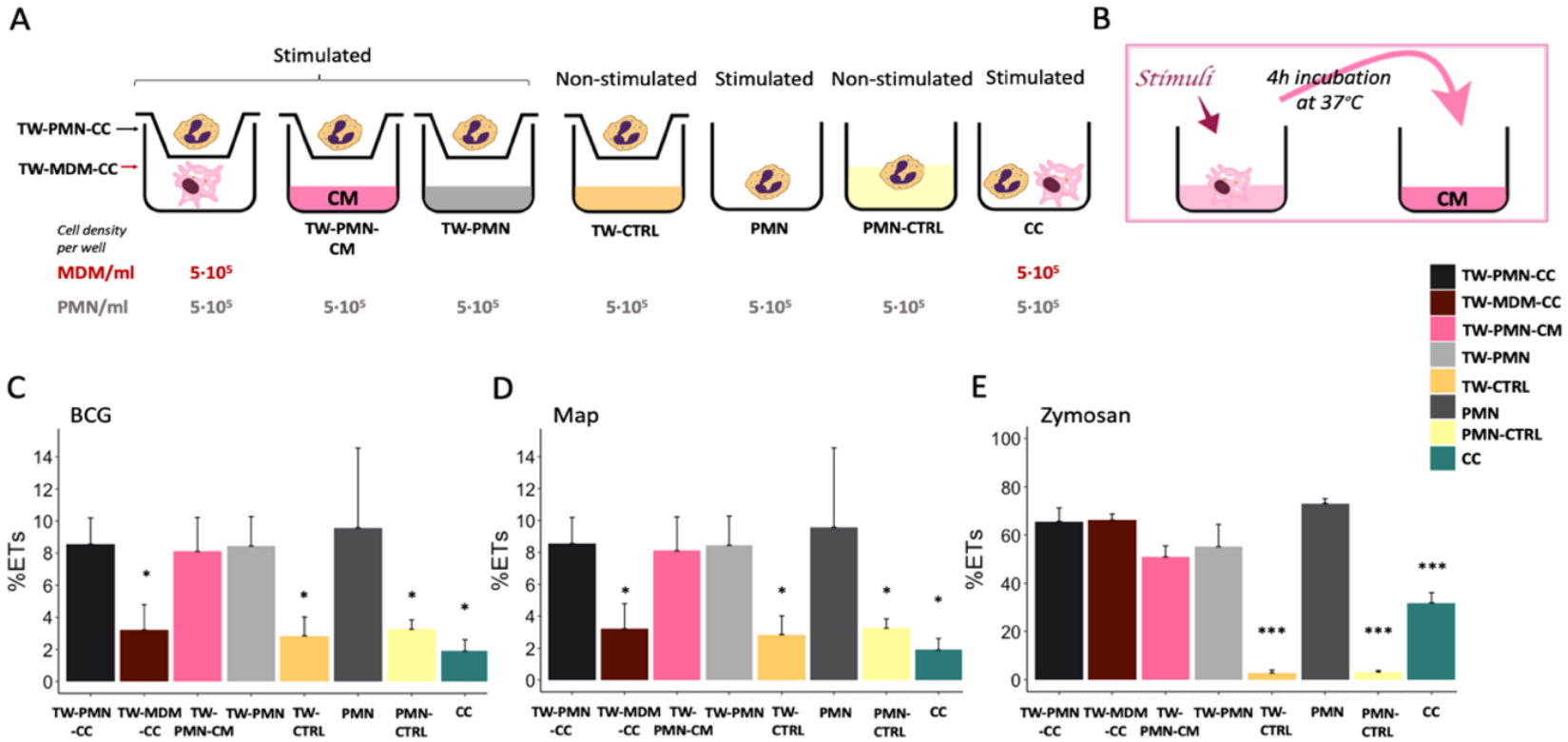

Figure 33. ET release quantified by fluorimetry of the transwell system experiment. (A) Culture types and conditions in 24 well plates. (B) Conditioned media preparation from stimulated macrophages for PMN stimulation. Fluorimetric quantification of ET release of (C) BCG, (D) Map and (E) Zymosan stimulated cultures. Data composed of combined values obtained of all cows (n=3), with samples run in duplicate (p<0.05, **; p<0.01; *** p<0.001). TW: transwell, CC: co-culture, CM: conditioned media, CTRL: non-stimulated control.*

Statistical analysis revealed significant differences between MDMs, PMNs and CCs showing higher killing of BCG in MDM cultures compared to PMNs (84.85% vs 34.15%, p=0.0016), and higher Map killing in PMN cultures than in MDMs (38.36% vs 9.14%, p=0.045). PMN culture killing rate against BCG was lower than in co-cultures (34.15% vs 88.19%; p=0.001), whereas MDM culture killing rate against Map was lower compared to co-cultures (9.14% vs 26.10%; p=0.065), although it was not statistically significant. Considering that CCs include half of the amount of each cell type, and that each cell type shows a certain killing capacity in individual culture, a theorical killing rate for CCs against each mycobacterium was calculated by dividing each individual culture (PMN, MDM) killing rate by two and adding both obtained values. Results indicate that co-cultures infected with BCG showed improved killing results (expected killing: 59.49% vs observed killing: 88.19%) than individual cultures. In contrast, this synergic effect was not evident in co-cultures infected with Map, showing only 2.52% of improvement (expected killing: 23.58 % vs observed killing: 26.1%).

When bacterial survival inside adherent cells of each cell-culture type was compared (Figures 34B and 34D), significant differences were not observed for either BCG or Map. However, non-internalized BCG survival in PMN cultures (46.23%) was higher than in MDM cultures (3.44%, p=0.021) and in co-cultures (8.65%, p=0.021), whereas non-internalized Map survival in PMN cultures was lower than in MDM cultures (54.46% vs 32.17%, p=0.03). Map-GFP survival inside adherent cells was higher than BCG-GFP as expected.

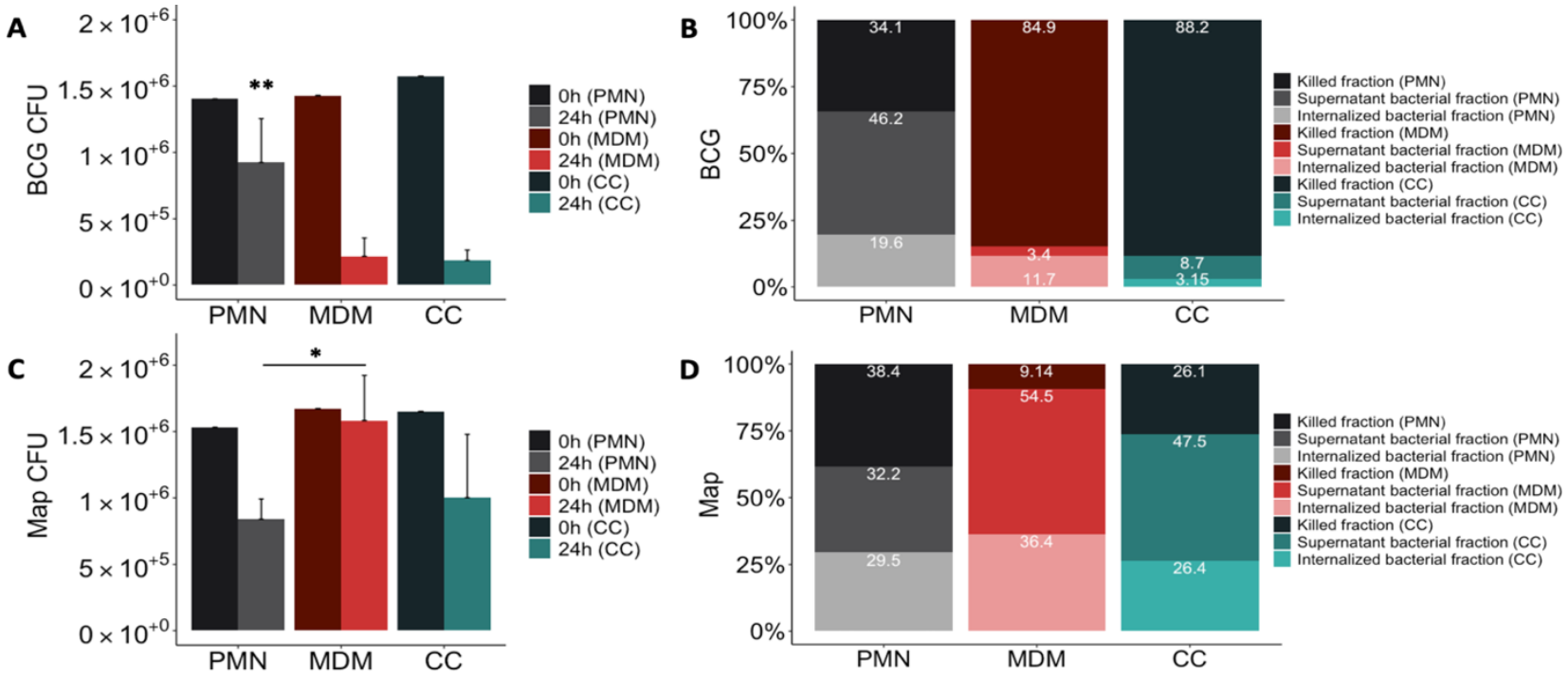

Figure 34. Mycobacterial killing assay results. of mycobacteria (A) total CFUs of BCG-GFP, (B) % BCG-GFP, (C) total CFUs Map-GFP and (D) % Map-GFP in 24 h cultures of PMNs in grey, MDMs in red and in direct contact co-cultures (CC) in green. In (A) and (C) in the dark colour the 0h control and in the light colour the 24 h assay of the corresponding culture type. In (B) and (D) in the darkest colours the fraction of killed bacteria, in the intermediate intensity colours the fraction of live bacteria non-internalized from the supernatant and in the lightest colours the proportion of internalized bacteria that survived inside the adherent cells of the corresponding culture type. Data composed of combined values obtained of all cows (n=4), with samples run in duplicate (p=<0.05, **, p=<0.01).*

2.5. MDMs alone release higher cytokine levels compared to PMNs independent of culture condition

Having assessed the killing capacity of both cell types to different mycobacterial strains, we next investigated whether their cytokine response follows a similar pattern. Considering that IL-8 is a major ET inducer in PMNs (Krupa *et al.*, 2015) and IL-1β is a key mediator of the inflammatory response that attracts macrophages to the infection site (Lamont *et al.*, 2012), we analysed the levels of both cytokines in the supernatant. IL-1β release after 24 h showed significant differences between the cells involved as well as in response to both mycobacteria. MDM cultures released higher concentrations of IL-1β (Figure 35A) in response to BCG compared to PMN ($p<0.001$) and CC ($p=0.009$) and in response to Map compared to PMN ($p=0.035$). Furthermore, MDM released significantly more IL-1β in response to BCG compared to Map.

Similar as seen for IL-1β, MDMs secreted more IL-8 into the supernatant in response to both mycobacteria (Figure 35B) compared to co-cultures (BCG; $p< 0.001$, Map; $p=0.013$) or PMNs alone (BCG; $p=0.001$, Map; $p=0.005$). As before, MDMs challenged with BCG produced significantly more IL-8 than challenge with Map ($p=0.011$).

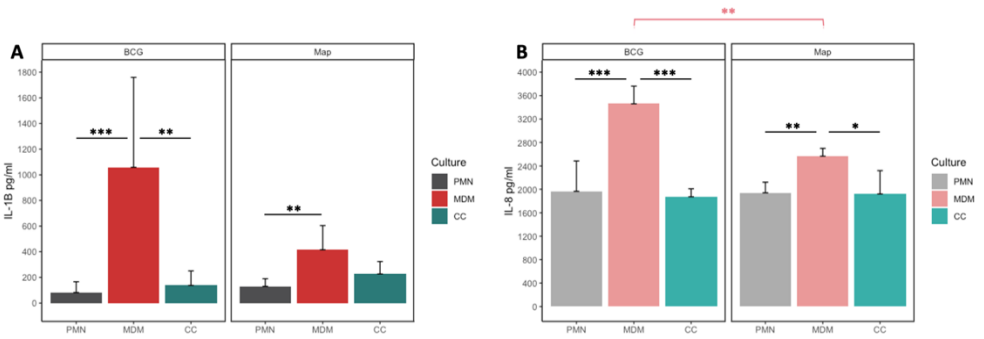

Figure 35. Cytokine release of (A) IL-1β and (B) IL-8 in PMN, MDM and CC cultures stimulated with BCG and Map after 24h. Data composed of combined values obtained of all cows (n=4), with samples run in duplicate (p<0.05, **; p<0.01; *** p<0.001).*

2.6. Correlation analysis of cytokine production and bacteria killing rates suggest different mechanism interplay between MDMs and PMNs against BCG and Map.

Correlation analyses were performed between cytokine levels, and mycobacteria killing rates to evaluate the strength of relationship between both parameters (Table 9). The correlation study was performed including the data from all the culture types together and then subdivided by culture type and stimuli. IL-1β and IL-8 levels were positively correlated at 24 h including all culture types in the analysis indicating that both cytokines are secreted in the same culture conditions in our assay. This correlation improved when eliminating the CCs from the analysis suggesting that cytokine release follows a different pattern in CCs maybe due to the difference in cell number. BCG-stimulated cultures showed a positive correlation between IL-1β and killing rate, which increased when eliminating CCs from the analysis. On the other hand, Map-stimulated cultures showed a negative correlation between IL-1β and killing rates, and in this case, power was increased when analysing

PMNs alone. IL-8 and killing capacity were positively correlated in MDM cultures. IL-8 and killing rates were negatively correlated in Map-stimulated cultures.

Table 9. Correlation analyses results between cytokine levels and mycobacteria killing rates.

Culture			**Stimuli**		**Parameters**			**Correlation**		
PMN	MDM	CC	BCG	Map	IL-1β	IL-8	killing	n	coefficient	p
✓	✓	✓	✓	✓	✓	✓		24	0.64	<0.0001
✓	✓		✓	✓	✓	✓		16	0.75	0.0011
✓	✓	✓	✓		✓		✓	12	0.75	0.0074
✓	✓		✓		✓		✓	8	0.95	0.0011
✓	✓			✓	✓		✓	8	-0.7	0.011
✓				✓	✓		✓	4	-0.98	0.016
	✓		✓	✓		✓	✓	8	0.87	0.0044
✓	✓	✓		✓		✓	✓	12	-0.8	0.002

Discussion

Paratuberculosis (PTB) is an enteric granulomatous disease caused by *Mycobacterium avium* subsp *paratuberculosis* (Map). PTB mainly affects ruminant livestock causing significant economic problems. Map can also affect other animal species including humans, making it a potential zoonotic agent (Whittington *et al.*, 2019). In ruminants, subcutaneous vaccination with inactivated Map vaccines not only has shown to be an adequate control method conferring protection against PTB (Bastida and Juste, 2011), but also has shown to exert beneficial non-specific effects by reducing overall mortality in vaccinated herds (Juste *et al.*, 2021). Despite these apparent benefits the use of these vaccines is banned in many countries due to cross interference with bovine tuberculosis (bTB) diagnosis (Patton, 2011; Garrido *et al.*, 2013).

Previous work by others has shown that administrating mycobacterial vaccines through the oral route can avoid this cross-reactivity (Roy *et al.*, 2017), but further knowledge on protection, mucosal immunity activation and possible generation of trained immunity through this route is needed. Further supporting this route is the fact that oral vaccination mimics natural exposure to Map. Another alternative route that has not been explored in PTB but can be attractive due to the generation of novel inoculation devices is the intradermal.

Apart from studying other administration routes, tackling knowledge gaps in pathogenesis can aid PTB vaccinology. Most research has been focused on the action of macrophages since they are the main immune cell subset invaded by Map, where this pathogen is able to survive and replicate

intracellularly inhibiting phagosome maturation. Less attention has been addressed to neutrophils (PMNs) although their presence has been recognized at disease sites during the early stages of infection (Sigurdardóttir *et al.*, 1999; Khare *et al.*, 2009). Recent transcriptomic studies suggest that Map infection causes an impairment of PMN recruitment (Park *et al.*, 2018; Alonso-Hearn *et al.*, 2019) making this immune cell worth studying.

In this Thesis work, administration routes have been assessed for protection, effect on local macrophages and peripheral immune response and interference with bTB. The oral route has been studied in depth with both mycobacterial and non-mycobacterial vaccines, showing signs of trained immunity in peripheral PMNs and heterologous protection (Figure 36).

Having studied the effect of vaccines in local macrophages and PMNs *ex vivo*, there was a need to study the effect of both cell types upon infection. It was also necessary to validate the PMN functional assay methodology developed in rabbits in the PTB target species. Therefore, the action of bovine PMNs alone and in co-culture with macrophages against Map and BCG was investigated. To our knowledge, this is the first work reporting bovine PMN ET release and killing capacity against Map. The performance of *ex vivo* functional assays with bovine PMNs have shed light on the possible mechanisms that these immune cells display to combat Map, alone or in cooperation with macrophages (Figure 37).

The first aim of the present thesis work was to evaluate an experimental vaccine through the oral (VOR) and intradermal (VID) routes in the rabbit model of PTB in terms of Map clearance and immune responses

and compare to the subcutaneously administered commercial vaccine (CV) used as control. In general, Map-challenged animals, including vaccinated and non-vaccinated groups showed weight reduction in comparison with non-infected controls (NIC) animals, although significant differences were only observed between the CV and the NIC groups. This could be a consequence of the stress of the animals due to the itching generated by the granuloma at the inoculation site of the CV vaccine.

Regarding the necropsy findings, 40–80% of the challenged animals showed PTB like gross lesions, consisting of caseous necrosis in SR and VA, intestinal wall thickening and lymphangiectasia. In spite of not having found significant differences between groups, the VID group was the one with more animals without visible lesions. Interestingly, this was also the group with less Map positive tissues evaluated by PCR. These events suggest that the intradermally delivered experimental vaccine could be more effective at Map clearance and thus, exert higher protection upon infection. On the other hand, CV did not completely clear the bacteria since 80% of the animals tested positive in the PCR. Additionally, the reduction in microscopic lesions, that is considered important in terms of protection (Huang *et al.*, 2015), was not significant when compared to the infected control (IC) group.

Macrophages are a doble edge sword in PTB, they display their bactericidal functions at the infection place, while providing a refuge for Map (Arsenault *et al.*, 2014). Depending on their state of polarization, macrophages acquire a phenotype with variable functional characteristics, for which a heterogeneous variety of macrophage populations is known. As with

the lymphocyte Th1/Th2 classification system, M1/M2 macrophage nomenclature was introduced to establish two polarized activation states. M1 macrophages exert a set of pro-inflammatory functions while promoting Th1 responses, whereas the M2 phenotype is specialized in tissue repair functions and promoting Th2 responses (Bekker *et al.*, 2000).

In PTB M1 macrophages have been considered more abundant in focal and multifocal forms in Map infected cattle, associating these with the ability to control Map infection in latent lesions. On the contrary, M2 macrophages are considered the main type in diffuse multibacillary forms related with the immunoregulatory phenotype that permits the infection to continue (Begg *et al.*, 2011). Furthermore, in human tuberculosis (hTB), M1 macrophages have been linked to the early stages of infection and protective responses, whereas M2 macrophages have been linked to the advanced stages of infection, in which host responses lose control of the infection (Green *et al.*, 2013). Previous studies address infection-associated macrophage polarization, while this is the first time that tissue macrophage polarization in vaccinated and Map-challenged animals is reported.

IFN-γ, historically considered a key cytokine in mycobacterial diseases, is directly responsible for M1 polarization of macrophages favoring pro-inflammatory responses and increasing macrophages' microbicidal abilities. Indeed, when IFN-γ acts in concert with TNF, macrophage phagocytosis and microbicidal capacities are enhanced and have been reported to be necessary in the control of Mtb (Fernández *et al.*, 2017b).

Analyzing immunohistochemistry (IHC)-scores of *sacculus rotundus*, IFN-γ achieved higher scores for VID, VOR, and IC groups when compared to CV animals, whereas higher scores for TNF were detected for CV and VID groups compared to VOR and IC. CD163 immunolabeled cells were more numerous for VOR and CV groups, indicating a more M2 polarized phenotype. Taken together, *sacculus rotundus* IHC suggests that the VID group presents a more M1 polarized response, which connects with the fact that lower bacterial loads were detected in the analyzed tissue.

In vermiform appendix the IHC-score for TNF was fairly low in all infected groups. This could mean that functional differences exist between both intestinal sections, and that the vermiform appendix lymphoid tissue possesses lower protective immune capacity than *sacculus rotundus*, at least at the studied time point. CD163 scores were again higher in the VOR and CV groups, associating these groups with the M2 polarization state. These results are consistent with the fact that all infected groups exhibited more severe lesions in the vermiform appendix in comparison to the *sacculus rotundus*.

Another remarkable result of the IHC is that the IC group scored higher for calprotectin in both *sacculus rotundus* and vermiform appendix, than the vaccinated groups. Calprotectin is a cytosolic protein complex present in peripheral blood monocytes, whose expression is maintained for a short period of time in recently recruited macrophages but that is lost after further differentiation (Elguezabal *et al.*, 2011). This suggests that the lesions of the IC group are more active than those in the vaccinated groups that seem

to be recruiting less new macrophages. In this sense, together with the high calprotectin levels, some of the IC animals also presented higher IFN-γ scores in comparison to vaccinated animals, indicating to some extent that vaccination had promoted healing. In line with these results, a previous study in cattle revealed that the diffuse forms in tissues from infected animals harbor higher calprotectin immunolabeled cells compared to the focal ones and focal and diffuse paucibacillary forms showed more IFN-γ expression (Duluc *et al.*, 2009).

It must be highlighted that macrophage polarization can be reversible both *in vitro* and *in vivo* (Dannenberg and Collins, 2001; Hagemann *et al.*, 2008) and also that the immune response is a dynamic process thus, obtaining conclusions based on data from just one point may lead to inaccurate interpretations. Moreover, recent studies associate the subclinical cases to a more balanced M1/M2 ratio opposed to control animals or clinically infected animals, showing a M1 and M2 pattern, respectively (Jenvey *et al.*, 2019). For these reasons, in order to improve the characterization of macrophage polarization status upon infection and the modulatory effect that the different vaccination routes have in it, present results must be verified in more animals and at different time points.

Additionally to protection, a promising PTB vaccine candidate should also elude interference with the skin test used for bTB diagnosis. In this study, guinea pigs were used as a model for tuberculin skin testing because they develop a strong delayed-type hypersensitivity response. The intradermal vaccination caused some degree of skin test reaction and did not show

increased PPA-3 levels by the end of the study. This means that in the event of considering the intradermal route for vaccination, this vaccination strategy should be combined with a diagnostic differentiation against both bTB and PTB. On the contrary, oral vaccination showed promising results causing no skin reactivity.

The oral route showed absence of interference with bTB diagnosis in the guinea pig model and low protection against Map in the rabbit model. This could be due to the lack of immune stimulation as a result of using an inactivated bacteria without adjuvant. Therefore, the following attempt was to improve oral vaccine formulation, utilizing the QuilA adjuvant and also to investigate the possible priming of innate cells derived from vaccination. Inactivated vaccines, based on Map (MPV), Mbv (MBV) and *C. pseudotuberculosis* (CPV) were formulated with QuilA, whereas a live attenuated vaccine (LAV) was tested without adjuvant. Including the QuilA adjuvant in the formulation of inactivated vaccines showed that mucosal activation and protection upon Map challenge was possible through oral vaccination (even with inactivated vaccines), and that PTB vaccination (with oral experimental vaccines and with the commercial vaccine) is able to enhance PMN functionality (showing trained immunity effects) as seen by increased phagocytosis and extracellular trap (ET) release, important mechanisms for bacterial clearance.

Some of the tested vaccines increased the capability of PMNs to phagocytose naked Map, in other words, in the absence of opsonization with inactivated autologous plasma. This type of phagocytosis is most prominent

one month after vaccination, but resulted temporary, lasting for three months after vaccination for the CPV vaccine and up to four months for CV.

PMNs are able to efficiently phagocytose pathogens by opsonization with complement factors or antibodies (Bournazos *et al.*, 2015). Also, they have been reported to express several membrane TLRs (Conejeros *et al.*, 2011), which in human and bovine PMNs, have shown to increase phagocytosis (Hayashi *et al.*, 2003; Conejeros *et al.*, 2015).

The described non-opsonized phagocytosis in this study could be linked to an increased expression of pattern recognition receptors on the surface of PMNs from vaccinated animals as seen in vaccination against leishmaniosis in dogs (Moreira *et al.*, 2016) and with BCG in humans (Moorlag *et al.*, 2020). Also, lactate levels were correlated with non-opsonized phagocytosis in PV3, being the CV group the main contributor to this correlation. It may be that CV is inducing high levels granulopoiesis in bone marrow, phenomenon that has been reported for BCG (Brook *et al.*, 2020). These high granulocyte demands would require elevated aerobic glycolysis that result in lactate increase as described previously (Khatib-Massalha *et al.*, 2020).

Phagocytosis of antibody-opsonized bacteria was higher than non-opsonized phagocytosis in most cases and highest in the CV control group correlating with higher levels of specific anti-Map-antibody levels in plasma. As for the tested oral vaccines, in the absence of antibodies, phagocytosis rates of Map pre-incubated with autologous plasma and non-treated-Map were equivalent.

Attending to the humoral response, PPA-3 antibody titers only were significantly higher in the animals immunized with the commercial vaccine (CV) during the course of the experiments. The humoral immune response against Map has been traditionally related to clinical stages of the disease and severe lesions (Sweeney, 2011) and thus, it has not been considered important in terms of protection. However, some studies argue that antibodies could be relevant against mycobacteria (Juste *et al.*, 1994; Balu *et al.*, 2011; Pooley *et al.*, 2019). The findings derived from the phagocytosis assay of the present work, suggest that during the first months after vaccination with CV, PMN activation may occur through upregulation of superficial pattern recognition receptors, but once antibody levels increase, phagocytosis of opsonized Map would be predominant and, in this case, antibodies would be helpful if phagocytes encounter extracellular opsonized-Map. For this reason, the antibody response triggered by the commercial vaccine should be considered as one of the factors behind this vaccine's protective effects. Indeed, previous studies in rabbits, cattle and goats (Juste *et al.*, 2009b; Hines *et al.*, 2014; Arrazuria *et al.*, 2016b) report a connection between the high antibody titers promoted by the commercial vaccine and protection. Furthermore, a recent study conducted in sheep using a similar commercial vaccine, Gudair®, (Barros *et al.*, 2013) directly states that the humoral response is necessary for adequate protection against Map. As a fact, the size of the granuloma at the inoculation point resulted positively correlated with the antibody levels. Anyhow, the high antibody titers observed with this kind of vaccines can present an obstacle for PTB diagnosis as long as there is no test to differentiate infected from vaccinated animals (DIVA).

ET formation is an important effector mechanism for pathogen clearance (Brinkmann *et al.*, 2004). ET release results presented in this second study also suggest a certain degree of immunity training exerted by oral vaccination that correlates with protection. Firstly, groups with the lowest Map tissue positivity (CV, CPV and MPV) show, at some point (one month or three months after vaccination) higher ET release compared to the non-infected control group when challenged *in vitro* with Map. Secondly, PMNs from CPV and CV groups are the ones showing the highest ET release, which also happened to be the groups showing the best PMN phagocytosis response, meaning that these are the groups with highest PMN activation or training levels.

Interestingly, in some cases this training or functional activation is heightened by Map oral challenge. One month after vaccination (PV1), PMNs of all orally vaccinated groups, showed lower ET level release against *E. coli* compared to CV and control groups, whereas after Map challenge (PV3) ET release levels increased for all challenged groups. This phenomenon was also observed against *S. aureus*. Also, worth mentioning is the finding that vaccines CPV and MBV did not show antigen specific response to self-antigen. This could be due to some type of self-tolerance as that seen in macrophages when low doses of LPS fail to activate histone marks in promoters of genes involved in phagocytosis pathways resulting in a lower inflammatory response of macrophages to subsequent stimulation (Novakovic *et al.*, 2016) or the activation of different defense mechanisms due to vaccination.

What takes PMNs to release ETs or to phagocytose pathogens remains a mystery (Ley *et al.*, 2018) and many microorganisms have not been tested yet for their ability to stimulate ET release. Interestingly, high ET release is not always associated with the control of the disease (Gunderson and Seifert, 2015). Indeed evidence is accumulating that excessive production of NETs is related to the exacerbation of inflammation and the development of autoimmunity, cancer metastasis and inappropriate thrombosis (Honda and Kubes, 2018). We believe that a good PTB vaccine should potentiate phagocytosis, rather than NETosis considering that Map is an intracellular bacterium.

Regarding cytokine expression in circulating PBMCs, oral vaccines enhanced early IL-4 expression, which is known to be a relevant cytokine for mucosal immunity shaping (Boyaka *et al.*, 2001). Added to this, total serum IgA increased after vaccination in the oral vaccinated groups being highest for CPV, which also shows high PMN activation and low Map tissue positivity. However, the subcutaneous administration of CV did not elevate either IL-4 or serum IgA, but in contrast with the oral vaccines, CV caused an early increase in IL-10 and also high TNF and low IL-4 expression in circulating PBMCs probably due to granuloma formation at the inoculation site as seen for Mycopar®, another commercially available whole cell bacterin containing inactivated Map (Lei *et al.*, 2008). This elevation of IL-10 has also been reported for this vaccine in a study that involved *in vitro* infection of caprine monocyte derived macrophages with Map (Arteche-Villasol *et al.*, 2021).

MPV vaccine showed the most convenient basal profile of immune modulation regarding protection at PV1 showing the highest IL-4 expression, significant TNF and IFN-γ increases and lowest IL-10 expression. IL-10 has been described to have a role in immune tolerance (Maurer *et al.*, 2003) and the blockage of IL-10 during immunization has demonstrated better pathogen clearance results in some studies (Ni *et al.*, 2015). In this context, maintaining IL-10 levels low during immunization could be the best approach to avoid mucosal tolerance of Map.

Upon *in vitro* re-stimulation of PBMCs with Map sonicate (*ex vivo* secondary exposure), in general, an innate immune activation driving inflammatory response was characterized by increased IL-1β, TNF and IL-23A expression, accompanied by an increase of the regulatory IL-10. MPV was the only group showing high IL-12B and IL-23A levels. High levels of IL-23 should be desirable since it has been linked to maintaining homeostasis in the intestinal barrier by preventing the entrance of inappropriate bacteria (Fatkhullina *et al.*, 2018).

Primed IL-1β response by gut monocytes and DCs, is considered to enhance gut protection, due to its role in inflammatory cell recruitment (Chase, 2018) and PBMC derived IL-1β participates in PMN recruitment and activation and inhibition of PMN apoptosis (William *et al.*, 1998; Prince *et al.*, 2004). In our study, all vaccinated animals showed increased IL-1β expression one month after vaccination (just before challenge) upon re-stimulation with Map sonicate. Furthermore, early IL-1β basal increase

correlated with increased phagocytosis activity of PMNs. In this sense, the vaccine triggering highest basal levels of IL-1β was CPV.

The GALT cytokine expression profile at the end point of the experiment showed a discrete pro-inflammatory response in most of the challenged animals, including all vaccinated groups and CC. The subclinical nature of the infection model is probably contributing to this fact. CV showed the highest lymphoproliferative expression in comparison to the oral vaccines probably due to the administration route and the persistence of the granuloma generated at the injection site, which, in the first study, has shown to correlate in size to anti-PPA3 antibody levels.

There has been controversy on whether inactivated vaccines maintain their innate training effects, mainly because evidence from human clinical data has claimed that the beneficial non-specific effects would be limited to live vaccines (Aaby *et al.*, 2014), as seen by comparison of BCG and gamma-irradiated BCG (Arts *et al.*, 2015). On the other hand, there is proof that a vaccine composed of cell wall components from *Mycobacterium phlei* in oil-emulsion was able to decrease overall mortality in feedlot cattle (Masic *et al.*, 2017), and also to improve survival after Enterotoxigenic *E. coli* challenge in neonatal cattle (Radoslaw *et al.*, 2017). In any case, we believe that this training effect in inactivated vaccines should be revised since we have demonstrated cross protective effects of heterologous inactivated vaccines against PTB in the present study.

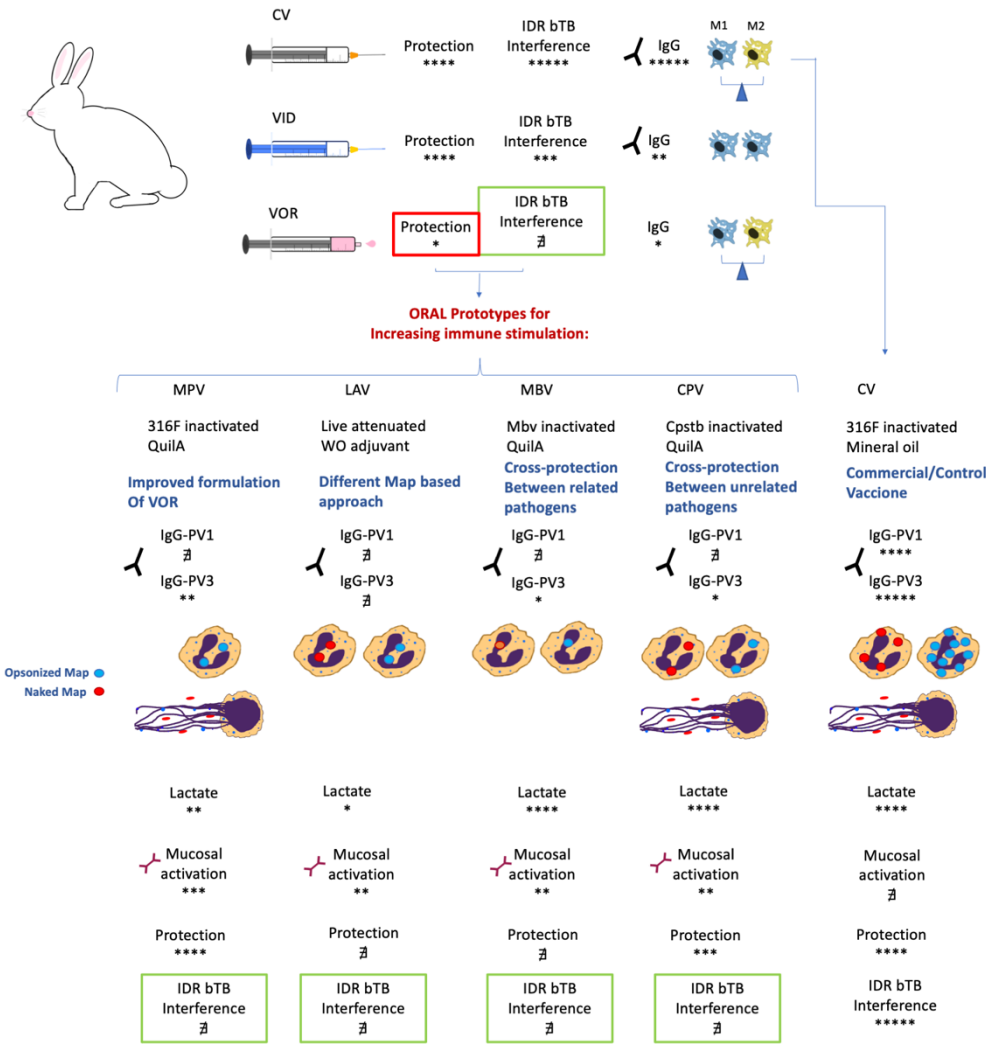

Figure 36. Schematic representation of the most remarkable results of the different vaccination routes and vaccines tested in this Thesis.

Data here presented should be confirmed in ruminants. The results regarding trained immunity mechanisms obtained in the rabbit model in this study are most probably similar in ruminants and will include training of

PMNs and monocytes as seen in this study and in that conducted by Arteche Villasol *et al* (Arteche-Villasol *et al.*, 2021) respectively. Attending to the properties exerted by the presented vaccine prototypes, CPV has shown interesting characteristics enhancing unspecific, but protective, PMN activation levels. This immunostimulatory capacity of the CPV vaccine is not surprising since different *Corynebacterium* species have shown to be potent immunostimulants (Ebisawa *et al.*, 2017; Palmieri *et al.*, 2020).

Having observed that trained PMNs could be responsible for the improvement in the sequence of events in the pathology of PTB, and that vaccination could also interfere in macrophage polarization, the following question that this Thesis work intended to address was related with the interaction between PMN and macrophages against Map. More concretely, the intention was to test whether a cooperation of both professional phagocytes would present an advantage for the host resulting in successful clearance of the mycobacteria. In addition, the developed PMN techniques in the rabbit model needed to be validated in the target species. With all this in mind, bovine monocytes were isolated and differentiated to macrophages (MDMs) cultured *ex vivo* separately or together with PMNs isolated from the same individual and were challenged with Map and a less pathogenic mycobacterium, *M. bovis* BCG. For the evaluation of this cooperation, ET release, the levels of the pro-inflammatory cytokines IL-1β and IL-8 and the destruction of mycobacteria were evaluated.

With respect to ET release, PMNs released more ETs against killed mycobacteria than live bacteria and more ETs than MDMs in all cases. This

is in agreement with the findings of previous studies, one of which reports that glycolipids from heat-inactivated mycobacteria allow their recognition by TLR2 and Mincle (Ishikawa *et al.*, 2009) and the other that demonstrated the formation of NET after activation of Mincle expressed in PMN (Sharma *et al.*, 2017). The direct interaction of MDM and PMN, in contrast, resulted in lower ET detection compared to PMNs cultured alone or PMNs cultured with MDM but in the transwell system. Furthermore, this effect was independent of the stimuli and whether the bacteria were alive or dead.

This lower presence of ET in direct contact might be due to the elimination of ET by a process in which apoptotic cells and the products of inflammation are eliminated by macrophages, known as efferocytosis. However, there is also a possibility that PMN respond differently in the presence of MDMs.

Indeed, the observation in micrographs that PMNs in CC present more internalized BCG bacilli and less detectable ETs than in separate cultures is in line with the hypothesis that PMNs may not release ETs when they are in direct contact with MDMs. In Map stimulated CCs, however, PMNs acquire an apoptotic aspect, without histone immunolabeling, few ETs and almost no internalized Map bacilli, whereas MDMs showed a red dotted histone containing cytoplasm. With the data obtained from this the experiment, it is not possible to know if it is a direct effect of Map on PMNs or if it is due to the process of efferocytosis. Activated inflammatory cells have shown to actively secrete histones into the extracellular space (Xu *et al.*, 2011), and histones are part of ET composition (Papayannopoulos and Zychlinsky, 2009)

and that they can come from apoptotic and necrotic cells (Xu *et al.*, 2011). Furthermore, extracellular histones have been reported to inhibit the efferocytosis process *in vitro* and *in vivo* (Friggeri *et al.*, 2012). Thus, it is possible that in our experimental conditions, Map infection drives PMNs to release ETs with the consequent histone liberation to the extracellular space, which would be then engulfed by MDMs, an event which ultimately would suppress the efferocytosis process and could explain why apoptotic PMNs remain while ETs are not detectable.

Regarding the bacterial killing results, in our experimental conditions, MDMs demonstrated being highly efficient in killing the attenuated *M. bovis* BCG, while they seemed unable to kill Map. PMNs, however, showed equivalent killing rates against both BCG and Map. Intriguingly, when these were co-cultured in a 1:1 ratio, the killing capacity against BCG was similar to that obtained by MDMs, but in the case of Map it was comparable to that obtained by PMNs. Moreover, taking into account that half of the numbers of each phagocyte type were present in CCs, the obtained killing % for CC indicates a synergistic effect of both cell types in BCG-infected co-cultures (observed killing > expected killing), whereas in Map-infected co-cultures both cells killed in an additive way (observed killing = expected killing). Therefore, the presence of PMN at the site of infection during the initial stages of Map could compensate for the difficulties that macrophages have in killing Map. In fact, an *ex vivo* study on human PMNs (Brown *et al.*, 1987; Jones *et al.*, 1990) demonstrated that these were capable of controlling Mtb infection and another one carried out with murine PMN demonstrated that following

G-CSF activation *in vivo*, these were able to kill *Mycobacterium avium ex vivo* (Bermúdez *et al.*, 1998).

Attending to the pro-inflammatory cytokines, not surprisingly MDMs produced significantly higher cytokine levels compared to PMNs and CCs in response to both mycobacteria. Unexpectedly, cytokine levels of CCs were low against both mycobacteria, being similar to those obtained in cultures of PMNs. In contrast, in a similar co-culture system using guinea pig PMNs and alveolar macrophages challenged *in vitro* with Mtb, Sawant and McMurray, (Sawant and McMurray, 2007) obtained higher IL-8 and IL-1β levels in comparison with separate cultures of these cells alone. There are some differences between both experiments that could explain the different outcomes. First, their co-cultures harboured the double number of final cells compared to separate cultures, whereas in our study we have used half of each phagocyte type for CCs, maintaining the final cell numbers in the three culture settings. Second, cell origins were different in terms of species (guinea pigs versus cattle) and of tissue source (lung versus peripheral blood).

Regarding the analysis of released cytokines, IL-8 secretion of the phagocytes against BCG and Map was compared. IL-8 expression has been described to be higher in monocytes from Map infected animals stimulated *ex vivo* with Map (Weiss *et al.*, 2002; Coussens *et al.*, 2004) than in those from healthy controls. In the present thesis work, the lower IL-8 release by MDMs infected with Map versus BCG infected MDMs could be related to the higher pathogenicity of Map. In line with this findings is the observation that a multi-drug resistant Mtb strain decreased the release of IL-8 by infected

bronchial epithelial cells, which limited PMN recruitment to the infection place (Kviatcovsky *et al.*, 2017). Similarly, although not significant due to the dispersion of the data, IL-1β release by MDMs was also higher against BCG than against Map. Together these findings clearly reflect the capability of Map to reduce the inflammatory response enough to ensure its survival but also to permit the slow but constant recruitment of leucocytes to the site of infection.

Attending to the effect observed in CCs, it is possible that similarly as described before (Vandivier *et al.*, 2006), anti-inflammatory mediators released by PMNs suppress the production of pro-inflammatory cytokines by MDMs, as well as it is also possible that macrophages themselves release anti-inflammatory cytokines during the efferocytosis process to promote homeostasis (Chung *et al.*, 2007; Korns *et al.*, 2011). In fact, the efferocytosis process that leads to homeostasis, is known to supress the inflammatory response, therefore, the increased IL-1β and IL-1α levels described in PTB by others (Chiang *et al.*, 2007) could be due to PMN activation and recruitment impairment (David *et al.*, 2014; Gossner *et al.*, 2017; Ibeagha-Awemu *et al.*, 2018; Park *et al.*, 2018; Alonso-Hearn *et al.*, 2019) and the resulting absence of PMNs at PTB granulomatous lesions (Lee *et al.*, 2001; Krüger *et al.*, 2015). Additionally, the increase of these cytokines at the infection site is thought to have a role in the enteric inflammatory process and also promote the development of the Th17 response during the advanced stages of PTB (DeKuiper and Coussens, 2019b).

The analyses of the relation between cytokine levels and bactericidal activity of cultures, showed that the release of IL-1β and IL-8 cytokines resulted positively correlated with the killing of the attenuated BCG strain, especially in MDMs, while, the release of both cytokines was negatively correlated with the killing of Map, showing a stronger negative correlation in PMNs. In this sense, in hTB, low IL-8 levels are associated to bad prognosis (Krupa *et al.*, 2015) and to Mtb survival inside macrophages by producing alterations in PMN functionality (Kviatcovsky *et al.*, 2017). Regarding IL-1β, a previous study carried out in IL-1 knock-out mice showed that these were more susceptible to infection by Mtb, showing higher bacterial loads and mortality than the wild type (Mayer-Barber *et al.*, 2010). Taking all this into account, it was expected that the cultures with the highest levels of the studied cytokines would be those exhibiting lowest mycobacterial survival rates. Although this was the case in cultures infected with BCG, this was not what happened in Map infected cultures, indicating, that there are more factors involved. Indeed, *in vitro* studies suggest that Map infection drives the epithelium to a self-destruction state resulting from the increased IL-1β levels, which would attract macrophages, thus facilitating Map's escape from being destroyed (Lamont *et al.*, 2012).

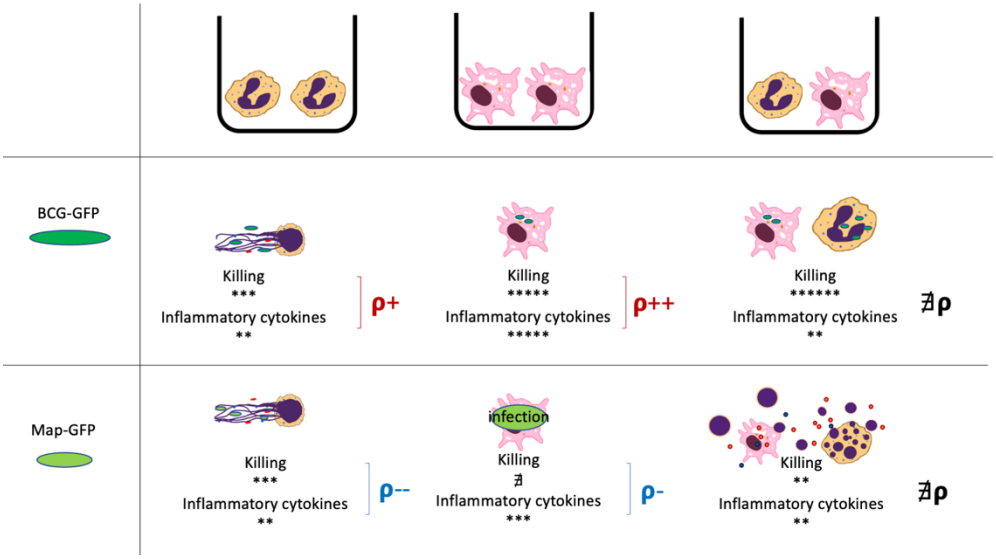

Figure 37. Summary of the most remarkable results of the ex vivo *infection cultures of bovine PMNs and MDMs alone and in co-culture. Red and blue ρ symbols indicate positive and negative correlations.*

In light of the results of this Thesis, we hypothesized that bovine PMNs may play an important role against Map. An effective defence against Map would take place if, once PMNs have reach the infection place attracted by the released local alarm signals they would collaborate amplifying the inflammatory responses together with M1 macrophages through the release of cytokines such as IL-1β and IL-8 while exerting their effective microbicidal functions of phagocytosis, degranulation and ET release. As part of the inflammatory response, together with other effector leucocytes, peripheral blood monocytes would be activated and attracted by the pro-inflammatory cascade to the site of infection. In order to prevent self-damage, macrophages would phagocytose inflammation products and apoptotic PMNs and their ETs, which provide them with valuable antimicrobial compounds

produced by PMNs and Map antigens. This efferocytosis activity, executed by M2 macrophages, combined with an effective cooperative work between both phagocytes in killing Map, would shut the inflammation and decrease the expression of its promoters (IL-1β, IFN-γ, TNF, IL-8, IL-23, IL-17 among others), ending ultimately in controlling Map invasion and tissue repair. The timing may be crucial in this operation and if PMNs arrive at the infection site too late, these might not be able to expand their antimicrobial mechanisms and cooperative functions before Map interferes in the inflammatory response from the inside of macrophages. Once Map has taken control of the situation inside macrophages, it acts as a Trojan horse, interfering in the normal functioning of inflammatory and regulatory mediators in order to keep a discrete influx of cells, not enough to end the infection, but sufficient to keep the invasion going.

PMNs have been shown to possess and expand effective antimicrobial mechanisms during the initial stage of hTB and thus, they have been postulated as innate effectors of tuberculosis resistance (Kroon *et al.*, 2018). Applied to Map and the presented vaccination studies, harbouring a number of tightly regulated and competent PMNs trained to exert the strong antimicrobial mechanisms combined with long-lasting high specific antibody levels at the beginning of the infection, could make the difference between controlling the infection or acquiring the disease.

Conclusions

1. The paratuberculosis vaccination route determines the host immune response, both against infection and the tuberculin intradermal reaction test used in the diagnosis of bovine tuberculosis.
2. The inactivated Map vaccine without adjuvant showed promising results when administered intradermally, in terms of protection against Map infection and less reaction in the tuberculin intradermal test, compared to the commercial vaccine.
3. The oral inactivated Map vaccine without adjuvant did not produce cross reactivity in the tuberculin test in guinea pigs, however, it did not induce a sufficient stimulation of the immune system in relation to the elimination of Map.
4. The use of the adjuvant, QuilA, in the formulation of the oral inactivated Map vaccine has shown increased immune responses and the stimulation of the immunity at the gut mucosa, thus improving its results in terms of protection against Map infection.
5. The CPV oral vaccine has shown high levels of stimulation of the immune system, conferring good levels of heterologous protection against Map. This is probably due to the combination of the observed training effect on innate immunity, observed in the increased functionality of neutrophils, and more specific responses directed towards homologous antigens shared with Map.

6. The efficacy of the commercial Silirum® vaccine may be due to a combined effect between the strong initial training effect on the innate immune response, observed in the increased functionality of neutrophils, and the activation of the humoral response, characterized by high levels of systemically detectable antibodies.
7. Neutrophils are capable of exerting a bactericidal effect against Map while macrophages have shown less efficacy.
8. Bovine and rabbit neutrophils release extracellular traps in response to Map and Mbv, although at lower levels when compared to the induction observed to other pathogens, such as *Escherichia coli* or *Staphylococcus aureus*.
9. The cooperation of neutrophils with macrophages *ex vivo* against Map and BCG is positive in terms of improved mycobactericidal capacity together with a lower inflammatory response, as reflected by the lower detection of macrophage inflammatory cytokines and the reduced presence of neutrophil extracellular traps.

Conclusiones

1. La ruta de vacunación utilizada frente a la paratuberculosis condicionó las respuestas inmunitarias del huésped, tanto a la infección por Map como a la prueba de intradermoreacción con tuberculinas utilizada en el diagnóstico de la tuberculosis bovina.
2. La vacuna de Map inactivada sin adjuvante mostró buenos resultados cuando se administró por la vía intradérmica, en cuanto a protección frente a la infección por Map y menor reactividad en la prueba de intradermoreacción con tuberculinas en comparación con la vacuna comercial.
3. La vacuna oral de Map inactivada sin adyuvante por la vía oral no produjo reactividad en la prueba de la tuberculina en cobaya, sin embargo, tampoco produjo una estimulación suficiente del sistema inmunitario en relación a la protección frente a Map.
4. El uso del adyuvante QuilA en la formulación de la vacuna oral de Map inactivada ha mostrado un aumento de las respuestas inmunitarias y ha conseguido estimular la inmunidad de la mucosa intestinal, mejorando así los resultados en cuanto a protección de la misma frente a la infección por Map.
5. La vacuna oral CPV, ha mostrado muy buenos niveles de estimulación del sistema inmunitario, confiriendo buenos niveles de protección heteróloga frente a Map. Esto probablemente se deba a la combinación del efecto de entrenamiento observado en la inmunidad innata, reflejado en el incremento de funcionalidad de los neutrófilos, y respuestas más específicas dirigidas hacia antígenos homólogos compartidos con Map.

6. La eficacia de la vacuna comercial Silirum® puede deberse a un efecto combinado entre el fuerte efecto de entrenamiento inicial de la respuesta inmune innata, reflejado en el incremento de funcionalidad de los neutrófilos, y la activación de la respuesta humoral, caracterizada por altos niveles de anticuerpos detectables a nivel sistémico.
7. Los neutrófilos son capaces de ejercer un efecto bactericida frente a Map mientras que los macrófagos han mostrado menor eficacia eliminando Map.
8. Los neutrófilos bovinos y de conejo liberan trampas extracelulares frente a Map y Mbv, aunque en menor proporción que frente a otros patógenos, como *Escherichia coli* o *Staphylococcus aureus*.
9. La cooperación de los neutrófilos con los macrófagos *ex vivo* frente a Map y BCG resulta positiva en cuanto a que mejora la capacidad micobactericida con una menor respuesta inflamatoria, reflejado esto último en la menor producción de citoquinas inflamatorias de macrófagos y menor presencia de trampas extracelulares de neutrófilos.

Supplementary Material

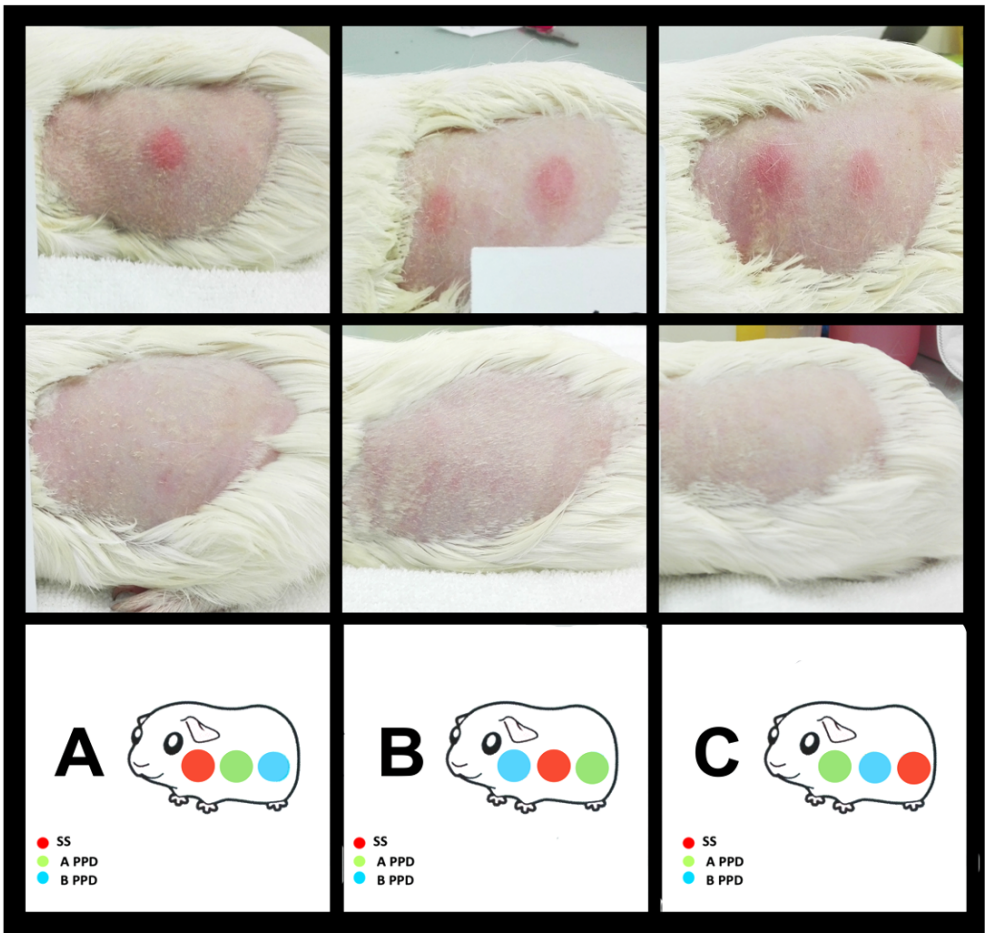

Supplementary figure. Images of the DTH results in guinea pigs 5 weeks after vaccination with CV, in the first line, and MPV, in the second line. In the third line a schematic representation of the inoculation location that corresponds with each column. Red dots represent saline solution (SS), green dots A PPD and blue dots B PPD.

References

Aaby, P., Kollmann, T. R. and Benn, C. S. (2014). Nonspecific effects of neonatal and infant vaccination: Public-health, immunological and conceptual challenges. *Nat. Immunol.* **15**, 895–899.

Achkar, J. M. and Casadevall, A. (2013). Antibody-mediated immunity against tuberculosis: Implications for vaccine development. *Cell Host Microbe* **13**, 250–262.

Aduriz, G., Juste, R. A., Garrido, J. M. and Geijo, M. V. (2000). Epidemiología y control de la paratuberculosis bovina. *Bovis* **93**, 063–073.

Aduriz, J. J., Juste, R. A. and Cortabarria, N. (1995). Lack of mycobactin dependence of mycobacteria isolated on Middlebrook 7H11 from clinical cases of ovine paratuberculosis. *Vet. Microbiol.* **45**, 211–217.

Albarrak, S. M. (2018). Investigating immunological responses of WC1+ gamma delta T cells in cattle naturally infected with *Mycobacterium avium* subspecies *paratuberculosis* (MAP). *Grad. Theses Diss.* 16305.

Albarrak, S. M., Waters, W. R., Stabel, J. R. and Hostetter, J. M. (2018). Evaluating the cytokine profile of the WC1+ γδ T cell subset in the ileum of cattle with the subclinical and clinical forms of MAP infection. *Vet. Immunol. Immunopathol.* **201**, 26–31.

Alderwick, L. J., Harrison, J., Lloyd, G. S. and Birch, H. L. (2015). The mycobacterial cell wall—peptidoglycan and arabinogalactan. *Cold Spring Harb. Perspect. Med.* **5**, 1–16.

Alonso-Hearn, M., Canive, M., Blanco-Vázquez, C., Torremocha, R., Balseiro, A., Amado, J., Varela-Martínez, E., Ramos, R., Jugo, B. M. *et al.* (2019). RNA-Seq analysis of ileocecal valve and peripheral blood from Holstein cattle infected with *Mycobacterium avium* subsp. *paratuberculosis* revealed dysregulation of the CXCL8/IL8 signaling pathway. *Sci. Rep.* **9**, 14845.

Alonso-Hearn, M., Molina, E., Geijo, M., Vázquez, P., Sevilla, I. A., Garrido, J. M. and Juste, R. A. (2012). Immunization of adult dairy cattle with a new heat-killed vaccine is associated with longer productive life prior to cows being sent to slaughter with suspected paratuberculosis. *J. Dairy Sci.* **95**, 618–629.

Alzuherri, H. M., Woodall, C. J. and Clarke, C. J. (1996). Increased intestinal TNF-α, IL-1 β and IL-6 expression in ovine paratuberculosis. *Vet. Immunol. Immunopathol.* **49**, 331–345.

Andersen, C. L., Jensen, J. L. and Ørntoft, T. F. (2004). Normalization of real-time quantitative reverse transcription-PCR data: A model-based variance estimation approach to identify genes suited for normalization, applied to bladder and colon cancer data sets. *Cancer Res.* **64**, 5245–5250.

Andersson-Rolf, A., Zilbauer, M., Koo, B. K. and Clevers, H. (2017). Stem cells in repair of gastrointestinal epithelia. *Physiology* **32**, 278–289.

Angus, R. D. (1978). Production of reference PPD tuberculins for veterinary use in the United States. *J. Biol. Stand.* **6**, 221–227.

Arrazuria, R., Elguezabal, N., Juste, R. A., Derakhshani, H. and Khafipour, E. (2016a). *Mycobacterium avium* subspecies *paratuberculosis* infection modifies gut microbiota under different dietary conditions in a rabbit model. *Front. Microbiol.* **7**, 446.

Arrazuria, R., Molina, E., Garrido, J. M., Pérez, V., Juste, R. A., Elguezabal, N., Pérez, V., Juste, R. A. and Elguezabal, N. (2016b). Vaccination sequence effects on immunological response and tissue bacterial burden in paratuberculosis infection in a rabbit model. *Vet. Res.* **47**, 77.

Arrazuria, R., Molina, E., Mateo-Abad, M., Arostegui, I., Garrido, J. M., Juste, R. A. and Elguezabal, N. (2015a). Effect of various dietary regimens on oral challenge with *Mycobacterium avium* subsp. *paratuberculosis* in a rabbit model. *Res. Vet. Sci.* **101**.

Arrazuria, R., Sevilla, I. A., Molina, E., Pérez, V., Garrido, J. M., Juste, R. A. and Elguezabal, N. (2015b). Detection of *Mycobacterium avium* subspecies in the gut associated lymphoid tissue of slaughtered rabbits. *BMC Vet. Res.* **11**, 130.

Arsenault, R. J., Li, Y., Bell, K., Doig, K., Potter, A., Griebel, P. J., Kusalik, A. and Napper, S. (2012). *Mycobacterium avium* subsp. *paratuberculosis* inhibits gamma interferon-induced signaling in bovine monocytes: Insights into the cellular mechanisms of Johne's disease. *Infect. Immun.* **80**, 3039–3048.

Arsenault, R. J., Maattanen, P., Daigle, J., Potter, A., Griebel, P. and Napper, S. (2014). From mouth to macrophage: Mechanisms of innate immune subversion by *Mycobacterium avium* subsp. *paratuberculosis*. *Vet. Res.* **45**, 1–15.

Arteche-Villasol, N., Gutiérrez-Expósito, D., Vallejo, R., Espinosa, J., Elguezabal, N., Ladero-Auñon, I., Royo, M., del Carmen Ferreras, M., Benavides, J. *et al.* (2021). Early response of monocyte-derived macrophages from vaccinated and non-vaccinated goats against *in vitro* infection with *Mycobacterium avium* subsp. *paratuberculosis*. *Vet. Res.* **52**, 69.

Arts, R. J. W., Blok, B. A., Aaby, P., Joosten, L. A. B., de Jong, D., van der Meer, J. W. M., Benn, C. S., van Crevel, R. and Netea, M. G. (2015). Long-term *in vitro* and *in vivo* effects of γ-irradiated BCG on innate and adaptive immunity. *J. Leukoc. Biol.* **98**, 995–1001.

Aulik, N. A., Hellenbrand, K. M. and Czuprynski, C. J. (2012). *Mannheimia haemolytica* and its leukotoxin cause macrophage extracellular trap formation by bovine macrophages. *Infect. Immun.* **80**, 1923–1933.

Ayele, W. Y., Svastova, P., Roubal, P., Bartos, M. and Pavlik, I. (2005). *Mycobacterium avium* subspecies *paratuberculosis* cultured from locally and commercially pasteurized cow's milk in the Czech Republic. *Appl. Environ. Microbiol.* **71**, 1210–1214.

Balu, S., Reljic, R., Lewis, M. J., Pleass, R. J., McIntosh, R., van Kooten, C., van Egmond, M., Challacombe, S., Woof, J. M. *et al.* (2011). A Novel Human IgA Monoclonal Antibody Protects against Tuberculosis. *J. Immunol.* **186**, 3113–3119.

Bannantine, J. P., Everman, J. L., Rose, S. J., Babrak, L., Katani, R., Barletta, R. G., Talaat, A. M., Gröhn, Y. T., Chang, Y. F. *et al.* (2014). Evaluation of eight live attenuated vaccine candidates for protection against challenge with virulent *Mycobacterium avium* subsp. *paratuberculosis*in mice. *Front. Cell. Infect. Microbiol.* **4**, 88.

Bannantine, J. P. and Bermúdez, L. E. (2013). No holes barred: Invasion of the intestinal mucosa by *Mycobacterium avium* subsp. *paratuberculosis*. *Infect. Immun.* **81**, 3960–3965.

Baquero, M. M. and Plattner, B. L. (2017a). Bovine WC1+ and WC1neg γδ T lymphocytes influence monocyte differentiation and monocyte-derived dendritic cell maturation during *in vitro Mycobacterium avium* subsp. *paratuberculosis* infection. *Front. Immunol.* **8**, 534.

Baquero, M. M. and Plattner, B. L. (2017b). Bovine peripheral blood WC1+ and WC1neg γδ T lymphocytes modulate monocyte-derived macrophage effector functions during *in vitro Mycobacterium avium* subspecies *paratuberculosis* infection. *Cell. Immunol.* **315**, 34–44.

Barros, M. H. M., Hauck, F., Dreyer, J. H., Kempkes, B. and Niedobitek, G. (2013). Macrophage Polarisation: an Immunohistochemical Approach for Identifying M1 and M2 Macrophages. *PLoS One* **8**, e80908.

Bastida, F. and Juste, R. A. (2011). Paratuberculosis control: A review with a focus on vaccination. *J. Immune Based Ther. Vaccines* **9**, 1–17.

Beard, P. M., Rhind, S. M., Buxton, D., Daniels, M. J., Henderson, D., Pirie, A., Rudge, K., Greig, A., Hutchings, M. R. *et al.* (2001). Natural paratuberculosis infection in rabbits in Scotland. *J. Comp. Pathol.* **124**, 290–9.

Begg, D. J., De Silva, K., Carter, N., Plain, K. M., Purdie, A. and Whittington, R. J. (2011). Does a Th1 over Th2 dominancy really exist in the early stages of *Mycobacterium avium* subspecies *paratuberculosis* infections? *Immunobiology* **216**, 840–846.

Bekker, L. G., Moreira, A. L., Bergtold, A., Freeman, S., Ryffel, B. and Kaplan, G. (2000). Immunopathologic effects of tumor necrosis factor alpha in murine mycobacterial infection are dose dependent. *Infect. Immun.* **68**, 6954–6961.

Benati, D., Ferro, M., Savino, M. T., Ulivieri, C., Schiavo, E., Nuccitelli, A., Pasini, F. L. and Baldari, C. T. (2010). Opposite effects of simvastatin on the bactericidal and inflammatory response of macrophages to opsonized *S. aureus*. *J. Leukoc. Biol.* **87**, 433–442.

Bennett, R., McClement, I. and McFarlane, I. (2010). An economic decision support tool for simulating paratuberculosis control strategies in a UK suckler beef herd. *Prev. Vet. Med.* **93**, 286–293.

Benoit, M., Desnues, B. and Mege, J.-L. (2008). Macrophage Polarization in Bacterial Infections. *J. Immunol.* **181**, 3733–3739.

Bermúdez, L. E., Petrofsky, M. and Stevens, P. (1998). Treatment with recombinant granulocyte colony-stimulating factor (Filgrastin ^{TM}) stimulates neutrophils and tissue macrophages and induces an effective non-specific response against *Mycobacterium avium* in mice. *Immunology* **94**, 297–303.

Bickett, T. E., McLean, J., Creissen, E., Izzo, L., Hagan, C., Izzo, A. J., Silva Angulo, F. and Izzo, A. A. (2020). Characterizing the BCG Induced Macrophage and Neutrophil Mechanisms for Defense Against *Mycobacterium tuberculosis*. *Front. Immunol.* **11**, 1202.

Botsaris, G., Swift, B. M. C., Slana, I., Liapi, M., Christodoulou, M., Hatzitofi, M., Christodoulou, V. and Rees, C. E. D. (2016). Detection of viable *Mycobacterium avium* subspecies *paratuberculosis* in powdered infant formula by phage-PCR and confirmed by culture. *Int. J. Food Microbiol.* **216**, 91–94.

Bournazos, S., DiLillo, D. J. and Ravetch, J. V. (2015). The role of Fc-FcγR interactions in IgG-mediated microbial neutralization. *J. Exp. Med.* **212**, 1361–1369.

Bower, K. L., Begg, D. J. and Whittington, R. J. (2010). Optimisation of culture of *Mycobacterium avium* subspecies *paratuberculosis* from blood samples. *J. Microbiol. Methods* **80**, 93–99.

Bower, K. L., Begg, D. J. and Whittington, R. J. (2011). Culture of *Mycobacterium avium* subspecies *paratuberculosis* (MAP) from blood and extra-intestinal tissues in experimentally infected sheep. *Vet. Microbiol.* **147**, 127–132.

Boyaka, P. N., Marinaro, M., Jackson, R. J., van Ginkel, F. W., Cormet-Boyaka, E., Kirk, K. L., Kensil, C. R. and McGhee, J. R. (2001). Oral QS-21 Requires Early IL-4 Help for Induction of Mucosal and Systemic Immunity. *J. Immunol.* **166**, 2283–2290.

Bozza, F. A., Salluh, J. I., Japiassu, A. M., Soares, M., Assis, E. F., Gomes, R. N., Bozza, M. T., Castro-Faria-Neto, H. C. and Bozza, P. T. (2007). Cytokine profiles as markers of disease severity in sepsis: A multiplex analysis. *Crit. Care* **11**, R49.

Brinkmann, V., Reichard, U., Goosmann, C., Fauler, B., Uhlemann, Y., Weiss, D. S., Weinrauch, Y. and Zychlinsky, A. (2004). Neutrophil Extracellular Traps Kill Bacteria. *Science.* **303**, 1532–1535.

Brook, B., Harbeson, D. J., Shannon, C. P., Cai, B., He, D., Ben-Othman, R., Francis, F., Huang, J., Varankovich, N. *et al.* (2020). BCG vaccination-induced emergency granulopoiesis provides rapid protection from neonatal sepsis. *Sci. Transl. Med.* **12**, eaax4517.

Brown, A. E., Holzer, T. J. and Andersen, B. R. (1987). Capacity of Human Neutrophils to Kill *Mycobacterium tuberculosis*. *J. Infect. Dis.* **156**, 985–9.

Bull, T. J., Munshi, T., Mikkelsen, H., Hartmann, S. B., Sørensen, M. R., García, J. S., López-Pérez, P. M., Hofmann, S., Hilpert, K. *et al.* (2017). Improved culture medium (TiKa) for *Mycobacterium avium* subspecies *paratuberculosis* (MAP) Matches qPCR Sensitivity and Reveals Significant Proportions of Non-viable MAP in Lymphoid Tissue of Vaccinated MAP Challenged Animals. *Front. Microbiol.* **7**, 1–8.

Bull, T. J. (2020). Development of New Paratuberculosis Vaccines. In: Behr, M. A., Stevenson, K. & Kapur, V. (eds) *Paratuberculosis Org. Dis. Control*, 380–408.

Bull, T. J., Gilbert, S. C., Sridhar, S., Linedale, R., Dierkes, N., Sidi-Boumedine, K. and Hermon-Taylor, J. (2007). A novel multi-antigen virally vectored vaccine against *Mycobacterium avium* subspecies *paratuberculosis*. *PLoS One* **2**, e1229.

Bull, T. J., McMinn, E. J., Sidi-Boumedine, K., Skull, A., Durkin, D., Neild, P., Rhodes, G., Pickup, R. and Hermon-Taylor, J. (2003). Detection and verification of *Mycobacterium avium* subsp. *paratuberculosis* in fresh ileocolonic mucosal biopsy specimens from individuals with and without Crohn's disease. *J. Clin. Microbiol.* **41**, 2915–2923.

Bull, T. J., Vrettou, C., Linedale, R., McGuinnes, C., Strain, S., McNair, J., Gilbert, S. C. and Hope, J. C. (2014). Immunity, safety and protection of an Adenovirus 5 prime - Modified Vaccinia virus Ankara boost subunit vaccine against *Mycobacterium avium* subspecies *paratuberculosis* infection in calves. *Vet. Res.* **45**, 112.

Burrells, C., Clarke, C. J., Colston, A., Kay, J. M., Porter, J., Little, D. and Sharp, J. M. (1998). A study of immunological responses of sheep clinically-affected with paratuberculosis (Johne's disease). The relationship of blood, mesenteric lymph node and intestinal lymphocyte responses to gross and microscopic pathology. *Vet. Immunol. Immunopathol.* **66**, 343–358.

Bustin, S. A., Benes, V., Garson, J. A., Hellemans, J., Huggett, J., Kubista, M., Mueller, R., Nolan, T., Pfaffl, M. W. *et al.* (2009). The MIQE guidelines: Minimum information for publication of quantitative real-time PCR experiments. *Clin. Chem.* **55**, 611–622.

Butot, S., Ricchi, M., Sevilla, I. A., Michot, L., Molina, E., Tello, M., Russo, S., Arrigoni, N., Garrido, J. M. *et al.* (2019). Estimation of performance characteristics of analytical methods for *Mycobacterium avium* subsp. *paratuberculosis* detection in dairy products. *Front. Microbiol.* **10**, 509.

Capitini, C. M., Fry, T. J. and Mackall, C. L. (2009). Cytokines as adjuvants for vaccine and cellular therapies for cancer. *Am. J. Immunol.* **5**, 65–83.

Carvalho, I. A., Pietralonga, P. A. G., Schwarz, D. G. G., Faria, A. C. S. and Moreira, M. A. S. (2012). Short communication: Recovery of viable *Mycobacterium avium* subspecies *paratuberculosis* from retail pasteurized whole milk in Brazil. *J. Dairy Sci.* **95**, 6946–6948.

Carvalho, N. B., Oliveira, F. S., Durães, F. V., de Almeida, L. A., Flórido, M., Prata, L. O., Caliari, M. V., Appelberg, R. and Oliveira, S. C. (2011). Toll-like receptor 9 is required for full host resistance to *Mycobacterium avium* infection but plays no role in induction of Th1 responses. *Infect. Immun.* **79**, 1638–1646.

Casanova, J. L. (1999). IL-12 and IFN-γ in host defense against mycobacteria and salmonella in mice and men. *Curr. Opin. Immunol.* **11**, 346–351.

Casey, M. E., Meade, K. G., Nalpas, N. C., Taraktsoglou, M., Browne, J. A., Killick, K. E., Stephen, S. D., Gormley, E., Hokamp, K. *et al.* (2015). Analysis of the bovine monocyte-derived macrophage response to *Mycobacterium avium* subspecies *paratuberculosis* infection using RNA-seq. *Front. Immunol.* **6**, 23.

Cassatella, M. A., Locati, M. and Mantovani, A. (2009). Never underestimate the power of a neutrophil. *Immunity* **31**, 698–700.

Cebra, J. J., Periwal, S. B., Lee, G., Lee, F. and Shroff, K. E. (1998). Development and maintenance of the gut-associated lymphoid tissue (GALT): The roles of enteric bacteria and viruses. *Dev. Immunol.* **6**, 13–18.

Chan, J., Mehta, S., Bharrhan, S., Chen, Y., Achkar, J. M., Casadevall, A. and Flynn, J. A. (2014). The role of B cells and humoral immunity in *Mycobacterium tuberculosis* infection. *Semin. Immunol.* **26**, 588–600.

Chase, C. C. L. (2018). Enteric Immunity: Happy Gut, Healthy Animal. *Vet. Clin. North Am. - Food Anim. Pract.* **34**, 1–18.

Chen, J. W., Faisal, S. M., Chandra, S., McDonough, S. P., Moreira, M. A. S., Scaria, J., Chang, C. F., Bannantine, J. P., Akey, B. *et al.* (2012). Immunogenicity and protective efficacy of the *Mycobacterium avium* subsp. *paratuberculosis* attenuated mutants against challenge in a mouse model. *Vaccine* **30**, 3015–3025.

Chen, L. H., Kathaperumal, K., Huang, C. J., McDonough, S. P., Stehman, S., Akey, B., Huntley, J., Bannantine, J. P., Chang, C. F. *et al.* (2008). Immune responses in mice to *Mycobacterium avium* subsp. *paratuberculosis* following vaccination with a novel 74F recombinant polyprotein. *Vaccine* **26**, 1253–1262.

Chiang, S. K., Sommer, S., Aho, A. D., Kiupel, M., Colvin, C., Tooker, B. and Coussens, P. M. (2007). Relationship between *Mycobacterium avium* subspecies *paratuberculosis*, IL-1α, and TRAF1 in primary bovine monocyte-derived macrophages. *Vet. Immunol. Immunopathol.* **116**, 131–144.

Chiodini, R. J., Van Kruiningen, H. J. and Merkal, R. (1984). Ruminant paratuberculosis (Johne's disease): The current status and future prospects. *Cornell Vet* **74**, 218–262.

Chung, E. Y., Liu, J., Homma, Y., Zhang, Y., Brendolan, A., Saggese, M., Han, J., Silverstein, R., Selleri, L. *et al.* (2007). Interleukin-10 Expression in Macrophages during Phagocytosis of Apoptotic Cells Is Mediated by Homeodomain Proteins Pbx1 and Prep-1. *Immunity* **27**, 952–

964.

Clarke, C. J. (1997). The pathology and pathogenesis of paratuberculosis in ruminants and other species. *J. Comp. Pathol.* **116**, 217–261.

Clarke, C. J. and Little, D. (1996). The Pathology of Ovine Paratuberculosis: Gross and Histological Changes in the Intestine and Other Tissues. *J. Comp. Path* **114**, 419–437.

Click, R. E. (2011). Successful treatment of asymptomatic or clinically terminal bovine *Mycobacterium avium* subsp. *paratuberculosis* infection (Johne's disease) with the bacterium Dietzia used as a probiotic alone or in combination with dexamethasone: Adaption to. *Virulence* **2**, 131–43.

Collins, E. J. B. M. and M. T. (2010). Epidemiology of Paratuberculosis. In: Behr, M. A. & Collins, D. M. (eds) *Paratuberculosis Org. Dis. Control*, 22–28.

Conejeros, I., Gibson, A. J., Werling, D., Muñoz-Caro, T., Hermosilla, C., Taubert, A. and Burgos, R. A. (2015). Effect of the synthetic Toll-like receptor ligands LPS, Pam3CSK4, HKLM and FSL-1 in the function of bovine polymorphonuclear neutrophils. *Dev. Comp. Immunol.* **52**, 215–225.

Conejeros, I., Patterson, R., Burgos, R. A., Hermosilla, C. and Werling, D. (2011). Induction of reactive oxygen species in bovine neutrophils is CD11b, but not dectin-1-dependent. *Vet. Immunol. Immunopathol.* **139**, 308–312.

Conejeros, I., Velásquez, Z. D., Grob, D., Zhou, E., Salecker, H., Hermosilla, C. and Taubert, A. (2019). Histone h2a and bovine neutrophil extracellular traps induce damage of *Besnoitia besnoiti*-infected host endothelial cells but fail to affect total parasite proliferation. *Biology (Basel).* **8**, 78.

Coombes, J. L. and Powrie, F. (2008). Dendritic cells in intestinal immune regulation. *Nat. Rev. Immunol.* **8**, 435–446.

Corneli, S., Di Paolo, A., Vitale, N., Torricelli, M., Petrucci, L., Sebastiani, C., Ciullo, M., Curcio, L., Biagetti, M. *et al.* (2021). Early Detection of *Mycobacterium avium* subsp. *paratuberculosis* Infected Cattle: Use of Experimental Johnins and Innovative Interferon-Gamma Test Interpretative Criteria. *Front. Vet. Sci.* **8**, 638890.

Corpa, J., Garrido, J., García, J. and Pérez, V. (2000). Classification of Lesions Observed in Natural Cases of Paratuberculosis in Goats. *J. Comp. Pathol.* **122**, 255–265.

Cousins, D. V., Whittington, R., Marsh, I., Masters, A., Evans, R. J. and Kluver, P. (1999). Mycobacteria distinct from *Mycobacterium avium* subsp. *paratuberculosis* isolated from the

faeces of ruminants possess IS900-like sequences detectable by IS900 polymerase chain reaction: Implications for diagnosis. *Mol. Cell. Probes* **13**, 431–442.

Coussens, P., DeKuiper, J. L., Shoyama, F. M., Brenner, E., Lamont, E. A., Kabara, E. and Sreevatsan, S. (2020). Host-Pathogen Interactions and Intracellular Survival of *Mycobacterium avium* subsp. *paratuberculosis*. In: Behr, M. A., Stevenson, K. & Kapur, V. (eds) *Paratuberculosis Org. Dis. Control*, 120–138.

Coussens, P. M. (2004). Model for immune responses to *Mycobacterium avium* subsp. *paratuberculosis* in cattle. *Infect. Immun.* **72**, 3089–3096.

Coussens, P. M., Verman, N., Coussens, M. A., Elftman, M. D. and McNulty, A. M. (2004). Cytokine gene expression in peripheral blood mononuclear cells and tissues of cattle infected with *Mycobacterium avium* subsp. *paratuberculosis*: evidence for an inherent proinflammatory gene expression pattern. *Infect Immun* **72**, 1409–1422.

Covián, C., Fernández-Fierro, A., Retamal-Díaz, A., Díaz, F. E., Vásquez, A. E., Lay, M. K., Riedel, C. A., González, P. A., Bueno, S. M. *et al.* (2019). BCG-Induced Cross-Protection and Development of Trained Immunity: Implication for Vaccine Design. *Front. Immunol.* **10**, 2806.

Cuenda, A. and Rousseau, S. (2007). p38 MAP-Kinases pathway regulation, function and role in human diseases. *Biochim. Biophys. Acta - Mol. Cell Res.* **1773**, 1358–1375.

D'Arboval, H. (1826). Dictionnaire de médecine et de chirurgie vétérinaires. In: Baillière, J.-B. (ed.) *Vol 1*, 1–604.

Dannenberg, A. M. and Collins, F. M. (2001). Progressive pulmonary tuberculosis is not due to increasing numbers of viable bacilli in rabbits, mice and guinea pigs but is due to a continuous host response to mycobacterial products. *Tuberculosis* **81**, 229–242.

Darwich, L., Coma, G., Peña, R., Bellido, R., Blanco, E. J. J., Este, J. A., Borras, F. E., Clotet, B., Ruiz, L. *et al.* (2009). Secretion of interferon-γ by human macrophages demonstrated at the single-cell level after costimulation with interleukin (IL)-12 plus IL-18. *Immunology* **126**, 386–393.

David, J., Barkema, H. W., Guan, L. L. and De Buck, J. (2014). Gene-expression profiling of calves 6 and 9 months after inoculation with *Mycobacterium avium* subspecies *paratuberculosis*. *Vet. Res.* **45**, 96.

De Almeida, D. E., Colvin, C. J. and Coussens, P. M. (2008). Antigen-specific regulatory T cells in

bovine paratuberculosis. *Vet. Immunol. Immunopathol.* **125**, 234–245.

De Oliveira, S., Rosowski, E. E. and Huttenlocher, A. (2016). Neutrophil migration in infection and wound repair: Going forward in reverse. *Nat. Rev. Immunol.* **16**, 378–391.

De Silva, K., Begg, D. J., Plain, K. M., Purdie, A. C., Kawaji, S., Dhand, N. K. and Whittington, R. J. (2013). Can early host responses to mycobacterial infection predict eventual disease outcomes? *Prev. Vet. Med.* **112**, 203–212.

De Silva, K., Plain, K. M., Begg, D. J., Purdie, A. C. and Whittington, R. J. (2015). CD4+ T-cells, γδ T-cells and B-cells are associated with lack of vaccine protection in *Mycobacterium avium* subsp. *paratuberculosis* infection. *Vaccine* **33**, 149–155.

De Silva, K., Plain, K., Purdie, A., Begg, D. and Whittington, R. J. (2018). Defining resilience to mycobacterial disease: Characteristics of survivors of ovine paratuberculosis. *Vet. Immunol. Immunopathol.* **195**, 56–64.

DeKuiper, J. L. and Coussens, P. M. (2019a). *Mycobacterium avium* subsp. *paratuberculosis* (MAP) induces IL-17a production in bovine peripheral blood mononuclear cells (PBMCs) and enhances IL-23R expression in-vivo and in-vitro. *Vet. Immunol. Immunopathol.* **218**, 109952.

DeKuiper, J. L. and Coussens, P. M. (2019b). Inflammatory Th17 responses to infection with *Mycobacterium avium* subsp. *paratuberculosis* (MAP) in cattle and their potential role in the development of Johne's disease. *Vet. Immunol. Immunopathol.* **218**, 109954.

Dennis, M. M., Reddacliff, L. A. and Whittington, R. J. (2011). Longitudinal study of clinicopathological features of Johne's disease in sheep naturally exposed to *Mycobacterium avium* subspecies *paratuberculosis*. *Vet. Pathol.* **48**, 565–575.

Diebold, S. S. (2008). Determination of T-cell fate by dendritic cells. *Immunol. Cell Biol.* **86**, 389–397.

Dorshorst, N. C., Collins, M. T. and Lombard, J. E. (2006). Decision analysis model for paratuberculosis control in commercial dairy herds. *Prev. Vet. Med.* **75**, 92–122.

Dotta, U., Guglielmino, R., Cagnasso, A., D'Angelo, A., Prato, S. and Bosso, M. (1999). Effects of subclinical bovine paratuberculosis on in-vitro polymorphonuclear neutrophil migration. *J. Comp. Pathol.* **121**, 399–403.

Dudemaine, P. L., Fecteau, G., Lessard, M., Labrecque, O., Roy, J. P. and Bissonnette, N. (2014). Increased blood-circulating interferon-γ, interleukin-17, and osteopontin levels in bovine

paratuberculosis. *J. Dairy Sci.* **97**, 3382–3393.

Duluc, D., Corvaisier, M., Blanchard, S., Catala, L., Descamps, P., Gamelin, E., Ponsoda, S., Delneste, Y., Hebbar, M. *et al.* (2009). Interferon-γ reverses the immunosuppressive and protumoral properties and prevents the generation of human tumor-associated macrophages. *Int. J. Cancer* **125**, 367–373.

Ebisawa, M., Tsukahara, T., Fudou, R., Ohta, Y., Tokura, M., Onishi, N. and Fujieda, T. (2017). Heat-killed cell preparation of *Corynebacterium glutamicum* stimulates the immune activity and improves survival of mice against enterohemorrhagic *Escherichia coli*. *Biosci. Biotechnol. Biochem.* **81**, 995–1001.

Ekundayo, T. C. and Okoh, A. I. (2020). Systematic Assessment of *Mycobacterium avium* subspecies *paratuberculosis* Infections from 1911-2019: A Growth Analysis of Association with Human Autoimmune Diseases. *Microorganisms* **8**, 1212.

Elguezabal, N., Bastida, F., Sevilla, I. A., González, N., Molina, E., Garrido, J. M. and Juste, R. A. (2011). Estimation of *Mycobacterium avium* subsp. *paratuberculosis* growth parameters: Strain characterization and comparison of methods. *Appl. Environ. Microbiol.* **77**, 8615–8624.

Faisal, S. M., Yan, F., Chen, T. T., Useh, N. M., Guo, S., Yan, W., Wang, S. J., Glaser, A. L., McDonough, S. P. *et al.* (2013a). Evaluation of a *Salmonella* Vectored Vaccine Expressing *Mycobacterium avium* subsp. *paratuberculosis* Antigens Against Challenge in a Goat Model. *PLoS One* **8**, e70171.

Faisal, S. M., Chen, J. W., Yan, F., Chen, T. T., Useh, N. M., Yan, W., Guo, S., Wang, S. J., Glaser, A. L. *et al.* (2013b). Evaluation of a *Mycobacterium avium* subsp. *paratuberculosis* leuD mutant as a vaccine candidate against challenge in a caprine model. *Clin. Vaccine Immunol.* **20**, 572–581.

Fatkhullina, A. R., Peshkova, I. O., Dzutsev, A., Trinchieri, G., Grivennikov, S. I. and Koltsova Correspondence, E. K. (2018). An Interleukin-23-Interleukin-22 Axis Regulates Intestinal Microbial Homeostasis to Protect from Diet-Induced Atherosclerosis. *Immunity* **49**, 943–957.

Fecteau, M. E. and Whitlock, R. H. (2011). Treatment and Chemoprophylaxis for Paratuberculosis. *Vet. Clin. North Am. - Food Anim. Pract.* **27**, 547–557.

Fernández, M., Benavides, J., Castaño, P., Elguezabal, N., Fuertes, M., Muñoz, M., Royo, M., Ferreras, M. C. and Pérez, V. (2017a). Macrophage Subsets Within Granulomatous Intestinal Lesions in Bovine Paratuberculosis. *Vet. Pathol.* **54**, 82–93.

Fernández, M., Fuertes, M., Elguezabal, N., Castaño, P., Royo, M., Ferreras, M. C., Benavides, J. and Pérez, V. (2017b). Immunohistochemical expression of interferon-γ in different types of granulomatous lesions associated with bovine paratuberculosis. *Comp. Immunol. Microbiol. Infect. Dis.* **51**, 1–8.

Fielding, C. A., McLoughlin, R. M., McLeod, L., Colmont, C. S., Najdovska, M., Grail, D., Ernst, M., Jones, S. A., Topley, N. *et al.* (2008). IL-6 Regulates Neutrophil Trafficking during Acute Inflammation via STAT3. *J. Immunol.* **181**, 2189–2195.

Fox, N. J., Smith, L. A., Stevenson, K., Davidson, R. S., Marion, G. and Hutchings, M. R. (2020). Infection of Non-ruminant Wildlife by *Mycobacterium avium* subsp. *paratuberculosis*. In: Behr, M. A., Stevenson, K. & Kapur, V. (eds) *Paratuberculosis Org. Dis. Control*, 200–212.

Francis, J. (1943). Infection of Laboratory Animals with *Mycobacterium Johnei*. *J. Comp. Pathol. Ther.* **53**, 140-IN12.

Friggeri, A., Banerjee, S., Xie, N., Cui, H., de Freitas, A., Zerfaoui, M., Dupont, H., Abraham, E. and Liu, G. (2012). Extracellular histones inhibit efferocytosis. *Mol. Med.* **18**, 825–833.

Fuchs, T. A., Abed, U., Goosmann, C., Hurwitz, R., Schulze, I., Wahn, V., Weinrauch, Y., Brinkmann, V. and Zychlinsky, A. (2007). Novel cell death program leads to neutrophil extracellular traps. *J. Cell Biol.* **176**, 231–241.

García, A. B. and Shalloo, L. (2015). Invited review: The economic impact and control of paratuberculosis in cattle. *J. Dairy Sci.* **98**, 5019–5039.

Garrido, J. M., Sevilla, I. A., Beltrán-Beck, B., Minguijón, E., Ballesteros, C., Galindo, R. C., Boadella, M., Lyashchenko, K. P., Romero, B. *et al.* (2011). Protection against tuberculosis in eurasian wild boar vaccinated with heat-inactivated *Mycobacterium bovis*. *PLoS One* **6**, e24905.

Garrido, J. M., Vázquez, P., Molina, E., Plazaola, J. M., Sevilla, I. A., Geijo, M. V., Alonso-Hearn, M. and Juste, R. A. (2013). Paratuberculosis vaccination causes only limited cross-reactivity in the skin test for diagnosis of bovine tuberculosis. *PLoS One* **8**, e80985.

Ghosh, P., Shippy, D. C. and Talaat, A. M. (2015). Superior protection elicited by live-attenuated vaccines in the murine model of paratuberculosis. *Vaccine* **33**, 7262–7270.

Gilmour, N. J. L. and Angus, K. W. (1974). Absence of immunogenicity of an oral vaccine against *Mycobacterium johnei* in sheep. *Res. Vet. Sci.* **16**, 269–70.

Golan, L., Livneh-Kol, A., Gonen, E., Yagel, S., Rosenshine, I. and Shpigel, N. Y. (2009). *Mycobacterium avium paratuberculosis* Invades Human Small-Intestinal Goblet Cells and Elicits Inflammation. *J. Infect. Dis.* **199**, 350–354.

Gonda, M. G., Chang, Y. M., Shook, G. E., Collins, M. T. and Kirkpatrick, B. W. (2007). Effect of *Mycobacterium paratuberculosis* infection on production, reproduction, and health traits in US Holsteins. *Prev. Vet. Med.* **80**, 103–119.

González, J., Geijo, M. V., García-Pariente, C., Verna, A., Corpa, J. M., Reyes, L. E., Ferreras, M. C., Juste, R. A., García Marín, J. F. *et al.* (2005). Histopathological classification of lesions associated with natural paratuberculosis infection in cattle. *J. Comp. Pathol.* **133**, 184–196.

Gossner, A. G., Venturina, V. M., Peers, A., Watkins, C. A. and Hopkins, J. (2012). Expression of sheep interleukin 23 (IL23A, alpha subunit p19) in two distinct gastrointestinal diseases. *Vet. Immunol. Immunopathol.* **150**, 118–122.

Gossner, A., Watkins, C., Chianini, F. and Hopkins, J. (2017). Pathways and Genes Associated with Immune Dysfunction in Sheep Paratuberculosis. *Sci. Rep.* **7**, 1–12.

Grant, I. R. (2005). Zoonotic potential of *Mycobacterium avium* subsp. *paratuberculosis*: The current position. *J. Appl. Microbiol.* **98**, 1282–1293.

Green, A. M., DiFazio, R. and Flynn, J. L. (2013). IFN-γ from CD4 T Cells Is Essential for Host Survival and Enhances CD8 T Cell Function during *Mycobacterium tuberculosis* Infection. *J. Immunol.* **190**, 270–277.

Gunderson, C. W. and Seifert, H. S. (2015). *Neisseria gonorrhoeae* elicits extracellular traps in primary neutrophil culture while suppressing the oxidative burst. *MBio* **6**, e02452-14.

Gupta, A. K., Hasler, P., Holzgreve, W., Gebhardt, S. and Hahn, S. (2005). Induction of neutrophil extracellular DNA lattices by placental microparticles and IL-8 and their presence in preeclampsia. *Hum. Immunol.* **66**, 1146–1154.

Guzman, E., Hope, J., Taylor, G., Smith, A. L., Cubillos-Zapata, C. and Charleston, B. (2014). Bovine γδ T Cells Are a Major Regulatory T Cell Subset. *J. Immunol.* **193**, 208–222.

Hagemann, T., Lawrence, T., McNeish, I., Charles, K. A., Kulbe, H., Thompson, R. G., Robinson, S. C. and Balkwill, F. R. (2008). "Re-educating" tumor-associated macrophages by targeting NF-κB. *J. Exp. Med.* **205**, 1261–1268.

Harris, N. B. and Barletta, R. G. (2001). *Mycobacterium avium* subsp. *paratuberculosis* in Veterinary Medicine. *Clin. Microbiol. Rev.* **14**, 489–512.

Hatton, R. D. (2011). TGF-β in Th17 cell development: The truth is out there. *Immunity* **34**, 288–290.

Hayashi, F., Means, T. K. and Luster, A. D. (2003). Toll-like receptors stimulate human neutrophil function. *Blood* **102**, 2660–2669.

Hein, W. R., Barber, T., Cole, S. A., Morrison, L. and Pernthaner, A. (2004). Long-term collection and characterization of afferent lymph from the ovine small intestine. *J. Immunol. Methods* **293**, 153–168.

Hellebrekers, P., Hietbrink, F., Vrisekoop, N., Leenen, L. P. H. and Koenderman, L. (2017). Neutrophil functional heterogeneity: Identification of competitive phagocytosis. *Front. Immunol.* **8**, 1498.

Heuertz, R. M., Tricomi, S. M., Ezekiel, U. R. and Webster, R. O. (1999). C-reactive protein inhibits chemotactic peptide-induced p38 mitogen- activated protein kinase activity and human neutrophil movement. *J. Biol. Chem.* **274**, 17968–17974.

Hilda, J. N., Das, S., Tripathy, S. P. and Hanna, L. E. (2020). Role of neutrophils in tuberculosis: A bird's eye view. *Innate Immun.* **26**, 240–247.

Hines, M. E., Stabel, J. R., Sweeney, R. W., Griffin, F., Talaat, A. M., Bakker, D., Benedictus, G., Davis, W. C., de Lisle, G. W. *et al.* (2007). Experimental challenge models for Johne's disease: A review and proposed international guidelines. *Vet. Microbiol.* **122**, 197–222.

Hines, M. E., Turnquist, S. E., Ilha, M. R. S. S., Rajeev, S., Jones, A. L., Whittington, L., Bannantine, J. P., Barletta, R. G. R. G., Gröhn, Y. T. *et al.* (2014). Evaluation of novel oral vaccine candidates and validation of a caprine model of Johne's disease. *Front. Cell. Infect. Microbiol.* **4**, 26.

Hoek, A., Rutten, V. P. M. G., Kool, J., Arkesteijn, G. J. A., Bouwstra, R. J., Rhijn, I. Van and Koets, A. P. (2009). Subpopulations of bovine WC1+γδ T cells rather than CD4+CD25highFoxp3+ T cells act as immune regulatory cells *ex vivo*. *Vet. Res.* **40**, 6.

Holland, D., Booy, R., Looze, F. De, Eizenberg, P., McDonald, J., Karrasch, J., McKeirnan, M., Salem, H., Mills, G. *et al.* (2008). Intradermal Influenza Vaccine Administered Using a New Microinjection System Produces Superior Immunogenicity in Elderly Adults: A Randomized Controlled Trial. *J. Infect. Dis.* **198**, 650–8.

Honda, M. and Kubes, P. (2018). Neutrophils and neutrophil extracellular traps in the liver and

gastrointestinal system. *Nat. Publ. Gr.* **15**, 206–221.

Hope, J. C., Thom, M. L., Villarreal-Ramos, B., Vordermeier, H. M., Hewinson, R. G. and Howard, C. J. (2005). Exposure to *Mycobacterium avium* induces low-level protection from *Mycobacterium bovis* infection but compromises diagnosis of disease in cattle. *Clin. Exp. Immunol.* **141**, 432–439.

Huang, Z., Luo, Q., Guo, Y., Chen, J., Xiong, G., Peng, Y., Ye, J. and Li, J. (2015). *Mycobacterium tuberculosis*-Induced Polarization of Human Macrophage Orchestrates the Formation and Development of Tuberculous Granulomas *In Vitro*. *PLoS One* **10**, e0129744.

Ibeagha-Awemu, E., Do, D., Dudemaine, P. and Bissonnette, N. (2018). PSXIV-17 Gene co-expression network analysis identifies important modules and genes for cow's response to *Mycobacterium avium* ssp. *paratuberculosis* infection in the small intestine. *J. Anim. Sci.* **96**, 39.

Imada, J., Kelton, D. F. and Barkema, H. W. (2020). Epidemiology, Global Prevalence and Economics of Infection. In: Behr, M. A., Stevenson, K. & Kapur, V. (eds) *Paratuberculosis Org. Dis. Control*, 1–13.

Ishikawa, E., Ishikawa, T., Morita, Y. S., Toyonaga, K., Yamada, H., Takeuchi, O., Kinoshita, T., Akira, S., Yoshikai, Y. *et al.* (2009). Direct recognition of the mycobacterial glycolipid, trehalose dimycolate, by C-type lectin Mincle. *J. Exp. Med.* **206**, 2879–2888.

Iwakura, Y. and Ishigame, H. (2006). The IL-23/IL-17 axis in inflammation. *J. Clin. Invest.* **116**, 1218–1222.

Janeway, C. A. J., Travers, P., Walport, M. and Shlomchik, M. J. (2001). Macrophage activation by armed CD4 TH1 cells. In: Science., G. (ed.) *Immunobiol. Immune Syst. Heal. Dis.*, 333-338.

Janssen and Arkitek, S. (2013). *Immunology in the Gut Mucosa*. *Nat. video*.

Jenvey, C. J., Shircliff, A. L., Bannantine, J. P. and Stabel, J. R. (2019). Phenotypes of macrophages present in the intestine are impacted by stage of disease in cattle naturally infected with *Mycobacterium avium* subsp. *paratuberculosis*. *PLoS One* **14**, e0217649.

Jimbo, S., Suleman, M., Maina, T., Prysliak, T., Mulongo, M. and Pérez-Casal, J. (2017). Effect of *Mycoplasma bovis* on bovine neutrophils. *Vet. Immunol. Immunopathol.* **188**, 27–33.

Jöhne, H. A. and Frothingham, L. (1895). Ein eigentümlicher Fall von Tuberulose beim Rinde. *Dtsch. Zeitschrift für Tiermedizin und vergleichende Pathol.* **21**, 438–454.

Jolly, A., Morsella, C., Bass, L., Fiorentino, M. A., Paolicchi, F. A. and Mundo, S. L. (2013). Bovine response to lipoarabinomannan vaccination and challenge with *Mycobacterium paratuberculosis*. *Brazilian J. Microbiol.* **44**, 511–514.

Jones, G. J., Steinbach, S., Sevilla, I. A., Garrido, J. M., Juste, R. and Vordermeier, H. M. (2016). Oral vaccination of cattle with heat inactivated *Mycobacterium bovis* does not compromise bovine TB diagnostic tests. *Vet. Immunol. Immunopathol.* **182**, 85–88.

Jones, G. S., Amirault, H. J. and Andersen, B. R. (1990). Killing of *Mycobacterium tuberculosis* by neutrophils: A nonoxidative process. *J. Infect. Dis.* **162**, 700–704.

Jung, C., Hugot, J.-P. and Barreau, F. (2010). Peyer's Patches: The Immune Sensors of the Intestine. *Int. J. Inflam.* **2010**, 1–12.

Juste, R. A., Elguezabal, N., Pavón, A., Garrido, J. M., Geijo, M., Sevilla, I., Cabriada, J. L., Tejada, A., García-Campos, F. *et al.* (2009a). Association between *Mycobacterium avium* subsp. *paratuberculosis* DNA in blood and cellular and humoral immune response in inflammatory bowel disease patients and controls. *Int. J. Infect. Dis.* **13**, 247–254.

Juste, R. A., Alonso-Hearn, M., Molina, E., Geijo, M., Vázquez, P., Sevilla, I. A. and Garrido, J. M. (2009b). Significant reduction in bacterial shedding and improvement in milk production in dairy farms after the use of a new inactivated paratuberculosis vaccine in a field trial. *BMC Res. Notes* **2**, 1–6.

Juste, R. A., García Marín, J. F., Peris, B., Sáez de Ocáriz, C. and Badiola, J. J. (1994). Experimental infection of vaccinated and non-vaccinated lambs with *Mycobacterium paratuberculosis*. *J. Comp. Pathol.* **110**, 185–194.

Juste, R. A., Garrido, J. M., Elguezabal, N. and Sevilla, I. A. (2020). Paratuberculosis vaccine and vaccination. In: Behr, M. A., Stevenson, K. & Kapur, V. (eds) *Paratuberculosis Org. Dis. Control*, 365–379.

Juste, R. A., Geijo, M. V., Elguezabal, N., Sevilla, I. A., Alonso-Hearn, M. and Garrido, J. M. (2021). Paratuberculosis vaccination specific and non-specific effects on cattle lifespan. *Vaccine* **39**, 1631–1641.

Juste, R. A. and Pérez, V. (2011). Control of Paratuberculosis in Sheep and Goats. *Vet. Clin. North Am. - Food Anim. Pract.* **27**, 127–138.

Kabara, E. and Coussens, P. M. (2012). Infection of primary bovine macrophages with *Mycobacterium avium* subsp. *paratuberculosis* suppresses host cell apoptosis. *Front. Microbiol.* **3**, 215.

Kalis, C. H. J., Collins, M. T., Hesselink, J. W. and Barkema, H. W. (2003). Specificity of two tests for the early diagnosis of bovine paratuberculosis based on cell-mediated immunity: The Johnin skin test and the gamma interferon assay. *Vet. Microbiol.* **97**, 73–86.

Kantele, A., Kantele, J. M., Savilahti, E., Westerholm, M., Arvilommi, H., Lazarovits, A., Butcher, E. C. and Mäkelä, P. H. (1997). Homing potentials of circulating lymphocytes in humans depend on the site of activation: oral, but not parenteral, typhoid vaccination induces circulating antibody-secreting cells that all bear homing receptors directing them to the gut. *J. Immunol.* **158**, 574–9.

Karcher, E. L., Beitz, D. C. and Stabel, J. R. (2008). Modulation of cytokine gene expression and secretion during the periparturient period in dairy cows naturally infected with *Mycobacterium avium* subsp. *paratuberculosis*. *Vet. Immunol. Immunopathol.* **123**, 277–288.

Kathaperumal, K., Kumanan, V., McDonough, S., Chen, L. H., Park, S. U., Moreira, M. A. S., Akey, B., Huntley, J., Chang, C. F. *et al.* (2009). Evaluation of immune responses and protective efficacy in a goat model following immunization with a coctail of recombinant antigens and a polyprotein of *Mycobacterium avium* subsp. *paratuberculosis*. *Vaccine* **27**, 123–135.

Kathaperumal, K., Park, S.-U., McDonough, S., Stehman, S., Akey, B., Huntley, J., Wong, S., Chang, C.-F. and Chang, Y.-F. (2008). Vaccination with recombinant *Mycobacterium avium* subsp. *paratuberculosis* proteins induces differential immune responses and protects calves against infection by oral challenge. *Vaccine* **26**, 1652–63.

Kenefick, K. B., Adams, J. L., Steinberg, H. and Czuprynski, C. J. (1994). *In vivo* administration of a monoclonal antibody against the type I IL-1 receptor inhibits the ability of mice to eliminate *Mycobacterium paratuberculosis*. *J. Leukoc. Biol.* **55**, 719–722.

Kennedy, H. E., Welsh, M. D., Bryson, D. G., Cassidy, J. P., Forster, F. I., Howard, C. J., Collins, R. A. and Pollock, J. M. (2002). Modulation of immune responses to *Mycobacterium bovis* in cattle depleted of WC1+ γδ T cells. *Infect. Immun.* **70**, 1488–1500.

Khare, S., Lawhon, S. D., Drake, K. L., Nunes, J. E. S., Figueiredo, J. F., Rossetti, C. A., Gull, T., Everts, R. E., Lewin, H. A. *et al.* (2012). Systems Biology Analysis of Gene Expression during *in vivo Mycobacterium avium paratuberculosis* Enteric Colonization Reveals Role for Immune

Tolerance. *PLoS One* **7**, e42127.

Khare, S., Drake, K. L., Lawhon, S. D., Nunes, J. E. S., Figueiredo, J. F., Rossetti, C. A., Gull, T., Everts, R. E., Lewin, H. A. *et al.* (2016). Systems analysis of early host gene expression provides clues for transient *Mycobacterium avium* ssp *avium* vs. Persistent *Mycobacterium avium* Ssp *paratuberculosis* intestinal infections. *PLoS One* **11**, e0161946.

Khare, S., Nunes, J. S., Figueiredo, J. F., Lawhon, S. D., Rossetti, C. A., Gull, T., Rice-Ficht, A. C. and Adams, L. G. (2009). Early phase morphological lesions and transcriptional responses of bovine ileum infected with *Mycobacterium avium* subsp. *paratuberculosis*. *Vet. Pathol.* **46**, 717–728.

Khatib-Massalha, E., Bhattacharya, S., Massalha, H., Biram, A., Golan, K., Kollet, O., Kumari, A., Avemaria, F., Petrovich-Kopitman, E. *et al.* (2020). Lactate released by inflammatory bone marrow neutrophils induces their mobilization via endothelial GPR81 signaling. *Nat. Commun.* **11**, 1–18.

Köckritz-Blickwede, M. von, Chow, O., Ghochani, M., Nizet, V., von Köckritz-Blickwede, M., Chow, O., Ghochani, M. and Nizet, V. (2010). Visualization and functional evaluation of phagocyte extracellular traps. *Methods Microbiol.* **37**, 139–160.

Koenig, G., Hoffsis, G., Shulaw, W., Bech-Nielsen, S., Rings, D. M. and St-Jean, G. (1993). Isolation of *Mycobacterium paratuberculosis* from mononuclear cells in tissues, blood, and mammary glands of cows with advanced paratuberculosis. *Am J Vet Res* **54**, 1441–5.

Koets, A., Hoek, A., Langelaar, M., Overdijk, M., Santema, W., Franken, P., Van Eden, W. and Rutten, V. (2006). Mycobacterial 70 kD heat-shock protein is an effective subunit vaccine against bovine paratuberculosis. *Vaccine* **24**, 2550–9.

Koets, A. P., Eda, S. and Sreevatsan, S. (2015). The within host dynamics of *Mycobacterium avium* ssp. *paratuberculosis* infection in cattle: Where time and place matter. *Vet. Res.* **46**, 61.

Koets, A., Rutten, V., Hoek, A., Van Mil, F., Müller, K., Bakker, D., Gruys, E. and Van Eden, W. (2002). Progressive bovine paratuberculosis is associated with local loss of CD4+ T cells, increased frequency of γδ T cells, and related changes in T-cell function. *Infect. Immun.* **70**, 3856–3864.

Korns, D., Frasch, S. C., Fernández-Boyanapalli, R., Henson, P. M. and Bratton, D. L. (2011). Modulation of macrophage efferocytosis in inflammation. *Front. Immunol.* **2**, 57.

Kroon, E. E., Coussens, A. K., Kinnear, C., Orlova, M., Möller, M., Seeger, A., Wilkinson, R. J., Hoal, E. G. and Schurr, E. (2018). Neutrophils: Innate effectors of TB resistance? *Front. Immunol.* **9**, 2637.

Krüger, C., Köhler, H. and Liebler-Tenorio, E. M. (2015). Cellular composition of granulomatous lesions in gut-associated lymphoid tissues of goats during the first year after experimental infection with *Mycobacterium avium* subsp. *paratuberculosis*. *Vet. Immunol. Immunopathol.* **163**, 33–45.

Krupa, A., Fol, M., Dziadek, B. R., Kepka, E., Wojciechowska, D., Brzostek, A., Torzewska, A., Dziadek, J., Baughman, R. P. *et al.* (2015). Binding of CXCL8/IL-8 to *Mycobacterium tuberculosis* Modulates the Innate Immune Response. *Mediators Inflamm.* **2015**, 124762.

Kryczek, I., Wei, S., Vatan, L., Escara-Wilke, J., Szeliga, W., Keller, E. T. and Zou, W. (2007). Cutting Edge: Opposite Effects of IL-1 and IL-2 on the Regulation of IL-17 + T Cell Pool IL-1 Subverts IL-2-Mediated Suppression. *J. Immunol.* **179**, 1423–1426.

Kuehnel, M. P., Goethe, R., Habermann, A., Mueller, E., Rohde, M., Griffiths, G. and Valentin-Weigand, P. (2001). Characterization of the intracellular survival of *Mycobacterium avium* ssp. *paratuberculosis*: Phagosomal pH and fusogenicity in J774 macrophages compared with other mycobacteria. *Cell. Microbiol.* **3**, 551–566.

Kuenstner, J. T., Naser, S., Chamberlin, W., Borody, T., Graham, D. Y., McNees, A., Hermon-Taylor, J., Hermon-Taylor, A., Dow, C. T. *et al.* (2017). The Consensus from the *Mycobacterium avium* ssp. *paratuberculosis* (MAP) Conference 2017. *Front. Public Heal.* **5**, 27.

Kviatcovsky, D., Rivadeneyra, L., Balboa, L., Yokobori, N., López, B., Ritacco, V., Schattner, M., Sasiain, M. D. C. and De La Barrera, S. (2017). *Mycobacterium tuberculosis* Multidrug-Resistant Strain M Induces Low IL-8 and Inhibits TNF- α Secretion by Bronchial Epithelial Cells Altering Neutrophil Effector Functions. *Mediators Inflamm.* **72**, 1409–22.

Lambrecht, R. S. and Collins, M. T. (1993). Inability to detect mycobactin in mycobacteria-infected tissues suggests an alternative iron acquisition mechanism by mycobacteria *in vivo*. *Microb. Pathog.* **14**, 229–238.

Lamont, E. A., O'Grady, S. M., Davis, W. C., Eckstein, T. and Sreevatsan, S. (2012). Infection with *Mycobacterium avium* subsp. *paratuberculosis* results in rapid interleukin-1β release and Macrophage transepithelial migration. *Infect. Immun.* **80**, 3225–3235.

Lamont, E. A., Talaat, A. M., Coussens, P. M., Bannantine, J. P., Grohn, Y. T., Katani, R., Li, L. L., Kapur, V. and Sreevatsan, S. (2014). Screening of *Mycobacterium avium* subsp. *paratuberculosis* mutants for attenuation in a bovine monocyte-derived macrophage model. *Front. Cell. Infect. Microbiol.* **4**, 87.

Lechuga, S. and Ivanov, A. I. (2017). Disruption of the epithelial barrier during intestinal inflammation: Quest for new molecules and mechanisms. *Biochim. Biophys. Acta - Mol. Cell Res.* **1864**, 1183–1194.

Lee, H., Stabel, J. R. and Kehrli, M. E. (2001). Cytokine gene expression in ileal tissues of cattle infected with *Mycobacterium paratuberculosis*. *Vet. Immunol. Immunopathol.* **82**, 73–85.

Lei, L., Plattner, B. L. and Hostetter, J. M. (2008). Live *Mycobacterium avium* subsp. *paratuberculosis* and a killed-bacterium vaccine induce distinct subcutaneous granulomas, with unique cellular and cytokine profiles. *Clin. Vaccine Immunol.* **15**, 783–793.

Lemon, J. K., Miller, M. R. and Weiser, J. N. (2015). Sensing of interleukin-1 cytokines during *Streptococcus pneumoniae* colonization contributes to macrophage recruitment and bacterial clearance. *Infect. Immun.* **83**, 3204–3212.

Ley, K., Hoffman, H. M., Kubes, P., Cassatella, M. A., Zychlinsky, A., Hedrick, C. C. and Catz, S. D. (2018). Neutrophils: New insights and open questions. *Sci. Immunol.* **3**, eaat4579.

Li, L., Bannantine, J. P., Campo, J. J., Randall, A., Grohn, Y. T., Katani, R., Schilling, M., Radzio-Basu, J. and Kapur, V. (2017). Identification of sero-reactive antigens for the early diagnosis of Johne's disease in cattle. *PLoS One* **12**, e0184373.

Li, M. O., Wan, Y. Y., Sanjabi, S., Robertson, A. K. L. and Flavell, R. A. (2006). Transforming growth factor-β regulation of immune responses. *Annu. Rev. Immunol.* **24**, 99–146.

Liao, W., Lin, J. X. and Leonard, W. J. (2013). Interleukin-2 at the Crossroads of Effector Responses, Tolerance, and Immunotherapy. *Immunity* **38**, 13–25.

Luckheeram, R. V., Zhou, R., Verma, A. D. and Xia, B. (2012). CD4 +T cells: Differentiation and functions. *Clin. Dev. Immunol.* **2012**, 12.

Luo, Y. Y. (2018). Creating a Marked *Mycobacterium avium* subsp. *paratuberculosis*Vaccine Strain and Detecting Marker-Specific Immune Responses in Calves. *(Unpublished master's thesis).University Calgary, Calgary, AB.* 155.

Lutaty, A., Soboh, S., Schif-Zuck, S., Zeituni-Timor, O., Rostoker, R., Podolska, M. J., Schauer, C., Herrmann, M., Muñoz, L. E. *et al.* (2018). A 17-kDa fragment of lactoferrin associates with the termination of inflammation and peptides within promote resolution. *Front. Immunol.* **9**, 28.

Lybeck, K. R., Tessema, G. T., Kampen, A. H., Djønne, B. and Agdestein, A. (2020). Paratuberculosis in Goats. In: Behr, M. A., Stevenson, K. & Kapur, V. (eds) *Paratuberculosis Org. Dis. Control*, 174–187.

MacKintosh, C., Clark, G., Tolentino, B., Liggett, S., De Lisle, G. and Griffin, F. (2012). Longitudinal pathogenesis study of young red deer (*Cervus elaphus*) after Experimental Challenge with *Mycobacterium avium* subsp. *paratuberculosis* (MAP). *Vet. Med. Int.* **2012**, 931948.

Mackintosh, C. G., De Lisle, G. W., Collins, D. M. and Griffin, J. F. T. (2004). Mycobacterial diseases of deer. *N. Z. Vet. J.* **52**, 163–174.

Marcé, C., Ezanno, P., Weber, M. F., Seegers, H., Pfeiffer, D. U. and Fourichon, C. (2010). Invited review: Modeling within-herd transmission of *Mycobacterium avium* subsp. *paratuberculosis* in dairy cattle: A review. *J. Dairy Sci.* **93**, 4455–4470.

Marino, R., Capoferri, R., Panelli, S., Minozzi, G., Strozzi, F., Trevisi, E., Snel, G. G. M., Ajmone-Marsan, P. and Williams, J. L. (2017). Johne's disease in cattle: an *in vitro* model to study early response to infection of *Mycobacterium avium* subsp. *paratuberculosis* using RNA-seq. *Mol. Immunol.* **91**, 259–271.

Masic, A., Nosky, B., Biwer, J., Alkemade, S., Prunic, B., Milovanovic, A., Maletic, M. and Masic, A. (2017). Effect of a non-specific immune stimulant (AMPLIMUNE^{TM}) on the health and production of light feedlot calves. *Acta Vet.* **6**, 179.

Matthews, C., Cotter, P. D. and O' Mahony, J. (2021). MAP, Johne's disease and the microbiome; current knowledge and future considerations. *Anim. Microbiome* **3**, 34.

Maurer, M., Seidel-Guyenot, W., Metz, M., Knop, J. and Steinbrink, K. (2003). Critical role of IL-10 in the induction of low zone tolerance to contact allergens. *J. Clin. Invest.* **112**, 432–439.

Mayer-Barber, K. D., Barber, D. L., Shenderov, K., White, S. D., Wilson, M. S., Cheever, A., Kugler, D., Hieny, S., Caspar, P. *et al.* (2010). Cutting Edge: Caspase-1 Independent IL-1β Production Is Critical for Host Resistance to *Mycobacterium tuberculosis* and Does Not Require TLR Signaling *In Vivo*. *J. Immunol.* **184**, 3326–3330.

Merkal, R. S., Lyle, P. and Whipple, D. L. (1982a). Decontamination, media and culture methods for *Mycobacterium avium* subsp. *paratuberculosis*. *Proc. 86th Annu. Meet. Unites States Anim. Heal. Assoc.*, 519–523.

Merkal, R. S., Miller, J. M., Hintz, A. M. and Bryner, J. H. (1982b). Intrauterine inoculation of *Mycobacterium paratuberculosis* into guinea pigs and cattle. *Am J Vet Res* **43**, 676–8.

Meyer, A., Bond, K., Van Winden, S., Green, M. and Guitian, J. (2018). A probabilistic approach to the interpretation of milk antibody results for diagnosis of Johne's disease in dairy cattle. *Prev. Vet. Med.* **150**, 30–37.

Mita, A., Mori, Y., Nakagawa, T., Tasaki, T., Utiyama, K. and Mori, H. (2016). Comparison of fecal pooling methods and DNA extraction kits for the detection of *Mycobacterium avium* subspecies *paratuberculosis*. *Microbiologyopen* **5**, 134–142.

Mokresh, A. H. and Butler, D. G. (1990). Granulomatous enteritis following oral inoculation of newborn rabbits with *Mycobacterium paratuberculosis* of bovine origin. *Can. J. Vet. Res.* **54**, 313.

Mokresh, A. H., Czuprynski, C. J. and Butler, D. G. (1989). A rabbit model for study of *Mycobacterium paratuberculosis* infection. *Infect. Immun.* **57**, 3798–3807.

Molina, J. M., Anguiano, A. and Ferrer, O. (1996). Study on immune response of goats vaccinated with a live strain of *Mycobacterium paratuberculosis*. *Comp. Immunol. Microbiol. Infect. Dis.* **19**, 9–15.

Momotani, E., Whipple, D. L. and Thiermann, A. B. (1988a). The distribution of ferritin, lactoferrin and transferrin in granulomatous lymphadenitis of bovine paratuberculosis. *J. Comp. Pathol.* **99**, 205–214.

Momotani, E., Whipple, D. L., Thiermann, A. B. and Cheville, N. F. (1988b). Role of M Cells and Macrophages in the Entrance of *Mycobacterium paratuberculosis* into Domes of Ileal Peyer's Patches in Calves. *Vet. Pathol.* **25**, 131–137.

Moorlag, S., Rodríguez-Rosales, Y., Gillard, J., Fanucchi, S., Theunissen, K., Novakovic, B., de Bont, C., Negishi, Y., Fok, E. *et al.* (2020). BCG Vaccination Induces Long-Term Functional Reprogramming of Human Neutrophils. *CellReports* **33**, 108387.

Moreira, M. L., Costa-Pereira, C., Alves, M. L. R., Marteleto, B. H., Ribeiro, V. M., Peruhype-

Magalhães, V., Giunchetti, R. C., Martins-Filho, O. A. and Araújo, M. S. S. (2016). Vaccination against canine leishmaniosis increases the phagocytic activity, nitric oxide production and expression of cell activation/migration molecules in neutrophils and monocytes. *Vet. Parasitol.* **220**, 33–45.

Muñoz-Caro, T., Silva, L. M. R., Ritter, C., Taubert, A. and Hermosilla, C. (2014). *Besnoitia besnoiti* tachyzoites induce monocyte extracellular trap formation. *Parasitol. Res.* **113**, 4189–4197.

Muñoz, M. (2014). Eficacia de una vacuna inactivada frente a la paratuberculosis bovina en un modelo experimental en terneros y su influencia en la patogenia de la enfermedad. *Tesis Dr. Univ. León* 548.

Musk, G. C., Kershaw, H., Tano, K., Niklasson, A., von Unge, M. and Dilley, R. J. (2019). Reactions to Gudair® vaccination identified in sheep used for biomedical research. *Aust. Vet. J.* **97**, 56–60.

Ni, G., Wang, T., Walton, S., Zhu, B., Chen, S., Wu, X., Wang, Y., Wei, M. Q. and Liu, X. (2015). Manipulating IL-10 signalling blockade for better immunotherapy. *Cell. Immunol.* **293**, 126–129.

Nicol, L., Wilkie, H., Gossner, A., Watkins, C., Dalziel, R. and Hopkins, J. (2016). Variations in T cell transcription factor gene structure and expression associated with the two disease forms of sheep paratuberculosis. *Vet. Res.* **47**, 83.

Nielsen, S. S. (2020). Immune-based diagnosis of paratuberculosis. In: Behr, M. A., Stevenson, K. & Kapur, V. (eds) *Paratuberculosis Org. Dis. Control*, 333–345.

Nielsen, S. S., Enevoldsen, C. and Gröhn, Y. T. (2002). The *Mycobacterium avium* subsp. *paratuberculosis* ELISA response by parity and stage of lactation. *Prev. Vet. Med.* **54**, 1–10.

Nielsen, S. S. and Toft, N. (2006). Age-specific characteristics of ELISA and fecal culture for purpose-specific testing for paratuberculosis. *J. Dairy Sci.* **89**, 569–579.

Nielsen, S. S., Toft, N. and Okura, H. (2013). Dynamics of Specific Anti-*Mycobacterium avium* Subsp. *paratuberculosis* Antibody Response through Age. *PLoS One* **8**, 63009.

Nisbet, D. I., Gilmour, N. J. and Brotherston, J. G. (1962). Quantitative studies of *Mycobacterium johnei* in tissues of sheep. III. Intestinal histopathology. *J. Comp. Pathol.* **72**, 80–91.

Novakovic, B., Habibi, E., Wang, S. Y., Arts, R. J. W., Davar, R., Megchelenbrink, W., Kim, B., Kuznetsova, T., Kox, M. *et al.* (2016). β-Glucan Reverses the Epigenetic State of LPS-Induced

Immunological Tolerance. *Cell* **167**, 1354-1368.e14.

O'Brien, R., Mackintosh, C. G. and Griffin, J. F. (2020). Paratuberculosis in Deer, Camelids and Other Ruminants. In: Behr, M. A., Stevenson, K. & Kapur, V. (eds) *Paratuberculosis Org. Dis. Control*, 188–199.

O'Reilly, M., Newcomb, D. E. and Remick, D. (1999). Endotoxin, sepsis, and the primrose path. *Shock* **12**, 411–420.

Okagawa, T., Konnai, S., Nishimori, A., Ikebuchi, R., Mizorogi, S., Nagata, R., Kawaji, S., Tanaka, S., Kagawa, Y. *et al.* (2015). Bovine immunoinhibitory receptors contribute to suppression of *Mycobacterium avium* subsp. *paratuberculosis*-specific T-cell responses. *Infect. Immun.* **84**, 77–89.

Onishi, R. M. and Gaffen, S. L. (2010). Interleukin-17 and its target genes: Mechanisms of interleukin-17 function in disease. *Immunology* **129**, 311–321.

Ott, S. L., Wells, S. J. and Wagner, B. A. (1999). Herd-level economic losses associated with Johne's disease on US dairy operations. *Prev. Vet. Med.* **40**, 179–192.

Padilla-Carlin, D. J., McMurray, D. N. and Hickey, A. J. (2008). The guinea pig as a model of infectious diseases. *Comp. Med.* **58**, 324–340.

Palmieri, B., Vadalà, M., Roncati, L., Garelli, A., Scandone, F., Bondi, M. and Cermelli, C. (2020). The long-standing history of *Corynebacterium parvum*, immunity, and viruses. *J. Med. Virol.* **92**, 2429–2439.

Paolicchi, F. A., Zumarraga, M. J., Gioffre, A., Zamorano, P., Morsella, C., Verna, A., Cataldi, A., Alito, A. and Romano, M. (2003). Application of different methods for the diagnosis of paratuberculosis in a dairy cattle herd in Argentina. *J. Vet. Med. Ser. B* **50**, 20–26.

Papayannopoulos, V. and Zychlinsky, A. (2009). NETs: a new strategy for using old weapons. *Trends Immunol.* **30**, 513–521.

Park, H.-E., Park, H.-T., Jung, Y. H. and Yoo, H. S. (2018). Gene expression profiles of immune-regulatory genes in whole blood of cattle with a subclinical infection of *Mycobacterium avium* subsp. *paratuberculosis*. *PLoS One* **13**, e0196502.

Park, K. T., Allen, A. J., Bannantine, J. P., Seo, K. S., Hamilton, M. J., Abdellrazeq, G. S., Rihan, H. M., Grimm, A. and Davis, W. C. (2011). Evaluation of two mutants of *Mycobacterium avium*

subsp. *paratuberculosis* as candidates for a live attenuated vaccine for Johne's disease. *Vaccine* **29**, 4709–4719.

Park, K. T., Allen, A. J. and Davis, W. C. (2014). Development of a novel DNA extraction method for identification and quantification of *Mycobacterium avium* subsp. *paratuberculosis* from tissue samples by real-time PCR. *J. Microbiol. Methods* **99**, 58–65.

Park, S.-U., Kathaperumal, K., McDonough, S., Akey, B., Huntley, J., Bannantine, J. P. and Chang, Y.-F. (2008). Immunization with a DNA vaccine cocktail induces a Th1 response and protects mice against *Mycobacterium avium* subsp. *paratuberculosis* challenge. *Vaccine* **26**, 4329–37.

Parker, A. E. and Bermúdez, L. E. (1997). Expression of the green fluorescent protein (GFP) in *Mycobacterium avium* as a tool to study the interaction between Mycobacteria and host cells. *Microb. Pathog.* **22**, 193–198.

Patton, E. A. (2011). Paratuberculosis Vaccination. *Vet. Clin. North Am. - Food Anim. Pract.* **27**, 573–580.

Pavić, K., Perković, I., Pospíšilová, Š., Machado, M., Fontinha, D., Prudêncio, M., Jampilek, J., Coffey, A., Endersen, L. *et al.* (2018). Primaquine hybrids as promising antimycobacterial and antimalarial agents. *Eur. J. Med. Chem.* **143**, 769–779.

Pérez, V., Tellechea, J., Badiola, J. J., Gutiérrez, M. and García Marín, J. F. (1997). Relation between serologic response and pathologic findings in sheep with naturally acquired paratuberculosis. *Am. J. Vet. Res.* **58**, 799–803.

Petretto, A., Bruschi, M., Pratesi, F., Croia, C., Candiano, G., Ghiggeri, G. and Migliorini, P. (2019). Neutrophil extracellular traps (NET) induced by different stimuli: A comparative proteomic analysis. *PLoS One* **14**, e0218946.

Phanse, Y., Wu, C. W., Venturino, A. J., Hansen, C., Nelson, K., Broderick, S. R., Steinberg, H. and Talaat, A. M. (2020). A protective vaccine against johne's disease in cattle. *Microorganisms* **8**, 1–18.

Phillips, I. L., Everman, J. L., Bermúdez, L. E. and Danelishvili, L. (2020). *Acanthamoeba castellanii* as a screening tool for *Mycobacterium avium* subspecies *paratuberculosis* virulence factors with relevance in macrophage infection. *Microorganisms* **8**, 1–21.

Pieters, J. (2001). Entry and survival of pathogenic mycobacteria in macrophages. *Microbes Infect.* **3**,

249–255.

Pilsczek, F. H., Salina, D., Poon, K. K. H., Fahey, C., Yipp, B. G., Sibley, C. D., Robbins, S. M., Green, F. H. Y., Surette, M. G. *et al.* (2010). A Novel Mechanism of Rapid Nuclear Neutrophil Extracellular Trap Formation in Response to *Staphylococcus aureus*. *J. Immunol.* **185**, 7413–7425.

Plain, K. M., Marsh, I. and Purdie, A. C. (2020). Diagnosis of Paratuberculosis by PCR. In: Behr, M. A., Stevenson, K. & Kapur, V. (eds) *Paratuberculosis Org. Dis. Control*, 305–332.

Plattner, B. L., Doyle, R. T. and Hostetter, J. M. (2009). Gamma-delta T cell subsets are differentially associated with granuloma development and organization in a bovine model of mycobacterial disease. *Int. J. Exp. Pathol.* **90**, 587–597.

Plattner, B. L., Huffman, E., Jones, D. E. and Hostetter, J. M. (2014). T lymphocyte responses during early enteric *Mycobacterium avium* subspecies *paratuberculosis* infection in cattle. *Vet. Immunol. Immunopathol.* **157**, 12–19.

Plattner, B. L., Huffman, E. L. and Hostetter, J. M. (2013). Gamma-delta T-cell responses during subcutaneous *Mycobacterium avium* subspecies *paratuberculosis* challenge in sensitized or naïve calves using matrix biopolymers. *Vet. Pathol.* **50**, 630–637.

Pooley, H. B., Begg, D. J., Plain, K. M., Whittington, R. J., Purdie, A. C. and De Silva, K. (2019). The humoral immune response is essential for successful vaccine protection against paratuberculosis in sheep. *BMC Vet. Res.* **15**, 223.

Pooley, H. B., Plain, K. M., Purdie, A. C., Begg, D. J., Whittington, R. J. and De Silva, K. (2018). Integrated vaccine screening system: using cellular functional capacity *in vitro* to assess genuine vaccine protectiveness in ruminants. *Pathog. Dis.* **76**.

Prince, L. R., Allen, L., Jones, E. C., Hellewell, P. G., Dower, S. K., Whyte, M. K. B. and Sabroe, I. (2004). The role of interleukin-1β in direct and toll-like receptor 4-mediated neutrophil activation and survival. *Am. J. Pathol.* **165**, 1819–1826.

Propst, T., Propst, A., Lhotta, K., Vogel, W. and Konig, P. (1998). Reinforced intradermal hepatitis B vaccination in hemodialysis patients is superior in antibody response to intramuscular or subcutaneous vaccination. *Am. J. Kidney Dis.* **32**, 1041–5.

Purdie, A. C., Plain, K. M., Begg, D. J., De Silva, K. and Whittington, R. J. (2012). Expression of genes

associated with the antigen presentation and processing pathway are consistently regulated in early *Mycobacterium avium* subsp. *paratuberculosis* infection. *Comp. Immunol. Microbiol. Infect. Dis.* **35**, 151–162.

Radoslaw, R., Rick, C., Stan, A., Maira, M.-P., Dejan, B., Aleksandar, M., Sladjan, N. and Aleksandar, M. (2017). *Mycobacterium* cell wall fraction immunostimulat (AMPLIMUNE^{TM}) efficacy in the reduction of the severity of the severity of ETEC induced diarrhea in neonatal calves. *Acta Vet.* **67**, 222–237.

Reboldi, A. and Cyster, J. G. (2016). Peyer's patches: Organizing B-cell responses at the intestinal frontier. *Immunol. Rev.* **271**, 230–245.

Reddacliff, L., Eppleston, J., Windsor, P., Whittington, R. and Jones, S. (2006). Efficacy of a killed vaccine for the control of paratuberculosis in Australian sheep flocks. *Vet. Microbiol.* **115**, 77–90.

Ricchi, M., Bertasio, C., Boniotti, M. B., Vicari, N., Russo, S., Tilola, M., Bellotti, M. A. and Bertasi, B. (2017). Comparison among the quantification of bacterial pathogens by qPCR, dPCR, and cultural methods. *Front. Microbiol.* **8**, 1174.

Richardson, E. K. B. and More, S. J. (2009). Direct and indirect effects of Johne's disease on farm and animal productivity in an Irish dairy herd. *Ir. Vet. J.* **62**, 526–532.

Rigden, R. C., Jandhyala, D. M., Dupont, C., Crosbie-Caird, D., López-Villalobos, N., Maeda, N., Gicquel, B. and Murray, A. (2006). Humoral and cellular immune responses in sheep immunized with a 22 kilodalton exported protein of *Mycobacterium avium* subspecies *paratuberculosis*. *J. Med. Microbiol.* **55**, 1735–1740.

Roupie, V., Viart, S., Leroy, B., Romano, M., Trinchero, N., Govaerts, M., Letesson, J. J., Wattiez, R. and Huygen, K. (2012). Immunogenicity of eight *Mycobacterium avium* subsp. *paratuberculosis* specific antigens in DNA vaccinated and Map infected mice. *Vet. Immunol. Immunopathol.* **145**, 74–85.

Roussey, J. A., Oliveira, L. J., Langohr, I. M., Sledge, D. G. and Coussens, P. M. (2016). Regulatory T cells and immune profiling in johne's disease lesions. *Vet. Immunol. Immunopathol.* **181**, 39–50.

Roussey, J. A., Steibel, J. P. and Coussens, P. M. (2014). Regulatory T cell activity and signs of T cell unresponsiveness in bovine paratuberculosis. *Front. Vet. Sci.* **1**, 20.

Roy, A., Risalde, M. A., Casal, C., Romero, B., De Juan, L., Menshawy, A. M., Díez-Guerrier, A., Juste, R. A., Garrido, J. M. *et al.* (2017). Oral vaccination with heat-inactivated *Mycobacterium bovis* does not interfere with the antemortem diagnostic techniques for tuberculosis in goats. *Front. Vet. Sci.* **4**, 124.

Santema, W. J., Poot, J., Segers, R. P. A. M., Van den Hoff, D. J. P., Rutten, V. P. M. G. and Koets, A. P. (2012). Early infection dynamics after experimental challenge with *Mycobacterium avium* subspecies *paratuberculosis* in calves reveal limited calf-to-calf transmission and no impact of Hsp70 vaccination. *Vaccine* **30**, 7032–7039.

Santema, W., Rutten, V., Segers, R., Poot, J., Hensen, S., Heesterbeek, H. and Koetsa, A. (2013). Postexposure subunit vaccination against chronic enteric mycobacterial infection in a natural host. *Infect. Immun.* **81**, 1990–1995.

Santocki, M. and Kolaczkowska, E. (2020). On Neutrophil Extracellular Trap (NET) Removal: What We Know Thus Far and Why So Little. *Cells* **9**, 2079.

Savi, R., Ricchi, M., Cammi, G., Garbarino, C., Leo, S., Pongolini, S. and Arrigoni, N. (2015). Survey on the presence of *Mycobacterium avium* subsp. *paratuberculosis* in ground beef from an industrial meat plant. *Vet. Microbiol.* **177**, 403–408.

Sawant, K. V. and McMurray, D. N. (2007). Guinea pig neutrophils infected with *Mycobacterium tuberculosis* produce cytokines which activate alveolar macrophages in noncontact cultures. *Infect. Immun.* **75**, 1870–1877.

Scandurra, G. M., De Lisle, G. W., Cavaignac, S. M., Young, M., Kawakami, R. P. and Collins, D. M. (2010). Assessment of live candidate vaccines for paratuberculosis in animal models and macrophages. *Infect. Immun.* **78**, 1383–1389.

Schrader, C., Schielke, A., Ellerbroek, L. and Johne, R. (2012). PCR inhibitors - occurrence, properties and removal. *J. Appl. Microbiol.* **113**, 1014–1026.

Schülke, S. (2018). Induction of interleukin-10 producing dendritic cells as a tool to suppress allergen-specific T helper 2 responses. *Front. Immunol.* **9**, 1.

Schwalm, A. K., Obiegala, A., Pfeffer, M. and Sting, R. (2018). Enhanced sensitivity and fast turnaround time in laboratory diagnosis for bovine paratuberculosis in faecal samples. *J. Microbiol. Methods* **152**, 39–47.

Sechi, L. A., Mara, L., Cappai, P., Frothingam, R., Ortu, S., Leoni, A., Ahmed, N. and Zanetti, S. (2006). Immunization with DNA vaccines encoding different mycobacterial antigens elicits a Th1 type immune response in lambs and protects against *Mycobacterium avium* subspecies *paratuberculosis* infection. *Vaccine* **24**, 229–235.

Secott, T. E., Lin, T. L. and Wu, C. C. (2001). Fibronectin attachment protein homologue mediates fibronectin binding by *Mycobacterium avium* subsp. *paratuberculosis*. *Infect. Immun.* **69**, 2075–2082.

Secott, T. E., Lin, T. L. and Wu, C. C. (2002). Fibronectin attachment protein is necessary for efficient attachment and invasion of epithelial cells by *Mycobacterium avium* subsp. *paratuberculosis*. *Infect. Immun.* **70**, 2670–2675.

Secott, T. E., Lin, T. L. and Wu, C. C. (2004). *Mycobacterium avium* subsp. *paratuberculosis* fibronectin attachment protein facilitates M-cell targeting and invasion through a fibronectin bridge with host integrins. *Infect. Immun.* **72**, 3724–3732.

Secott, T. E., Ohme, A. M., Barton, K. S., Wu, C. C. and Rommel, F. A. (1999). *Mycobacterium paratuberculosis* detection in bovine feces is improved by coupling agar culture enrichment to an *IS900*-specific polymerase chain reaction assay. *J. Vet. Diagnostic Investig.* **11**, 441–447.

Serrano, M., Elguezabal, N., Sevilla, I. A., Geijo, M. V, Molina, E., Arrazuria, R., Urkitza, A., Jones, G. J., Vordermeier, M. *et al.* (2017a). Tuberculosis Detection in Paratuberculosis Vaccinated Calves: New Alternatives against Interference. *PLoS One* **12**, e0169735.

Serrano, M., Elguezabal, N., Sevilla, I. A., Geijo, M. V., Molina, E., Juste, R. A. and Garrido, J. M. (2017b). Preliminary results indicate that inactivated vaccine against paratuberculosis could modify the course of experimental *Mycobacterium bovis* infection in calves. *Front. Vet. Sci.* **4**, 175.

Settles, E. W., Kink, J. A. and Talaat, A. (2014). Attenuated strains of *Mycobacterium avium* subspecies *paratuberculosis* as vaccine candidates against Johne's disease. *Vaccine* **32**, 2062–2069.

Sevilla, I. A., Garrido, J. M., Molina, E., Geijo, M. V., Elguezabal, N., Vázquez, P. and Juste, R. A. (2014). Development and evaluation of a novel multicopy-element-targeting triplex PCR for detection of *Mycobacterium avium* subsp. *paratuberculosis* in feces. *Appl. Environ. Microbiol.* **80**, 3757–3768.

Sharma, A., Simonson, T. J., Jondle, C. N., Mishra, B. B. and Sharma, J. (2017). Mincle-Mediated

Neutrophil Extracellular Trap Formation by Regulation of Autophagy. *J. Infect. Dis.* **215**, 1040–1048.

Shin, M. K., Park, H., Shin, S. W., Jung, M., Lee, S. H., Kim, D. Y., Yoo, H. S. and Dellagostin, O. A. (2015). Host Transcriptional Profiles and Immunopathologic Response following *Mycobacterium avium* subsp. *paratuberculosis* Infection in Mice. *PLoS One* **10**, e0138770.

Shin, S. J., Wu, C. W., Steinberg, H. and Talaat, A. M. (2006). Identification of novel virulence determinants in *Mycobacterium paratuberculosis* by screening a library of insertional mutants. *Infect. Immun.* **74**, 3825–3833.

Shippy, D. C., Lemke, J. J., Berry, A., Nelson, K., Hines, M. E. and Talaat, A. M. (2017). Superior protection from live- attenuated vaccines directed against johne's disease. *Clin. Vaccine Immunol.* **24**, e00478-16.

Shrestha, S., Lee, J. M. and Hong, C. W. (2020). Autophagy in neutrophils. *Korean J. Physiol. Pharmacol.* **24**, 1–10.

Siemsen, D. W., Malachowa, N., Schepetkin, I. A., Whitney, A. R., Kirpotina, L. N., Lei, B., Deleo, F. R. and Quinn, M. T. (2014). Neutrophil Isolation from Nonhuman Species. *Methods Mol. Biol.*, 19–37.

Sigurdardóttir, Ó. G., Bakke-McKellep, A. M., Djønne, B. and Evensen, Ø. (2005). *Mycobacterium avium* subsp. *paratuberculosis* enters the small intestinal mucosa of goat kids in areas with and without Peyer's patches as demonstrated with the everted sleeve method. *Comp. Immunol. Microbiol. Infect. Dis.* **28**, 223–230.

Sigurdardóttir, Ó. G., Press, C. M. L., Saxegaard, F. and Evensen, Ø. (1999). Bacterial isolation, immunological response, and histopathological lesions during the early subclinical phase of experimental infection of goat kids with *Mycobacterium avium* subsp. *paratuberculosis*. *Vet. Pathol.* **36**, 542–550.

Silva, M. T. (2010). When two is better than one: macrophages and neutrophils work in concert in innate immunity as complementary and cooperative partners of a myeloid phagocyte system. *J. Leukoc. Biol.* **87**, 93–106.

Silva, M. T., Silva, M. N. and Appelberg, R. (1989). Neutrophil-macrophage cooperation in the host defence against mycobacterial infections. *Microb. Pathog.* **6**, 369–380.

Skendros, P., Mitroulis, I. and Ritis, K. (2018). Autophagy in neutrophils: From granulopoiesis to neutrophil extracellular traps. *Front. Cell Dev. Biol.* **6**, 109.

Smeed, J. A., Watkins, C. A., Rhind, S. M. and Hopkins, J. (2007). Differential cytokine gene expression profiles in the three pathological forms of sheep paratuberculosis. *BMC Vet. Res.* **3**, 18.

Smith, R. L., Al-Mamun, M. A. and Gröhn, Y. T. (2017). Economic consequences of paratuberculosis control in dairy cattle: A stochastic modeling study. *Prev. Vet. Med.* **138**, 17–27.

Smith, R. L., Schukken, Y. H. and Gröhn, Y. T. (2015). A new compartmental model of *Mycobacterium avium* subsp. *paratuberculosis* infection dynamics in cattle. *Prev. Vet. Med.* **122**, 298–305.

Smith, S. L., Wilson, P. R., Collett, M. G., Heuer, C., West, D. M., Stevenson, M. and Chambers, J. P. (2014). Liver Biopsy Histopathology for Diagnosis of Johne's Disease in Sheep. *Vet. Pathol.* **51**, 915–918.

Sommer, S., Pudrith, C. B., Colvin, C. J. and Coussens, P. M. (2009). *Mycobacterium avium* subsp. *paratuberculosis* suppresses expression of IL-12p40 and iNOS genes induced by signalling through CD40 in bovine monocyte-derived macrophages. *Vet. Immunol. Immunopathol.* **128**, 44–52.

Soulas, C., Conerly, C., Kim, W. K., Burdo, T. H., Alvarez, X., Lackner, A. A. and Williams, K. C. (2011). Recently infiltrating MAC387+ monocytes/ macrophages: A third macrophage population involved in SIV and HIV encephalitic lesion formation. *Am. J. Pathol.* **178**, 2121–2135.

Souza, C. D., Evanson, O. A. and Weiss, D. J. (2006). Mitogen activated protein kinasep38 pathway is an important component of the anti-inflammatory response in *Mycobacterium avium* subsp. *paratuberculosis*-infected bovine monocytes. *Microb. Pathog.* **41**, 59–66.

Souza, C. D., Evanson, O. A. and Weiss, D. J. (2008). Role of cell membrane receptors in the suppression of monocyte anti-microbial activity against *Mycobacterium avium* subsp. *paratuberculosis*. *Microb. Pathog.* **44**, 215–223.

St-Jean, G. (1996). Treatment of clinical paratuberculosis in cattle. *Vet. Clin. North Am. Food Anim. Pract.* **12**, 417–430.

St-Jean, G. and Jernigan, A. D. (1991). Treatment of *Mycobacterium paratuberculosis* infection in

ruminants. *Vet. Clin. North Am. Food Anim. Pract.* **7**, 793–804.

Stabel, J. R. (1998). Johne's Disease: A Hidden Threat. *J. Dairy Sci.* **81**, 283–288.

Stabel, J. R. (2000). Transitions in immune responses to *Mycobacterium paratuberculosis*. *Vet. Microbiol.* **77**, 465–473.

Stabel, J. R. and Bannantine, J. P. (2005). Development of a nested PCR method targeting a unique multicopy element, *ISMap02*, for detection of *Mycobacterium avium* subsp. *paratuberculosis* in fecal samples. *J. Clin. Microbiol.* **43**, 4744–4750.

Stabel, J. R. and Bannantine, J. P. (2021). Reduced tissue colonization of *Mycobacterium avium* subsp. *paratuberculosis* in neonatal calves vaccinated with a cocktail of recombinant proteins. *Vaccine* **39**, 3131–3140.

Stabel, J. R., Koets, A. and De Silva, K. (2020). Immunology of Paratuberculosis Infection and Disease. In: Behr, M. A., Stevenson, K. & Kapur, V. (eds) *Paratuberculosis Org. Dis. Control*, 248–265.

Storset, A. K., Hasvold, H. J., Valheim, M., Brun-Hansen, H., Berntsen, G., Whist, S. K., Djønne, B., Press, C. M. L., Holstad, G. *et al.* (2001). Subclinical paratuberculosis in goats following experimental infection: An immunological and microbiological study. *Vet. Immunol. Immunopathol.* **80**, 271–287.

Streeter, M. N., Barron, S. J., Wagner, D. G., Hibberd, C. A., Owens, F. N. and McCollum, F. T. (1991). Technical note: a double L intestinal cannula for cattle. *J. Anim. Sci.* **69**, 2601–2607.

Suda, Y., Miyazaki, A., Miyazawa, K., Shibahara, T. and Ohashi, S. (2021). Systemic and intestinal porcine epidemic diarrhea virus-specific antibody response and distribution of antibody-secreting cells in experimentally infected conventional pigs. *Vet. Res.* **52**, 2.

Sweeney, R. W. (1996). Transmission of paratuberculosis. *Vet. Clin. North Am. Food Anim. Pract.* **12**, 305–312.

Sweeney, R. W. (2011). Pathogenesis of Paratuberculosis. *Vet. Clin. North Am. - Food Anim. Pract.* **27**, 537–546.

Taddei, R., Barbieri, I., Pacciarini, M. L., Fallacara, F., Belletti, G. L. and Arrigoni, N. (2008). *Mycobacterium porcinum* strains isolated from bovine bulk milk: Implications for *Mycobacterium avium* subsp. *paratuberculosis* detection by PCR and culture. *Vet. Microbiol.* **130**, 338–347.

Talaat, A. M., Wu, C.-W. and Hines, M. E. (2020). Experimental animal models of paratuberculosis. In: Behr, M. A., Stevenson, K. & Kapur, V. (eds) *Paratuberculosis Org. Dis. Control*, 213–247.

Tan, B. H., Meinken, C., Bastian, M., Bruns, H., Legaspi, A., Ochoa, M. T., Krutzik, S. R., Bloom, B. R., Ganz, T. *et al.* (2008). Macrophages acquire neutrophil granules for antimicrobial activity against intracellular pathogens. *J. Immunol.* **180**, 664.2-664.

Tecchio, C. and Cassatella, M. A. (2016). Neutrophil-derived chemokines on the road to immunity. *Semin. Immunol.*, 119–128.

Tejedor, F. J. (1994). Estudio epidemiológico de la Paratuberculosis ovina en la provincia de Segovia.

Tessema, M. Z., Koets, A. P., Rutten, V. P. M. G. and Gruys, E. (2001). How does *Mycobacterium avium* subsp. *paratuberculosis* resist intracellular degradation? *Vet. Q.* **23**, 153–162.

Tewari, D., Hovingh, E., Linscott, R., Martel, E., Lawrence, J., Wolfgang, D. and Griswold, D. (2014). *Mycobacterium avium* subsp. *paratuberculosis* antibody response, fecal shedding, and antibody cross-reactivity to *Mycobacterium bovis* in *M. avium* subsp. *paratuberculosis*-infected cattle herds vaccinated against Johne's dis. *Clin. Vaccine Immunol.* **21**, 698–703.

Tiwari, A., VanLeeuwen, J. A., McKenna, S. L. B., Keefe, G. P. and Barkema, H. W. (2006). Johne's disease in Canada Part I: Clinical symptoms, pathophysiology, diagnosis, and prevalence in dairy herds. *Can. Vet. J.* **47**, 874–882.

Tizard, I. (2017a). Lymphocytes. *Vet. Immunol.*, 122–130.

Tizard, I. (2017b). Helper T Cells and Their Response to Antigens. *Vet. Immunol.*, 131–146.

Tizard, I. (2017c). Regulation of Adaptive Immunity. *Vet. Immunol.*, 207–220.

Tizard, I. (2017d). Dendritic Cells and Antigen Processing. *Vet. Immunol.*, 89–99.

Tizard, I. (2017e). Humoral Innate Immunity: Inflammatory Mediators. *Vet. Immunol.*, 18–25.

Toft, N., Nielsen, S. S. and Jørgensen, E. (2005). Continuous-data diagnostic tests for paratuberculosis as a multistage disease. *J. Dairy Sci.* **88**, 3923–3931.

Trentini, M. M., de Oliveira, F. M., Kipnis, A. and Junqueira-Kipnis, A. P. (2016). The role of neutrophils in the induction of specific Th1 and Th17 during Vaccination against tuberculosis. *Front. Microbiol.* **7**, 898.

Twort, F. W. and Ingram, G. L. Y. (1912). A method for isolating and cultivating the *Mycobacterium*

enteritidis chronicæ pseudotuberculosæ bovis, Johne, and some experiments on the preparation of a diagnostic vaccine for pseudo-tuberculous enteritis of bovines. *Proc. R. Soc. London. Ser. B, Contain. Pap. a Biol. Character* **84**, 517–542.

Vallée, H. and Rinjard, P. (1926). Etudes sur l´entérite paratuberculeuse des bovides. *Rev. Gén. Méd. Vét.* **409**, 1–9.

Vandesompele, J., De Preter, K., Pattyn, F., Poppe, B., Van Roy, N., De Paepe, A. and Speleman, F. (2002). Accurate normalization of real-time quantitative RT-PCR data by geometric averaging of multiple internal control genes. *Genome Biol.* **3**, 1–12.

Vandivier, R., Henson, P. and Douglas, I. (2006). Burying the Dead: The Impact of Failed Apoptotic Cell Removal (Efferocytosis) on Chronic Inflammatory Lung Disease. *Chest* **129**, 1673–82.

Vaughan, J. A., Lenghaus, C., Stewart, D. J., Tizard, M. L. and Michalski, W. P. (2005). Development of a Johne's disease infection model in laboratory rabbits following oral administration of *Mycobacterium avium* subsp. *paratuberculosis*. *Vet. Microbiol.* **105**, 207–13.

Vázquez, P., Garrido, J. M., Molina, E., Geijo, M. V., Gómez, N., Pérez, V., Sevilla, I. A., Alonso-Hearn, M., Cortés, A. *et al.* (2014). Latent infections are the most frequent form of paratuberculosis in slaughtered Friesian cattle. *Spanish J. Agric. Res.* **12**, 1049–1060.

Vázquez, P., Garrido, J. M. and Juste, R. A. (2013). Specific Antibody and Interferon-Gamma Responses Associated with Immunopathological Forms of Bovine Paratuberculosis in Slaughtered Friesian Cattle. *PLoS One* **8**, e64568.

Wang, J., Moolji, J., Dufort, A., Staffa, A., Domenech, P., Reed, M. B. and Behr, M. A. (2016). Iron acquisition in *Mycobacterium avium* subsp. *paratuberculosis*. *J. Bacteriol.* **198**, 857–866.

Warren, E., Teskey, G. and Venketaraman, V. (2017). Effector Mechanisms of Neutrophils within the Innate Immune System in Response to *Mycobacterium tuberculosis* Infection. *J. Clin. Med.* **6**, 15.

Watanabe, S., Alexander, M., Misharin, A. V. and Budinger, G. R. S. (2019). The role of macrophages in the resolution of inflammation. *J. Clin. Invest.* **129**, 2619–2628.

Weber, M. F. (2006). Risk management of paratuberculosis in dairy herds. *Ir. Vet. J.* **59**, 555–561.

Weiss, D. J., Evanson, O. A., de Souza, C. and Abrahamsen, M. S. (2005). A critical role of interleukin-10 in the response of bovine macrophages to infection by *Mycobacterium avium* subsp.

paratuberculosis. *Am. J. Vet. Res.* **66**, 721–726.

Weiss, D. J., Evanson, O. A., Moritz, A., Deng, M. Q. and Abrahamsen, M. S. (2002). Differential responses of bovine macrophages to *Mycobacterium avium* subsp. *paratuberculosis* and *Mycobacterium avium* subsp. *avium*. *Infect. Immun.* **70**, 5556–5561.

Whittington, R. (2020). Cultivation of *Mycobacterium avium* subsp. *paratuberculosis*. In: Behr, M. A., Stevenson, K. & Kapur, V. (eds) *Paratuberculosis Org. Dis. Control*, 266–304.

Whittington, R. J., Donat, K., Weber, M. F., Kelton, D., Nielsen, S. S., Eisenberg, S., Arrigoni, N., Juste, R., Sáez, J. L. *et al.* (2019). Control of paratuberculosis: Who, why and how. A review of 48 countries. *BMC Vet. Res.* **15**, 1–29.

Whittington, R. J., Begg, D. J., De Silva, K., Plain, K. M. and Purdie, A. C. (2012). Comparative immunological and microbiological aspects of paratuberculosis as a model mycobacterial infection. *Vet. Immunol. Immunopathol.* **148**, 29–47.

Whittington, R. J., Begg, D. J., De Silva, K., Purdie, A. C., Dhand, N. K. and Plain, K. M. (2017). Case definition terminology for paratuberculosis (Johne's disease). *BMC Vet. Res.* **13**, 328.

Whittington, R. J., Marsh, I. B., Saunders, V., Grant, I. R., Juste, R., Sevilla, I. A., Manning, E. J. B. and Whitlock, R. H. (2011). Culture phenotypes of genomically and geographically diverse *Mycobacterium avium* subsp. *paratuberculosis* isolates from different hosts. *J. Clin. Microbiol.* **49**, 1822–1830.

William, R., Watson, G., Rotstein, O. D., Parodo, J., Bitar, R. and Marshall, J. C. (1998). The IL-1β-Converting Enzyme (Caspase-1) Inhibits Apoptosis of Inflammatory Neutrophils Through Activation of IL-1β. *J. Immunol.* **161**, 957–962.

Windsor, P. A., Bush, R., Links, I. and Eppleston, J. (2005). Injury caused by self-inoculation with a vaccine of a Freund's complete adjuvant nature (Gudair^{TM}) used for control of ovine paratuberculosis. *Aust. Vet. J.* **83**, 216–220.

Wong, K. W. and Jacobs, W. R. (2013). *Mycobacterium tuberculosis* exploits human interferon γ to stimulate macrophage extracellular trap formation and necrosis. *J. Infect. Dis.* **208**, 109–119.

World Organisation for Animal Health (OIE) (2018). Bovine tuberculosis. *Man. Diagnostic Tests Vaccines Terr. Anim.*, 1058–1074.

Wright, K., de Silva, K., Plain, K. M., Purdie, A. C., Blair, T. A., Duggin, I. G., Britton, W. J. and

Oehlers, S. H. (2021). Mycobacterial infection-induced miR-206 inhibits protective neutrophil recruitment via the CXCL12/CXCR4 signalling axis. *PLoS Pathog.* **17**, e1009186.

Wu, C. W., Livesey, M., Schmoller, S. K., Manning, E. J. B., Steinberg, H., Davis, W. C., Hamilton, M. J. and Talaat, A. M. (2007). Invasion and persistence of *Mycobacterium avium* subsp. *paratuberculosis* during early stages of Johne's disease in calves. *Infect. Immun.* **75**, 2110–2119.

Xu, J., Zhang, X., Monestier, M., Esmon, N. L. and Esmon, C. T. (2011). Extracellular Histones Are Mediators of Death through TLR2 and TLR4 in Mouse Fatal Liver Injury. *J. Immunol.* **187**, 2626–2631.

Yamane, K., Ihn, H., Asano, Y., Jinnin, M. and Tamaki, K. (2003). Antagonistic Effects of TNF-α on TGF-β Signaling Through Down-Regulation of TGF-β Receptor Type II in Human Dermal Fibroblasts. *J. Immunol.* **171**, 3855–3862.

Yates, R. M. and Russell, D. G. (2005). Phagosome maturation proceeds independently of stimulation of toll-like receptors 2 and 4. *Immunity* **23**, 409–417.

Research Contributions of the author

Academic record

Veterinary Medicine Degree. University of Extremadura (UEX), Spain (2008-2013). Degrees obtained: 7.26/10.

Master on Molecular Biotechnology. University of Barcelona (UB) (2014-2015). Degrees obtained: 8.6/10.

Master`s internship studying "*Caenorhabditis elegans* as a model for the study of Parkinson Disease" **IDIBELL** (Institut d'Investigació Biomèdica de Bellvitge).

Scientific contributions

Arrazuria R, **Ladero I**, Molina E, Fuertes M, Juste R, Fernández M, Pérez V, Garrrido J, Elguezabal N. "Alternative vaccination routes against paratuberculosis modulate local immune response and interference with tuberculosis diagnosis in laboratory animals". *Veterinary Sciences* (2020).

Ladero-Auñon I, Molina E, Holder A, Kolakowski J, Harris H, Urkitza A, Anguita J, Werling D, Elguezabal N. "Bovine Neutrophils Release Extracellular Traps and Cooperate With Macrophages in *Mycobacterium avium* subsp. *paratuberculosis* clearance *in vitro*". *Frontiers in Immunology* (2021).

Arteche N, Gutiérrez-Expósito D; Vallejo R; Espinosa J; Elguezabal N; **Ladero-Auñon I**; Royo M; Ferreras M; Benavides J; Pérez V. "Early response of monocyte-derived macrophages from vaccinated and non-vaccinated goats against *in vitro* infection with *Mycobacterium avium* subsp. *paratuberculosis*" *Veterinary Research* (2021).

Ladero-Auñon I, Molina E, Oyanguren M, Barriales D, Fuertes M, Sevilla I, Luo L, Arrazuria R, De Buck J, Anguita J, Elguezabal N. "Oral vaccination stimulates neutrophil functionality and exerts protection in a *Mycobacterium avium* subsp. *paratuberculosis* infection model". Accepted*, npj Vaccines,* July 2021.

Ladero-Auñon I, Elguezabal N. "Neutrophil Function Assays". Chapter for the *Encyclopedia of Infection and Immunity, ELSEVIER.* Submitted May, 2021.

Congress communications

Ladero I, Arrazuria A, Molina E, Fernández M, Royo M, Garrido J, Juste R, Pérez V, Elguezabal N**. "**Effects of vaccination route on the immune response in the rabbit paratuberculosis infection model". 14th International Colloquium of Paratuberculosis. Riviera Maya, México. June*,* 2018.

Serna S, Artschawager R, Gracía R, Dupin D, **Ladero I**, Molina E, Elguezabal N, Reichardt N. "Towards the production of anti-N-glycan antibodies. An immunization study

with a bi-antennary N-glycan with terminal LacdiNAc (LDN) residues" Glycobasque. March, 2020.

Ladero I, Molina E, Barriales D, De Buck J, Garrido J, Anguita J, Elguezabal N. "Oral mycobacterial vaccines stimulate rabbit neutrophil extracellular trap formation and phagocytosis". Accepted and Awarded with the Richard Merkal Award. for 15th International Colloquium of Paratuberculosis. May, 2020. Cancelled due to COVID-19 pandemic.

Ladero-Auñon I, Holder A, Kolakowski J, Harris H, Garrido JM, Elguezabal N, Werling D. "Macrophages regulate neutrophils' IL-1β release in the presence of *Mycobacterium avium* subsp. *paratuberculosis*". Accepted for 15th International Colloquium of Paratuberculosis. May, 2020. Cancelled due to COVID-19 pandemic.

Goikoetxea-Usandizaga N, Egia-Mendikute L, Serrano-Maciá M, Delgado T, **Ladero I**, Molina E, Lachiondo-Ortega S *et al*. "Metabolic rewiring by increased mitochondrial respiration drives immune evasion in liver cancer". The International Liver Congress™. June, 2021.

Scholarships

EMBO short-term fellowship (number 8407): Cattle innate response against mycobacterial infections: neutrophil extracellular trap release and inflammasome complex formation in caspase-1 activation. September-December 2019.

FEMS research and training grant (ID FEMS-GO-2019-507): Cattle innate response against mycobacterial infections: neutrophil extracellular trap release and inflammasome complex formation in caspase-1 activation. September-December 2019.

PhD Scholarship from the Department of Economic Development and Infrastructure of the **Basque Government** February 2017-January 2021.

Collaboration scholarship granted by the Education Ministry of the **Spanish Government**. October 2012-July 2013.